ErbB inhibitors as a potential future treatment for chronic obstructive pulmonary disease

K. D. Herman

A thesis submitted in partial fulfilment of the requirements for the degree of Doctor of Philosophy

2022

ErbB inhibitors as a potential future treatment for chronic obstructive pulmonary disease

Kimberly Dana Herman

Supervised by Dr Lynne Prince and Professor Stephen Renshaw

Department of Infection, Immunity and Cardiovascular Disease

A thesis submitted in partial fulfilment of the requirements for the degree of Doctor of Philosophy

May 2022

Acknowledgements

Abstract

Despite substantial improvements in the efficacy of therapeutics used to treat chronic inflammatory diseases over the last several decades, there is a significant unmet need for the treatment for chronic obstructive pulmonary disease (COPD), the third leading cause of death worldwide in 2019. The increasing knowledge of cellular and molecular mechanisms that underpin inflammation in COPD has not yet translated into the successful development of improved therapeutics for patients. There is a clear role for dysregulated neutrophil apoptosis in driving tissue damage in COPD, and small molecule therapeutics that increase the apoptotic rate of neutrophils are available for research use. Kinase-targeting therapeutics are of particular interest, due to the well-characterised role of kinases in mediating a variety of apoptotic pathways, and clinically approved therapies targeting these pathways being well-tolerated by patients. This PhD aims to assess whether inhibitors of the ErbB family of receptor tyrosine kinases have potential efficacy in the treatment of COPD, via the induction of neutrophil apoptosis. ErbB inhibitors are currently used clinically for different disease indications, and re-purposing these for the treatment of COPD or other neutrophil-driven inflammatory diseases could bring new treatment strategies to patients.

Abbreviations

ACTB – beta actin

ASPA – Animals (Scientific Procedures) Act

ATP – adenosine triphosphate

BAD - BCL2-associated agonist of cell death

BAK – BCL2 homologous antagonist killer

BAL – bronchoalveolar lavage

BAX – BCL2-associated X protein

BCL-2 – B-cell lymphoma 2

bFGF – basic fibroblast growth factor

BH3 – BCL2 homology 3

BID – BH3-interacting domain death agonist

BIM – BCL2-like protein 11

cAMP – cyclic adenosine monophosphate

Cas9 – CRISPR-associated protein 9

CCL – C-C chemokine ligand

CD3E – T cell receptor epsilon chain

CDK – cyclin dependant kinase

cDNA – complementary DNA

CHT – caudal haematopoietic tissue

COPD – chronic obstructive pulmonary disease

CRISPR – clustered regularly interspaced short palindromic repeats

CXCL – C-X-C chemokine ligand

CXCR – C-X-C chemokine receptor

DAMP – damage-associated molecular pattern

DEFA3 – defensin alpha 3

DMSO – dimethyl sulfoxide

DNA – deoxyribonucleic acid

dpf – days post-fertilisation

dpi – days post-injury

EDTA – ethylenediaminetetraacetic acid

EGF – epidermal growth factor

EGFR – epidermal growth factor receptor

ELISA – enzyme-linked immunosorbent assay

EMA – European Medicines Agency

ERK – extracellular signal-regulated kinase

FBS – fetal bovine serum

FDR – false discovery rate

FPKM – fragments per kilobase million

GAPDH – glyceraldehyde 3-phosphate dehydrogenase

GFP – green fluorescent protein

GM-CSF – granulocyte macrophage-colony stimulating factor

GRO – growth-regulated oncogene

H&E – hematoxylin and eosin

HLA – human leukocyte antigen

hpf – hours post-fertilisation

hpi – hours post-injury

HPLC-MS – high performance liquid chromatography-mass spectrometry

HPRT1 – hypoxanthine phosphoribosyltransferase 1

IC50 – half maximal inhibitory concentration

ICU – intensive care unit

IFN – interferon

Ig – immunoglobulin

IL – interleukin

IMAC – immobilised metal affinity chromatography

JAK – Janus kinase

JNK – c-Jun N-terminal kinase

KC – keratinocyte-derived chemokine

LPS – lipopolysaccharide

LTB4 – leukotriene B4

MAPK – mitogen-activated protein kinase

MCL-1 – myeloid cell leukaemia 1

MCP-1 – monocyte chemoattractant protein 1

MEK – mitogen-activated protein kinase kinase

MIP-1 – macrophage inflammatory protein 2

MMP – matrix metalloproteinase

MPO – myeloperoxidase

mpx – myeloid-specific peroxidase

mTOR – mammalian target of rapamycin

NADPH – nicotinamide adenine dinucleotide phosphate

NET – neutrophil extracellular trap

NFκB – nuclear factor kappa B

NK – natural killer

NPM1 – nucleophosmin 1

PAK – p21-activated kinase

PAMP – pathogen-associated molecular patter

PBS – phosphate-buffered saline

PCR – polymerase chain reaction

PDE – phosphodiesterase

PFA – paraformaldehyde

PI3K – phosphoinositide 3-kinase

PKA – protein kinase A

PMBC – peripheral blood mononuclear cell

PRR – pattern recognition receptor

PS – phosphatidylserine

RBC – red blood cell

RMA – robust multiarray average

RNA – ribonucleic acid

RNAseq – RNA sequencing

ROS – reactive oxygen species

RPKM – reads per kilobase million

RPS3 – ribosomal protein S3

SD – standard deviation

Ser – serine

SIRT1 – NAD-dependant protein deacetylase sirtuin 1

STAT – signal transducer and activator of transcription

TGF – transforming growth factor

TLR – toll-like receptor

TNF – tumour necrosis factor

TPM – transcripts per million

tracr – trans-activating RNA

TSA – Tyramide Signal Amplification

TUNEL – terminal deoxynucleotidyl transferase dUTP nick end labelling

tyr – tyrosinase

v/v – volume/volume percentage

VEGF – vascular endothelial growth factor

w/v – weight/volume percentage

WBC – white blood cell

WHO – World Health Organisation

Table of Contents

List of Figures

List of Tables

1 Introduction

1.1 Inflammation in health and disease

Of the leading causes of death globally, seven of the top ten are non-communicable, and the top three (ischemic heart disease, stroke, and chronic obstructive pulmonary disease) accounted for 33% of all deaths in 2019 (World Health Organisation, 2019). Numbers of deaths from the three leading infectious causes of mortality (lower respiratory infections, neonatal conditions and diarrhoeal diseases) all decreased significantly in the last 20 years, with treatments and preventative measures becoming more widely available in the lower income countries that are most in need of them. On the other hand, the number of deaths from every non-communicable disease in the top ten have increased since 2000 (World Health Organisation, 2019), with a rapidly ageing population giving rise to increasing numbers of people with untreatable chronic diseases that impact on morbidity and quality of life. Chronic inflammation plays a role in a number of diseases that together account for approximately 50% of deaths globally, including cardiovascular disease, diabetes mellitus, chronic kidney disease, non-alcoholic fatty liver disease, neurodegenerative disorders and chronic obstructive pulmonary disease (Furman *et al.*, 2019). Due to the complex nature of these diseases, and the increased likelihood of multimorbidity in patients with one chronic disease, treatment availability is patchy, often expensive, and not always effective. Investment in research to generate new, more effective treatments is clearly needed to counteract this increasing global incidence of chronic disease.

1.1.1 The inflammatory response

When the body is exposed to harmful stimuli, such as pathogens, cancerous cells, heat, chemical irritants, or physical injury, the immune system is activated to clear the stimuli, defend against further damage and promote healing (Chen *et al.*, 2017). The two arms of the immune system, the innate and adaptive, work together but differ in their cell phenotypes, timing of response, and methods utilised to clear the threat. The initial inflammatory response is mediated by innate immune cells recognising inflammatory stimuli such as pathogens or damaged cells, and releasing a range of soluble mediators to co-ordinate local changes that create a tissue environment unfavourable to pathogens (Kaur and Secord, 2019). This includes increasing blood supply to the inflamed tissue by inducing vasodilation, and increasing local capillary permeability. Circulating leukocytes follow chemotactic gradients released by cells at the site of inflammation, transmigrating through endothelial cell walls and into the

inflamed tissue (Muller, 2013). Together, these changes result in the cardinal features of inflammation: heat, redness and swelling (Pober and Sessa, 2014).

1.1.2   The innate and adaptive immune response

Of the cells in the innate immune system, neutrophils are one of the first to reach the site of inflammation (Witko-Sarsat *et al.*, 2000). Neutrophils are the most abundant leukocyte in humans, and play a key role in the clearance of pathogens, described below (1.1.3). Monocytes also migrate rapidly towards the inflammatory stimuli, and upon entry to a tissue differentiate into macrophages and dendritic cells to aid pathogen clearance and tissue healing (Chen *et al.*, 2017). Eosinophils, basophils and mast cells are more commonly recruited in allergic responses and diseases such as asthma, and in response to parasitic infections (Denburg, 1998). Natural killer cells are lymphocytes of the innate immune system that are key in killing virally infected cells or potentially cancerous cells (Vivier *et al.*, 2008). Dendritic cells have a wide and complex range of roles, and are a key link between the innate and adaptive immune responses (Liu *et al.*, 2021).

The innate immune response is not specific to an individual antigen, but rather these cells respond to pathogen-associated molecular patterns (PAMPs), which are released by, or are structural components of pathogens, such as lipopolysaccharide (LPS) which is present in all Gram-negative bacterial cell walls. Damage-associated molecular patterns (DAMPs) are components of the body's own cells, such as DNA or adenosine triphosphate (ATP) and are usually sequestered intracellularly, and thus their presence in the extracellular space indicates tissue damage (Tang *et al.*, 2012). PAMPs and DAMPs bind to pattern-recognition receptors (PRRs) on innate immune cells, a family of receptors that include toll-like receptors such as TLR4 which binds specifically to LPS (Amarante-Mendes *et al.*, 2018).

In comparison to the minutes and hours in which an innate immune response is initiated, the adaptive immune response takes days to mount in humans, as cells of the adaptive immune system respond poorly to primary inflammatory stimuli (Luster, Alon and von Andrian, 2005). The T and B lymphocyte response is highly specific to individual antigenic epitopes, which they recognise via the presentation of an antigen by immune cells such as macrophages, dendritic cells and other B cells (Pennock *et al.*, 2013). This primarily occurs in lymphoid tissues rather than at the site of inflammation, in which the T or B cells with antigen-specific receptors undergo clonal expansion, generating large numbers of cells that can bind the specific antigen with high affinity (Luster, Alon and von Andrian, 2005). These effector cells produce antibodies, release cytokines that modulate the response of other immune cells

to best resolve the specific threat, directly induce apoptosis of infected or cancerous cells, and regulate the immune response to avoid prolonged inflammation and induce resolution (Cano and Lopera, 2013). Another key aspect of the adaptive immune system is the immunological memory: if a particular antigen is detected again, the adaptive immune response is significantly quicker at recognising and eliminating it (Pennock *et al.*, 2013).

1.1.3 Neutrophils and their role in the innate immune response

Being one of the first to reach the site of inflammation, neutrophils must mount a rapid and effective response that initiates pathogen destruction and encourages the response of other immune cells. However, they must first reach the site of inflammation, and importantly they must later be removed from the inflamed tissue to prevent excessive inflammation, as summarised in Figure 1.1.
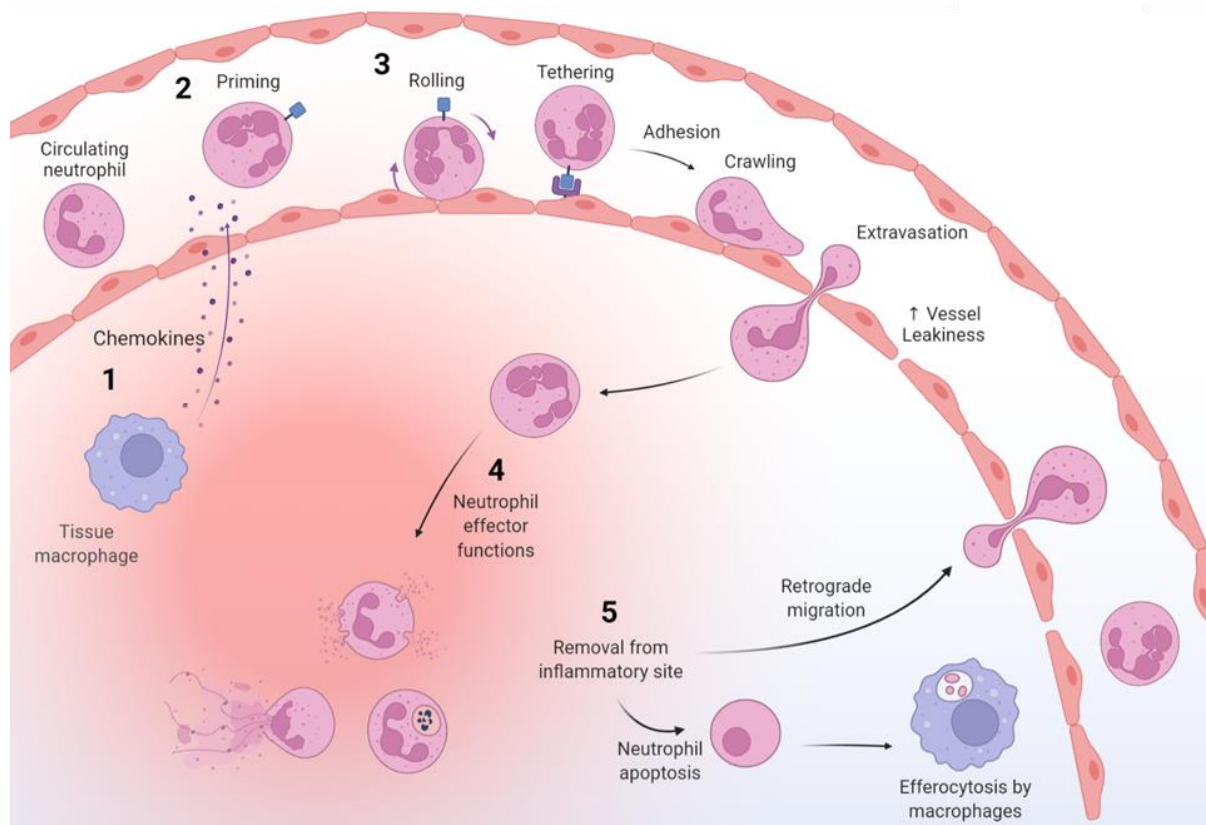
Figure 1.1. Neutrophil migration into inflamed tissues.
Tissue resident immune cells such as macrophages release chemokines upon exposure to inflammatory stimuli from tissue damage (1). These chemokines prime neutrophils, resulting in the upregulation of adhesion receptors (2), which bind to cognate receptors on the endothelium. This slows circulating neutrophils, allowing them to roll, tether, adhere and crawl along the endothelium (3), followed by extravasation of the neutrophil through the vessel and into the inflamed tissue. After carrying out effector functions such as phagocytosis, degranulation and NETosis (4), neutrophils are removed from the tissue (5) by either apoptosis and engulfment by macrophages, or retrograde migration back into circulation.

1.1.3.1 Neutrophil maturation and release into circulation

Neutrophils are formed in the bone marrow in a process known as granulopoiesis, in which neutrophils, basophils and eosinophils (granulocytes) differentiate from a common myeloid precursor cell. The differentiation into neutrophils is characterised by the sequential formation of different types of neutrophilic granules (see 1.1.3.3), and the segmentation of the nucleus into lobes (Yvan-Charvet and Ng, 2019). Mature neutrophils are stored in the bone marrow until their release into circulation; this occurs at a steady-state level in homeostatic conditions, but emergency granulopoiesis can also occur to increase the production and release of neutrophils in cases of infection (Lawrence, Corriden and Nizet, 2018). In an effort to meet the increased demand for neutrophils to combat the infection, emergency granulopoieses also results in the increased release of immature neutrophils, known as band cells, into circulation (Manz and Boettcher, 2014).

1.1.3.2 Neutrophil priming and response to chemotactic cues

In a homeostatic environment, neutrophils exist in a basal state, patrolling the environment for noxious stimuli but having a limited capacity to respond. The transition from this to a state of activation, in which effector mechanisms are carried out, is known as neutrophil priming, and can be induced by DAMPs and PAMPs such as ATP, LPS and flagellin, and inflammatory cytokines (Miralda, Uriarte and McLeish, 2017). Primed neutrophils have increased responsiveness to inflammatory stimuli, including the upregulated expression of adhesion molecules and response to chemotactic agents (Miralda, Uriarte and McLeish, 2017). These can be primary inflammatory stimuli, such as hydrogen peroxide and other DAMPs released by damaged tissue, or chemoattractive cytokines (chemokines) released by other inflammatory cells, key neutrophil ones being CXCL8 and leukotriene B4 (LTB4) (Afonso *et al.*, 2012; Capucetti, Albano and Bonecchi, 2020). Primed neutrophils in circulation respond to a chemokine gradient in a stepwise manner, by first tethering and rolling along the endothelial cell wall, followed by "firm" adhesion, and migration either directly through the endothelial cells (transcellular migration) or through gaps between the cells (paracellular cell migration), the latter facilitated by the increased capillary permeability in inflamed tissue (Morikis and Simon, 2018).

1.1.3.3 Neutrophil effector mechanisms

Neutrophils have three key effector functions in their repertoire to combat pathogens: phagocytosis, degranulation, and the formation of neutrophil extracellular traps (NETosis). To initiate a response as

quickly as possible, mature neutrophils contain high concentrations of antimicrobial and pro-inflammatory peptides and enzymes, which in a non-activated state are sequestered in cytoplasmic vesicles, called granules, to prevent cellular damage (Sheshachalam *et al.*, 2014). Neutrophilic granules are categorised into primary, secondary and tertiary based on their contents, summarised in Table 1.1, with their names (primary to tertiary) reflecting their successive formation during neutrophil maturation.

Phagocytosis occurs when neutrophils detect antibody-coated or complement-coated (opsonised) pathogens and engulf them into a membrane-derived vacuole, which then fuses with granules and lysosomes to generate the phagosome (Nordenfelt and Tapper, 2011). The respiratory, or oxidative burst is considered a key mechanisms by which internalised pathogens are killed, in which the NADPH oxidative complex on the membrane of the phagosome rapidly generates reactive oxygen species (Panday *et al.*, 2015). Some pathogens however are able to escape this process, such as *Streptococcus pyogenes* which inhibits fusion of intracellular granules with the phagosome, and *Staphylococcus aureus* which secretes several proteins to prevent opsonisation and thus detection by neutrophils (Staali *et al.*, 2006; Ko *et al.*, 2013).

In addition to the intracellular fusion of granules with phagosomes containing pathogens, granules can also be expelled from the neutrophil in a process known as degranulation to combat external pathogens (Witko-Sarsat *et al.*, 2000). The contents of granules are effective at killing pathogens: enzymes such as lysozyme cleave bacterial cell walls, lactoferrin is directly microbicidal, serine proteases can attenuate bacterial virulence factors, and myeloperoxidase catalyses the formation of hypochlorous acid and other reactive oxygen species that are strongly oxidative, interacting with bacterial proteins to induce aggregation, dysfunction and subsequent bacterial cell death (Table 1.1) (López-Boado *et al.*, 2004; Valenti and Antonini, 2005; da Cruz Nizer, Inkovskiy and Overhage, 2020).

The third main neutrophil effector mechanism is the formation of neutrophil extracellular traps (NETs), which are primarily implicated in clearing infections, but can also induce tissue damage in sterile inflammation (Kaplan and Radic, 2012). NETosis usually occurs later in the immune response and is a sign of escalation of the response to pathogens, for example larger pathogens such as fungi that are not killed by the initial immune response (Branzk *et al.*, 2014). During NETosis, the neutrophil nuclear chromatin decondenses, breaks from the nucleoplasm into the cytoplasm, perforates the cell membrane and is released into the extracellular space as a web of chromatin decorated with histones and antimicrobial agents such as myeloperoxidase and neutrophil elastase (Papayannopoulos *et al.*, 2010; Yipp and Kubes, 2013). Numerous NETs may aggregate and serve as a physical barrier to stop pathogen spread, trap bacteria in their sticky negatively-charged DNA fibres, and provide a high local

Table 1.1. Role of neutrophilic granules in pathogen clearance and tissue damage.

Granule	Role in pathogen clearance	Role in inflammation and tissue damage
Primary/azurophilic granules: • **Neutrophil elastase** • **Myeloperoxidase** • **Cathespin G** • **Azurocidin** • **Proteinase 3** • **Defensins**	• Disrupt microbial membrane integrity, bacterial DNA and proteins • Activation of host anti-microbial peptides • Inactivate bacterial virulence factors • Myeloperoxidase generates hypochlorous acids which disrupt bacterial DNA and proteins	• Degradation of elastin, fibronectin and collagen in lung tissue • Activation of matrix metalloproteinases • Hypochlorous acid stimulates collagen synthesis which is pro-fibrogenic
Secondary/specific granules: • **Collagenase** • **Gelatinase** • **NADPH-oxidase** • **Lysozyme** • **Lactoferrin**	• Production of reactive oxygen species (ROS) which damage bacterial DNA, lipids and proteins • Hydrolysis of bacterial cell wall • Sequestration of free iron to inhibit bacterial growth	• Oxidisation of host proteins and lipids, damage to DNA which can induce apoptosis • ROS act as a second messenger of inflammatory signalling via NFkB activation
Tertiary/gelatinase granules: • **Gelatinase** • **Cathespin** • **Collaginase** • **Matrix metalloproteinases**	• Allow neutrophil migration through endothelium and extracellular matrix to site of infection	• Excess degradation of basement membranes damages lung tissue

(Kolaczkowska and Kubes, 2013; Stapels, Geisbrecht and Rooijakkers, 2015; Cowland and Borregaard, 2016; Nita and Grzybowski, 2016; Rawat, Syeda and Shrivastava, 2021)

concentration of antimicrobial agents to kill bacteria (Daniel *et al.*, 2019). NETosis can be a form of cell death, but there is also evidence that neutrophils can retain some function: NETosing cells do not stain for vital dyes, are still able to phagocytose pathogens, and can crawl along endothelium toward a chemotactic gradient (Yipp *et al.*, 2012). Both degranulation and NETosis can be induced without pathogenic insult: the formation of NETs has been demonstrated in inflammation induced by a sterile foreign body, and synthetic inhibition of degranulation results in reduced liver injury in a murine model of chemically induced liver injury (Jhunjhunwala *et al.*, 2015; Alvarenga *et al.*, 2018).

1.1.3.4 Neutrophil phenotypes and class switching

Although neutrophils are traditionally viewed as pro-inflammatory cells whose primary function is to kill bacteria, they are a heterogenous population and several subsets with other roles in homeostasis and disease have been defined. Pro-angiogenic neutrophils are characterised by high expression of vascular endothelial growth factor (VEGF), and contribute to healthy vasculature formation but are also implicated in tumour angiogenesis (Bekes *et al.*, 2011; Christoffersson *et al.*, 2012). Myeloid-derived suppressor cells are derived from both granulocytic and monocytic precursors, and use mediators such as arginase and prostaglandin E2 to supress the activity of T and B lymphocytes and NK cells. In cancer, they are considered to exacerbate the disease by supressing the anti-tumour immune response, however in chronic inflammatory and autoimmune conditions they have positive effects by supressing the aberrant inflammation (Veglia, Sanseviero and Gabrilovich, 2021). Neutrophils in infected tissues also undergo class switching to produce different phenotypes. In mice infected with *Staphylococcus aureus*, distinct neutrophil populations were identified: those that classically activated macrophages and expressed cytokines such as IL-12, resulting in a pro-inflammatory phenotype, and those that alternatively activated macrophages and expressed IL-10, resulting in a pro-resolution phenotype (Tsuda *et al.*, 2004). The signals biasing neutrophils towards a specific phenotype are thought to derive from the local tissue environment, and can also influence the lifespan of the neutrophil (Ballesteros *et al.*, 2020).

1.1.3.5 Neutrophils recruit other immune cells

In addition to their own effector mechanisms, neutrophils produce chemokines that initiate the recruitment of additional immune cells. These include monocyte chemoattractant protein-1 (MCP-1) which induces monocyte/macrophage migration, CXCL9 which is a T cell and NK cell chemoattractant, and CCL-5, a dendritic cell chemokine (Green *et al.*, 2006; Amatschek *et al.*, 2011; Schuster, Hurrell and Tacchini-Cottier, 2013). ATP released by damaged cells induces a calcium flux within neutrophils, which in turn induces the neutrophil to continually synthesise the chemokine LTB4, a secondary chemoattract that amplifies the migratory response of primary chemoattractants (Afonso *et al.*, 2012; Poplimont *et al.*, 2020). The recruited immune cells further sustain the pro-inflammatory environment via their own specific effector mechanisms; macrophages for example produce CXCL8, which is a potent neutrophil chemoattractant that induces neutrophil elastase secretion and upregulation of mucin production (Kuwahara *et al.*, 2007).

1.1.4 Inflammation resolution

Historically, it was thought that the acute inflammatory response resolves spontaneously, due to the destruction of the inflammatory stimuli by immune cells (and thus loss of migratory cues) and dilution of chemotactic gradients over time. It is now known however that the resolution of the acute inflammatory response is a tightly controlled and active process (Headland and Norling, 2015). For inflammation to resolve two key events must occur: the numbers of inflammatory cells at the site of inflammation must decline, and pro-inflammatory mediators such as lipids and cytokines must be neutralised (Schett and Neurath, 2018). Neutrophils, macrophages and regulatory T cells are key regulators of these processes. In neutrophils, the class switch from the production of inflammatory and chemoattractive mediators such as LTB4, to the pro-resolving lipid mediators including lipoxins and resolvins, prevents further neutrophil recruitment to the inflammatory site (Sogawa *et al.*, 2011). In humans and other mammals, removal of neutrophils from inflamed tissue is thought to be primarily mediated by apoptosis, an immunologically silent mechanism of cell death in which the neutrophil essentially "switches off" and no longer responds to external cues or produces inflammatory mediators (Haslett *et al.*, 1991; Fox *et al.*, 2010). There is also evidence of neutrophils undergoing reverse migration away from the site of inflammation, and back to the bone marrow where they undergo apoptosis, which is mediated by the CXCR4/CXCL12 signalling axis (Buckley *et al.*, 2006; De Filippo and Rankin, 2018). Although this has been demonstrated with human neutrophils *in vivo*, much of the research on neutrophil reverse migration is carried out in the zebrafish larvae, mouse or *in vitro* models, and so the impact of this mechanism on the inflammatory response in humans is still unclear (Mathias *et al.*, 2006; Nourshargh, Renshaw and Imhof, 2016; J. Wang *et al.*, 2017).

Typically, apoptotic neutrophils are rapidly cleared by macrophages or other phagocytes *in vivo* by efferocytosis, a multi-step process in which the macrophage detects, engulfs and digests apoptotic cells or cell debris (Silva, 2011). Apoptotic cells release "find me" signals, such as nucleotides and the membrane-associated protein CX3CL1, that are chemotactic for macrophages and other phagocytes (Park and Kim, 2017). The macrophage then confirms the cell is apoptotic by the presence of "eat me" cues on the cell surface, the most prominent being the exposure of phosphatidylserine (PS) on the outer leaflet of the cell membrane (Naeini *et al.*, 2020). The binding of PS by macrophages receptors induces intracellular signalling cascades that result in the engulfment of the apoptotic cell and formation of a phagosome, in which the cell is digested by molecules such as hydrolytic enzymes and cationic peptides (Boada-Romero *et al.*, 2020).

The process of efferocytosis can result in the macrophage switching to an anti-inflammatory phenotype, resulting in the release of interleukin 10 (IL-10) and transforming growth factor beta

(TGFβ), both of which are pro-resolution cytokines (El Kebir and Filep, 2013; Sun *et al.*, 2015). The production of TGFβ and other growth factors by macrophages and other cell types promotes cellular proliferation and the secretion of collagen by fibroblasts to facilitate wound healing (Wynn and Vannella, 2016). Efferocytosis also induces macrophage desensitisation to bacterial LPS, allowing the macrophage to migrate away from the inflammatory site and into lymphoid organs (Schif-Zuck *et al.*, 2011).

Of the adaptive immune response, regulatory T cells play a direct role in mediating inflammation resolution by secreting IL-13, which promotes IL-10 production by macrophages, enhancing the ability of macrophages to engulf apoptotic cells (Proto *et al.*, 2018). They also supress the activity of neutrophils by decreasing the expression of chemoattractants CXCL1 and CXCL2 and inhibiting production of the inflammatory cytokine IL-6 (Richards *et al.*, 2010; Lewkowicz *et al.*, 2013). Clonally expanded effector T cells die primarily by apoptosis, as do short-lived antibody-producing plasma B cells, although a small number of memory T and B cells remain for years and can rapidly mount an immune response upon repeated exposure to the antigen (Krammer, Arnold and Lavrik, 2007; Auner *et al.*, 2010).

1.1.5 Chronic inflammation

While the acute inflammatory response is a vital mechanism for the defence against pathogens and removal of potentially cancerous cells, the failure of inflammation resolution results in chronic inflammation: a prolonged, low grade and superfluous inflammatory response that damages tissue and is detrimental to the host (Furman *et al.*, 2019). Acute inflammation may last days or weeks before being resolved, whereas chronic inflammation spans months and often years. Why inflammation does not resolve is often specific to individual diseases, and in many cases the mechanisms are yet to be fully elucidated. Certain pathogens such as *Mycobacterium tuberculosis* and *Trypanosoma cruzi* are able to evade immune destruction and remain in the host tissue, eliciting a prolonged but ineffective inflammatory response (Duthie *et al.*, 2007; Muefong and Sutherland, 2020). Other diseases can result in the accumulation of pro-inflammatory residues in the body, such as uric acid crystals in gout, or excessive reactive oxygen species production in metabolic diseases of mitochondrial dysfunction (Ragab, Elshahaly and Bardin, 2017; Geto *et al.*, 2020). Genetic risk factors can also result in an exaggerated immune response that does not resolve, such as IL-10 and IL-10 receptor polymorphisms in severe infantile colitis, and allelic variants of HLA-DRB1 that are severe disease risk genes for rheumatoid arthritis (Weyand and Goronzy, 2000; Moran *et al.*, 2013). Autoimmune disorders such as rheumatoid arthritis and systemic lupus erythematosus are defined by an aberrant and prolonged

immune response against host tissue, or in the case of inflammatory bowel disease, against the gut microbiota (Wong and Lord, 2004; Muñoz *et al.*, 2010; Lee and Chang, 2021). Persistent exposure to an inhaled inflammatory agent that cannot be cleared by the immune system, such as cigarette smoke or silica dust, similarly results in chronic inflammatory diseases of the lungs (Pahwa *et al.*, 2021). Although all cigarette smokers develop airway inflammation, only approximately 15-20% develop chronic obstructive pulmonary disease (COPD), suggesting additional mechanisms that lead to the more severe inflammatory phenotype observed in patients with COPD; however these mechanisms are currently unknown (Agustí *et al.*, 2003; Terzikhan *et al.*, 2016).

1.2   Chronic Obstructive Pulmonary Disease

COPD is an umbrella term for a group of chronic inflammatory diseases of the lungs, primarily chronic bronchitis and emphysema, that is estimated to have caused 3.23 million deaths globally in 2019, approximately 6% of all deaths that year (World Health Organisation, 2019). The disease is associated with long-term exposure to, and inhalation of, harmful substances such as cigarette smoke, pollution, dusts or fumes. People with COPD present with a broad spectrum of clinical phenotypes that can include emphysema, chronic bronchitis, exacerbations (acute worsening of symptoms) and a faster decline in lung function than would be expected in a patient of that age (Kim and Criner, 2013). This manifests as breathlessness, fatigue, chronic cough and frequent infections.

Treatments are available that give symptomatic relief, such as bronchodilators and corticosteroids designed to reduce airway inflammation and frequency of exacerbations (Vogelmeier *et al.*, 2017). Smoking cessation (if relevant) is the only method shown to reduce the long-term decline in lung function, with no other therapy being conclusively shown to modify this outcome (Vogelmeier *et al.*, 2017). Prolonged abstinence rates are not high however, with one trial of 296 smokers with COPD showing 10% people remained abstinent after one year (van Eerd *et al.*, 2017). The predictors of successful abstinence are often not readily in the control of the patient, and include education level, perception of health, having a partner who also smoked, and availability of high-intensity behavioural support and medication (van Eerd *et al.*, 2016, 2017). Other sources such as pollution or occupational exposure to fumes can also be very difficult to avoid without major lifestyle changes, and these are the most common cause of COPD in lower and middle-income countries (World Health Organisation, 2019). The latest (and only) treatment to be approved for COPD that was not an iteration of existing bronchodilators/corticosteroids was the phosphodiesterase type-4 inhibitor Roflumilast in 2011, which was shown to improve lung function in patients, but did not improve exacerbation frequency (Martinez *et al.*, 2016). There is a clear unmet treatment need for patients with COPD, and targeting

specific components of the chronic inflammatory response may unlock the development of new therapies with increased efficacy.

1.2.1 Pathophysiology of COPD

The causative agents of COPD are not pathogenic (although infections can induce exacerbations) however they illicit an inflammatory response, and long-term exposure results in a chronic inflammatory infiltrate of immune cells in the lungs that persist despite being unable to clear the stimulus (Gahring *et al.*, 2017). These activated immune cells release a wide variety of pro-inflammatory agents that have evolved to kill pathogens, but are also histotoxic and result in cellular injury and tissue damage (Tuder and Petrache, 2012). All areas of the lower respiratory tract – the bronchi, bronchioles, and alveoli - can be inflamed, although this varies between patients (Figure 1.2). Chronic bronchitis is a common but variable phenotype in COPD in which the epithelium of the central airways is inflamed, resulting in airway remodelling: thickening of the basement membrane, smooth muscle hypertrophy, goblet cell hyperplasia, increased mucus production, and reduced mucociliary clearance (Kim and Criner, 2013). These changes result in the narrowing of the airway lumen and obstruction of airflow. Within the smaller airways (bronchioles), this can lead to complete closure of airways, resulting in trapped air (Barnes, 2019). This is premature closure is also facilitated by damage to alveolar attachments, elastin fibres radiating from the outer airway walls to nearby alveoli to hold the small airways open (Saetta *et al.*, 1985). In COPD these fibres are damaged by proteases and reactive oxygen species released from the infiltrating inflammatory cells in the lung, which can result in airway collapse upon expiration (Barnes *et al.*, 2015; Pandey, De and Mishra, 2017).

The destruction of alveoli in emphysema is considered to be partly due to oxidative and protease-mediated damage leading to death of the epithelial cells, with neutrophil elastase considered key (Craig, Scott and Mitzner, 2017; Pandey, De and Mishra, 2017). Emphysema is usually observed in later stages of the disease, whereas small airway disease is observed in the earlier stages (Galbán *et al.*, 2012). The resulting irreversible enlargement of airspaces reduces surface area for gas exchange, leading to low oxygen saturation in the blood (hypoxemia), which in the short term manifests as breathlessness and fatigue, but long term increases the likelihood of extra-pulmonary morbidities including hypertension, skeletal muscle dysfunction, polycythaemia, systemic inflammation and neurocognitive dysfunction (Kent, Mitchell and McNicholas, 2011). Although emphysema is strongly associated with cigarette smoking, interestingly it is not widespread in COPD caused by biomass smoke exposure, which is more common in developing countries (Zhao *et al.*, 2018).
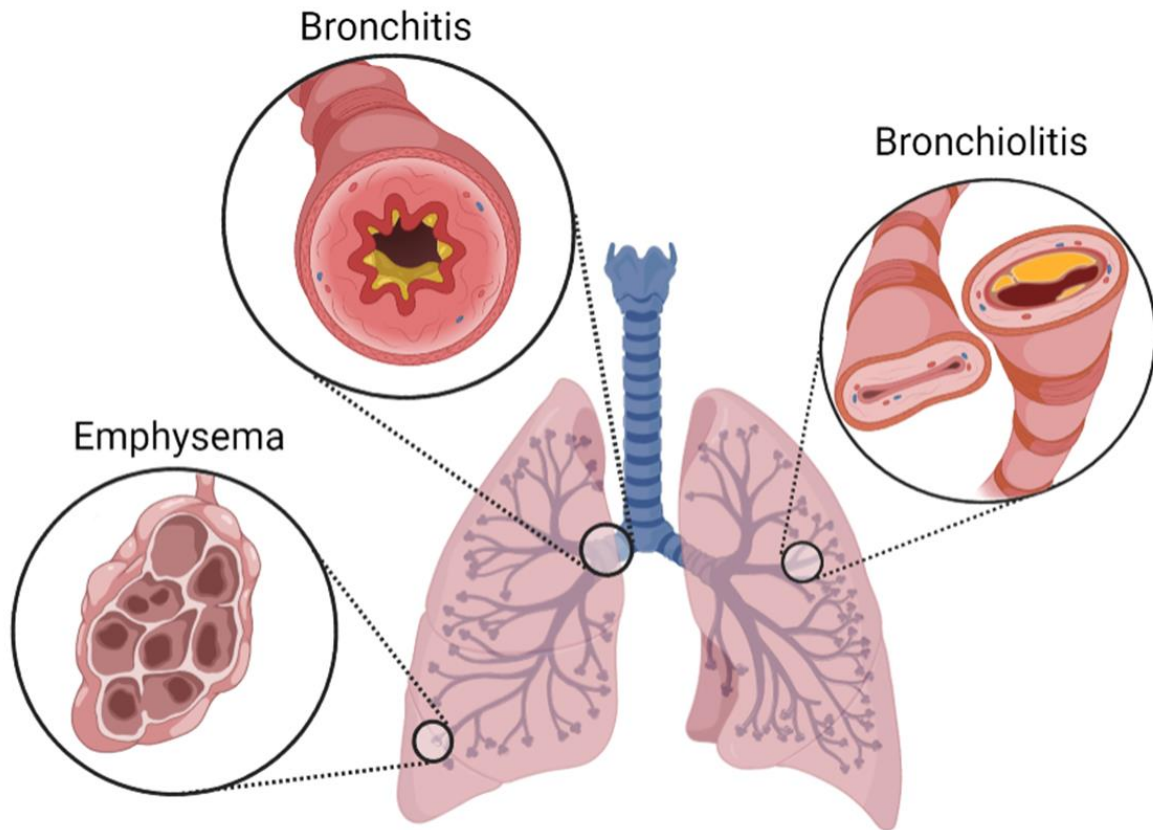
Figure 1.2. Pathophysiology of chronic obstructive pulmonary disease.
COPD covers a number of diseases, the frequency and severity of which can vary widely between different patients. Chronic bronchitis, in which the bronchi are inflamed, results in thickened walls due to smooth muscle hypertrophy and excessive mucus production. Similar inflammatory changes are observed in the smaller airways, known as bronchiolitis, and due to their smaller size these airways can become completely blocked with mucus or collapse, preventing airflow. In emphysema, alveolar membranes are destroyed, reducing the surface area for gas exchange with the blood. Created in BioRender.

1.2.2   The inflammatory response in COPD

A variety of inflammatory cells in the lungs regulates and perpetuates the inflammatory response in chronic obstructive pulmonary disease, however neutrophils, macrophages and T cells are considered the primary effector cells, with airway epithelial cells also playing a role (King, 2015). Bronchial epithelial cells are the first to encounter inhaled noxious substances, and when exposed to cigarette smoke and other toxins they secrete a variety of inflammatory mediators including cytokines, chemokines and reactive oxygen species, which can recruit and activate inflammatory cells (Gao *et al.*, 2015). Inhaled toxins can also directly damage epithelial cells, resulting in the release of their contents, which act as DAMPS and induce further inflammation (Gindele *et al.*, 2020).

1.2.2.1 Neutrophils and macrophages

Neutrophils are considered a key driver of the damage to lung tissue observed in this disease, with airway neutrophilia correlating with disease severity, mucus production and decline in lung function (Thompson *et al.*, 1989; Hogg *et al.*, 2004; Donaldson *et al.*, 2005). The continual activation of neutrophils and their release of histotoxic mediators contributes to the chronic inflammatory environment in the lungs, resulting in tissue damage and declining lung function (Figure 1.3). Myeloperoxidase activity is a key marker of activated neutrophil function and is similarly associated with disease severity, mediating local tissue damage by oxidising cellular proteins and lipids, and resulting in DNA damage-induced apoptosis (Brown *et al.*, 2004; Zhu *et al.*, 2014; Nita and Grzybowski, 2016). Reactive oxygen species can induce gene expression via the activation of redox-sensitive transcription factors, such as those controlling the nuclear factor kappa B (NFκB) pathway, a central mediator of inflammatory signal transduction (Asehnoune *et al.*, 2004). This increases production of inflammatory mediators such as tumour necrosis factor alpha (TNFα), IL-1β and matrix metalloproteinases (Le Rossignol, Ketheesan and Haleagrahara, 2018). The release of neutrophil proteases, particularly neutrophil elastase and matrix metalloproteinases, induces the destruction of alveolar cells and contributes to airway remodelling by cleaving components of the extracellular matrix in alveoli and small airways (Chen *et al.*, 2008; Yao *et al.*, 2013; Guo *et al.*, 2016). NETs correlate with COPD severity, and are increased during exacerbations (Dicker *et al.*, 2018). NETs also activate platelets, leading to the release of TGFβ and subsequent tissue remodelling (Narasaraju *et al.*, 2011; Bosmann and Ward, 2014).
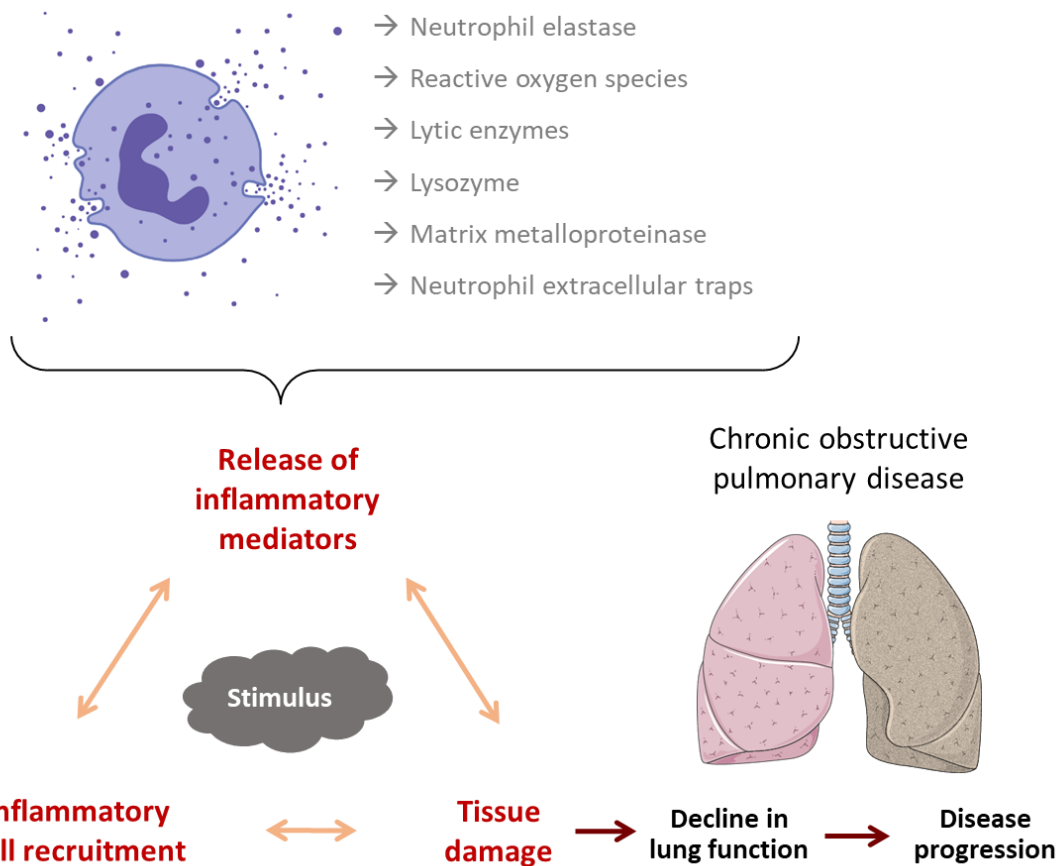
Figure 1.3. Role of neutrophils in the progression of COPD.
Neutrophils release a range of inflammatory mediators when activated, which while beneficial for removing pathogens in acute inflammation, in chronic inflammatory environments contribute to tissue damage and induce further inflammation. In diseases such as COPD, this failure of inflammation resolution results in declining lung function and disease progression. Created using BioRender and Servier Medical Art.

Inflammatory macrophages also release cytokines, reactive oxygen species and proteases in the lungs of patients with COPD, with the release of matrix metalloproteinases in particular shown to contribute to the breakdown of elastin and development of emphysema, as well as airway remodelling (Russell *et al.*, 2002; Churg, Zhou and Wright, 2012). Cytokines secreted by alveolar macrophages in COPD include IL-1β, TNFα, MCP-1 and CXCL8, which collectively are chemotactic, cytotoxic, and modulate the inflammatory response of other immune cells such as neutrophils and lymphocytes (Mukhopadhyay, Hoidal and Mukherjee, 2006; Wang *et al.*, 2018). Interestingly, studies have shown that although alveolar macrophages from people with COPD are pro-inflammatory, they have reduced capacity to phagocytose bacteria and engulf dead cells (Hodge *et al.*, 2007; Martí-Lliteras *et al.*, 2009; Todt *et al.*, 2013). This may contribute to the increased susceptibility to infection observed in patients with COPD, as well as further perpetuating the inflammatory response due to increased numbers of uncleared dead cells. The latter is particularly problematic due to the chronic influx of short-lived

neutrophils to the lungs, which will undergo secondary necrosis if not cleared efficiently, spilling their highly inflammatory contents onto the tissue (Vlahos and Bozinovski, 2014).

In addition to the influx of newly-recruited neutrophils and macrophages to the lungs, there are also tissue-resident macrophages, and a small population of patrolling neutrophils residing in the lungs that can initiate the early acute inflammatory response. A large proportion of circulating neutrophils are also localised to the lung microvasculature in homeostatic conditions, which upon respiratory infection can rapidly migrate into the respiratory airspace (Lin and Fessler, 2021). These lung-resident neutrophils also migrate to lymphoid tissues and present opsonised cargo in the absence of infection, suggesting a role for these cells in homeostatic immune surveillance (Lok *et al.*, 2019). In COPD this may be a pathway for the activation of the adaptive immune response, although this has not been well studied, and in some cases neutrophil interactions with lymphoid cells are shown to be immunosuppressive (Lok and Clatworthy, 2021).

1.2.2.2   Lymphocytes

The role of lymphocytes in the pathology of COPD is less defined. Levels of CD4+ helper T cells, CD8+ cytotoxic T cells, and B cells are elevated in the lungs of patients, with cytotoxic T cells being the most abundant lymphocyte (Turato *et al.*, 2002; Hogg *et al.*, 2004). Secretion of the pro-inflammatory cytokine interferon gamma (IFNγ) by cytotoxic T cells correlates with COPD disease severity (Freeman, Curtis and Chensue, 2007). Cytotoxic T cells are able to directly kill cells of the lung parenchyma, but this is an antigen-specific process and it is unclear whether this is triggered by a secondary infection, which is common in people with COPD, or another mechanism such as oxidant-induced damage leading to antigenic modification that renders these cells a target for destruction (Freeman *et al.*, 2010).

The number of lymphoid follicles (aggregates of lymphocytes in which B cells mature) in bronchial tissue is increased in patients with severe COPD, although the antigenic specificity of the maturing B cells is unknown (Hogg *et al.*, 2004; Brusselle *et al.*, 2009; Higham *et al.*, 2019). Circulating IgG autoantibodies specific to epithelial cell markers were detected in lung explants from COPD patients, suggesting an autoimmune aspect in the later stages of the disease (Feghali-Bostwick *et al.*, 2008; Karayama *et al.*, 2010; Núñez *et al.*, 2011). Decreased numbers of regulatory T cells, which protect against autoimmune responses, are also found in COPD patients, which may contribute to this autoantibody production (Barceló *et al.*, 2008). Evidence suggests helper T cells also orchestrate the immune response via the release of cytokines, potentially priming cytotoxic T cells and inducing

antibody production and differentiation of antibody-producing B cells, although this is not well studied in COPD (Gadgil and Duncan, 2008).

1.2.2.3 Systemic inflammation in COPD

Inflammation in COPD extends beyond the lungs: chronic systemic inflammation is observed in patients, shown by increased peripheral blood levels of pro-inflammatory cytokines and reactive oxygen species (Kaźmierczak *et al.*, 2015). The leakage of cytokines from the lungs into circulation can prime patrolling neutrophils, monocytes other leukocytes, and induce the expression of adhesion molecules to increase their extravasation into tissue (Selvarajah *et al.*, 2016; Lokwani *et al.*, 2019). Some studies demonstrate correlations between circulating leukocyte numbers and lung function or disease severity, but this is not always replicable and is considered a weak predictive factor (Weiss *et al.*, 1995; Kim, 2017; Koo *et al.*, 2017). Interestingly, shortened telomeres were found in circulating leukocytes from patients with COPD, which is induced by oxidative stress and inflammatory damage and is a marker of premature ageing (Savale *et al.*, 2009). Systemic inflammation is considered the cause of muscle wasting observed in severe disease, with possible implications for elevated TNFα levels in circulation (Oudijk, Lammers and Koenderman, 2003; Sinden and Stockley, 2010). In combination with the systemic inflammatory response, chronic hypoxemia is considered to play a key role in the development of comorbidities such as cardiovascular disease, osteoporosis, anaemia, and neurocognitive disorders (Barnes and Celli, 2009; Kent, Mitchell and McNicholas, 2011; Furman *et al.*, 2019).

1.2.2.4 Hypoxia alters the immune response in COPD

In addition to the chronic hypoxemia caused by reduced lung function in the later stages of COPD, local areas of tissue hypoxia are observed in the lungs of COPD patients, which can have a profound impact on the immune response. Markers of hypoxia in the airway epithelial cells of COPD patients correlated with airway remodelling, and chronic and progressive hypoxia is a hallmark of disease severity (Polosukhin *et al.*, 2007; Hoenderdos and Condliffe, 2013). The upregulation of the hypoxia inducible factor (HIF) pathway in neutrophils results in extended lifespan, NFκB pathway activation, and enhanced degranulation (Ryan, Whyte and Walmsley, 2019; Lodge *et al.*, 2020). Hypoxia-mediated upregulation of integrins results in increased adherence of neutrophils and other immune cells to endothelia, and neutrophils in hypoxic conditions generally show increased rates of phagocytosis, although this appears pathogen-dependant and some studies have shown a suppression

or no change in bacterial killing in hypoxia (Kong *et al.*, 2004; Lodge *et al.*, 2020). Although oxygen is a requirement for the generation of reactive oxygen species, evidence regarding ROS generation in hypoxia is conflicting (Lodge *et al.*, 2020). *In vitro* studies have shown decreased respiratory burst and killing of *S. aureus* by human neutrophils in hypoxic conditions (McGovern *et al.*, 2011). On the other hand, neutrophils taken from patients with sleep apnoea, which correlates with intermittent hypoxia, show increased superoxide production (Schulz *et al.*, 2000). Hypoxic conditions may also inhibit tissue repair, by reducing the production of elastin by lung fibroblasts (Berk *et al.*, 2005).

1.3   Neutrophil cell death as a regulator of inflammation

Being terminally differentiated and with highly destructive potential, neutrophils are one of the shortest lived cells in the body, undergoing spontaneous (or constitutive) apoptosis within hours or days *in vivo*, even in the absence of extracellular stimuli (Xu, Loison and Luo, 2010; Yuyun *et al.*, 2021). This is regulated by the mitochondrial/intrinsic apoptotic pathway, in which the intracellular ratio of pro and anti-apoptotic members of the BCL-2 family of proteins control the activation of caspases, which initiate the sequential degradation of cellular components in apoptosis (Geering and Simon, 2011). Mature neutrophils have relatively low numbers of mitochondria which are not considered to carry out much respiration or ATP synthesis; their primary role is thought to be in regulating apoptosis (Geering and Simon, 2011). A number of BCL-2 family proteins are expressed in neutrophils, including the pro-apoptotic BAX, BAD, BH3, BID and BIM, while the key anti-apoptotic family member is MCL-1 (Milot and Filep, 2011). MCL-1 is degraded as the neutrophil ages, allowing BIM/BAK to translocate to the mitochondrial membrane, which permeabilises and releases additional proapoptotic factors such as cytochrome c, activating the caspase cascade and inducing apoptosis (Derouet *et al.*, 2004; Luo and Loison, 2008; Milot and Filep, 2011). At sites of inflammation neutrophil apoptosis can also be induced by external cues in the death receptor/extrinsic pathway, in which macrophages and other inflammatory cells release soluble Fas-ligand and TNFα, which bind to neutrophil death receptors (Fas and TNF receptor 1) to induce apoptosis by activating caspases (Croker *et al.*, 2011).

1.3.1   Modalities of neutrophil cell death

A number of different modalities of neutrophil cell death exist in addition to apoptosis: autophagy, pyroptosis, necroptosis, NETosis, and necrosis, and each can skew the inflammatory response to further inflammation or resolution (Pérez-Figueroa *et al.*, 2021) (Figure 1.4). Neutrophil apoptosis is

an immunologically silent process as the cell stops functioning and remains intact, however subsequent efferocytosis generates a pro-resolution phenotype in macrophages, as described in 1.1.4. Neutrophil necrosis often occurs in response to a severely adverse environment, such as oxygen or nutrient deprivation, high temperature, toxins or radiation, and results in the rupture of the cell membrane and uncontrolled release of neutrophil contents into the extracellular space (Krysko *et al.*, 2008). Necrosis can also occur if an apoptotic neutrophil is not efficiently cleared by macrophages or other efferocytic cells, termed secondary necrosis (Krysko *et al.*, 2008; Whelan *et al.*, 2012). Like NETosis, necrosis is highly inflammatory due to the release of the neutrophilic contents into the surrounding tissue, including histotoxic reactive oxygen species, and DAMPs which initiate inflammation (Li *et al.*, 2001).

Necroptosis is considered to be a controlled form of necrosis, whereby cell membrane rupture is triggered by a series of signalling events that results in the oligomerisation and translocation of a protein complex (MLKL) to the cell membrane (Samson *et al.*, 2020). Pyroptosis is a cell death pathway triggered by inflammation, in which the inflammasome (an intracellular protein complex required for the maturation of IL-1β amongst other functions) activates caspase-1, inducing cell swelling and lysis (Yu *et al.*, 2021). Both necroptosis and pyroptosis result in cell lysis and the release of neutrophil contents, and are thus pro-inflammatory: however they also prevent the neutrophil carrying out further effector functions, and so in the long term may be less inflammatory than a neutrophil that continued to carry out effector functions (Lawrence, Corriden and Nizet, 2020).

Autophagy is a process observed in all eukaryotes in which the cell digests its own contents when deprived of nutrients or energy (Jiang *et al.*, 2019). This occurs at a basal level in all cells and is essential for the maintenance of intracellular homeostasis, removal of dysfunctional or damaged organelles and recycling of cellular contents, but can result in cell death if a sufficient level is reached (Pérez-Figueroa *et al.*, 2021). Similar to apoptosis, autophagy downregulates neutrophil function such as ROS and cytokine production and so can be considered anti-inflammatory, particularly if the autophagic cell is engulfed by macrophages; but autophagy can also induce NETosis and undergo secondary necrosis, and so its overall impact on inflammation is highly contextual (Skendros, Mitroulis and Ritis, 2018; Liang *et al.*, 2020; Yu and Sun, 2020). Therapeutics targeting specific cell death mechanisms are not currently present in the clinic, but present a novel approach in an area with significant unmet patient need.
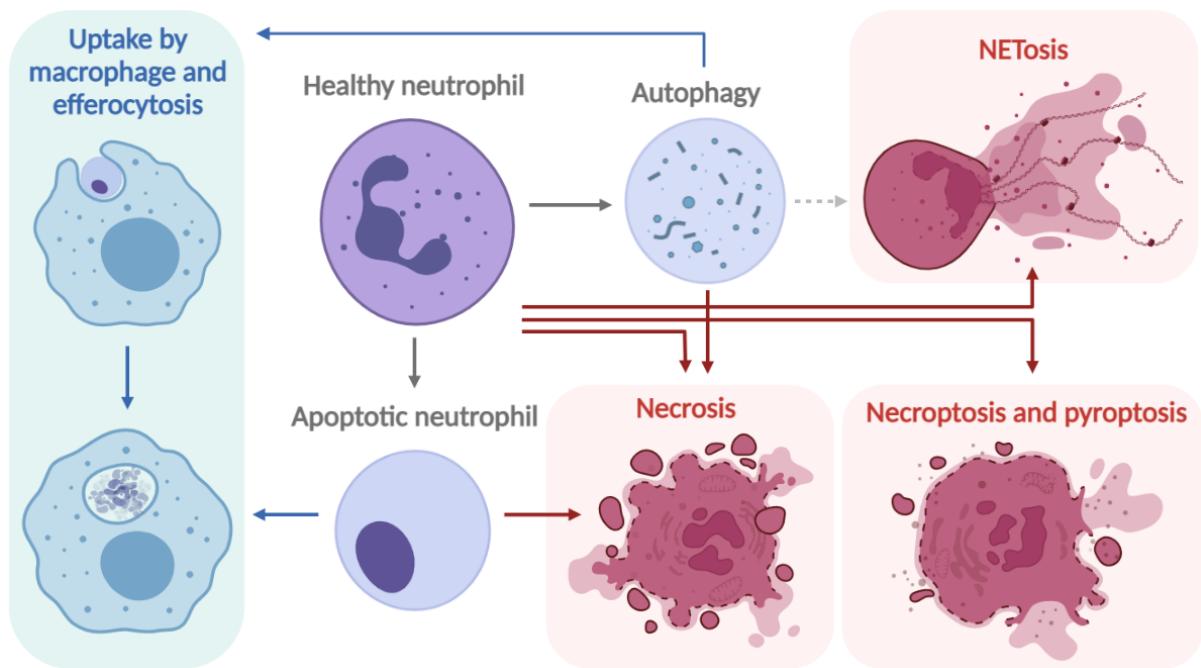
Figure 1.4. Impact of neutrophil cell death modalities on the inflammatory phenotype.
Neutrophil apoptosis and autophagy are immunologically silent; however their fate can alter the inflammatory context. Engulfment by macrophages and subsequent efferocytosis is anti-inflammatory. Alternatively, autophagy can initiate NETosis, and apoptotic and autophagic neutrophils that are not cleared efficiently can undergo secondary necrosis, leading to a pro-inflammatory phenotype due to the leakage of the cytoplasmic contents onto the tissue. NETosis, necroptosis and pyroptosis similarly induce inflammation for this reason. Created in BioRender.

Neutrophils are extremely sensitive to factors that prolong survival such as granulocyte macrophage-colony stimulating factor (GM-CSF), a cytokine secreted by macrophages and epithelial cells in inflammatory settings, and PAMPs and DAMPs such as LPS and extracellular DNA, which supress constitutive neutrophil apoptosis and extend functional capacity (Pillay *et al.*, 2010). Local tissue hypoxia is also considered a key mechanism by which neutrophil lifespan is extended in inflammatory sites, as the activation of HIF pathways supresses neutrophil apoptosis via NFκB signalling (Walmsley *et al.*, 2005). Neutrophil lifespan is therefore prolonged in sites of inflammation, which in acute inflammatory settings is beneficial and allows the neutrophil to carry out effector mechanisms and clear the pathogen. In chronic inflammation however this prolongs the tissue damage that the neutrophil is inflicting and prevents inflammation resolution (Brown *et al.*, 2009).

1.3.2 Evidence of dysregulated neutrophil apoptosis in COPD

COPD is commonly associated with airway neutrophilia (Qiu *et al.*, 2003), but whether this is primarily due to an increase in migration of neutrophils to the lungs, or decrease in the rate of neutrophil cell death is disputed. Some studies have demonstrated that sputum samples from patients with COPD contained significantly fewer apoptotic neutrophils than a healthy control group, with the rate of apoptosis in the 'healthy smoker' group (i.e. smokers with no clinical disease) being between the two (Brown *et al.*, 2009). Other researchers however have found no significant differences in apoptotic rates in sputum neutrophils (Rytilä *et al.*, 2006). This discrepancy may be due to differences in the disease severity of patients sampled, as a third study demonstrated reduced rates of apoptosis only in samples from patients with a more severe clinical disease, and not those with mild COPD (Makris *et al.*, 2009). A correlation between the suppression of apoptosis and disease severity suggests that the effector mechanisms of persistent neutrophils in the lungs of patients may be contributing to the pathology of the disease, or alternatively that the severity of the inflammation is supressing neutrophil apoptosis. Due to the limitations surrounding the investigation of airway neutrophil function in COPD patients *in vivo*, this cannot be confirmed.

The relationship between severity of disease and rate of neutrophil apoptosis is also found in peripheral blood neutrophils from people with COPD. No differences in the rate of neutrophil apoptosis were found in peripheral blood of clinically stable patients (Noguera *et al.*, 2004). In studies of patients admitted to hospital for acute COPD exacerbations, neutrophil apoptosis was decreased on the day of admission, but three days later was no different to healthy aged-matched controls (Pletz *et al.*, 2004; Schmidt-Ioanas *et al.*, 2006). This correlation with disease-phenotype is not always supported in COPD, as stable patients with mild to moderate disease were also shown to have significantly less apoptosis of peripheral blood neutrophils compared to both healthy controls and smokers with no clinical disease (Zhang *et al.*, 2012). It is likely that variables between patient cohorts, particularly relating to medication, are contributing to the discrepancy between results from different data sets, and a meta-analysis of data from different studies may lead to a clearer understanding of the significance of individual parameters such as disease phenotype. Reduced neutrophil apoptosis is observed in other inflammatory lung diseases, such as chronic bronchitis (Strassburg *et al.*, 2004), acute respiratory distress syndrome (Fialkow *et al.*, 2006), and pneumonia (Moret *et al.*, 2011), so it is not surprising that this is also observed in some studies of patients with COPD.

1.3.3   Induction of neutrophil apoptosis as a therapeutic strategy

Reversing the dysregulation of neutrophil apoptosis in inflammatory diseases such as COPD has been investigated by others, via mechanisms relating to death-receptor pathways, NFκB signalling, and adhesion molecule expression (Noguera *et al.*, 2004; Dupont and Warrens, 2007; Brown *et al.*, 2009). Cytokines and growth factors in particular are recognised as being key to maintaining the persistent inflammatory environment that contributes towards the suppression of neutrophil apoptosis. The haematopoietic cytokine and growth factor GM-CSF is known to profoundly delay neutrophil apoptosis *in vitro* (Kobayashi *et al.*, 2005). GM-CSF is increased in both the sputum and peripheral blood of patients with COPD compared to both healthy smokers and healthy non-smokers (Day, Barnes and Donnelly, 2014; Mitra *et al.*, 2018). Since GM-CSF is clearly implicated in extending neutrophil lifespan in inflammatory environments, it may be an effective therapeutic target, and murine models indicated a positive reduction in clinical disease phenotype as well as reduced pro-inflammatory biomarkers when treated with a GM-CSF neutralising antibody (Vlahos *et al.*, 2006, 2010; Puljic *et al.*, 2007). However a randomised clinical trial in which patients requiring intensive care with systemic inflammation were treated with recombinant human GM-CSF showed no differences in the rates of peripheral blood neutrophil apoptosis (or phagocytosis, the primary outcome measured) compared to a placebo treatment group (Pinder *et al.*, 2018).

Although not specifically focused on neutrophil apoptosis, inhibition of cytokines for the treatment of COPD has also been investigated. These have shown promising results in animal models of pulmonary inflammation pre-clinically, however this has not always translated into successful treatment of human disease. Both TNFα knockout mice and IL-1 receptor (IL-1R) knockout mice have significantly lower pulmonary inflammation when exposed to cigarette smoke (Churg *et al.*, 2004; Pauwels *et al.*, 2011). On the other hand, clinical trials in which COPD patients were treated with infliximab (an anti-TNFα antibody) or an anti-IL-1R antibody showed no treatment benefit compared to a placebo (Rennard *et al.*, 2007; Calverley *et al.*, 2017). As both IL-1 and TNFα signalling converge at the NFκB signalling pathway, it is possible that redundancy in these pathways is playing a role in the lack of efficacy of these treatments (Butler, Walton and Sapey, 2018). The redundancy in many inflammatory cell signalling pathways, and potential compensation when the activity of one specific cytokine is attenuated, has led to the alternative therapeutic approach of inhibiting common signalling pathways that regulate inflammation (Foster *et al.*, 2012).

The pro-survival effects of GM-CSF in neutrophils are induced by preventing the degradation of the anti-apoptotic MCL-1, which occurs via the phosphoinositide 3-kinase (PI3K)/AKT and ERK/MEK signalling pathways (Derouet *et al.*, 2004). Other neutrophil survival factors such as type I interferon

and components of cigarette smoke also inhibit neutrophil apoptosis via the PI3K pathway (Wang *et al.*, 2003). The activation of the NFκB pathway, either induced by AKT signalling or independently by other inflammatory mediators, similarly supresses neutrophil apoptosis (Castro-Alcaraz *et al.*, 2002; Hussain *et al.*, 2012; Ratajczak-Wrona *et al.*, 2014) (Figure 1.5). Both cigarette smoke extract and nicotine prevent the decline in activity of the pro-survival AKT pathway in human neutrophils *in vitro,* delaying spontaneous apoptosis, which could be reversed using pharmacological inhibitors of either AKT and the upstream PI3K (Xu *et al.*, 2013). This finding translated into murine *in vivo* models in which knock-out of InsP6K1, a kinase that prevents the decline in AKT pathway, lead to an increase in cigarette smoke-induced neutrophil recruitment to the lungs (Xu *et al.*, 2013).

Pharmacological inhibitors of PI3K and ERK also induced apoptosis of neutrophils isolated from healthy volunteers *in vitro* (Klein *et al.*, 2000). Inhibitors of PI3K (particularly PI3K delta) are of potential therapeutic interest for COPD and other inflammatory diseases, although the focus is not always on neutrophil apoptosis specifically, as this pathway controls a wide variety of inflammatory phenotypes in immune cells (Fung-Leung, 2011). In mouse models of LPS-induced lung injury, an aerosolised PI3Kδ inhibitor reduced pulmonary neutrophil numbers, and reduced the migration of polymorphonuclear leukocytes *in vitro* (Doukas *et al.*, 2009; Reutershan *et al.*, 2010). Additional research has demonstrated the efficacy of PI3K inhibitors in repairing alveolar cell damage in murine models (Horiguchi *et al.*, 2015) and restoring migration accuracy in human neutrophils *in vitro* (Sapey *et al.*, 2014). A clinical trial of COPD patients with exacerbations found that an inhaled PI3Kδ inhibitor (Nemiralisib) improved lung function and reduced further exacerbations after 12 weeks of treatment (Hessel *et al.*, 2018). However a second, similar study which tested a range of doses of Nemiralisib showed no difference to lung function or re-exacerbations (Fahy *et al.*, 2021).
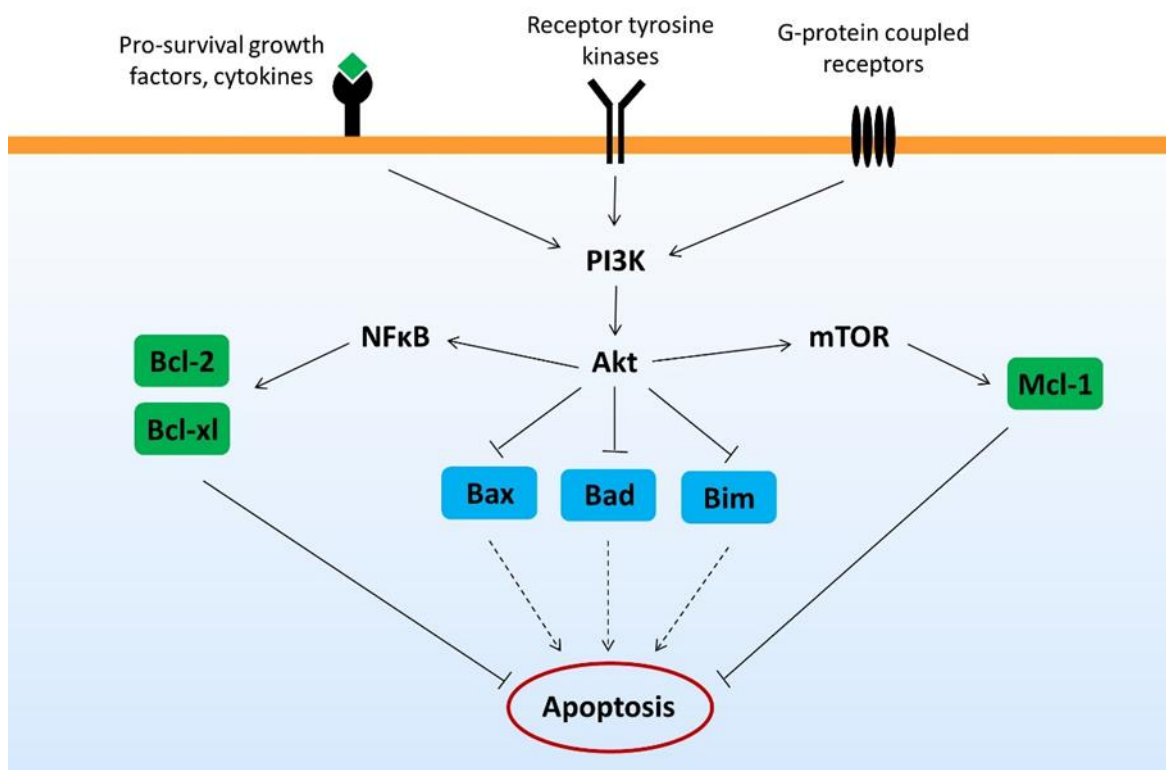
Figure 1.5. Inhibition of apoptosis via the PI3K/AKT signalling pathway.
External signalling through a variety of receptors activates the PI3K/AKT pathway, resulting in suppression of pro-apoptotic factors (blue), or prevents the degradation of anti-apoptotic factors (green) through the induction of other signalling pathways such as NFκB and mTOR. (Sousa *et al.*, 2010; Perciavalle *et al.*, 2012; Hein, Ouellette and Yan, 2014).

Phosphorylation of the Janus kinase 2 (JAK2) tyrosine kinase in response to GM-CSF results in the phosphorylation and activation of the signal transducer and activator of transcription (STAT) family of proteins, and may also play a role in neutrophil survival, as a JAK2 inhibitor abolished the anti-apoptotic effects of GM-CSF in neutrophils isolated from young subjects *in vitro* (Fortin *et al.*, 2007)*.* Interestingly it had no effect on apoptotic rates in the neutrophils of elder subjects (65-85 years) (Fortin *et al.*, 2007). Since COPD is a progressive disease and thus disproportionately affects older people, identifying differences in cellular mechanisms that are altered with age may lead to increased efficacy of therapeutics. JAK inhibitors are already used clinically for the treatment of myelofibrosis, a cancer in which fibrosis of the bone marrow causes aberrant haematopoiesis, and rheumatoid arthritis (Yamaoka, 2016; Bose and Verstovsek, 2017). The JAK/STAT signalling pathway is a central regulator of cytokine production, by initiating the transcription of inflammatory cytokines such as interferons,

interleukins including IL-6, and regulators of leukocyte proliferation and differentiation such as GM-CSF (Harrington, Al Nokhatha and Conway, 2020).

The therapeutic success of JAK inhibitors in human disease demonstrates that targeting central regulators of inflammation is an efficacious therapeutic strategy. Targeting specific kinases to alleviate dysregulated inflammation is an approach being investigated for a range of inflammatory diseases and cancers, as knowledge of the signalling pathways inducing particular disease phenotypes become more comprehensive (Zarrin *et al.*, 2021). Additionally, the wide range of small-molecule kinase inhibitors available to researchers is highly useful for collecting preliminary data, with these drugs having the advantages of being able to cross cellular membranes to interact with the intracellular target, therefore often having oral administration routes, and being less costly and easier to manufacture than biologics (Makurvet, 2021).

1.4 ErbB inhibitors as potential therapeutics for neutrophil-driven inflammatory diseases

1.4.1 ErbBs are a family of receptor tyrosine kinases

Receptor tyrosine kinases are cell surface receptors that bind a variety of external ligands including cytokines, growth factors, and hormones, inducing intracellular signalling pathways that regulate many aspects of cell function, including survival, migration, proliferation, differentiation and the inflammatory response (Page *et al.*, 2009). The ErbB family consists of four receptor tyrosine kinases: epidermal growth factor receptor (EGFR)/ErbB1, ErbB2/HER-2/Neu, ErbB3/HER-3 and ErbB4/HER-4 (Roskoski, 2014). Signal transduction is initiated by dimerization of two receptors on the cell membrane, which is either induced by ligand binding or (in the case of ErbB2, which has no known ligand) spontaneous dimerization (Muthuswamy, Gilman and Brugge, 1999). Dimerization induces phosphorylation of the intracellular C-terminal domain of the receptor, activating downstream signalling pathways that include ERK (MAPK), PI3K/AKT and JAK/STAT, which induce a wide range of effector functions (Ho *et al.*, 2017) (Figure 1.6). A variety of dimerization partners are possible between the four family members, including the formation of heterodimers as well as homodimers. ErbB3 is the only family member unable to form active homodimers, due to its lack of intrinsic kinase activity (Plowman *et al.*, 1990). ErbB2 has no known ligands, but is the preferred dimerization partner of other ErbB family members (Graus-Porta *et al.*, 1997). Ligand binding regulates the dimer type

formed; epidermal growth factor (EGF) for example binds to EGFR and promotes EGFR-ErbB2 heterodimers, whilst Neu differentiation factor, a ligand specific to ErbB3 and ErbB4, promotes heterodimer formation of either receptor with ErbB2 (Graus-Porta *et al.*, 1997). Research suggests that homodimer signalling is significantly weaker than that induced by heterodimers, with heterodimers containing ErbB2 being the most potent in mediating downstream signalling, and ErbB2-ErbB3 heterodimers being the most mitogenic (Yarden and Sliwkowski, 2001; Holbro *et al.*, 2003).
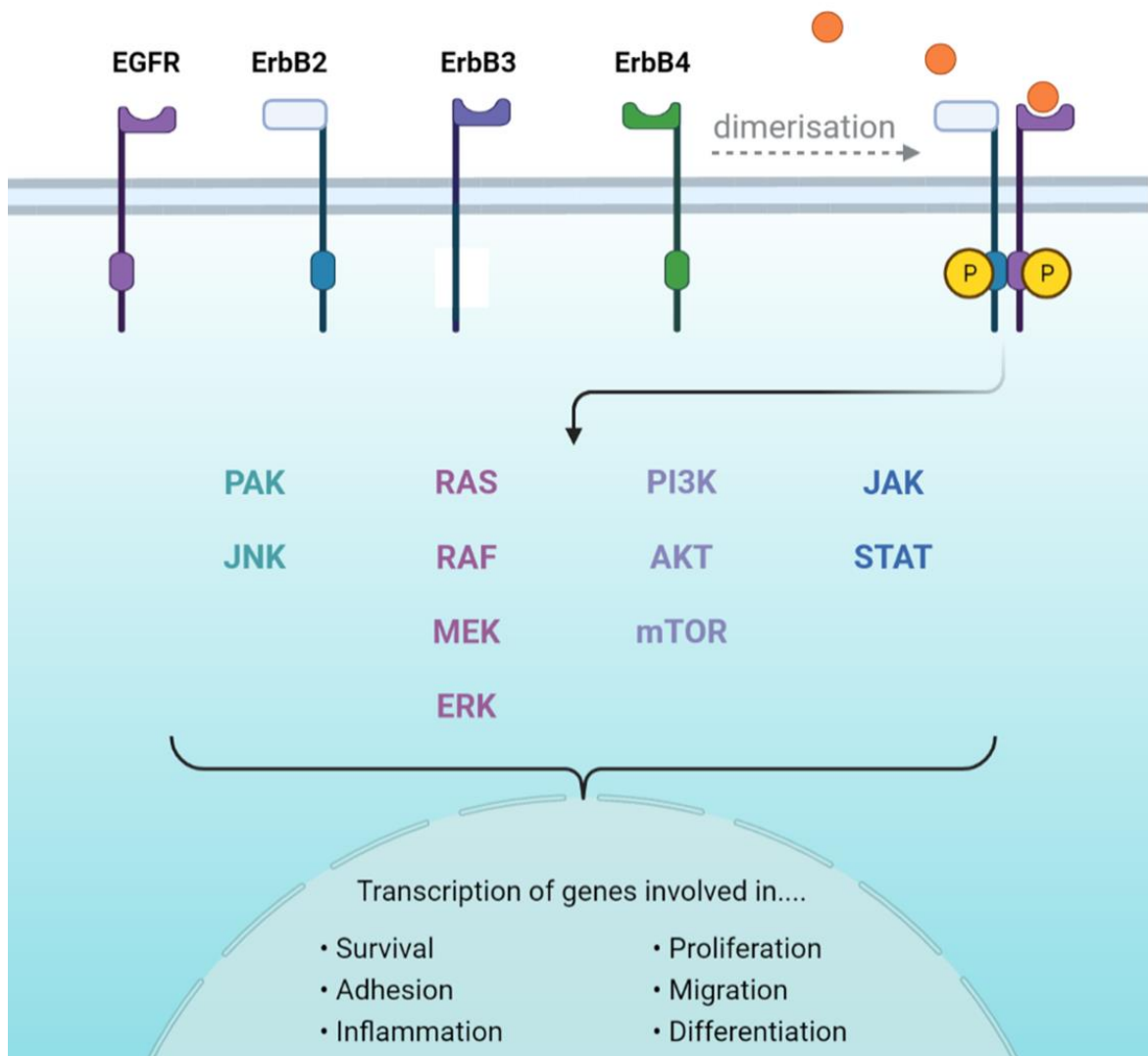
Figure 1.6. Signalling pathways and functional outcomes regulated by the ErbB family.
Of the four members of the ErbB family, ErbB2 has no known ligands and ErbB3 has no intrinsic kinase activity, but both can form fully functional heterodimers. Ligand binding induces dimerisation and phosphorylation of the intracellular kinase domain, which induces a variety of intracellular signalling pathways to alter cellular function and phenotype. Created in BioRender.

According to the Human Protein Atlas, an online database which integrates various "omics" technologies to map all the proteins in human cells, tissues and organs (Uhlén *et al.*, 2015), ErbB

expression is fairly ubiquitous across tissues in humans, although there is some variation. ErbB3 is detected at the protein level in every tissue analysed in this database, whereas EGFR is not detected in a number of tissues including the brain, spleen or adrenal gland; ErbB2 protein is not found in the brain, pancreas, gallbladder or spleen; and ErbB4 is not present in the heart muscle, spleen and cerebral cortex, amongst others. All four family members are detected in the lungs (Uhlén *et al.*, 2015). Expression of ErbBs on individual immune cell types does not appear widely researched, although there are some examples in the literature. EGFR on human neutrophils and ErbB2 and ErbB3 on human monocytes were detected by flow cytometry, and EGFR on murine macrophages by western blot (Lewkowicz *et al.*, 2005; Lu *et al.*, 2014; Ryzhov *et al.*, 2017). Research from my group suggests neutrophils express a 60kD version of ErbB2, which was upregulated by cyclic AMP (cAMP) and GM-CSF (Rahman *et al.*, 2019). The canonical form of ErbB2 according to the UniProt protein database is 138kD, although lower molecular weight isoforms are also documented (The UniProt Consortium, 2021).

1.4.2   Pharmacological ErbB inhibitors promote apoptosis in a number of cell types

ErbB signalling is inherently anti-apoptotic, as the activation of the AKT pathway prevents the interaction of pro-apoptotic BAD with BCL-2, thus inhibiting the intrinsic apoptosis pathway (Marmor, Skaria and Yarden, 2004). This has been demonstrated in our group in human neutrophils *in vitro*, by showing that GM-CSF-induced upregulation of phosphorylated AKT and MCL-1 can be reduced by an inhibitor of EGFR and ErbB2 (tyrphostin AG825) (Rahman *et al.*, 2019). The majority of research surrounding ErbBs is in the field of cancer, as therapeutic inhibition of ErbBs is used clinically to treat a number of solid tumours in which the respective receptor is overexpressed (Yarden and Sliwkowski, 2001; Rimawi *et al.*, 2010). In these cancers, the overexpression or aberrant activation of ErbB signalling pathways promotes carcinogenesis, as the cell does not undergo constitutive apoptosis as it should (Wei *et al.*, 2020). A number of clinically approved and research use ErbB inhibitors are available, with different selectivities for ErbB family members depending on the cancer type (Table 1.2).

The biology of the ErbB receptors is complex, with EGFR/ErbB1 paradoxically reported to be both pro- and anti-apoptotic (Jackson and Ceresa, 2017). This is suggested to vary with the subcellular location of the receptor, which may be mediated by ligand concentration (Hyatt and Ceresa, 2008; Rush *et al.*, 2012). My group has shown that in human neutrophils *in vitro*, a number of pharmacological ErbB inhibitors induce human neutrophils apoptosis in a dose-dependent manner (Rahman *et al.*, 2019). Although there is very little other research regarding the effect of ErbBs on immune cells, there is

plenty showing the efficacy of ErbB inhibitors in inducing apoptosis in cancer cells. In several lung adenocarcinoma cell lines, as well as in an immortalised keratinocyte cell line, the clinical ErbB inhibitor gefitinib was shown to induce apoptosis in a dose-dependent manner (Cho *et al.*, 2010; Yan *et al.*, 2015). Gefitinib similarly induced apoptosis in myeloid cell lines and primary cells isolated from patients with myelodysplastic syndrome or acute myeloid leukaemia, however interestingly this was also observed in cell lines that do not express EGFR, the target of gefitinib (Boehrer *et al.*, 2008).

Table 1.2. Mechanism of action and current use of several clinically approved and research use ErbB inhibitors.

Inhibitor	Selectivity	Mechanism of action	Current use
Trastuzumab (Herceptin)	ErbB2	Monoclonal anti-HER-2 antibody (Yakes *et al.*, 2002)	Used in clinic for HER-2 overexpressing breast cancers and gastric cancer (Valabrega, Montemurro and Aglietta, 2007; Bang *et al.*, 2010)
Neratinib	EGFR ErbB2	Small molecule competitive inhibitor of the ATP-binding domain (Hickinson *et al.*, 2010; Segovia-Mendoza *et al.*, 2015)	Clinical use for HER-2 overexpressing breast cancers (Segovia-Mendoza *et al.*, 2015)
Gefitinib	EGFR		Patients with NSCLC, clinical trials for other cancers (Soria *et al.*, 2015)
Erlotinib	EGFR		Clinical use for NSCLC and pancreatic cancer (Park *et al.*, 2012)
Sapitinib (AZD8931)	EGFR ErbB2 ErbB3		Clinical trials for breast cancer and other solid tumours (Adams *et al.*, 2016)
Lapatinib	EGFR ErbB2		Clinical use for breast cancer, clinical trials for other cancers (Ahmad *et al.*, 2011)
Tyrphostin (AG825)	ErbB2 (selective) EGFR		Research use (Ahmad *et al.*, 2011)
Erbstatin	EGFR		Research use (Breen and Soellner, 2015)
CP-724,714	ErbB2 (selective) EGFR		Research use (Jani *et al.*, 2007)

The second member of the ErbB family, ErbB2 or HER-2, is primarily known for its role in breast cancer in which ErbB2 is overexpressed. This aggressive tumour has a poorer prognosis than HER-2 negative

counterparts, but can be treated specifically with the anti-HER-2 monoclonal antibody, trastuzumab (Vogel *et al.*, 2002; dos Santos *et al.*, 2017). Initially ErbB2 was thought to require dimerisation with another ErbB receptor to drive downstream signalling pathways, specifically ErbB3 in cancer cells to drive tumorigenesis, however recent evidence has shown that residual ErbB2-driven PI3K signalling is present in a number of breast cancer cell lines in which ErbB3 is silenced (Ruiz-Saenz *et al.*, 2018). In other cell types such as keratinocytes however, knock-down of ErbB2 had no effect on the apoptotic rate, whereas knock-down of ErbB3 did induce apoptosis (Dahlhoff *et al.*, 2017). This may suggest that the function of these receptors, including apoptosis suppression, is cell specific.

The importance of ErbB3 signalling was further demonstrated in a study using primary human trophoblasts isolated from placental tissue, in which cells cultured in the presence of an ErbB3-blocking antibody and neuregulin 1 (a ligand of ErbB3) showed increased cell death rate compared to cells treated with the ligand alone (Fock *et al.*, 2015). This suggests a possible role of ErbB3-mediated cell death during tissue development in the placenta, which is supported by the fact that ErbB2 and ErbB3 gene deletion is lethal in mice (Lee *et al.*, 1995; Riethmacher *et al.*, 1997).

ErbB4 is the least therapeutically exploited member of the ErbB family, despite being upregulated in several solid tumours (Williams *et al.*, 2015). Ibrutinib, an inhibitor specific for Bruton's tyrosine kinase used clinically to treat leukaemia and other B-cell malignancies, was shown to inhibit ErbB4 activity and downstream signalling, and decrease mouse xenograft tumour volume (Rauf *et al.*, 2018). ErbB4 was upregulated in breast cancer cell lines with resistance to Lapatinib *in vitro*, and ErbB4 knockdown triggered apoptosis in Lapatinib- and Trastuzumab- resistant cancer cell lines in which ErbB2 is overexpressed, suggesting it may play a role in the development of resistance to these treatments (Canfield *et al.*, 2015).

1.4.3   EGFR as a target in inflammatory lung diseases

Targeting EGFR signalling specifically as a therapeutic strategy for inflammatory lung diseases has previously been investigated, although no research has been identified that used ErbB inhibitors to induce neutrophil apoptosis specifically. EGFR signalling is involved in a wide range of cellular responses, including inflammation: for example the binding of the EGFR ligand amphiregulin is required for TGFβ-dependant pulmonary fibrosis in mouse models (Andrianifahanana *et al.*, 2013). Bronchial epithelial cells from patients with COPD have increased production of CXCL8 and increased phosphorylation of EGFR and AKT, however both were reduced *in vitro* with erlotinib treatment (a clinical EGFR inhibitor) (Ganesan *et al.*, 2013). The EGFR signalling pathway was also shown to

contribute to the loss of muscle function that many patients with COPD experience (Ciano, Mantellato, *et al.*, 2019). Not all experiments have shown a benefit of blocking EGFR signalling however, as a clinical trial of an inhaled EGFR antagonist being assessed for its efficacy in reducing mucus production in patients with COPD showed no difference compared to a placebo (Woodruff *et al.*, 2010). Although EGFR inhibitors have to date only been approved for cancer treatment, research does suggest they may have potential benefit for inflammatory lung diseases such as COPD.

1.4.4 ErbB inhibitors are safe and tolerated in humans, with some adverse effects

Numerous ErbB inhibitors have been approved for use in the clinic, indicating their safety in patients. If these drugs were to be repurposed however, the new disease indication would need to be taken into account when assessing the toxicity profiles of these drugs. Treatment with gefitinib for example can increase the incidence of dry skin, itchiness, diarrhoea, nausea, vomiting and abnormal hepatic function (Wo *et al.*, 2018). Neratinib causes diarrhoea in almost all people who take it, and although this is often manageable with treatment, in some cases it can be severe, with one study showing 1.4% patients taking neratinib required hospital admission for diarrhoea, and 1.6% had serious diarrhoeal events (Mortimer *et al.*, 2019). Other common adverse effects of neratinib treatment are nausea, vomiting and fatigue, and this drug cannot be taken by people who are pregnant or plan to be as it can increase the risk of birth defects (Chilà *et al.*, 2021). Trastuzumab has been associated with low rates (0.5-4%) of mostly reversible cardiac toxicity, although this may be due to a dual-treatment regime (Procter *et al.*, 2007; Suter *et al.*, 2007). The most common toxicities observed with lapatinib treatment (currently in clinical trials) are diarrhoea, rash, nausea and fatigue (Moy and Goss, 2007). It is important to consider that many people with COPD have co-morbidities and will be taking other medications that may also have adverse effects, and so the potential benefits of adding a new drug treatment would need to be carefully considered.

1.5 Models for the investigation of neutrophil biology and lung inflammation

1.5.1 Primary human neutrophils *in vitro*

Use of the primary human neutrophil, isolated from blood samples of volunteers, is currently the gold standard method of studying neutrophil behaviour *in vitro*. A number of different isolation methods

exist and have been well described in the literature, including density gradient separation (Haslett *et al.*, 1985; Ward *et al.*, 1999), antibody-based immunomagnetic selection (Hasenberg *et al.*, 2011), and chip-based methods of isolation (Kotz *et al.*, 2010). Each technique has numerous variations and is often optimised further by individual research groups, resulting in a lack of consistency that can affect the replication of results from other groups. Neutrophil chemotaxis and phagocytic capacity in response to LPS for example was shown to be altered between neutrophils isolated by density gradient separation and spontaneous sedimentation (Mosca and Forte, 2016). Reactive oxygen species production and Fcγ receptor I expression were also found to be altered between neutrophils isolated by Percoll density gradient and gelatin spontaneous sedimentation method (Marchi *et al.*, 2014). As neutrophils are extremely sensitive to priming and activation *in vitro*, this is not particularly surprising.

Many of the key functions of neutrophils *in vivo*, in both homeostatic and inflammatory environments, can be modelled *in vitro* and are known to be conserved. Neutrophil biochemical and functional features that have been demonstrated *in vitro* include production of hydrogen peroxide and reactive oxygen species and myeloperoxidase activity, degranulation and cytokine release, phagocytosis and killing of pathogens, chemotaxis and migration, including transepithelial cell migration, NETosis, apoptosis and other forms of cell death (Naegelen *et al.*, 2015; Hoppenbrouwers *et al.*, 2017; Deng *et al.*, 2018; van Grinsven *et al.*, 2018; Pérez-Figueroa *et al.*, 2021).

In the absence of growth factors, human neutrophils undergo spontaneous apoptosis *in vitro* with the majority of cells becoming apoptotic by 24 hours. This can be suppressed by the addition of growth factors, bacterial products and inflammatory agents such as GM-CSF, LPS or cyclic AMP, or hypoxic conditions (Hannah *et al.*, 1995; Walmsley *et al.*, 2005; Rahman *et al.*, 2019). This model is therefore very useful for studying the effects of pharmacological inhibitors on neutrophil apoptosis, unlike *in vivo* models in which apoptotic neutrophils are rapidly cleared by macrophages and are significantly harder to detect.

Animal models are also commonly used to investigate the immune response of neutrophils; these have the obvious advantage of being able to administer drugs and other reagents *in vivo*, carry out procedures and control other experimental variables in ways that would not be possible in human studies. Many animal models however – rodents being the most commonly used – have similar limitations to humans, in that in order to investigate many parameters of immune cells specifically, these cells need to be removed from the animal and studied *ex vivo*.

1.5.2 Zebrafish larvae as a model for studying the innate immune system *in vivo*

Zebrafish larvae are an ideal model to study immune cell behaviour *in vivo*. The high genetic homology to humans and relative ease of genetic manipulation in this organism allows for stable transgenic lines of adult fish to be developed, in which specific cells or tissues express fluorescent markers. Combined with the optical transparency of zebrafish larvae, this allows for individual cells or tissue types to be visualised and imaged in real time at high resolution *in vivo*, an advantage that is lacking in many other animal models.

The immune system of the larval zebrafish parallels the mammalian immune systems in several ways. Two myeloid cell lineages are present in the larvae: the macrophage-like cell (primitive macrophage) is the first to develop at approximately 15 hours post-fertilisation (hpf), and is identifiable in the yolk-sac from approximately 22 hpf (Herbomel, Thisse and Thisse, 1999, 2001). A neutrophilic granulocyte cell (strictly, heterophil), referred to going forward as a neutrophil, can be found in circulation and in the caudal haematopoietic tissue (the primary site of haematopoiesis in the larvae) from approximately 48 hpf (Murayama *et al.*, 2006; Bertrand *et al.*, 2007). Neutrophils in the zebrafish larvae share many functions with human and other mammalian neutrophils. They contain primary and secondary granules, form structures such as neutrophil extracellular traps, phagocytose and kill pathogens, migrate to sites of injury or infection and undergo reverse migration and apoptosis as part of inflammation resolution (Herbomel, Thisse and Thisse, 1999; Palić *et al.*, 2007; Kaveh *et al.*, 2020; Manley *et al.*, 2020; Isles *et al.*, 2021). Primitive macrophages similarly respond to infection and inflammatory stimuli in the larvae, and play important roles in development, inflammation resolution and tissue regeneration through the engulfment of apoptotic and necrotic cell debris (Harvie and Huttenlocher, 2015; Loynes *et al.*, 2018). As fully functional adaptive immune cells are not produced in the zebrafish until approximately 4 weeks, the use of larvae allows for the function and responses of these two cell types to be studied independently.

A number of models of inflammation in the zebrafish larvae are well established, including the tail fin transection model of injury-induced inflammation which generates a clean injury site, comparable to a surgical wound, to which neutrophil and macrophage migration, function and death can be observed (Lieschke *et al.*, 2001; Renshaw *et al.*, 2006). The relative ease of genetic editing by CRISPR/Cas9 in zebrafish, as well as the ability to administer pharmacological inhibitors either by injection into the tissues or immersion of larvae in solution containing the drug of interest makes it a highly versatile model for the study of neutrophil biology (Henry *et al.*, 2013).

1.5.3   Mouse models of lung inflammation

COPD develops over decades in humans and of course this cannot be effectively replicated in animal models with any efficiency: although non-human primate models are the closest in terms of the respiratory anatomy, these require tightly regulated ethical approval, are expensive and not available to the majority of research groups (Polverino *et al.*, 2014). Rodent models of lung inflammation are much more commonly used to test the efficacy of potential therapeutics, and many are well-established in the literature. The immune system and inflammatory response of mice closely mirrors that of humans, with the vast majority of the immune system and inflammatory response detailed in this introduction being conserved (Mestas and Hughes, 2004; Shannon *et al.*, 2005).

Decades of research using mouse models for the study of immunology has resulted in a wealth of information regarding the translation of these models to human disease and differences are well documented (Mestas and Hughes, 2004). For example it is known that mice and rats lack the key neutrophil chemokine CXCL8, and instead have two related cytokines with similar functions, CXCL1/KC and macrophage inflammatory protein 2 (MIP2) (Tsai *et al.*, 2000; Zlotnik and Yoshie, 2000). Whereas the predominant leukocyte in human blood is the neutrophil, in mice lymphocytes account for 75-90% of all circulating white blood cells (Doeing, Borowicz and Crockett, 2003). Human and mouse toll-like receptor 4 (TLR-4), a receptor that binds bacterial LPS and is a key inducer of inflammatory responses, have an amino acid sequence similarity of 62% for the extracellular domain, and so may respond differently to specific LPS structures (Vaure and Liu, 2014).

Rather than model the entirety of COPD, which has not been achieved in rodent models, specific key pathophysiological features of COPD can be replicated in smaller, acute models of lung inflammation in mice, such as endotoxin (LPS) induced lung injury. The inhalation or intranasal instillation of LPS results in an influx of neutrophils, macrophages and lymphocytes, release of inflammatory mediators and structural changes such as airway remodelling and alveolar destruction (Matute-Bello, Frevert and Martin, 2008). These changes are observed after a single exposure to LPS, unlike other models such as cigarette smoke induced inflammation, making the LPS model particularly useful for collecting preliminary data on the efficacy of potential new therapeutics.

1.6   Hypothesis and aims

The use of ErbB inhibitors in cancer treatment has demonstrated their efficacy in inducing tumour cell death, and previous research in our group has shown this also occurs in human neutrophils *in vitro*. The signalling pathways mediating these effects in cancer treatment are also known to be regulators of apoptosis in human neutrophils, suggesting that these inhibitors may be attractive novel targets for diseases such as COPD, in which inducing neutrophil apoptosis is desirable. The hypothesis for this thesis is that ErbB inhibitors have therapeutic potential in neutrophil-driven inflammatory diseases such as COPD, via the upregulation of neutrophil apoptosis.

This hypothesis will be tested by three key aims. The first is to assess whether inhibition of ErbB signalling is able to induce neutrophil apoptosis and reduce neutrophilic inflammation in a larval zebrafish model of inflammation. This will be tested using pharmacological ErbB inhibitors, and genetic knock-down of ErbB genes using transient expression CRISPR/Cas9.

The second aim will be to determine whether pharmacological ErbB inhibitors are beneficial in a mammalian model of lung inflammation. A number of mouse models will be utilised for this, and a number of parameters will be tested, including the number and distribution of different leukocytes in bronchoalveolar lavage fluid, rates of neutrophil apoptosis and efferocytosis by macrophages, and whether lung tissue damage is reduced via histological analysis.

The final aim is to elucidate the signalling pathways that pharmacological ErbB inhibitors are inhibiting in human neutrophils, leading to be induction of apoptosis. Literature describes these signalling pathways in tumour cells; however these cells are intrinsically resistant to apoptosis, unlike short-lived neutrophils, and it will be interesting to determine whether the same pathways are being inhibited. This will be carried out using mass spectrometry-based phosphoproteomics analysis to identify phosphorylated proteins in ErbB inhibitor treated and untreated human neutrophils, and attempt to reconstruct signalling pathways based on those that are differentially detected between the treatment groups.

2 Methods

2.1 Human neutrophils *in vitro*

2.1.1 Collection of peripheral blood samples from healthy volunteers

In vitro experiments were conducted on neutrophils isolated from peripheral blood samples of healthy donors, in compliance with the guidelines of the South Sheffield Research Ethics Committee (reference number STH13927). Two isolation methods were utilised: plasma-Percoll™ gradient centrifugation (Haslett *et al.*, 1985; Ward *et al.*, 1999) (Figure 2.1), and immunomagnetic negative selection. For both methods of isolation, the volume of blood required was calculated prior to collection according to experimental requirements, based on approximately 1 million isolated neutrophils per 1 mL blood. Peripheral blood samples were obtained by venepuncture and collected into a 50mL syringe, then immediately transferred into a 50mL Falcon tube containing 3.8% Tri-sodium citrate (Martindale, MS156) (5mL per 40mL blood). Tubes were gently inverted to mix blood and citrate, to prevent coagulation. After collection, all further handling (other than centrifugation) was carried out in a Class II Biological Safety Cabinet. All isolation procedures were carried out at room temperature.

2.1.2 Dextran sedimentation and plasma-Percoll™ gradient centrifugation

A schematic of the process is shown in Figure 2.1. Blood was centrifuged at 330g for 20 minutes, separating the blood into two distinct layers of platelet-rich plasma and blood cells. Platelet-rich plasma was transferred to a separate falcon tube and centrifuged at 912g for 20 minutes, pelleting the platelets and leaving the platelet-poor plasma as supernatant. This platelet-poor plasma was transferred to a fresh tube, and the platelet pellet discarded. During the second centrifugation step, 6mL of 6% Dextran in saline (Dextran T500, Pharmacosmos, 5510050090007) was added to the blood cell layer from the initial centrifugation, and the volume topped up to 50mL with saline. After gentle mixing, this was left for approximately 20 minutes, allowing the red blood cells to sediment. When a clear interface layer was visible, the upper layer, containing leukocytes but not red blood cells, was transferred to a clean falcon tube and centrifuged at 230 g for 6 minutes. The supernatant was removed and cells resuspended in 2mL platelet-poor plasma. During the centrifugation step, the Percoll™ gradient was prepared. In fresh 15mL falcon tubes, 1.02mL of 90% Percoll™ (GE Healthcare, 17-0891-02) was mixed with 0.98mL platelet-poor plasma (producing the lower phase), and separately
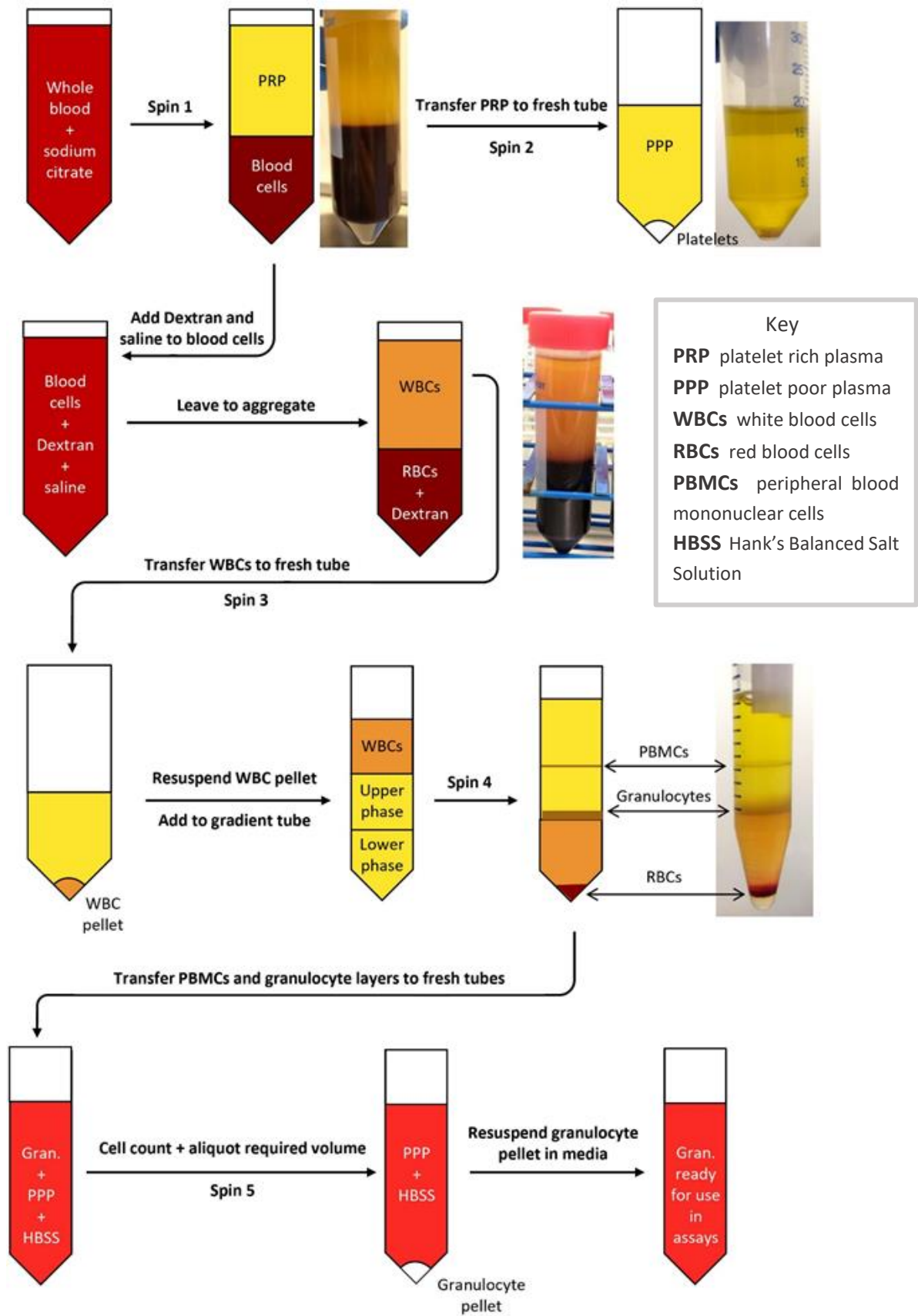
Figure 2.1. Dextran and Percoll-plasma gradient neutrophil isolation.
Schematic diagram of the steps involved in the isolation of human neutrophils using dextran sedimentation followed by plasma-Percoll gradient centrifugation (Herman, Rahman and Prince, 2020).

0.84mL 90% Percoll™ was combined with 1.16mL platelet-poor plasma (making the upper phase). The upper phase was slowly layered onto the lower phase in a clean falcon using a Pasteur pipette, after which the resuspended leukocytes were overlaid.

Centrifugation at 275g for 11 minutes yielded three layers of cells: remaining red blood cells pelleted at the bottom of the tube, granulocytes formed a layer in the middle, and peripheral blood mononuclear cells (PBMCs) formed a separate layer closer to the top. The PBMC and granulocyte layers were carefully removed and transferred to clean falcon tubes containing 10mL platelet-poor plasma, and to which Hank's Balanced Salt Solution (HBSS - Gibco, 14170-112) was added to obtain a final volume of 50mL. The number of cells in each suspension was counted using a haemocytometer, and the required number of cells for each experiment aliquoted and centrifuged at 511g for 6 minutes. The supernatant containing excess plasma proteins was removed, and cells resuspended in RPMI 1640 media (Lonza, BE12-702F) supplemented with 10% fetal bovine serum (FBS – Gibco, 10500-064), to a final concentration of 5 x 10^6 cell/mL.

Both granulocytes and PBMCs were shared between several researchers in the department, as requested, however for the experiments detailed in this thesis only granulocytes were used. After each isolation, the percentage of neutrophils, eosinophils, monocytes and lymphocytes were calculated using based on morphology (Figure 2.2A). For the majority of experiments, a purity of 95% neutrophils was required. Red blood cells were not included in purity counts.

2.1.3 Isolation of human neutrophils from peripheral blood samples using negative selection antibody kit

For experiments in which a higher purity of neutrophils was required, neutrophil isolation was carried out using an EasySep™ Human Neutrophil Isolation Kit (Stem Cell Technologies, catalogue 17957). Blood was collected into citrate as above, and centrifuged at 330g for 20 minutes, separating into the upper phase of platelet-rich plasma and a lower phase of cells. The plasma was carefully removed and discarded. Saline was added to the blood cells, to the volume of the original blood sample collected. Ethylenediaminetetraacetic acid (EDTA - 1mM) was added to the blood cells, and cells aliquoted into 15mL Falcon tubes, maximum 12mL per tube. HetaSep™ (Stem Cell Technologies, catalogue 07806) was added to each tube at a concentration of 1-part HetaSep™ to 5 parts blood. Tubes were centrifuged at 110g for 6 minutes, then placed back in the Class II Safety Cabinet and left for 15 minutes, undisturbed. During this step, the HetaSep™ sedimented red blood cells, resulting in red blood cells settling to the bottom of the tube and leaving a layer of leukocytes on top. This upper layer

of leukocytes was carefully transferred to fresh Falcon tubes. Leukocytes were centrifuged at 110g for 6 minutes, and cell pellets resuspended at 5×10^7 cells/mL in ice-cold buffer (phosphate-buffered saline (PBS) + 2% FBS + 1mM EDTA). From this point, samples were kept on ice.

Samples were transferred to sterile 5mL polystyrene round-bottomed tubes. Isolation cocktail from the EasySep™ kit was added to cells at a concentration of 25μL/mL sample, and mixed gently by pipetting. This cocktail of antibodies binds to surface proteins on all blood cells other than neutrophils. Samples were incubated on ice for 5 minutes, during which RapidSpheres™ (magnetic beads that can bind the Isolation Cocktail antibodies) from the EasySep™ kit were vortexed for 30 seconds to ensure an even suspension. RapidSpheres™ were then added to samples at a concentration of 40μL/mL, and samples incubated on ice for 3 minutes. Buffer was added to each sample to generate a final volume of 2.5mL, and mixed gently by pipetting. The tube was then placed in the EasySep™ magnet for 5 minutes. Neutrophils remain unbound, while all other cells bind the antibody/magnetic bead complex. Without removing the tube from the magnet, the enriched neutrophil suspension was poured into a fresh 5mL tube. This enriched neutrophil sample was placed into the magnet, and incubated at room temperature for 3 minutes to remove any remaining contaminating cells. The final enriched neutrophil suspension was poured into a fresh tube, ready for use in assays.

2.1.4   Treatment of human neutrophils with pharmacological agents

Neutrophils were treated with various pharmacological agents in 96-well flexible untreated polyvinyl chloride general assay plates (Corning, CLS2592), which minimise neutrophil adherence and activation. Plates were prepared in advance, with each well containing the 50μL of pharmacological agent at 2X desired concentration in RPMI 1640 + 10% FBS media. Immediately after isolation, 50uL neutrophils at a concentration of 5×10^6/mL were added to each well, diluting the pharmacological agent to the desired concentration. Lids were placed on plates, and plates incubated at 37°C in 5% CO_2 for 6 hours for experiments in which neutrophil apoptosis was assessed.

Pharmacological agents used for experiments in this thesis were: gefitinib (Toku-e, G039-100mg), lapatinib (Adooq Bioscience, A11752), sapitinib AZD8931 (Cayman Chemical, 24196), tyrphostin AG825 (Santa Cruz Biotechnology, sc-202045), neratinib HKI-272 (Selleck, S2150), EX527 (Santa Cruz Biotechnology, sc-203044), NSC348884 (Selleck, S8149), NU6102 (abcam, ab144317), dibutyryladenosine 3',5'-cyclic monophosphate sodium salt (db-cAMP) (Sigma Aldrich, D0627) (see Appendix 1 for concentrations). Stock solutions of each compound were solubilised in dimethyl sulfoxide (DMSO - Sigma) and stored in aliquots at -20C until use. DMSO-treated cells were therefore

used as a control. Duplicate wells were set up for each condition; for data analysis, the mean value of these replicates was used.

2.1.5 Assessment of neutrophil purity and apoptosis by microscopy

For the fixation, staining and analysis of neutrophils, cytocentrifugation was used to transfer and immobilise the cells on glass microscopy slides, referred to in this thesis as "cytospin slides". Cells in each well were gently pipetted to ensure an even cell suspension, and 100uL of each sample transferred to a cytospin funnel secured with a clamp onto a labelled glass microscope slide. After centrifugation in a Shandon Cytospin 4 cytocentrifuge (Thermo Electron Corporation) at 300rpm for 3 minutes, the cells (now immobilised on the microscope slide) were fixed with a drop of 100% methanol. Once dry, slides were stained for 3 minutes with Kwik-Diff Solution 2 (Shandon, 9990706) which contains eosin for cytoplasmic staining, followed by 3 minutes with Kwik-Diff Solution 3 (Thermo Electron Corporation, 9990707) which contains methylene blue for nuclear staining. Excess stain was washed from the slide using tap water, and slides left to dry completely. Slides were moved to a fume hood for the addition of a coverslip. Using a Pasteur pipette, a drop of DPX (Sigma Aldrich, 44581) was placed directly onto the cells, and a coverslip placed carefully on top. Slides were left in the fume hood at least overnight to allow the DPX to set.

A Nikon Eclipse TE300 inverted light microscope with 100X magnification oil immersion lens was used to analyse cytospin slides. Kwik-Diff stains allow differentiation of each type of blood cell by their morphology (Figure 2.2A). This is used to assess the purity of neutrophils from each isolation. As neutrophils have such distinct nuclear morphology, apoptotic neutrophils can similarly be identified by their rounded, condensed nucleus (Figure 2.2B). For assessing neutrophil apoptosis, 300 neutrophils per cytospin slide were counted and recorded as healthy or apoptotic, and the percentage of apoptotic neutrophils calculated.

A)

Red blood cell
Small, pink, anucleate

Eosinophil
Granular cytoplasm

Monocyte
Large kidney shaped nucleus

Neutrophil
Distinctive lobed nucleus

Lymphocyte
Large round nucleus, little cytoplasm

B)

Healthy neutrophil
Multi-lobed nucleus, chromatin bridges may be visible

Apoptotic neutrophil ◁
Condensed, round, darker nucleus
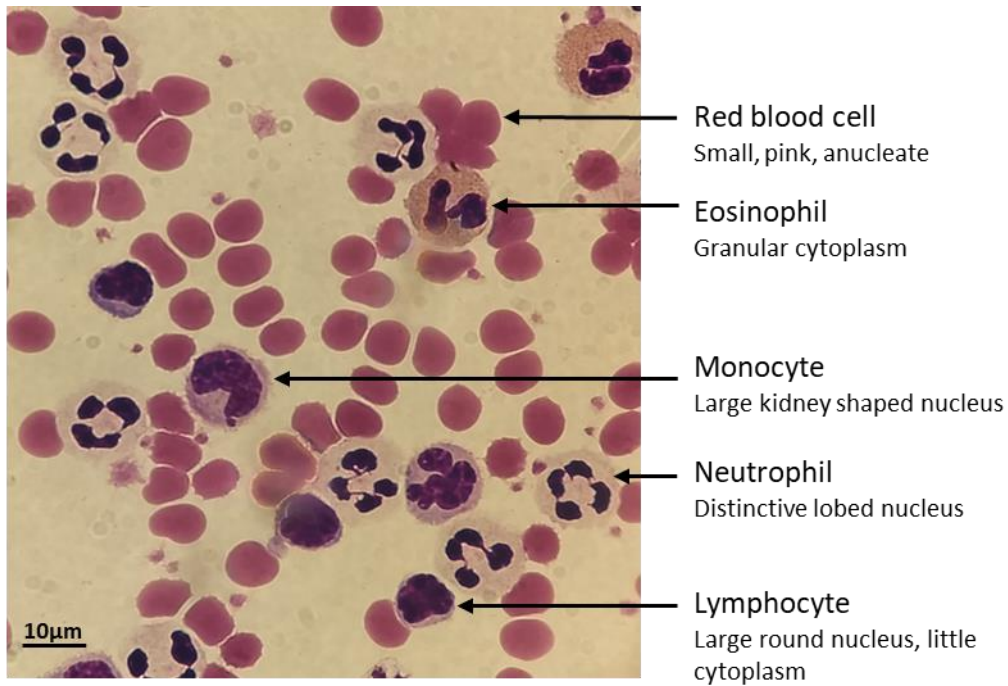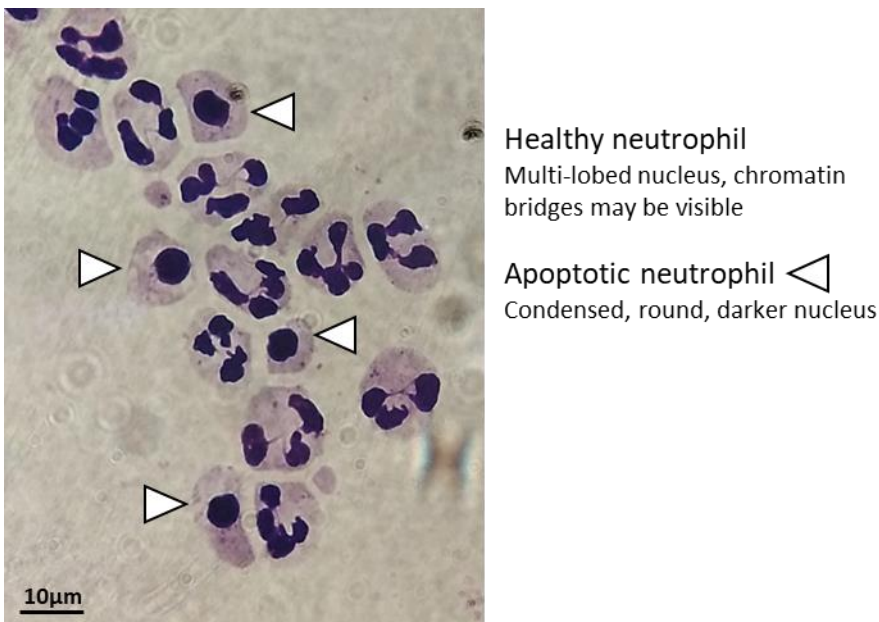
Figure 2.2. Identification of blood cells, and neutrophil apoptosis, by morphology.
Neutrophils, monocytes, eosinophils, lymphocytes and red blood cells are all identifiable based on their morphology when stained with Kwik-Diff (A). Image from the leukocyte isolation stage of the antibody-mediated negative selection neutrophil isolation, after the depletion of red blood cells (although some remain) but before enrichment for neutrophils. Neutrophil apoptosis can also be assessed using this stain, based on the morphology of the nucleus (B).

2.1.6 Mass spectrometry-based phosphoproteomics analysis of human neutrophils

Neutrophils obtained for phosphoproteomics analysis by mass spectrometry were isolated using the antibody-mediated negative selection kit, as detailed in 2.1.3. Neutrophils isolated from each donor were split into two samples of 15 million cells each and treated with 25μM neratinib or equivalent concentration (v/v) DMSO, and incubated for 1 hour at 37°C and 5% CO_2. All samples were then treated with 500μM db-cAMP for 30 minutes in the same incubation conditions. After incubation, samples were centrifuged at 400g for 3 minutes at 4°C to pellet the neutrophils, placed on ice and the cell pellet resuspended in 1mL ice-cold PBS. Cells were centrifuged again at 400g for 3 minutes at 4°C, the PBS supernatant removed, and cell pellets stored immediately at -80°C.

From this point, sample preparation and analysis by mass spectrometry was kindly carried out by Dr Mark Collins within the Faculty of Science Mass Spectrometry Centre at the University of Sheffield. To extract protein from samples, the following extraction buffer was added to the neutrophil pellets: 5% SDS, 50mM TEAB buffer, 50mM NaF, 50mM β-glyercophosphate, 10mM sodium orthovanadate, 1mM PMSF, and 5% Protease Inhibitor Cocktail Set III (Calbiochem, catalogue 535140) made up in HPLC-grade water. Neutrophil pellets were pipetted to mix, and DNA was sheared using a homogeniser. Samples were incubated at 70°C for 15 minutes, homogenised again and incubated for a further 5 minutes, or until no cellular material was visible. Samples were centrifuged at 16,000g to pellet any cell debris, and supernatants transferred to fresh Eppendorf tubes. At this point, aliquots were taken to measure protein concentration using a Pierce™ BCA Protein Assay Kit (Thermo Scientific™, 23225) as per kit instructions. Remaining samples were reduced with 10mM TCEP and alkylated with iodoacetamide.

Protein purification was carried out using suspension trapping (S-Trap™) columns which contain a protein-binding matrix (Protifi, K02-Micro-10). To each 120μL protein extract, 12μL 12% phosphoric acid and 840μL binding buffer (90% methanol, 100mM TEAB buffer) was added. Samples were transferred to the top chamber of an S-Trap™ spin column and centrifuged at 4000g for 15 seconds. The proteins (now "trapped" in the matrix) were washed four times by adding 400μL binding buffer to the column and centrifuging as before, to elute any impurities. The protein-binding matrix from the S-Trap™ spin column was transferred to a fresh Eppendorf for protein digestion. Proteins were digested into peptides by adding 12μL of 1:10 Trypsin Gold (Promega, V528A) in 50mM TEAB to each sample, and spinning briefly in a bench top centrifuge to push the trypsin into the matrix. Samples were incubated at 47°C for 1 hour. Peptides were then eluted from the matrix by adding 80μL 50mM TEAB, centrifuging at 1000g for 30 seconds, followed by 80μL 0.2% formic acid solution and

centrifuging again at 1000g for 30 seconds. Peptides were then desalted using Sep-Pak® Light C18 Cartridge (Waters, WAT023501) and dried down using a SpeedVac (Thermo Scientific).

Immobilised metal affinity chromatography (IMAC) was used to enrich samples for phosphorylated peptides, by firstly resuspending peptides in IMAC loading buffer (1M glycolic acid, 80% acetonitrile, 5% trifluoroacetic acid) and centrifuging at 1000rpm for 5 minutes at room temperature. MagReSyn® Ti-IMAC beads (ReSyn Biosciences, MR-THP002) were washed by centrifuging 30μL bead suspension in 500μL IMAC loading buffer for 5 minutes at 500 rpm. Beads were placed in a magnetic rack for 1 minute, and supernatant removed. Peptide samples were added to the beads and incubated for 20 minutes, centrifuging at 1000 rpm, after which supernatant was removed. Three washes were carried out, using 100μL IMAC loading buffer per wash, and phosphorylated peptides were then eluted from the beads with 80μL 1% ammonia. Enriched phosphorylated peptides (phosphopeptides) were acidified with 40μL 10% trifluoroacetic acid.

Phosphopeptides were analysed by high performance liquid chromatography-mass spectrometry, using HPLC column Acclaim® PepMap 100 C18 nano/capillary BioLC (ThermoFisher Scientific, 164535), EASY-Spray column (ThermoFisher Scientific, ES803), and analysis on an Orbitrap Elite™ Hybrid Ion Trap. Raw data was analysed using MaxQuant Version 1.6.10.43 software. Peptide spectra were searched against the human UniProt Knowledgebase (UniProtKB) database, and a false discovery rate (FDR) of 1% was set for peptide identification and FDR 5% for phosphosite localisation.

2.2 Zebrafish larvae as a model of neutrophilic inflammation

2.2.1 Zebrafish maintenance and husbandry

All zebrafish used in these experiments were raised and maintained according to standard protocols (Nüsslein-Volhard and Dahm, 2002) in UK Home Office approved aquaria at the University of Sheffield, according to institutional guidelines. Embryos refer to the stage of development before hatching; after this point, zebrafish are referred to as larvae. No larvae were raised beyond 5.2 days post-fertilisation (dpf), the defined time at which zebrafish are recognised as protected under the Animals (Scientific Procedures) Act (ASPA) and EU Directive (2010/63/EU). No personal license (PIL) was required for work carried out in this thesis, however the nominated delegate personal license holder was Catherine Loynes (PIL: I50A7A353). Work in this thesis was covered by the project license 70/8178, PPL holder: Professor Stephen Renshaw from 2018 – September 2019, and from October 2019 – present, project license P5983040C, PPL holders: Professor Stephen Renshaw and Catherine Loynes.

The transgenic zebrafish line *TgBAC(mpx:EGFP)i114*, in which neutrophils express green-fluorescent protein (GFP) under the myeloid-specific peroxidase (*mpx*) promoter, was used for all experiments (Mathias *et al.*, 2006; Renshaw *et al.*, 2006). For experiments requiring embryos in the single-cell stage, one male and one female adult zebrafish were placed in pair mating tanks overnight, separated by a divider. At 8am the following day dividers were removed and embryos collected after 20 minutes, at which point fertilisation had usually occurred but embryos were still in the single-cell stage. For all other experiments, a marble tank was placed inside a tank of adult zebrafish and embryos collected the following morning. Dead and unfertilised embryos were discarded by immersion in bleach, and healthy embryos maintained in petri dishes containing E3 medium with methylene blue, at 28°C in 14h light/10h dark cycles. Approximately 60 embryos per petri dish were maintained, with dead embryos removed and discarded daily.

Prior to hatching at 2-3 days post-fertilisation, embryos are surrounded by a membranous envelope, the chorion. Manual dechorination was carried out if required by piercing and removing the chorion with clean sharp tweezers. After experiments, embryos or larvae were sacrificed by anaesthetising in 0.017% 3-amino benzoic acid ethyl ester, or 'tricaine', followed by immersion in bleach. Tricaine was also used as an anaesthetic prior to experimental work such as tail fin transection or microscopy.

2.2.2 Injection of CRISPR/Cas9 components into single-cell stage embryos

The generation of zebrafish CRISPR/Cas9-mediated mutants, or "crispants" was used to generate larvae with genetic mutation of *egfra* (referred to as *egfra* crispants), *erbb2* (*erbb2* crispants) or both (double *egfra/erbb2* crispants). *tyrosinase* (*tyr*) crispants, in which the *tyrosinase* gene regulating pigment formation was mutated, were used as a control. Mutations in the gene of interest were induced by injecting three components into single-cell stage zebrafish embryos: synthetic guide RNA, complementary to the gene of interest; Cas9 endonuclease, which creates double-stranded DNA breaks; and trans-activating RNA (tracr) which allows the guide RNA to bind to the Cas9. This complex creates a double-stranded DNA break in the gene of interest, due to the complementary base pairing between the guide RNA and the intended gene target. Cellular DNA repair mechanisms such as non-homologous end joining often result in the insertion or deletion of nucleotides and thus a mutation in the gene, rendering the subsequent protein non-functional (**Figure 2.3**A). This can be visualised when *tyr* is mutated, as larvae often still have some pigment expression (**Figure 2.3**B).

Synthetic guide RNAs for each gene of interest were generated (Table 2.1) using the online tool CHOPCHOP by Dr Katy Henry, a postdoc in the Renshaw lab at the University of Sheffield.

TgBAC(mpx:EGFP)i114 zebrafish embryos in the one-cell stage were injected with a pre-combined injection solution of Cas9 nuclease protein [20µM] (New England Biolabs), tracr [20µM] (Merck) and guide RNA [20µM] (Merck) in a 1:1:1 ratio in sterile Eppendorf tubes. For the generation of double *egfra/erbb2* crispants, injections solutions for each guide were made up separately and then combined in a 1:1 ratio. 0.5µL phenol red was added to each final injection solution for visualisation, and all injection solutions were kept on ice until required.

A)
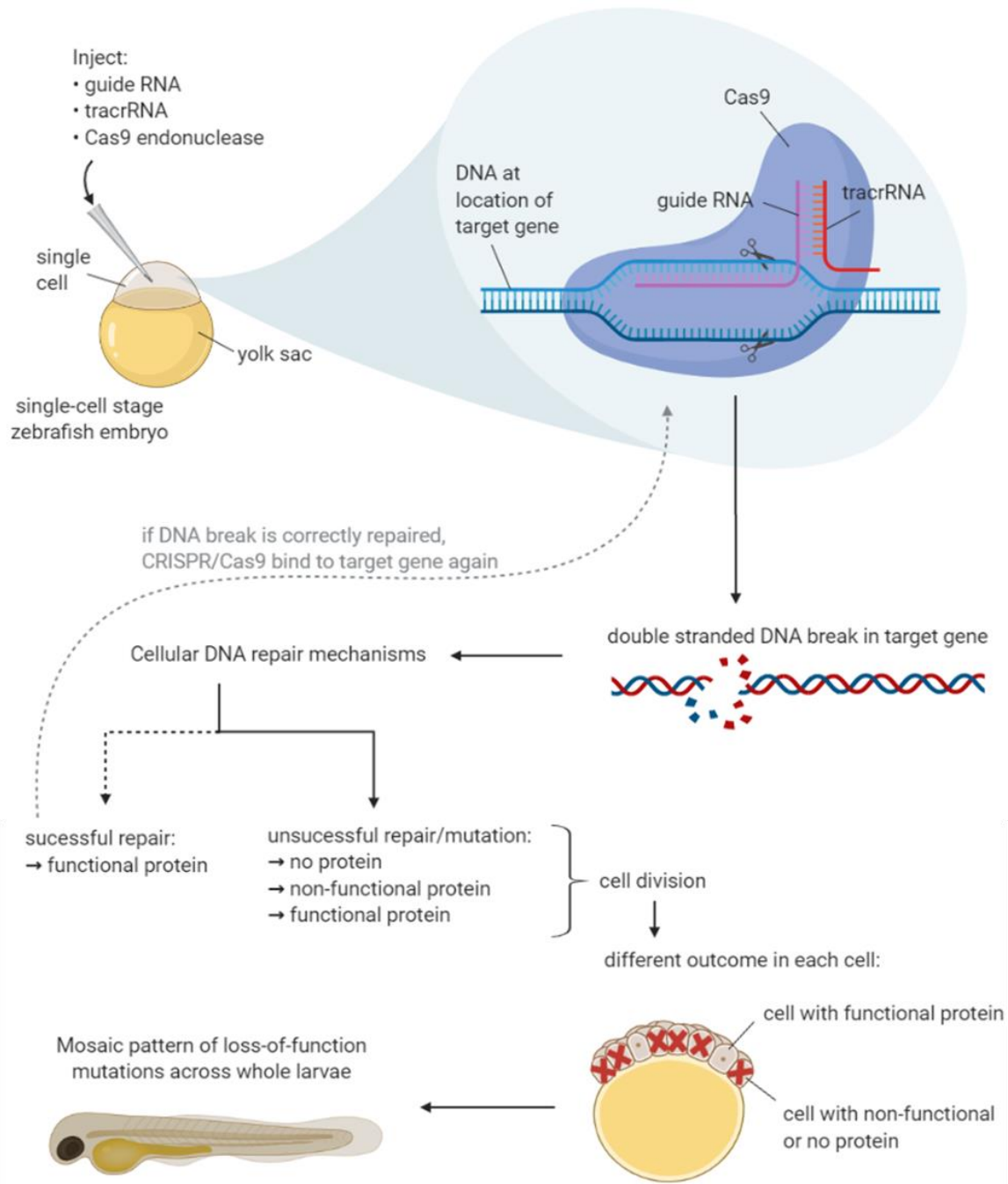
B)

Figure 2.3. Process of generating mutations using transient-expression CRISPR/Cas9.
Schematic diagram of the process of generating CRISPR/Cas9-mediated mutant larvae ("crispants"), generating using BioRender. As a cellular DNA repair mechanisms can have a range of outcomes for the gene, including correct repair, or repair that does not affect the amino acid sequence of the protein, some cells will contain functional protein. However the CRISPR/Cas9 complex can continue to bind to the target gene and induce further mutations, resulting in the likely outcome for the majority of cell being the production of a truncated or non-functional protein. Mutation of the tyrosinase gene results in loss of pigment in zebrafish larvae (B - uninjected control larvae on the left, 2 dpf tyr crispant larvae on the right). Due to mosaic pattern of loss-of-function mutation, some pigment may still be produced, and one batch of injected larvae may show varying degrees of pigmentation.

Injections were performed using a microinjection rig (World Precision Instruments) attached to a dissecting light microscope. A glass capillary needle was calibrated to dispense 0.5nL droplets of each injection solution, using a graticule. Embryos in the 1-cell stage were positioned against a glass microscope slide placed in a petri dish, and 1nL injected into the yolk sac. After injection, embryos were transferred to a petri dish containing clean E3, and maintained at 28°C.

Table 2.1. Synthetic guide RNA sequences

Gene	Sequence
egfra	TGAATCTCGGAGCGCGCAGGAGG
erbb2	AACGCTTTGGACCTACACGTGGG
tyr	GGACUGGAGGACUUCUGGGG

2.2.3   High resolution melt curve analysis to confirm genetic mutation

The appearance of the *tyrosinase* phenotype (reduced pigment formation) was used as an indicator of successful injections and mutation, however high-resolution melt curve analysis was also used to show specific mutation in the gene of interest. This technique can identify a single nucleotide difference in an amplified gene sequence, and thus is suitable for detecting mutations induced by CRISPR/Cas9 (Samarut, Lissouba and Drapeau, 2016). Figure 2.4 shows a schematic diagram of the process. Genomic DNA was collected from whole larvae, which in these experiments were at 2 dpf or 5 dpf. To extract genomic DNA, larvae were anaesthetised with tricaine and placed in individual wells of a 96-well qPCR plate. To each well, 90µL 50mM NaOH was added and the plate incubated at 95°C for 20 minutes. After incubation, 10µL Tris HCl (pH8) was added to each well as a pH buffer. The genomic DNA solution was stored at 4°C until required. High resolution melting curve analysis was carried out in a new qPCR plate, each well containing a master mix of: 0.5µL 10µM each forward and reverse primers (Integrated DNA technologies) (sequences in Table 2.2); 5µL 2X DyNAmo Flash SYBR Green (Thermo Scientific); 3µL MilliQ water. Genomic DNA (1µL per larvae) was added to each well. Samples were run and analysed using Bio-Rad Precision Melt Analysis software.

Table 2.2. Primer sequences used for high resolution melt curve analysis

Gene	Forward primer sequence	Reverse primer sequence
egfra	CCAGCGGTTCGGTTTATTCAG	CGTCTTCGCGTATTCTTGAGG
erbb2	ACAAAGAGCCCAAAAACAGGTTTA	TCCTTCAGTGCATACCCAGA
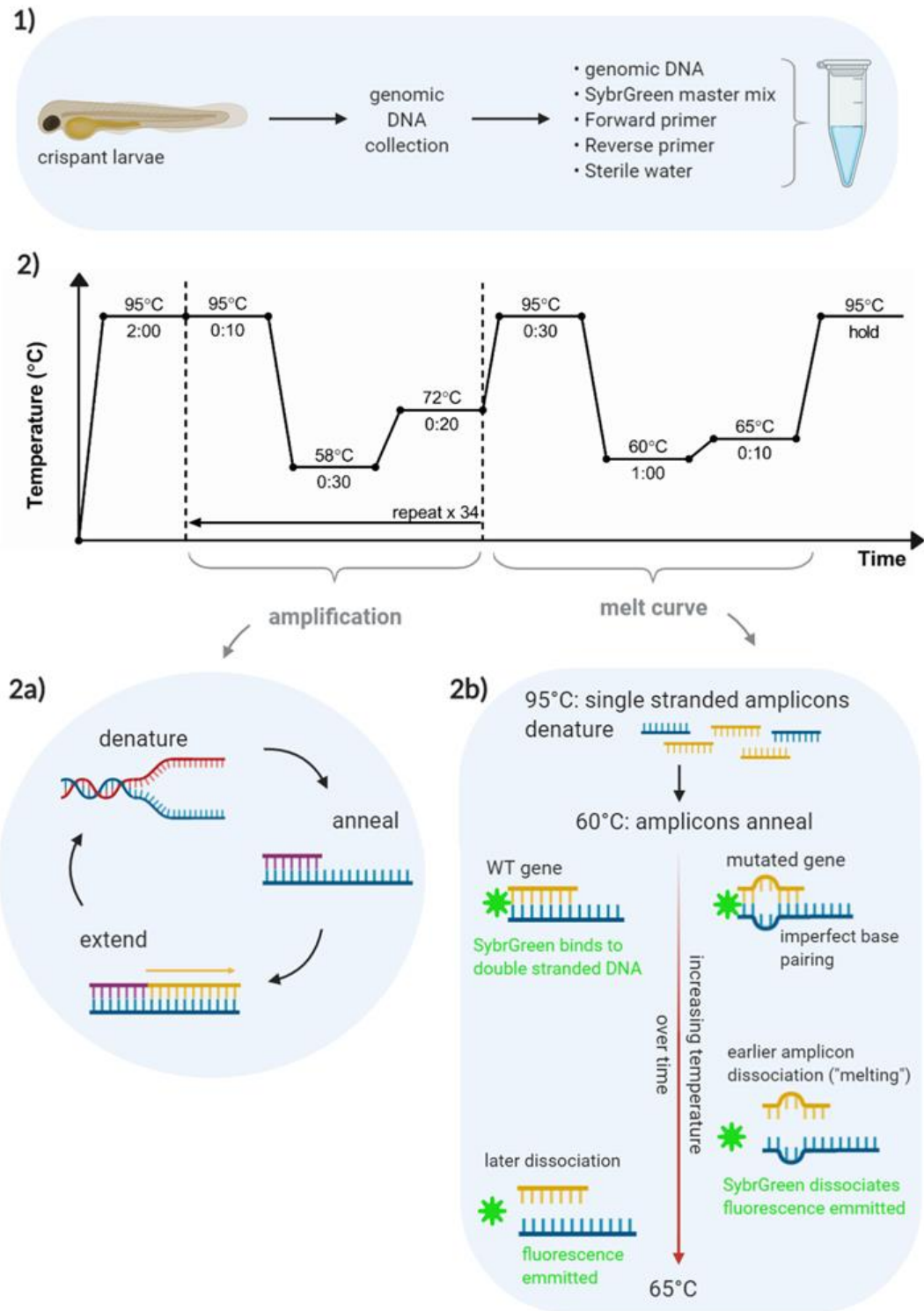
Figure 2.4. Schematic representation of high-resolution melt curve analysis.
After the extraction of genomic DNA (1) and amplification of egfra or erbb2 (2a), a melt curve step is carried out (2b). Mutated genes will imperfectly anneal with the primers and dissociate at an earlier temperature, generating a different melt curve profile to the wild type gene to which the primers were designed to bind perfectly. Created in BioRender.

2.2.4   Treatment of zebrafish larvae with pharmacological inhibitors

For experiments in which larvae were treated with pharmacological inhibitors, embryos were generated by marbling and maintained as described above, and larvae were dechorinated prior to treatment if required. Treatment with pharmacological inhibitors was achieved by immersing larvae in E3 without methylene blue containing inhibitor or control, and incubating at 28°C. This was carried out in 6-well plates, each well containing 6mL of E3 with 10µM inhibitor or equivalent volume DMSO as a control. Each well contained a maximum of 15 larvae. Inhibitors used for experiments were tyrphostin AG825 (Santa Cruz Biotechnology, sc-202045), CP-724,714 (Sigma Aldrich, PZ0335), and neratinib HKI-727 (Selleck, S2150), and DMSO as a control. Larvae were transferred to fresh treatment solution if tricaine was added to the plates (e.g. for tail fin transection or microscopy) or every 24 hours if multiple days of treatment was required (e.g. tail fin regeneration assays).

Larvae undergoing tail fin transection and neutrophil counts or TSA/TUNEL were incubated overnight (16 hours) in compound or control at 28°C, and assays performed the following day at 9am. For tail fin regeneration experiments, tail fin transection was performed at 2 dpf at 5pm, and larvae were then immediately transferred to plates containing compound or control for 48 hours.

2.2.5   Enumeration of total neutrophils in zebrafish larvae

To determine the number of neutrophils across the whole body of zebrafish larvae, larvae were anaesthetised with tricaine and mounted in low-melting point agarose. This was carried out either after 16 hours of treatment with inhibitors, or in crispant larvae at 2 dpf. Images were acquired using a Nikon Eclipse TE2000 U inverted compound fluorescence microscope with NIS-Elements software. Neutrophils were enumerated manually based on GFP expression in cells.

2.2.6   Tail fin transection model of injury-induced inflammation

To assess neutrophilic inflammation *in vivo,* a tail fin transection model of injury-induced inflammation was utilised. Larvae were anaesthetised in tricaine, and complete transection of the tail fin was carried out using a sterile scalpel as described previously (Lieschke *et al.*, 2001; Renshaw *et al.*, 2006). For experiments in which neutrophils were counted at the injury site, or TSA/TUNEL assays, the site of transection was adjacent (but distal to) the circulatory loop (Figure 2.5, orange line), transecting through a section of notochord to induce a large inflammatory response. For tail fin regeneration

assays a smaller amount of tissue was amputated, with the transection site distal to the notochord to allow faster regrowth of the tail fin (Figure 2.5, blue line). After transection, larvae were placed in fresh E3 containing pharmacological inhibitors (or E3 only in the case of crispant larvae) for the remainder of the assay.

To assess neutrophilic inflammation, larvae were anaesthetised and neutrophils at the injury site enumerated using fluorescence microscopy, either using a Leica Fluorescence Stereo Dissecting Microscope or a Nikon Eclipse TE2000 U with NIS-Elements software if images were required. Neutrophils were counted manually based on GFP expression. After counting, larvae were either discarded by complete immersion in bleach, or fixed in 4% paraformaldehyde (PFA) and stored at 4°C for TSA/TUNEL.
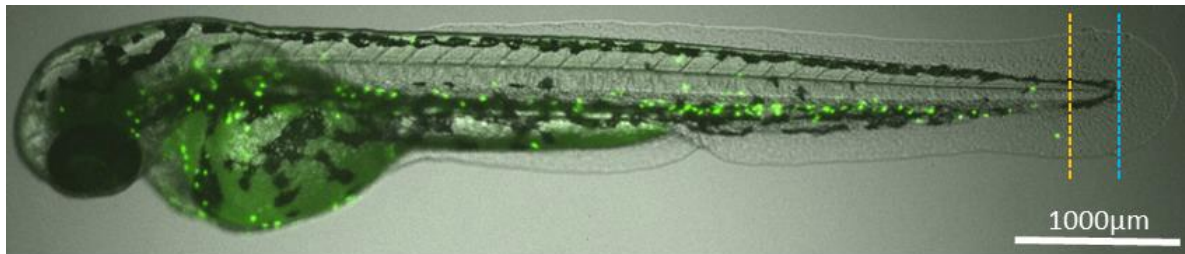
Figure 2.5. Tail fin transection model of injury-induced inflammation.
The tip of the tail fin of zebrafish larvae is completely transected using a sterile scalpel. For assessing neutrophilic inflammation, a larger amount of tissue is amputated (orange line) whereas for tail fin regeneration assays, a smaller amount of tissue is transected (blue line).   Image from 2 dpf *TgBAC(mpx:EGFP)i114* zebrafish larvae, showing GFP-labelled neutrophils in green.

2.2.7   Measuring tail fin regeneration

For tail fin regeneration assays, the tail fin was carefully transected at the end of the pigment (Figure 2.5), which was then used as a reference point for measuring regrowth. Uninjured larvae were also included in each experiment to ensure the treatment did not alter normal tail fin development. After incubation in compound/control for 2 days post-injury, larvae were mounted low melting point agarose, ensuring the tail fin was flat against the coverslip. Brightfield images were acquired using a Nikon TE2000 U and analysed using the open-source platform Fiji. Regrowth was assessed in two ways: the length of the regrown tissue was measured by drawing a straight line from the edge of the pigment to the end of the tail fin (Figure 2.6A). Area of regrown tissue was also measured by tracing the outline of the tail fin, after the point of transection, the area of which is calculated by Fiji (Figure 2.6B).

A)
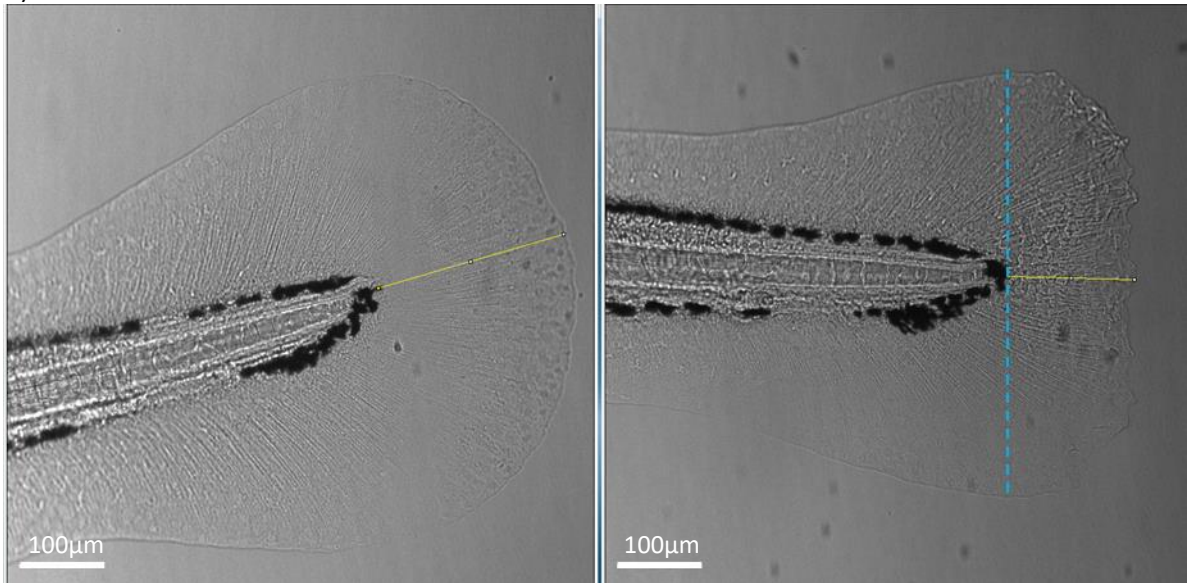
Uninjured – normal tail fin length

Injured – regrown tissue length

B)
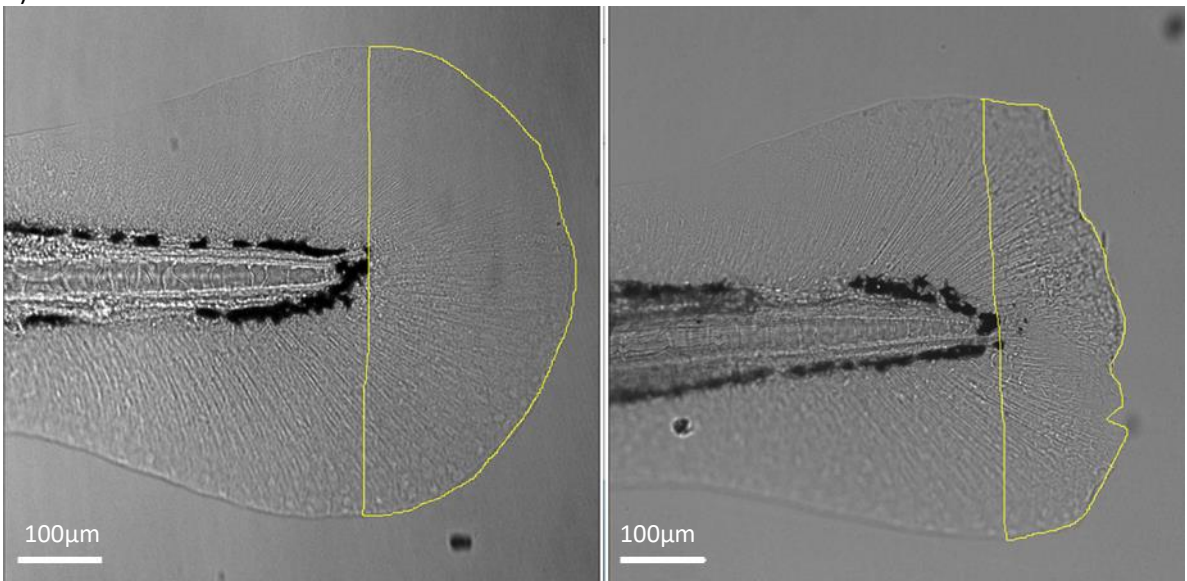
Uninjured – normal tail fin area

Injured – regrown tissue area

Figure 2.6. Assessment of tail fin regeneration in zebrafish larvae.
Tail fin regrowth (or length in uninjured larvae) was measured by two methods; length of regrown tissue (A – yellow line), where the blue line indicates the site of transection in injured larvae. Area of regrown tissue was also assessed (B).

2.2.8 TSA/TUNEL assay for the detection of apoptotic neutrophils in zebrafish larvae

To assess neutrophil apoptosis *in vivo*, TSA/TUNEL assay was carried out on fixed zebrafish larvae. Tyramide Signal Amplification (TSA) detects myeloperoxidase enzymatic activity, and thus neutrophils. Terminal deoxynucleotidyl transferase dUTP nick end labelling (TUNEL) binds to dUTP nick ends, which are generated in DNA by caspase activity during apoptosis, and this was used to detect apoptotic cells. Double TSA/TUNEL positive cells were counted as apoptotic neutrophils. This assay was carried out by the sequential removal and addition of reagents to groups of larvae (inhibitor treated or crispant) in Eppendorf tubes. For each removal step, a small amount of solution was left each tube to prevent larvae from being crushed. All steps were carried out at room temperature unless stated otherwise. Larvae had previously been fixed in 4% PFA at the desired timepoint, and stored at 4°C.

Three 5 minute incubations (washes) in PBS (1mL per Eppendorf) on a rocker were followed by a brief wash in 50µL Amp Diluent, from the TSA® Plus Fluorescein System kit (Perkin Elmer, NEL741E001KT). A 1:50 dilution of FITC TSA in Amp diluent was next added to each Eppendorf, and incubated for 10 minutes at 28°C. From this point, Eppendorfs were covered in aluminium foil for all incubation steps. Three 10 minute washes with PBS were followed by a 20 minute fixation in 4% PFA. Larvae were then stored overnight, remaining in PFA, at 4°C.

After overnight fixation, 10µg/mL Proteinase K was added to larvae, followed by incubation for 75 minutes (2 dpf larvae) or 90 minutes (3 dpf larvae). Two 5 minute PBS washes were followed by 20 minutes of fixation in 4% PFA. Another three 5 minute PBS washes were carried out, after which 50µL Equilibration Buffer from the ApopTag® Red In Situ Apoptosis Detection Kit (Millipore, S7165) was added to each Eppendorf. Larvae were incubated for 1 hour, following which a pre-mixed solution of 16µL TdT Enzyme and 30µL Reaction Buffer from the kit were added to each Eppendorf. Larvae were incubated at 37°C for 90 minutes. Stop Buffer, at 200µL per Eppendorf, was next added followed by a 2 hour incubation at 37°C. Three 5 minute PBS washes followed, after which a pre-combined solution of 62µL anti-Dig Rhodamine antibody and 68µL Blocking Solution was added. Overnight incubation at 4°C followed.

The following day, larvae underwent four 30 minute washes in PBS. A 30 minute fixation step in 4% PFA followed, after which larvae were stored at 4°C. Imaging was carried out within a week, by mounting larvae in low melting point agarose or 80% glycerol. As high magnification is required to identify co-localisation of TSA and TUNEL in a single cell, images were taken either of the tail fin injury site (Figure 2.7), or the caudal haematopoietic tissue. Images were acquired and analysed using UltraVIEWVoX spinning disc confocal laser imaging system with Volocity® 6.3 software (Perkin Elmer).
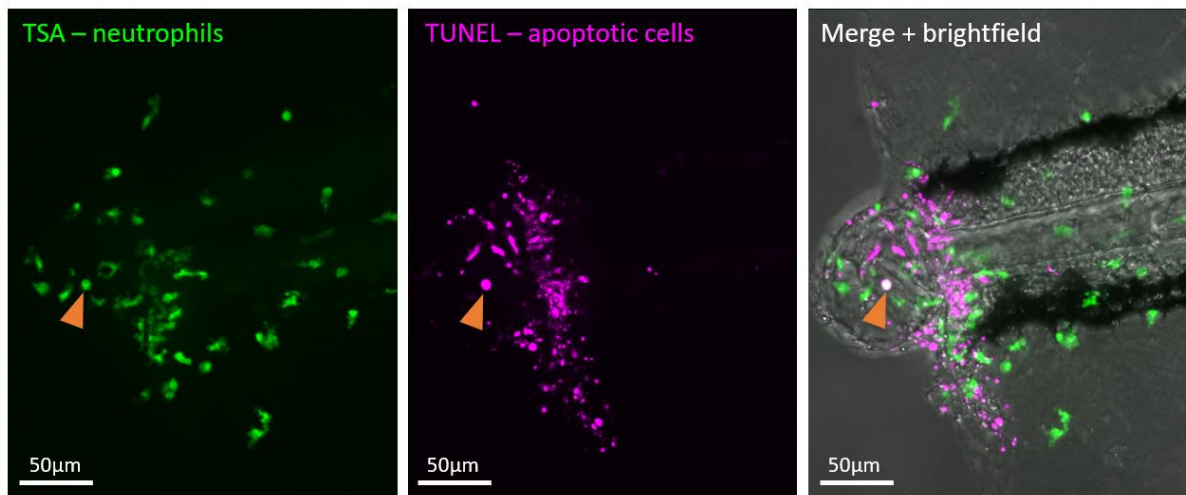
Figure 2.7. Identification of apoptotic neutrophils using TSA/TUNEL.
An apoptotic neutrophil (orange arrowhead) at the tail fin injury site of a zebrafish larvae is identified based on the co-localisation (right panel) of TSA (left panel) and TUNEL (middle panel).

2.2.9 Statistical analysis

Unless stated otherwise, each experiment consisted of groups of 10-15 larvae per condition from the same batch. Each experiment was repeated three times, and final datasets generated from collated data from every larva across the three experiments, containing approximately 30-45 larvae (n=30-45). Due to issues such as a small percentage of larvae dying or developing abnormally, or an imprecise tail fin transection, or imperfect staining during TSA/TUNEL assay, it is often not possible to use data from exactly the same number of larvae in each treatment group, hence the variability. Statistical analysis was carried out on collated datasets. P values indicated in graphs where appropriate. For normally distributed data such as whole body neutrophil counts or tail fin injury neutrophil counts, an unpaired t test was used to compare two groups. For three groups, a one-way ANOVA with Bonferroni's multiple comparisons was used, comparing each treatment condition to the control group (i.e. the DMSO-treated or *tyr* larvae).

Data collected from TSA/TUNEL experiments was not normally distributed, as in many zebrafish larvae no apoptotic neutrophils were detected. Therefore the non-parametric Mann-Whitney test was used to compare two groups, or Kruskal Wallis test for the comparison of three or more groups. In the latter case, Dunn's multiple comparisons test was also used, comparing each treatment group to the control group.

2.3   Mouse models of lung inflammation

2.3.1   Mouse husbandry

Approval for working with a murine model was obtained from the Animal Welfare and Ethical Review Body by the University of Sheffield. Three mouse studies were carried out for this thesis, under the project license (PPL): P4802B8AC, PPL holder: Dr Helen Marriott, personal license holders (PIL): Carl Wright and Dr Helen Marriot. All handling and procedures were kindly carried out by Carl Wright, Dr Helen Marriott and Sam McCaughran (all of the Department of Infection, Immunity and Cardiovascular Disease, University of Sheffield). To adhere to humane end-points, if mice appeared in distress and were not comfortably breathing 24 hours after procedure, or if 20% weight loss were reached, mice were culled to prevent excessive suffering.

2.3.2   Neratinib treatment in an LPS-induced acute lung injury mouse model

Female C57BL/6J mice, aged 9-10 weeks, were split into two groups of 6 mice each. Under anaesthesia (gaseous isoflurane), all animals were administered 7µg lipopolysaccharides from *E. Coli* O26:B6 (LPS – Sigma, L8274) in 50µL PBS, by intranasal delivery. This LPS was used for all mouse experiments. Immediately after, mice in group 1 were administered 200µL vehicle (0.5% methylcellulose + 0.4% Tween-80 + 1% DMSO) by oral gavage. Mice in group 2 were administered 20mg/kg neratinib (ApexBio Technology, A8322 – used in all mouse experiments), dissolved in vehicle, by oral gavage. After 48 hours, all mice were sacrificed by terminal anaesthesia, by intraperitoneal administration of 100µL pentobarbitone, and subject to bronchoalveolar lavage (3x 1mL administrations of PBS). Bronchoalveolar lavage fluid (approximately 2-2.5mL recovered) was placed immediately on ice for analysis.

2.3.3   Neratinib treatment in an LPS/elastase induced chronic lung injury mouse model

Female C57BL/6J mice, aged 10-12 weeks, were split into two groups of 8 mice each. On days 1, 8, 15 and 22, all animals were administered 1.2 units of porcine pancreatic elastase (Merck, 324682-250U) and 7µg LPS in 50µL PBS, by intranasal delivery under anaesthesia. Immediately after each LPS/elastase administration, all mice in group 1 were given 200µL vehicle, and all mice in group 2 administered 20mg/kg neratinib in vehicle by oral gavage. On day 29, all mice were sacrificed by terminal anaesthesia. Blood was collected by inferior vena cava (IVC) bleed, bronchoalveolar lavage

fluid was collected (3x 1mL administrations of PBS) and lungs removed for histology. Bronchoalveolar lavage fluid (approximately 2-2.5mL recovered) was placed immediately on ice for analysis. Blood was collected into EDTA-coated tubes and placed on ice. Lungs were placed into a solution of 4% paraformaldehyde and stored at room temperature until processing for histological analysis.

2.3.4 Neratinib treatment after disease onset in an LPS/elastase induced chronic lung injury model

Female C57BL/6J mice, aged 10-12 weeks, were split into two groups of 8 mice each. Under anaesthesia, all animals were administered 1.2 units elastase and 7μg LPS in 50μL PBS, by intranasal delivery, on days 1, 8, 15 and 22 of the study. On days 15, 16, 17, 18, 19, 22, 23, 24, 25 and 26, mice in group 1 were administered vehicle by oral gavage, and mice in group 2 administered 20mg/kg neratinib in vehicle by oral gavage. On day 29, all mice were sacrificed by terminal anaesthesia. All mice were then subjected to IVC bleed and bronchoalveolar lavage as above. Samples were collected and stored as above.

2.3.5 Analysis of mouse blood samples by automated haematology analyser and separation of plasma

Blood collected into EDTA-coated tubes were gently inverted to ensure thorough mixing of the EDTA with blood and prevent clotting. The majority of each sample was transferred to a fresh labelled Eppendorf, leaving 50μL blood from in each EDTA tube, which was stored at 4°C until analysis by an automated haematology blood analyser. The blood samples in Eppendorf tubes were centrifuged at 350g for 10 minutes at 4°C to separate the plasma from the blood cells. The upper plasma layer was transferred to a fresh Eppendorf and stored immediately at -80°C, for later analysis by ELISA.

Blood samples from the first chronic lung disease mouse study (2.3.3) were analysed using a Sysmex KX-21N™. This machine, normally used for human blood samples, had been adapted in-house to measure parameters from mouse blood cells, including leukocyte concentration, and differential detection of neutrophils, monocytes and lymphocytes. As the only analyser available was at the Northern General Hospital, analysis of blood samples from this study was carried out the following morning after collection of all samples.

For the second chronic lung disease study (2.3.3), blood samples were analysed using a scil Vet abc Plus⁺ automated haematology analyser. This machine was programmed to analyse blood samples from

a range of animals including mice, and was available in the Royal Hallamshire Hospital, so samples could be analysed on the same day they were collected. Data obtained showed leukocyte concentration per sample, and differential white blood cell count identifying concentration and percentage of granulocytes, monocytes, lymphocytes and eosinophils.

2.3.6 Preparation of mouse bronchoalveolar lavage samples for cell counting, microscopy and ELISA

Bronchoalveolar lavage (BAL) samples obtained from mice were transferred into 15mL Falcon tubes, and placed immediately on ice. Samples (remaining on ice) were placed in a Class II safety cabinet. The volume of fluid in each lavage sample was noted. Cells were gently resuspended with a Pasteur pipette, and 10uL of each BAL sample transferred to a haemocytometer chamber for counting. In a centrifuge pre-cooled to 4°C, BAL samples were centrifuged at 400g for 5 minutes to pellet the cells. Supernatant from each lavage fluid sample was transferred to fresh labelled Eppendorfs, and stored immediately at -80°C for later analysis by ELISA. The remaining cells were resuspended in ice-cold PBS at a concentration of 2 million/mL.

Cytospin funnels were assembled and 50uL fetal bovine serum (FBS) was placed into each funnel. From each BAL sample, 50uL was added directly to the FBS in each cytospin funnel, to prevent the cells from breaking during centrifugation. A cytocentrifuge was used to transfer the cells to microscope slides, and slides were fixed and stained with Kwik-Diff as described in 2.1.5.

2.3.7 Preparation of mouse bronchoalveolar lavage for flow cytometry

The cells remaining in each BAL sample were prepared for flow cytometry. For all mouse studies, cells were stained with FITC anti-mouse Ly6G/Ly6C antibody (Biolegend, 108405) to detect neutrophils; PE Annexin V (Biolegend, 640908) which binds to apoptotic cells; and TO-PRO™-3 Iodide (Invitrogen, T3605) a vital dye that only binds to dead cells in which the plasma membrane is broken. All samples were stained with all three markers, and an additional four samples were generated, for one unstained control and three single-stain controls. Still remaining on ice, aliquots of 250,000 cells from the four samples with the most cells remaining were placed into fresh falcon tubes, for the four controls. All samples were centrifuged at 400g for 3 minutes at 4°C to pellet the cells. During this time, Ly6G staining solution was prepared by diluting the FITC-Ly6G antibody 1:200 in FACS buffer (PBS + 10% FBS). Each cell pellet was resuspended in 50uL Ly6G staining solution, or 50uL FACS buffer for the

unstained control and Annexin-V and TO-PRO-3 single stain controls. Samples were incubated on ice, in the dark for 20 minutes.

After incubation, samples were centrifuged at 400g for 3 minutes at 4°C to pellet the cells. After this spin, samples were kept at room temperature. Annexin-V staining solution was prepared by diluting PE-Annexin-V antibody 1:20 with Annexin V Binding Buffer (BioLegend, 422201). BAL samples were resuspended in 50uL of Annexin-V staining solution, or 50uL Annexin V Binding Buffer in the case of the unstained control, and the Ly6G and TO-PRO-3 single stain controls. Samples were incubated in the dark at room temperature for 20 minutes. After incubation, 5uL of TO-PRO-3 solution (diluted 1:1000 in Annexin Binding Buffer) was added to each sample, and samples kept in the dark at room temperature while the flow cytometry analyser was set up (approximately 10 minutes). When samples were ready for analysis, 300uL of Annexin Binding Buffer was added to each sample, to ensure an adequate volume for analysis.

Samples were analysed on a BD LSRII Flow Cytometer using BD FACSDiva™ software. The following parameters were selected for acquisition: forward scatter area (FSC-A), forward scatter height (FSC-H), side scatter area (SSC-A), blue 488nm (FITC detection), blue 575/26Anm (PE detection), red 660/20Anm (TO-PRO-3-PI detection). Cells were gated based on FSC-A/SSC-A profiles and data for 10,000 events within that population acquired. Analysis was carried out using FlowJo software, in which compensation was applied to the PE and FITC parameters.

2.3.8 IL-6 and CXCL1 ELISA

An enzyme-linked immunosorbent assay (ELISA) was used to determine the concentration of cytokines in bronchoalveolar lavage fluid and plasma samples from mice. Kits used were Mouse IL-6 DuoSet ELISA (DY406-05, lot P278762) and Mouse CXCL1/KC DuoSet ELISA (DY453-05, lot P271865). All reagents described below were from these kits. Samples used were either supernatants from mouse bronchoalveolar lavage fluid, or plasma from mouse blood samples. Protocols were followed as per kit instructions, described here in brief. All steps were carried out at room temperature, and for all incubation steps plates were placed on a shaker. Plates were prepared by coating each well with 100μL reconstituted Capture Antibody, sealing the plate with a clear plate seal and incubating overnight. The following day (after approximately 16 hour incubation) plates were washed four times using a LabTech ELx50 Microplate Strip Washer. This automated washer aspirated each well of liquid and replaced it with 400μL Wash Buffer. After the final wash all liquid was aspirated from each well again, and plates were blocked by adding 300uL Reagent Diluent to each well. Plates were incubated for 1 hour. During

this time, samples and standards were prepared. All BAL samples were run neat. Plasma samples were diluted with Reagent Diluent between 1:2 – 1:16, dependant on the volume of plasma available – 100uL per well was required, and plasma sample volumes ranged from 32μL to 270μL. Technical replicates of all samples and standards were used.

After the incubation with the blocking reagent was complete, plates were washed using the plate washer as above. Samples and standards were added to plates, 100μL per well, with Reagent Diluent only used for blank wells. Plates were sealed and incubated for 2 hours, followed by washing using the plate washer. Reconstituted Detection Antibody was added to each well, at 100μL per well, and plates sealed and incubated for 2 hours. Plates were washed using the plate washer. Horseradish peroxidase-conjugated streptavidin was diluted to a working concentration and 100μL added to each well. Plates were sealed, covered in foil to protect from light and incubated for 20 minutes, followed by washing using the plate washer. Substrate Solution was added to the plate, 100μL per well, and plates sealed, covered in foil, and incubated for 20 minutes. After this incubation, 50μL of Stop Solution was added to each well without removing the Substrate Solution, and tapping the plates gently to mix the solutions. Plates were analysed immediately on a Thermo Scientific Varioskan® Flash microplate reader at 450nm, with wavelength correction at 540nm.

Cytokine concentration was calculated using interpolation of a standard curve. The average absorbance value of all blank wells from each plate was calculated, and this value subtracted from all other sample absorbance values, generating an optical density value for each well. A standard curve was generated using GraphPad Prism, using the known concentrations of standards and their optical density readings. Cytokine concentrations from all other samples were calculated by interpolation of the standard curve in Prism, using a 4-parameter logistic sigmoidal curve, as suggested by the ELISA kit instructions. For plasma samples, the dilution factor was then accounted for to calculate the final concentration in samples.

2.3.9 Histological analysis of mouse lung tissue samples

Lung tissue from mouse studies were kindly prepared for histological analysis by Fiona Wright and Sam McCaughran. After at least 48 hours in 4% PFA, lungs were transferred to PBS. Lungs were placed into a tissue cassette and embedded in paraffin wax, and 5μm sections generated and transferred to microscope slides using a microtome. Sections were stained with hematoxylin (Sigma, H3136) and eosin (Sigma, HT110116) (H&E), by moving slides sequentially though a series of reagents, spending

1-2 minutes in each reagent: xylene, 100% ethanol, 90% ethanol, water, hematoxylin, water, 95% ethanol, eosin, 95% ethanol, 100% ethanol, xylene.

Histology slides were analysed on a Nikon Eclipse E600 and images obtained using NIS Elements software. Within NIS Elements, the polygon tool was used to manually trace the edges of individual alveoli. This tool generates a perimeter and area measurement for each shape, which were exported for analysis. Twenty alveoli per mouse, across two sections of lung tissue, were measured.

2.3.10 Statistical analysis

Statistical analysis on the data collected from mouse studies compared the vehicle and neratinib treatment groups. Datasets contained a single data point for each mouse, which in some cases was calculated as an average of technical replicates within the assay (e.g. ELISA), but others was from a single measurement (e.g. leukocyte concentration in blood samples). For normally distributed data, an unpaired t test was used, and for non-normally distributed data, a Mann-Whitney test was used.

3 Genetic and pharmacological inhibition of ErbB signalling in zebrafish larvae alters neutrophilic inflammation

3.1 Introduction and aims

To explore the potential of ErbB inhibitors as novel therapeutics in an inflammatory disease setting, *in vivo* investigations were appropriate. A wealth of literature demonstrates the safety and efficacy of these inhibitors for cancer indications in humans and murine models, however very little research exists on their effect on neutrophils specifically. Previous research from our group identified ErbB inhibitors as inducers of human neutrophil apoptosis *in vitro,* and suppressors of neutrophilic inflammation in zebrafish larvae *in vivo* (Rahman *et al.*, 2019). One of the research questions of this thesis is whether clinically used ErbB inhibitors would be useful to treat aberrant neutrophilic inflammation. Therefore a number of clinical ErbB inhibitors were tested for their efficacy in inducing human neutrophil apoptosis *in vitro*, as well as in experiments with zebrafish larvae.

The zebrafish larvae was selected as a model for studying the effects of inhibiting ErbB signalling on inflammation and immune cell function *in vivo*, with a key advantage over other models being the ability to analyse individual cells *in vivo,* in their tissue microenvironments, in real time. For these studies, the *TgBAC*(*mpx:EGFP*)*i114* zebrafish transgenic line was used, in which green fluorescent protein (GFP) is expressed under the control of the zebrafish myeloid-specific peroxidase (*mpx*) promoter, allowing neutrophils specifically to be identified (Renshaw *et al.*, 2006; Gray *et al.*, 2011).

One key research question investigated in this chapter is whether genetic mutation of the ErbB genes targeted by ErbB inhibitors can also result in reduced neutrophilic inflammation. The complete characterisation of the zebrafish genome and the numerous tools available for genetic manipulation (Howe *et al.*, 2013; Liu *et al.*, 2017) further increased the suitability of the zebrafish for this project. Kinase inhibitors in general, and ErbB inhibitors specifically, are known to induce off-target effects in some systems (Boehrer *et al.*, 2008; Yamaura *et al.*, 2014; Bhullar *et al.*, 2018). This is likely due to the highly conserved ATP-binding domain within kinases that are the binding site of a number of these inhibitors, including all ErbB inhibitors used in this thesis (Bhullar *et al.*, 2018). Another potential issue is that although ErbB inhibitors are often, although not always, selective for at least one of the four ErbB family members in humans, and interactions with other family members with lower selectivity is common. Genetic loss-of-function mutation of individual ErbB family members may therefore provide further insight into whether inhibition of one particular ErbB family member is inducing the particular phenotypes observed.

Transient-expression CRISPR/Cas9 mediated genetic knockdown was chosen for these experiments for several reasons. The relative ease and speed at which transient-expression CRISPR/Cas9 mutant larvae (referred to as "crispants" or "crispant larvae") can be generated and used in subsequent assays, before the 120 hours post-fertilisation (hpf) protected life stage, averts the need to carry out regulated procedural work on protected animals. The mosaic loss-of-function mutation patterns in these larvae (**Figure 2.3**) is also hypothesised to be more similar to the effects of pharmacological ErbB inhibitor treatment, in comparison to complete loss of function that would be observed in a stable homozygous mutant. However, this hypothesis has not been investigated further in this work. For this research, zebrafish larvae with mutation of *egfra* or *erbb2*, or both simultaneously (*egfra/erbb2* double crispant larvae) were used. These are referred to collectively as "ErbB crispant larvae".

Other than *erbb2*, all ErbB family members are duplicated in zebrafish, but although *egfrb* has been described, it has not been mapped and no data is available on homology to human EGFR (Reischauer *et al.*, 2009; Ningappa *et al.*, 2015). Zebrafish Egfra protein shares 89% amino acid similarity with human EGFR in the tyrosine kinase domain, 80% similarity in the trans-membrane domain, and 58% similarity in the extracellular domain (Laisney *et al.*, 2010). The UniProt Align tool shows human ERBB2 and zebrafish Erbb2 share 53% similarity in amino acid sequence overall, with 700 identical positions and 258 similar positions, out of 1255 amino acids for the canonical human ERBB2 sequence and 1275 amino acids for the canonical Erbb2 zebrafish sequence (Sievers *et al.*, 2011).

The primary aim of this chapter is to investigate how genetic mutation and pharmacological inhibition of ErbB signalling affects neutrophil phenotypes in zebrafish larvae. An injury-induced inflammation model was used to measure these parameters in an inflammatory environment, as well as in uninjured larvae. In addition to enumerating neutrophils after blockade of ErbB signalling, the detection of apoptotic neutrophils in the zebrafish larvae was carried out. This allowed investigation into whether the pro-apoptotic phenotype of ErbB inhibitors in human neutrophils *in vitro* was recapitulated *in vivo*. As a more global measure of the effect of inhibition of ErbB signalling on injury, tail fin tissue regrowth after injury was also assessed in the presence of ErbB inhibitors.

3.2 Pharmacological ErbB inhibitors induce human neutrophil apoptosis *in vitro*

Previous research in my group demonstrated the efficacy of a number of pharmacological ErbB inhibitors, including tyrphostin AG825, CP-724,714, and erbstatin, to induce human neutrophil apoptosis in a dose-dependent manner, as well as reduce neutrophil number at the tail fin injury site of zebrafish larvae (Rahman *et al.*, 2019). These ErbB inhibitors are used only for research purposes,

and it was decided that a number of clinically-used ErbB inhibitors should also be tested in human neutrophils *in vitro* to determine if apoptosis is similarly induced, prior to using them for *in vivo* experiments. Four were selected: neratinib, gefitinib and lapatinib, all of which are used clinically, and sapitinib, which is currently in clinical trials (Table 1.2). A range of doses of each drug were incubated with human neutrophils for 6 hours, after which apoptosis was assessed by morphology. Both neratinib and gefitinib induced neutrophil apoptosis to statistically significant degrees, from a percentage neutrophil apoptosis of 14.30 ± 4.46 (mean ± standard deviation) in the DMSO control to 50.17 ± 6.40 with 50μm neratinib (Figure 3.1A), and 11.00 ± 9.25 in the DMSO control to 25.15 ± 12.61 with 50μm gefitinib (Figure 3.1B). Lapatinib and sapitinib treatment caused no significant increase in percentage apoptosis (Figure 3.1C-D). As neratinib appeared the most efficacious at inducing human neutrophil apoptosis, this drug was selected as a clinical ErbB inhibitor for experiments in the zebrafish larvae.
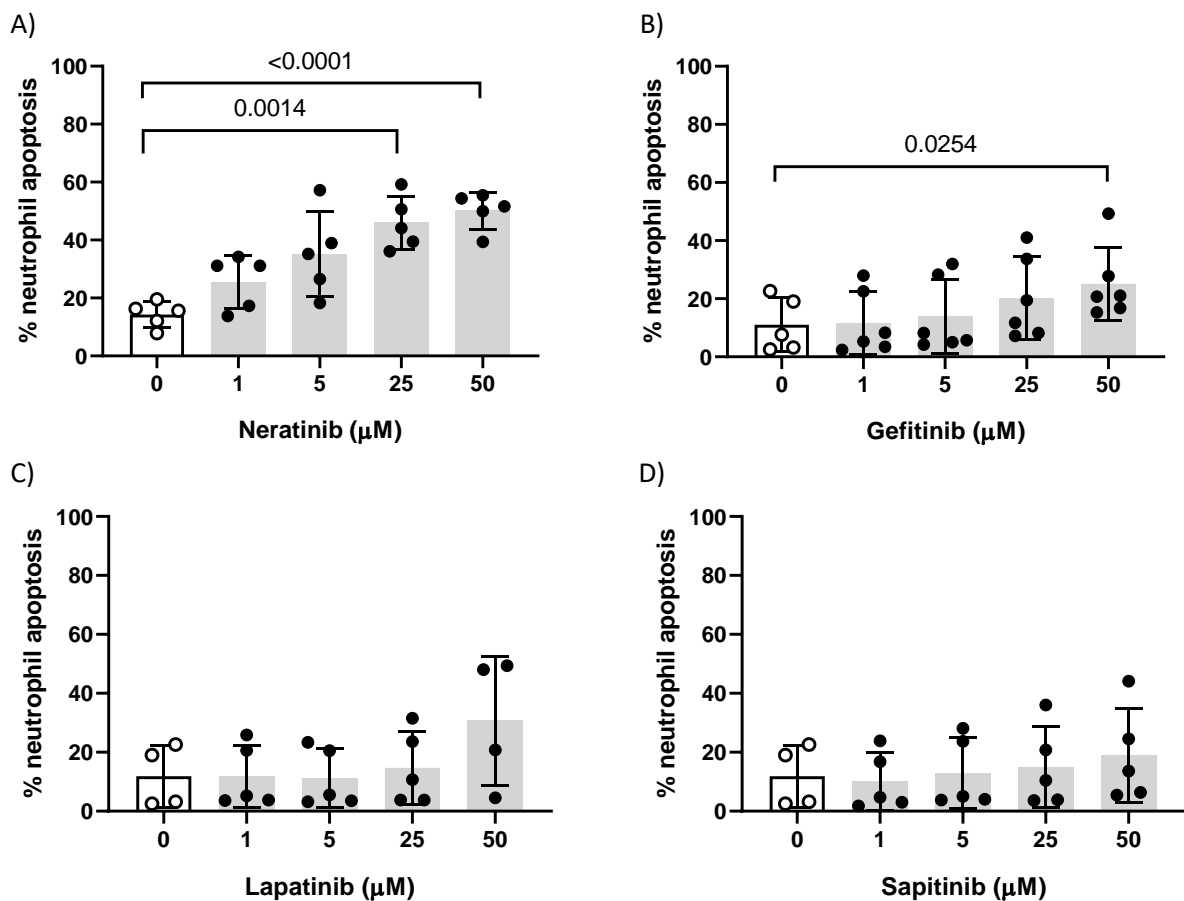
Figure 3.1. Human neutrophil apoptosis is induced by gefitinib and neratinib treatment.
Human neutrophils were treated with the ErbB inhibitors neratinib (A), gefitinib (B), lapatinib (C) and sapitinib (D) at a range of doses, and apoptosis assessed by morphology after 6 hours of treatment. DMSO (control) labelled as 0. Bars show mean, error bars show standard deviation. Each data point represents data from one biological replicate (neutrophil donor), n=4-6. One-way ANOVA with Dunnett's multiple comparisons used to analyse the data, with repeated measured to match data points from each biological replicate, p values shown where p<0.05.

3.3   Confirming genetic mutation in crispant zebrafish larvae by high resolution melt curve analysis

Tyrphostin AG825 and CP-724,714, which were shown by previous members of my group to reduce neutrophilic inflammation in the zebrafish larvae, are selective for ErbB2, but also target EGFR. Neratinib targets both EGFR and ErbB2 (Table 1.2), and therefore zebrafish genes *egfra* and *erbb2* were selected for mutation in larvae. Transient-expression CRISPR/Cas9 was used to achieve this, by injecting the components of the CRISPR/Cas9 system (guide RNA, tracrRNA, and Cas9 endonuclease) into zebrafish embryos in the single-cell stage, generating larvae ("crispants") with mosaic loss-of-function mutation patterns across the whole organism (**Figure 2.3**). In all experiments utilising crispants, the control group was comprised of larvae with transient-expression CRISPR/Cas9-induced mutation in the *tyrosinase* (*tyr*) gene, which results in a loss of pigment. The appearance of this albino phenotype indicates successful injections in this group, and although this cannot be extrapolated to assume that injections of other groups were also successful, it at least confirms that the aliquots of Cas9 protein and tracrRNA used for those particular injections were functional. However as neither *egfra*, *erbb2* or *egfra/erbb2* double crispants display such a phenotype, high resolution melt curve (referred to as "melt curve") analysis was used to confirm successful mutation.

Melt curve analysis is a PCR-based reaction that exploits the differences in dissociation rates of amplicon dimer binding in wild-type vs mutated DNA (detailed in Figure 2.4). This was carried out using genomic DNA extracted from a selection of 2 days post-fertilisation (dpf) crispant larvae, after single-cell injections to generate *tyr*, *egfra* and *erbb2* crispants, and *egfra/erbb2* double crispants (in which both *egfra and erbb2* are mutated simultaneously). The mutation rate of each crispant group was calculated based on the percentage of larvae in a particular injection group that showed an *egfra* or *erbb2* melt curve profile different to that of the *tyr* control group. Results indicate that the average successful mutation rate for a group of injected larvae was 73% in *egfra* crispants (n=4 experiments), 84% in *erbb2* crispants (n=4), and 98% and 90% (*egfra* and *erbb2* mutations respectively), in *egfra/erbb2* double crispants (n=6) (Figure 3.2). Although this indicates that a portion of larvae within each group will not have the intended mutation, creating more "noise" in the data, the average mutagenesis efficacy was considered high enough to be sufficient for assays.

It should be taken into account that melt curve analysis indicates differences in genomic DNA sequence; it does not indicate whether that mutation results in a non-functional gene product. In these experiments, a difference in mutation rate was assumed to correlate with non-functional ErbB

A)
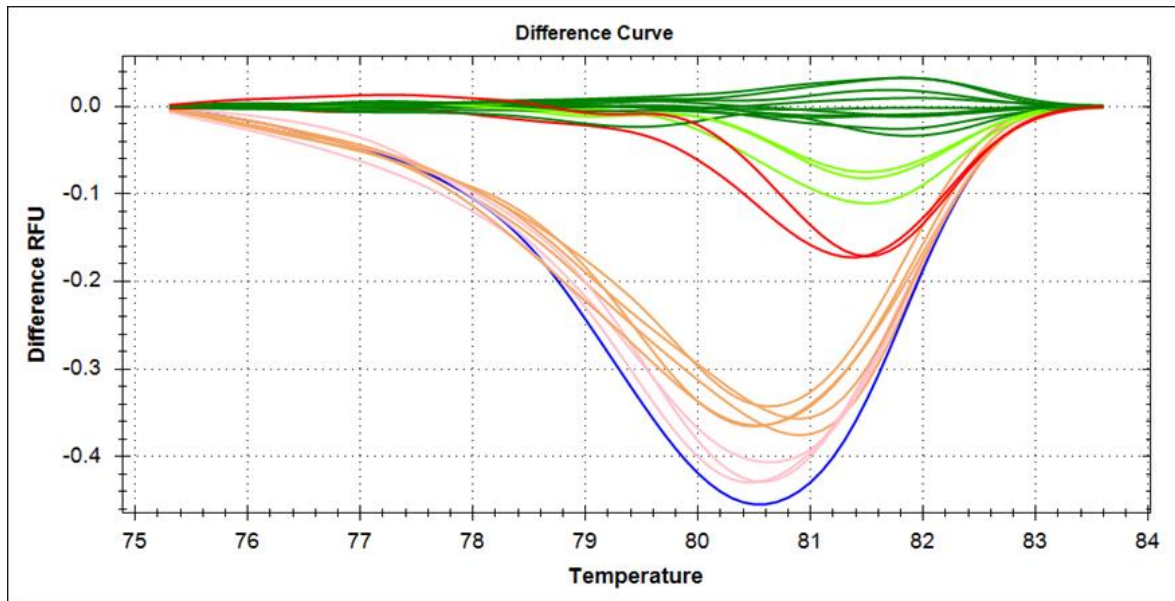
B)

Well	Sample	Cluster	Percentage confidence
A02	*tyr*	Cluster 02	99.5
A03	*tyr*	Cluster 02	97.9
A04	*tyr*	Cluster 02	97.8
A06	*tyr*	Cluster 02	99.3
A07	*tyr*	Cluster 02	99.3
A08	*tyr*	Cluster 02	99.6
A09	*tyr*	Cluster 02	89.1
A10	*tyr*	Cluster 02	97.2
B02	*egfra*	Cluster 02	99.3
B03	*egfra*	Cluster 02	99.0
B01	*egfra*	Cluster 04	98.3
B05	*egfra*	Cluster 04	97.7
B09	*egfra*	Cluster 04	98.2
B10	*egfra*	Cluster 04	97.8
B12	*egfra*	Cluster 04	92.3
B06	*egfra*	Cluster 05	95.6
B07	*egfra*	Cluster 05	89.8
B08	*egfra*	Cluster 05	95.8
A05	*tyr*	Cluster 06	93.3
A11	*tyr*	Cluster 06	98.3
B04	*egfra*	Cluster 06	97.0
A01	*tyr*	Cluster 08	98.0
A12	*tyr*	Cluster 08	99.9
B11	*egfra*	Cluster 10	98.0

C)

- Clusters containing *tyrosinase* larvae: 02, 06, 08
- Other clusters: 04, 05, 10
- Number of *egfra* crispants in *tyrosinase* clusters: 3
- Number of *egfra* crispants in other clusters: 9

Calculation of percentage mutation rate:

((*egfra* in other clusters) / (total *egfra*)) * 100
= (9 / 12) * 100 = 75%

D)

	% egfra mutation (mean ± SD)	% *erbb2* mutation (mean ± SD)
egfra crispants	73.25 ± 19.38	-
erbb2 crispants	-	84.18 ± 14.61
egfra/erbb2 double crispants	98.00 ± 4.47	90.34 ± 17.34

Figure 3.2. Confirming mutation of *egfra* and *erbb2* genes in zebrafish larvae by high resolution melt curve analysis.

Example readout (A) showing the melting curve profiles of genomic DNA isolated from *tyr* and *egfra* crispants. In this example, *egfra* primers were utilised to analyse differences in *egfra* gene sequence between the two crispant groups. Each line represents the melting curve profile of amplified *egfra* from one larva. Melting curve profiles are organised into 'clusters' by the Precision Melt Analysis™ software (B), which represent samples with statistically similar enough melting profiles to be considered to have identical DNA sequences (confidence intervals in far right column). Calculation of percentage mutation rate in this experiment showed 75% mutation rate in *egfra* crispants (C). Collated data showed an average mutation rate for all crispants to be between 73-100% (D). n=4 groups of *egfra* and *erbb2* crispants analysed, n=6 *egfra/erbb2* double crispant groups.

62

product. This is demonstrated in the *tyr* crispants by the presence of the albino phenotype, although further validation, such as whole-mount *in situ* hybridisation, would be useful to confirm.

As this method of identifying mutations in ErbB genes relies on *tyr* crispant larvae expressing the wild-type ErbB gene, the melt curve profiles *egfra* and *erbb2* genes in uninjected larvae and *tyr* crispants were compared. No differences in the melt curve profile of these genes were observed (data not shown). Previous research in our group also demonstrated no difference in whole body neutrophil count, or in neutrophil number at the injury site after tail fin transection between *tyr* larvae and uninjected control larvae, further validating the use of *tyr* crispants as a control (Isles *et al.*, 2019).

In early experiments, a selection of larvae from each group of crispants (*egfra, erbb2* or *egfra/erbb2* double crispant larvae) underwent melt curve analysis. After genetic mutation of the intended gene was confirmed in a series of successful injections, this technique was performed only on selected experiments going forward. Although it would be possible to carry out melt curve analysis on every larva used in experiments, and exclude data from those without the intended mutation, this would take significant amounts of time and resources. Not genotyping every larva results in the inclusion of data from non-mutant larvae, increasing the "noise" of the data, however results gathered from these experiments demonstrate that this is not enough to mask differences between groups, when they are present.

3.4 Genetic, but not pharmacological, inhibition of ErbB signalling reduces neutrophil number across the whole body of zebrafish larvae

In human neutrophils *in vitro*, ErbB inhibitors induce apoptosis. Initial experiments using zebrafish larvae aimed to determine whether inhibition of ErbB signalling affected the total number of neutrophils across the whole body of zebrafish larvae. There are several reasons why neutrophil number may be increased or reduced: a change in neutrophil production, an increase in neutrophil death, a global delay in larval development. This measure cannot determine which of these mechanisms may be responsible, however it is a simple indicator of whether neutrophil numbers are affected by inhibition of ErbB signalling in homeostatic conditions, under normal larval development. For these experiments, the clinical inhibitor neratinib, and the research use ErbB inhibitors used previously by my group, tyrphostin AG825 and CP-724,714, were utilised.

3.4.1 Treatment of zebrafish larvae with ErbB inhibitors does not affect total neutrophil number

To determine whether treatment with ErbB inhibitors alters total neutrophil number, *TgBAC(mpx:EGFP)i114* zebrafish larvae were used. The concentration of inhibitors (10 µM) was selected based on initial preliminary experiments, with larvae showing no visible abnormalities after treatment (data not shown). At 2.5 dpf, larvae were treated with 10 µM inhibitor or equivalent volume DMSO by adding the compounds to the E3 in which larvae were immersed. After 16 hours of treatment neutrophils were counted manually based on GFP expression using fluorescence microscopy (Figure 3.3A). No changes in neutrophil number were observed after treatment with either the research use ErbB inhibitors tyrphostin AG825 (mean ± standard deviation 171.0 ± 41.44) or CP-724,714 (164.2 ± 32.82) in comparison to the DMSO control (173.2 ± 46.22) (Figure 3.3B), or the clinical ErbB inhibitor neratinib (181.1 ± 29.19) in comparison to the DMSO control (180.5 ± 30.76) (Figure 3.3C).

A)
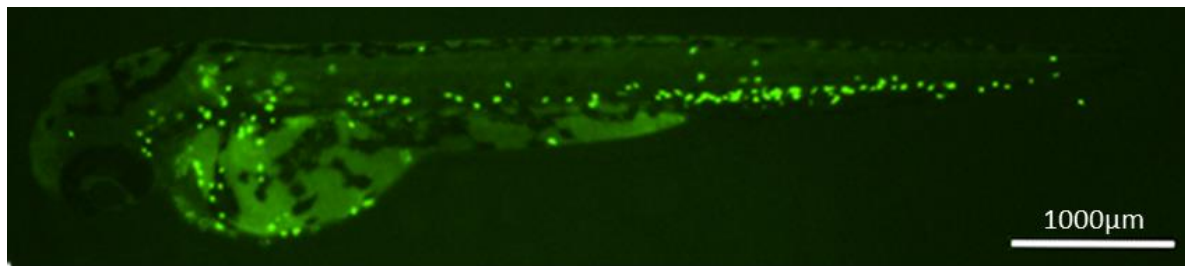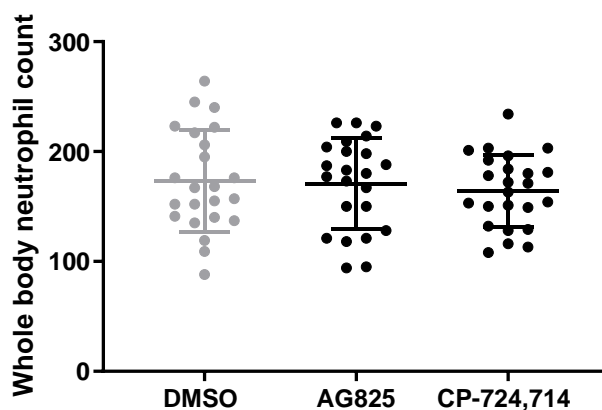
B) C)
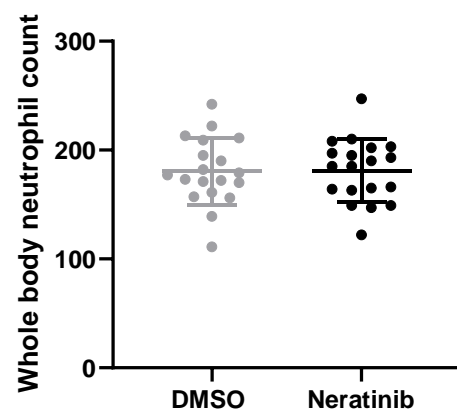
Figure 3.3. Whole body neutrophil counts are unchanged with ErbB inhibitor treatment.
Total number of neutrophils across the whole body of zebrafish larvae were counted by fluorescence microscopy, with each GFP-expressing (green) cell indicating one neutrophil (A). Neutrophil number was unchanged after 16h treatment with 10 µM tyrphostin AG825 or CP-724,714 (B), or 10 µM neratinib (C), in comparison to DMSO-treated larvae. Minimum 20 larvae per group across three independent experiments. Each data point represents one larva. Bars show mean ± SD. No statistically significant differences measured using one-way ANOVA with Bonferroni's multiple comparison post-test (B) or unpaired t test (C).

3.4.2 *egfra, erbb2* and *egfra/erbb2* double crispant larvae have a reduction in whole body neutrophil number

To determine whether genetic mutation of ErbB genes from the single-cell stage affects total neutrophil number across the whole body of zebrafish larvae, transient-expression CRISPR/Cas9 was used. Initial experiments used zebrafish larvae in which either *egfra* or *erbb2* was mutated, to determine if mutation of one particular ErbB family member resulted in a change in neutrophil number. However as the ErbB inhibitor neratinib targets both ErbB family members, larvae in which *egfra* and *erbb2* are mutated simultaneously were also generated (double *egfra/erbb2* crispant larvae).

After injection of the CRISPR/Cas9 components into single-cell embryos of the *TgBAC*(*mpx:EGFP*)*i114* line, larvae were left to develop to 2 dpf, at which point neutrophils were enumerated by fluorescence microscopy. At 2 dpf, both single crispant larvae had significantly reduced neutrophil numbers, at 87.39 ± 22.48 (mean ± standard deviation) in *egfra* crispants, 93.17 ± 23.75 in *erbb2* crispants, in comparison to 114.80 ± 21.19 in control *tyr* crispants (Figure 3.4A). Double *egfra/erbb2* crispant larvae similarly had significantly reduced numbers of neutrophils (97.55 ± 23.93) in comparison to control *tyr* larvae (119.30 ± 22.06) (Figure 3.4B). This suggests that blockade of *egfra* and *erbb2* signalling from the single-cell stage in zebrafish is affecting neutrophil biology in some manner.

There are many potential biological mechanisms that could be resulting in the reduction in total neutrophil number in ErbB crispant larvae, but not with ErbB inhibitor treatment, addressed in the Chapter Discussion. One of the mechanisms investigated here was whether the reduction in total neutrophil number is part of a global developmental defect in ErbB crispant larvae. This was partially addressed by observing *egfra/erbb2* double crispant larvae at 5 dpf. No obvious morphological changes were observed compared to uninjected controls. Swim bladder development, used as an indicator of normal development in these larvae, was also unchanged in comparison to uninjected control larvae (data not shown). It cannot be concluded that no developmental defects are present in these larvae based on this parameter alone, however these results suggest that the suppression of ErbB signalling does not result in any gross morphological changes before 5 dpf.
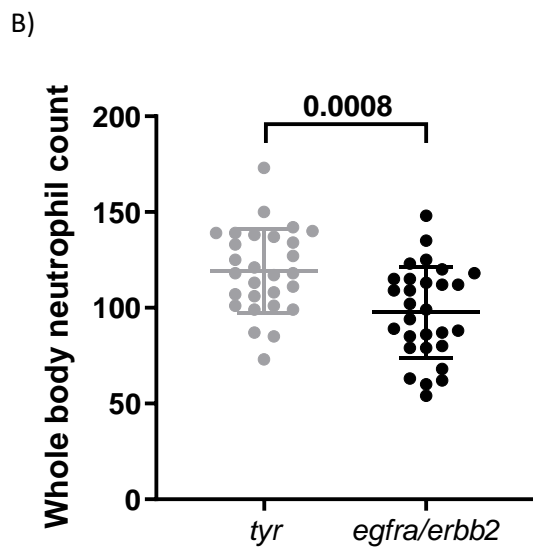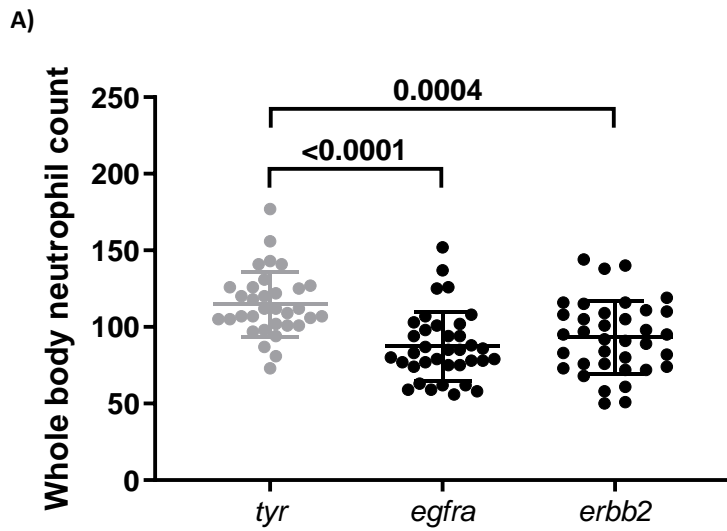
Figure 3.4. Whole body neutrophil count is reduced in *egfra* and *erbb2* crispant zebrafish larvae at 2 dpf. Whole body neutrophil count based on GFP expression was reduced in uninjured *egfra* and *erbb2* crispant larvae (A), and in double *egfra/erbb2* crispant larvae (B), compared to *tyr* control larvae at 2 dpf. Results representative of at least 30 larvae per condition across three independent experiments. Each data point represents data from one larva. Bars show mean ± SD. Significance calculated using one-way ANOVA with Bonferroni's multiple comparisons post-test (A) or unpaired t test (B); p values indicated.

3.5 Genetic and pharmacological inhibition of ErbB signalling alters neutrophil numbers in an inflammatory environment in zebrafish larvae

As the zebrafish has increased its popularity as a model of choice for biomedical research, a number of well-established protocols have been generated to create an inflammatory environment, in which the behaviour of primitive neutrophils and macrophages can be studied in real time *in vivo*. The tail fin transection model of injury-induced inflammation is one such model, in which transection of the tail fin of zebrafish larvae creates an injury site to which neutrophils and macrophages are recruited. The neutrophilic response to this particular injury is well documented, with neutrophil migration toward the injury site taking place over approximately 6 hours, after which neutrophil numbers deplete by reverse migration or apoptosis, indicating the onset of inflammation resolution (Renshaw *et al.*, 2006). For experiments in this chapter, neutrophils at the injury site are counted at 4 hours post-injury (hpi), during the migratory phase of neutrophilic inflammation, and 8 hours post-injury, the resolution phase.

Previous research by our group assessed the impact of pharmacological ErbB inhibitors on neutrophilic inflammation in this model. At 2.5 dpf, zebrafish larvae were treated with the ErbB inhibitors tyrphostin AG825 or CP-724,714 for 16 hours, followed by tail fin transection. Both ErbB inhibitor treated larvae were found to have significantly lower neutrophil numbers at the tail fin injury site, at both 4 and 8 hours post injury (Rahman *et al.*, 2019). Experiments carried out in this section aim to determine if the same phenotype is observed with the clinical ErbB inhibitor neratinib, as well as in larvae in which *egfra* and *erbb2* genes have been mutated using transient expression CRISPR/Cas9.

3.5.1 Treatment of zebrafish larvae with the clinical ErbB inhibitor neratinib reduces the number of neutrophils at the site of inflammation

TgBAC(*mpx:EGFP*)*i114 z*ebrafish larvae at 2.5 dpf were treated with 10 µM neratinib or equivalent concentration (v/v) of DMSO. Tail fin transection was carried out after 16h of treatment, and neutrophils at the tail fin injury site enumerated by fluorescence microscopy (Figure 3.5A). Neratinib treatment reduced the number of neutrophils at the injury site at 4-hours post injury, from 19.73 ± 7.66 (mean ± standard deviation) in control larvae to 15.22 ± 5.69 with neratinib treatment, and at 8-hours post-injury from 20.20 ± 8.36 in control larvae to 15.38 ± 5.85 with neratinib treatment (Figure 3.5B). This recapitulation of the phenotype observed using tyrphostin AG825 and CP-724,714 provides further support that the suppression of ErbB signalling in these larvae is responsible for the reduction in neutrophilic inflammation in this model, rather than an off-target effect of the drugs. However, to

confirm that this phenotype is an ErbB-specific effect, genetic mutation of ErbB genes in zebrafish larvae was carried out.

A)
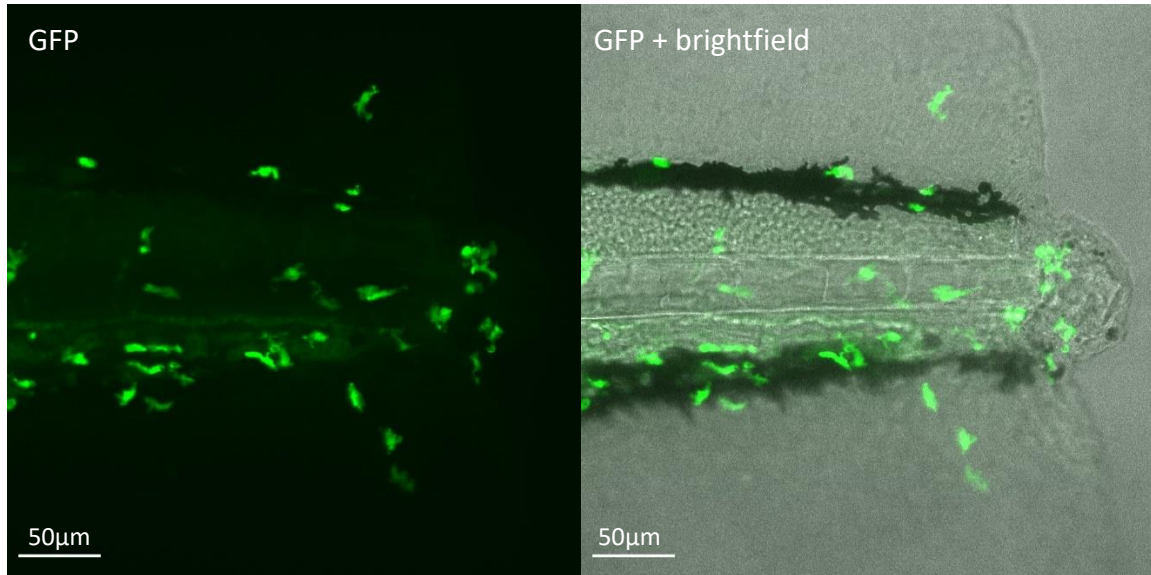
B)
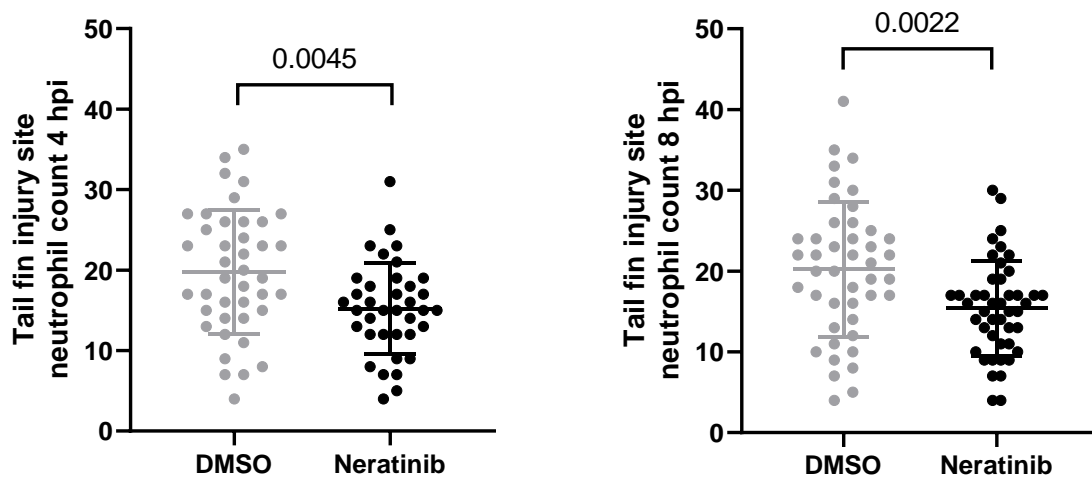
Figure 3.5. Neutrophil number at the tail fin injury site is reduced after 16h treatment with 10µM neratinib. Tail fin transection performed on 3 dpf zebrafish larvae, after 16h treatment with 10 µM neratinib. Neutrophils at the injury site were counted in live larvae at 4 and 8 hpi, based on GFP expression (A). At both timepoints, injury site neutrophil counts are reduced compared to DMSO-treated controls (B). At least 12 larvae per condition across three independent experiments. Each data point represents data from one larva. Bars show mean ± SD. Significance determined by unpaired t test; p values indicated.

3.5.2 Zebrafish larvae with mutation of *egfra* have increased neutrophilic retention at the tail fin injury site

Initial experiments using ErbB crispant larvae aimed to determine if mutation of either *egfra* or *erbb2* was sufficient to reduce neutrophil number at the tail fin injury site of zebrafish larvae. At 2 dpf, the tail fin transection assay was carried out on *egfra*, *erbb2*, and *tyr* crispant larvae, and neutrophils were enumerated at both 4- and 8-hours post injury. There was no change in neutrophil number at the injury site of *egfra* crispants (10.04 ± 4.32) or *erbb2* crispants (13.22 ± 5.75) in comparison to *tyr* control larvae (12.16 ± 5.39) at 4 hpi (Figure 3.6A). Interestingly there was a significant increase in the number of neutrophils in *egfra* crispant larvae (13.54 ± 6.90) at 8 hours post-injury, but not in *erbb2* crispant larvae (14.02 ± 7.32) in comparison to control larvae (10.31 ± 5.20) (Figure 3.6B). The increase in neutrophil retention at the injury site contradicts other experiments in this chapter, and several explanations are proposed (examined further in the chapter discussion), including functional over-compensation of other ErbB receptors after the loss of *egfra*, or mechanisms specific to the first member of the ErbB family that are overridden when other ErbB receptors are also inhibited.

To further investigate the possibility that the increase in neutrophil number at the tail fin injury site in *egfra* crispant larvae is specific to this ErbB family member, this assay was repeated in *egfra*/*erbb2* double crispant larvae. Tail fin transection was carried out at 2 dpf, and neutrophil numbers at the tail fin injury site enumerated as before. A significant reduction in neutrophil number was observed at the injury site of *egfra*/*erbb2* double crispant larvae at 4-hours post injury (8.79 ± 4.26) in comparison to control larvae (12.19 ± 5.43) (Figure 3.7A), and 8-hours post-injury (8.41 ± 5.14) compared to control larvae (12.17 ± 5.82) (Figure 3.7B).

It is important to note that as *egfra*/*erbb2* double crispant larvae also show a reduction in total neutrophil count across the whole body of larvae, it may be that the reduction in neutrophil number at the tail fin injury site is simply a reflection of the reduction in total neutrophil number. However *egfra* and *erbb2* single crispant larvae similarly had a reduction in total neutrophil number, without a corresponding reduction in neutrophil numbers at the site of injury. It is therefore possible that the reduction in total neutrophil number alone may not be enough to explain the reduction in numbers at the injury site. This result also supports the hypothesis that the increase in neutrophil number at the tail fin injury site of *egfra* crispant larvae may be specific to that ErbB family member, and additional inhibition of *erbb2* prevents that phenotype emerging.

The 4-hour post injury timepoint in this assay corresponds to the recruitment phase of neutrophilic inflammation in this particular model. Both pharmacological inhibition and double *egfra*/*erbb2* crispant larvae showed reduced neutrophil numbers at both timepoints measured in this assay,

A)
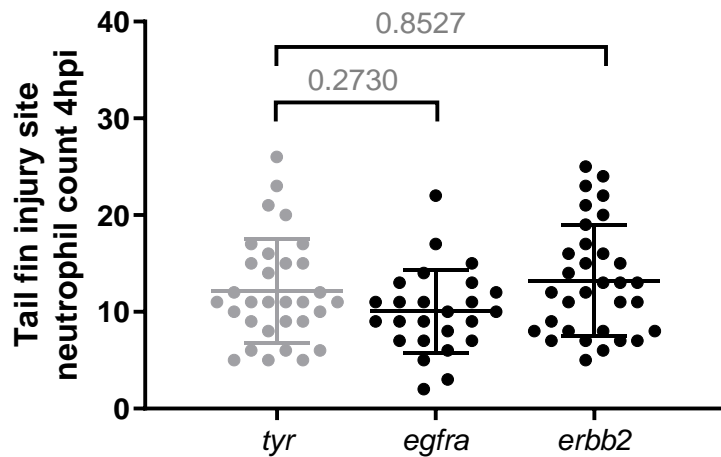
B)
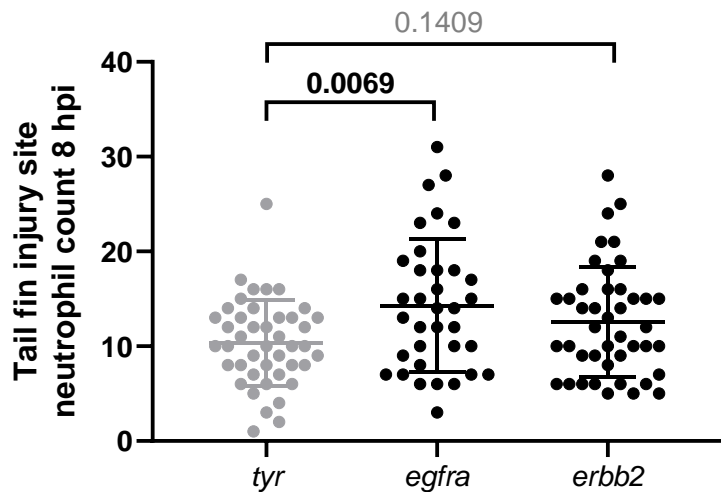
Figure 3.6. *egfra* crispants have increased numbers of neutrophils at the injury site at 8 hpi.
Tail fin transection was carried out on 2 dpf *egfra, erbb2* and *tyr* crispant larvae of the *TgBAC(mpx:EGFP)i114* transgenic line. Neutrophils at the tail fin injury site were enumerated by fluorescence microscopy at 4 (A) and 8 (B) hours post-injury. Datasets represent at least 25 larvae per group over three independent experiments. Each data point represents data from one larva. Bars show mean ± SD. Significance calculated using one-way ANOVA with Bonferroni's multiple comparisons post-test; p values indicated.

suggesting that blockade of ErbB signalling is resulting in a reduction in neutrophilic migration to the injury site. It is possible that blocking ErbB signalling is directly inhibiting migration, as this is a known role of ErbBs, however, it is also possible that this reduction in migration is indirect, for example due to neutrophils undergoing apoptosis in response to ErbB inhibition. This would correlate with *in vitro* data from human neutrophils, showing these inhibitors induce apoptosis in a dose-dependent manner. The next set of experiments in this chapter therefore investigated whether genetic and pharmacological blockade of ErbB signalling impacts neutrophil apoptosis in zebrafish larvae *in vivo*.
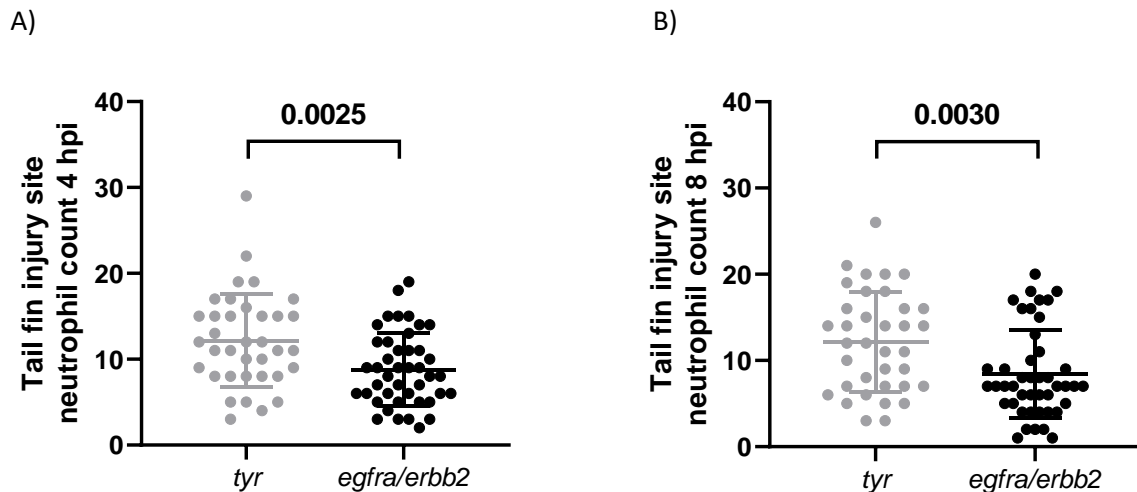
Figure 3.7. Neutrophil number at the tail fin injury site is reduced in *egfra/erbb2* double crispant larvae. Tail fin transection performed on double *egfra/erbb2* crispant larvae at 2 dpf. Injury site neutrophils counted in live larvae at 4 hpi (A) and 8 hpi (B), based on GFP expression. At both timepoints, injury site neutrophil counts are reduced compared to *tyr* controls. At least 35 larvae per condition across three independent experiments. Each data point represents data from one larva. Bars show mean ± SD. Significance determined using unpaired t test; p values indicated.

3.6 Neutrophil apoptosis within the caudal haematopoietic tissue is increased after treatment with ErbB inhibitors but unchanged in ErbB crispant larvae

Evidence so far has indicated that inhibition of ErbB signalling may reduce neutrophilic inflammation in response to tissue injury, but in some cases also reduces the total neutrophil number in uninjured zebrafish larvae. It was hypothesised that upregulation of neutrophil apoptosis, due to inhibition of ErbB signalling, was playing a role in both of these contexts. Therefore neutrophil apoptosis was investigated in the zebrafish larvae *in vivo*, both in uninjured larvae and at the site of tail fin transection.

Although apoptotic neutrophils do have a distinct, rounded morphology in zebrafish larvae, this parameter alone is not sufficient to reliably differentiate between healthy and apoptotic neutrophils. In addition, GFP expression used to visualise neutrophils in the *TgBAC*(*mpx:EGFP*)*i114* transgenic line may be quenched during apoptosis by the hypochlorous acid produced by the neutrophil, and so the fluorescence emitted by apoptotic neutrophils will gradually diminish (Schwartz *et al.*, 2009; Leliefeld *et al.*, 2018). Tyramide Signal Amplification (TSA) detects myeloperoxidase enzymatic activity (which is not affected by hypochlorous acid), and was used to detect neutrophils in apoptosis assays. Terminal deoxynucleotidyl transferase dUTP nick end labelling (TUNEL) binds to dUTP nick ends, which are

71

generated in DNA by caspase activity during apoptosis, and this was used to detect apoptotic cells. Double TSA/TUNEL positive cells were counted as apoptotic neutrophils.

When assessing neutrophil apoptosis *in vivo* in uninjured larvae, ideally every neutrophil in the zebrafish larvae would be analysed to determine whether inhibition of ErbB signalling resulted in an overall change in apoptotic rate. However due to the high magnification required to observe apoptotic neutrophils by TSA/TUNEL, assessing the whole body of each larva would not be feasible with the sample sizes in these experiments. As neutrophil apoptosis is already a rare event to capture, and 3-day old larvae may have only 200 neutrophils across the whole body, a region where neutrophils are known to be present in sufficient number was required. The caudal haematopoietic tissue (CHT) is the initial niche of haematopoietic stem cell expansion, equivalent to the foetal liver of mammals (Murayama *et al.*, 2015), and was chosen as an area in which neutrophils are likely to be present in sufficient numbers for analysis.

3.6.1   ErbB inhibitor treatment of zebrafish larvae upregulates neutrophil apoptosis within the CHT

Initial experiments aimed to determine if neutrophil apoptosis was upregulated within the CHT of uninjured larvae, after treatment with ErbB inhibitors. As with the tail fin transection assay, 2.5 dpf zebrafish larvae were treated with the ErbB inhibitors tyrphostin AG825 and CP-724,714, or equivalent volume of DMSO as a control. After 16h of treatment, larvae (now 3 dpf) were fixed in 4% PFA and TSA/TUNEL was carried out. Neutrophil numbers within the CHT were found to be unchanged after treatment with either ErbB inhibitor, at a mean ± standard deviation of 23.67 ± 10.95 with tyrphostin AG825, and 25.00 ± 6.17 with CP-724,714, compared to 27.80 ± 11.04 in DMSO control-treated larvae (Figure 3.8). This result is reflective of the unchanged numbers of neutrophil across the whole body after treatment with these ErbB inhibitors.
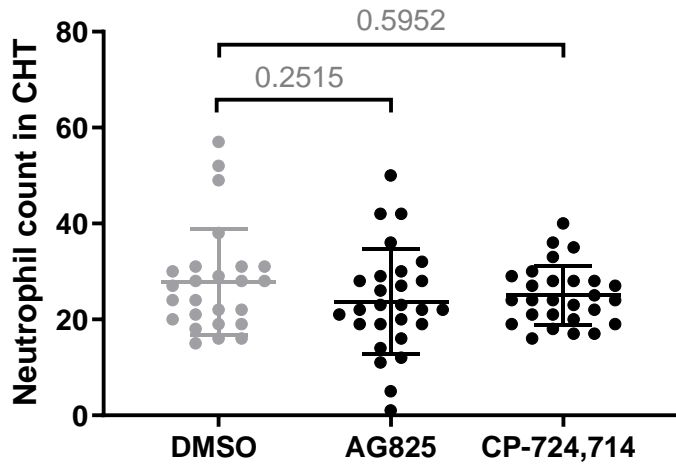
Figure 3.8. Neutrophil count in the caudal haematopoietic tissue is unchanged after treatment with tyrphostin AG825 or CP-724,714.
Neutrophil count in the CHT was determined using TSA, as part of the TSA/TUNEL assay, in 3 dpf larvae after 16h treatment with either 10 µM tyrphostin AG825 (AG825), CP-724,714, or DMSO (equivalent volume v/v). Neutrophil count in the CHT was unchanged with treatment. Minimum 25 larva per group across three independent experiments. Each data point represents data from one larva. Bars show mean ± SD. Statistical significance determined using or one-way ANOVA with Bonferroni's multiple comparisons post-test; p values indicated.

Apoptotic neutrophils were identified in the CHT based on TSA/TUNEL (Figure 3.9A). Although no differences were found in neutrophil numbers in the CHT, there was variation within each group, and therefore apoptotic neutrophil number was quantified as a percentage of the number of neutrophils in the CHT of each larva. Tyrphostin AG825 treatment was found to significantly increase the percentage of apoptotic neutrophils within the CHT, at 27.47 ± 28.77 (mean ± standard deviation), in comparison to the DMSO control (3.68 ± 4.48) (Figure 3.9B). Interestingly, the levels of neutrophil apoptosis were very variable in tyrphostin AG825-treated larvae, ranging from 0-100%, reflected by the high standard deviation. No significant differences were found in the percentage of apoptotic neutrophils in CP-724,714-treated larvae (7.47 ± 10.91) in comparison to the control.
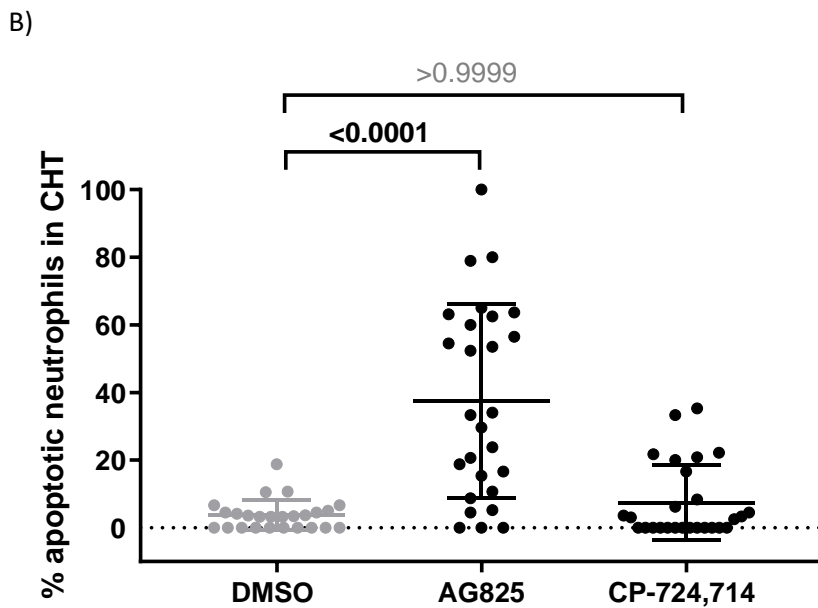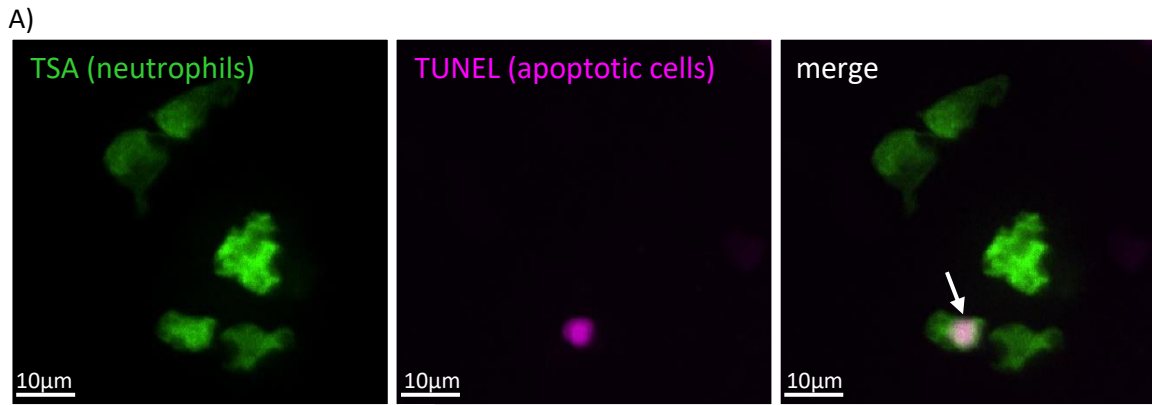
Figure 3.9. Percentage of apoptotic neutrophils within the caudal haematopoietic tissue is increased after treatment with tyrphostin AG825.

Neutrophil count and apoptotic neutrophil count in the CHT were determined using TSA to visualise neutrophils (A, left panel) and TUNEL to label apoptotic cells (A, middle panel). Apoptotic neutrophils identified based on co-localisation of the two reporters, and the rounded-up apoptotic morphology (A, right panel, arrow). A 16h pre-treatment of larvae with 10 µM tyrphostin AG825 (AG825) significantly increased the percentage of apoptotic neutrophils in the CHT compared to the DMSO control, however pre-treatment with 10 µM CP-724,714 did not (B). Minimum 25 larvae per group across three independent experiments. Each data point represents data from one larva. Bars show mean ± SD. Statistical significance determined using Kruskal-Wallis with Dunn's multiple comparisons test; p values indicated.

These results suggest that treatment with tyrphostin AG825 is having a profound, although very variable, effect on neutrophil apoptosis in zebrafish larvae. This dramatic increase in apoptosis is very likely impacting on the response of neutrophils to tissue injury, and may be responsible for the reduction in neutrophil numbers at the injury site after tail fin transection. However CP-724,714 was equally efficacious at reducing neutrophil number, but did not affect neutrophil apoptosis in the CHT.

3.6.2 Neutrophil apoptosis within the CHT is unchanged in ErbB crispant larvae

Neutrophil apoptosis was next examined within the CHT of ErbB crispant larvae. Due to the TSA/TUNEL protocol requiring larvae to be fixed, only one timepoint could be observed per experiment. Since 2 dpf was when the reduction in total neutrophil count was observed in all ErbB crispant larvae, this timepoint was selected for this assay. The generation of *tyr*, *egfra*, *erbb2* and *egfra/erbb2* double crispant larvae was carried out, and larvae were fixed uninjured at 2 dpf before undergoing TSA/TUNEL.

The number of neutrophils within the CHT was unchanged in both *egfra* (16.03 ± 5.76) and *erbb2* (17.03 ± 5.42) crispant larvae in comparison to *tyr* control larvae (18.42 ± 6.34) (Figure 3.10A). However neutrophil number was significantly reduced in the CHT of *egfra/erbb2* double crispant larvae (20.37 ±6.41) in comparison to control larvae (23.26 ± 5.35) (Figure 3.10B). This was slightly surprising as *egfra, erbb2* and double crispant larvae had reduced whole body neutrophil counts. However, it may be reflective of *egfra/erbb2* double crispant larvae having a more pronounced phenotype, due to blocking signalling of two ErbB family members rather than one (discussed in 3.9.2).

A)

B)
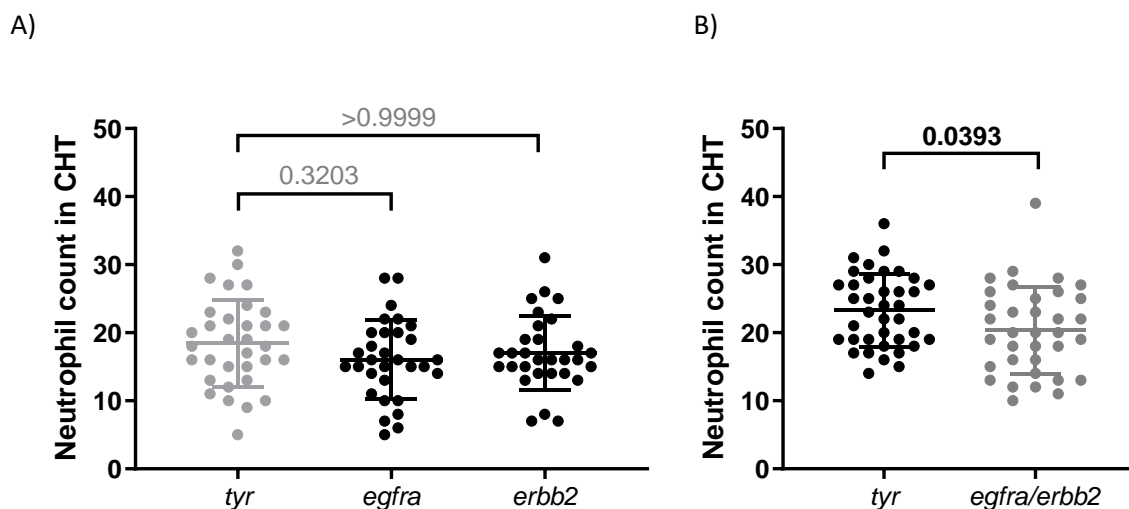
Figure 3.10. Neutrophil numbers within the caudal haematopoietic tissue are unchanged in *egfra* and *erbb2* crispant larvae, but reduced in *egfra/erbb2* double crispants at 2 dpf.
Neutrophils within the CHT of ErbB crispant larvae were enumerated based on TSA assay, in larvae fixed at 2 dpf. *egfra* and *erbb2* crispant larvae (A) showed no changes in neutrophil numbers in the CHT compared to *tyr* control crispants, whereas *egfra/erbb2* double crispant larvae (B) had significantly lower neutrophils than *tyr* controls. Minimum 30 larvae per group across three independent experiments. Each data point represents data from one larva. Bars show mean ± SD. Statistical significance determined using A) one-way ANOVA with Bonferroni's multiple comparisons test, and B) unpaired t-test; p values indicated.

Apoptotic neutrophils were detected by identifying cells that were TSA/TUNEL double positive. No alterations in the percentage neutrophil apoptosis within the CHT were observed in *egfra* larvae (3.66 ± 7.42), *erbb2* larvae (6.67 ± 9.94) in comparison to *tyr* control larvae (5.92 ± 8.46) (Figure 3.11A). Similarly, no changes in the percentage neutrophil apoptosis in *egfra/erbb2* double crispant larvae (8.49 ± 13.67) were found in comparison to *tyr* control larvae (6.91 ± 9.83), at 2 dpf (Figure 3.11B).

The differences in results from ErbB crispant larvae and ErbB inhibitor treated larvae suggests that neutrophil apoptosis within the CHT is not the only mechanism impacting neutrophilic inflammation at the tail fin injury site. Although it very likely is having an impact on tyrphostin AG825 treated larvae, it cannot explain the reduction in neutrophilic inflammation in other experiments. To further investigate, the next experiments assessed neutrophil apoptosis within the tail fin injury site of larvae.
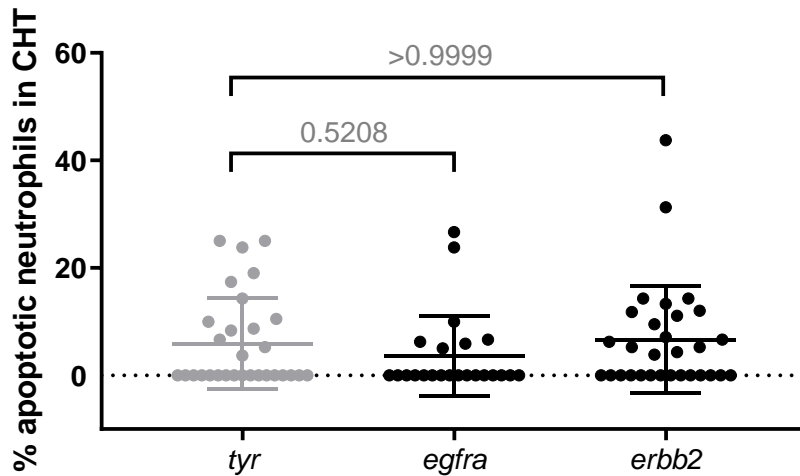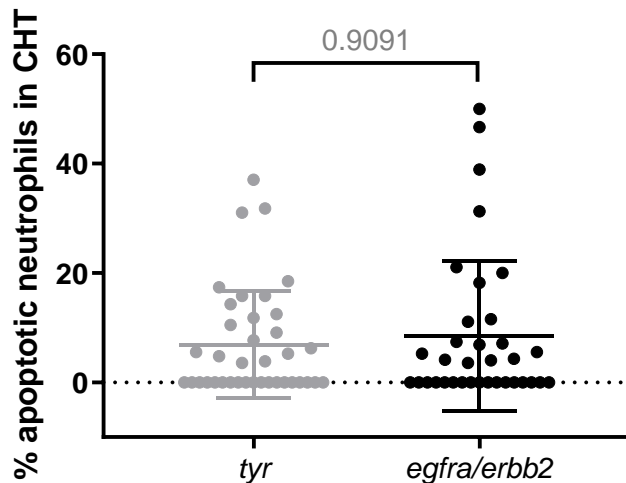
Figure 3.11. Percentage of apoptotic neutrophils within the caudal haematopoietic tissue is unchanged in ErbB crispant larvae at 2 dpf.

Apoptotic neutrophils within the CHT of *egfra*, *erbb2*, and *egfra/erbb2* double crispant larvae were enumerated by TSA/TUNEL and are shown as a percentage of the total number of neutrophils within the CHT. No changes in the percentage of apoptotic neutrophils between *egfra* or *erbb2* crispants and control *tyr* larvae (A), or *egfra/erbb2* double crispant larvae and controls, were found at 2 dpf. Minimum 30 larvae per group across three independent experiments. Each data point represents data from one larva. Bars show mean ± SD. Significance calculated using Kruskal-Wallis test with Dunn's multiple comparisons (A) or Mann Whitney test (B); p values indicated.

3.7 Neutrophil apoptosis at the tail fin injury site is increased with ErbB inhibitor treatment, and in double *egfra/erbb2* crispant larvae

The next set of experiments in this chapter aimed to determine whether inhibition of ErbB signalling, through both genetic and pharmacological means, induces apoptosis of neutrophils at a site of inflammation. Results indicating that tyrphostin AG825 is able to induce neutrophil apoptosis within the CHT of zebrafish larvae are promising, in that they recapitulate the efficacy of ErbB inhibitors in inducing human neutrophil apoptosis *in vitro*. However, one of the primary aims of this work is to determine whether ErbB inhibitors would be able to induce neutrophil apoptosis at the inflammatory site in disease, where neutrophils are typically more resistant to underdoing apoptosis. The tail fin transection model was once again used, to determine if inhibition of ErbB signalling upregulated neutrophil apoptosis at this site of inflammation.

3.7.1 Treatment with ErbB inhibitors induces neutrophil apoptosis at the tail fin injury site of zebrafish larvae

To assess whether ErbB inhibitors are able to induce neutrophil apoptosis at the site of inflammation, *TgBAC(mpx:EGFP)i114* zebrafish larvae were treated with 10 µM tyrphostin AG825, CP-724,714 or equivalent volume (v/v) of DMSO, at 2.5 dpf. After 16 hours, tail fin transection was carried out and larvae fixed at 8 hours post-injury, followed by TSA/TUNEL. Apoptotic neutrophil numbers were analysed as a percentage of the number of neutrophils at the site of injury. Treatment with either ErbB inhibitor resulted in a significant increase in the percentage of apoptotic neutrophils present at the tail fin injury site, to 5.69 ± 7.18 with AG825, 4.78 ± 5.37 with CP-724,714, compared to 1.81 ± 3.31 in DMSO-treated control larvae (Figure 3.12).

This result demonstrates the ability of tyrphostin AG825 and CP-724,714 to induce neutrophil apoptosis, in this particular inflammatory environment in zebrafish larvae. This was next examined in ErbB crispant larvae, to determine whether genetic blockade of ErbB signalling results in the same phenotype.
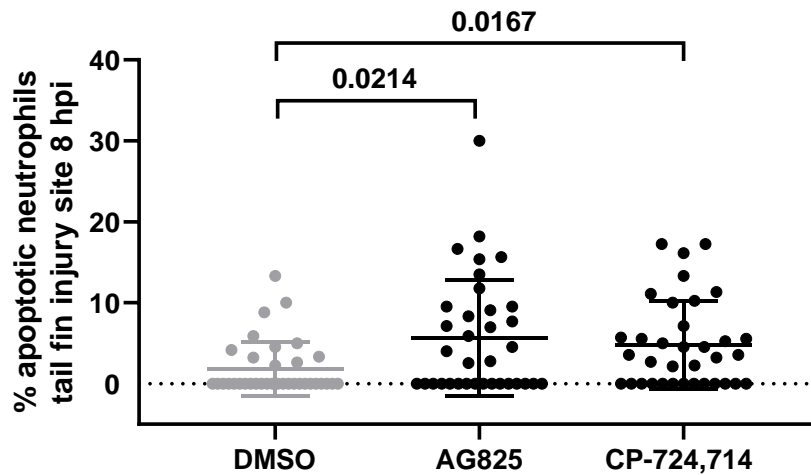
Figure 3.12. Neutrophil apoptosis at the tail fin injury site is increased after ErbB inhibitor treatment.
After 16h pre-treatment of zebrafish larvae with 10 µM Tyrphostin AG825 (AG825) or CP-724,714, tail fin transection was carried out, followed by fixation at 8 hpi and TSA/TUNEL. The percentage of apoptotic neutrophils at the tail fin injury site was increased with treatment with either ErbB inhibitor, compared to DMSO-treated control larvae. At least 35 larvae per group across three independent experiments. Each data point represents data from one larva. Bars show mean ± SD. Significance determined using Kruskal-Wallis test with Dunn's multiple comparisons; p values indicated.

3.7.2 Neutrophil apoptosis is unchanged at the tail fin injury site of *egfra* and *erbb2* crispant larvae

egfra and *erbb2* crispant larvae were used to determine whether a mutation in either ErbB family member affected the rate of neutrophil apoptosis. Tail fin transection of *egfra*, *erbb2* and *tyr* larvae was carried out at 2 dpf, and larvae were fixed in 4% PFA at 8-hours post-injury followed by TSA/TUNEL. No differences in the percentage of apoptotic neutrophils at the tail fin injury site of *egfra* (1.30 ± 3.59) or *erbb2* crispant larvae (1.53 ± 5.11), compared to *tyr* control larvae (1.18 ± 4.12), was observed (Figure 3.13).
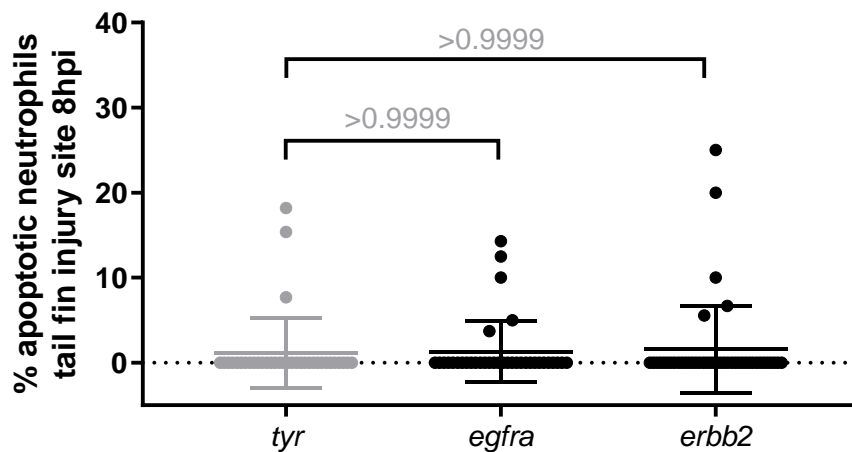
Figure 3.13. Neutrophil apoptosis is unchanged in *egfra* and *erbb2* crispants at the tail fin injury site at 8 hours post-injury.
TSA/TUNEL of 2 dpf *egfra* and *erbb2* crispant larvae showed no difference in the percentage of apoptotic neutrophils at the injury site at 8 hpi. At least 25 larvae per experimental group over 3 independent experiments. Each data point represents data from one larva. Bars show mean ± SD. Significance calculated using Kruskal-Wallis with Dunn's multiple comparison test; p values indicated.

This result was not particularly surprising, as neutrophil number at the tail fin injury site was unchanged in *egfra* and *erbb2* crispant larvae in comparison to *tyr* control larvae, and neutrophil apoptosis in the CHT of uninjured larvae was also unchanged. However, neutrophil numbers at the site of injury in *egfra*/*erbb2* double crispant were reduced compared to *tyr* larvae (Figure 3.7). This was not seen in single *egfra* and *erbb2* crispant larvae. This lends further support to the hypothesis that mutation of more than one ErbB family member is required to induce a phenotype, and this hypothesis was tested again by measuring neutrophil apoptosis at the injury site of *egfra*/*erbb2* double crispant larvae.

3.7.3 Neutrophil apoptosis is increased at the tail fin injury site of *egfra*/*erbb2* double crispant larvae

Neutrophil apoptosis was assessed at the tail fin injury site of *egfra/erbb2* double crispant larvae, as described previously. At 8 hpi, 22/44 *egfra/erbb2* double crispant larvae had at least one apoptotic neutrophil at the tail fin injury site, equating to 3.72 ± 4.88 (mean ± standard deviation) percentage apoptotic neutrophils, in comparison to 10/40 in *tyr* crispant larvae (1.39 ± 2.67). At this timepoint, the percentage neutrophil apoptosis at the injury site was significantly higher in *egfra/erbb2* double crispant larvae than in *tyr* controls (Figure 3.14).

This result demonstrates that genetic mutation of *egfra* and *erbb2* is able to induce neutrophil apoptosis in an inflammatory environment, recapitulating the phenotype observed in ErbB inhibitor treated larvae. This increase in apoptosis may at least partially explain the reduction in neutrophil number at the injury site of *egfra/erbb2* double crispant larvae; this is further explored in the Chapter Discussion. When considering this result alongside the reduction in neutrophil number at the injury site observed in both *egfra/erbb2* double crispant larvae and with ErbB inhibitor treatment, it suggests that inhibition of ErbB signalling is able to reduce neutrophilic inflammation in this model, which may be at least partially attributed to the induction of neutrophil apoptosis.
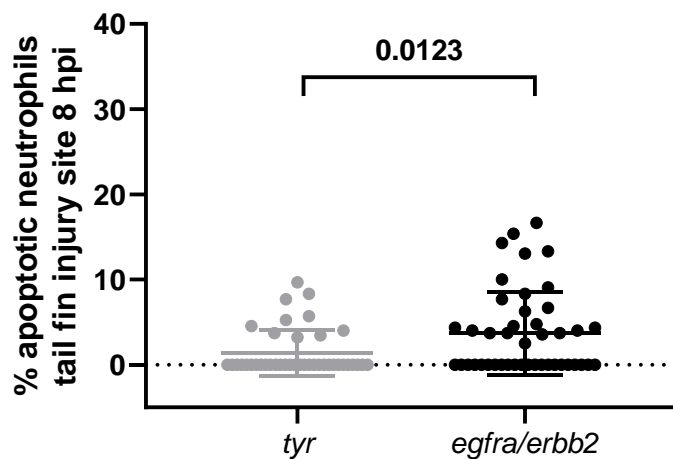
Figure 3.14. Neutrophil apoptosis at the tail fin injury site is increased in *egfra/erbb2* double crispants at 8 hpi.

Tail fin transection followed by TSA/TUNEL of double *egfra/erbb2* crispants was carried out to determine the number of apoptotic neutrophils at the tail fin injury site. The percentage of apoptotic neutrophils was increased in *egfra/erbb2* double crispants, compared to *tyr* control larvae. At least 28 larvae per group across three independent experiments. Each data point represents data from one larva. Bars show mean ± SD. Significance determined using Mann-Whitney test; p values indicated.

3.8 Treatment of zebrafish larvae with the ErbB inhibitor neratinib does not affect tail fin regeneration

Observing aspects of neutrophilic inflammation in the zebrafish larvae has yielded some important and interesting results within this chapter, namely that a reduction in inflammation at the tail fin injury site, and an increase in neutrophil apoptosis, is observed in some cases with inhibition of ErbB signalling. However, studying one particular innate immune cell type in isolation may not yield a complete picture of the inflammatory response and how it changes in response to ErbB inhibition. Therefore, the final assay carried out in this chapter aimed to determine whether treatment with an ErbB inhibitor affected a more global measure of inflammatory response in the zebrafish: tissue regeneration. The zebrafish has the ability to regenerate amputated tissue, and measuring the rate of regrowth of the tail fin after transection can indicate whether a particular genetic or pharmacological manipulation prevents tissue repair and healing. In this case, as ErbB signalling is involved in a wide range of biological processes, including cell proliferation, migration, differentiation and apoptosis, in normal development and disease, it was hypothesised that tissue growth after injury may be affected by ErbB inhibitor treatment.

For this assay, tail fin transection was carried out on the tail fin at the point where the pigment surrounding the notochord ends. This site is more distal than the transection site used for other experiments in this chapter, but it was chosen so that the pigment could be used as a reference point for measuring the start of regrowth. Under anaesthesia by tricaine, larvae underwent tail fin transection at 2.5 days post fertilisation, and were then immediately placed into E3 containing 10 µM neratinib or equivalent volume DMSO. At 2 days post injury, the length and area of the regrown tissue was measured (method described in Figure 2.6). A small number of uninjured fish were also included in each experiment, to determine whether neratinib treatment affected normal tail fin growth in larvae. The average tail fin length in uninjured fish was unchanged between DMSO-treated (mean ± standard deviation of 224.9 ± 7.8 µm) and neratinib-treated larvae (218.6 ± 4.6 µm), as was the area (mean 86075 µm^2 with neratinib treatment, and 90383 µm^2 with DMSO treatment). The length of regrown tissue in injured fish was also unchanged with neratinib treatment (122.3 ± 22.3 µm) compared to DMSO treatment (119.2 ± 22.5 µm), as was the area (mean 59420 µm^2 with neratinib treatment, 56555 µm^2 with DMSO treatment) (Figure 3.15).

This result suggests that neratinib treatment does not affect tail fin regrowth in zebrafish larvae in this particular assay. As regrowth of damaged tissue is a good indicator of inflammation resolution, it was important to establish that this ErbB inhibitor at least was not impeding this. This is particularly important as patients with chronic inflammatory diseases such as COPD will have tissue damage

induced by excess neutrophilic inflammation, and so treating with a drug that obstructed tissue healing may exacerbate the damage. In combination with other data in this chapter that indicates inhibition of ErbB signalling reduces neutrophilic inflammation and induces apoptosis in the zebrafish larvae, this paves the way for further research into whether ErbB inhibitors could be repurposed for treating neutrophil-driven inflammatory disease.

A)
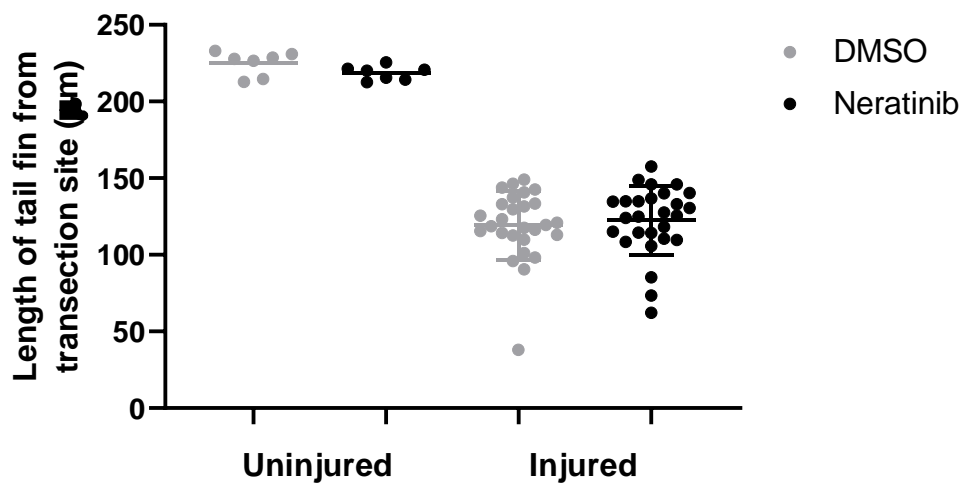
B)
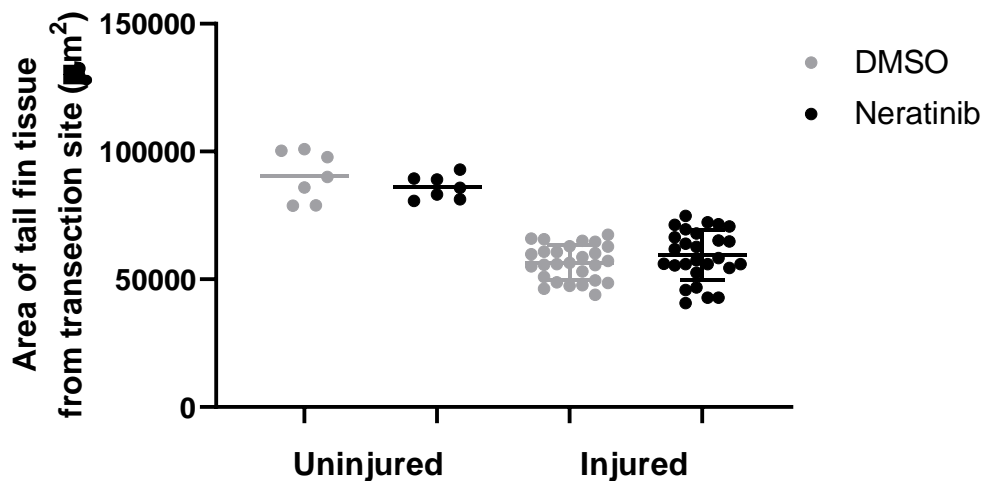
Figure 3.15. Tail fin regrowth in zebrafish larvae is unchanged after 2 days of treatment with neratinib. Tail fin transection was carried out in 2 dpf larvae, after which larvae were immediately placed into 10 µM neratinib or equivalent volume DMSO for 48 hours. Uninjured larvae were also included in each experiment to determine whether neratinib treatment affected normal tail fin growth. No differences between the treatment groups were detected in either uninjured or injured larvae, either in length (A) or area (B) of tissue from the site of transection. At least 30 larvae per injured group, and 7 per uninjured group, across three independent experiments. Each data point represents data from one larva. Bars show mean ± SD. Significance determined using unpaired t test between injured or uninjured treatment groups.

3.9   Chapter discussion

The data gathered from experiments in this chapter have demonstrated that blockade of ErbB signalling, both genetic and pharmacological, is able to reduce neutrophilic inflammation and in some cases induce neutrophil apoptosis in the zebrafish larvae *in vivo,* without inhibiting tissue regeneration. ErbB inhibitor treatment of zebrafish larvae reduced neutrophil number and increased neutrophil apoptosis at the tail fin injury site, and also increased neutrophil apoptosis in the caudal haematopoietic tissue of larvae. The only phenotypes observed in *egfra* and *erbb2* crispant larvae were a reduction in whole body neutrophil number, and an increase in neutrophils at the tail fin injury site of *egfra* crispant larvae at 8 hours post-injury. However double *egfra/erbb2* double crispant larvae additionally showed a reduction in neutrophil number, and an increase in neutrophil apoptosis, at the tail fin injury site. These results suggest that ErbB inhibitors are able to reduce neutrophilic inflammation in this model, potentially via the induction of apoptosis. These phenotypes are recapitulated in some cases when genetic mutation of ErbB genes was carried out, suggesting an ErbB-specific effect, rather than an off-target effect of these inhibitors.

One limitation of the experiments in this chapter is the order in which they were performed. The majority of the experiments using crispant larvae, and the inhibitors tyrphostin AG825 and CP-724,714 were carried out in 2018-2019 prior to the COVID-shutdown. Neratinib only became of interest due to its use in the mouse studies in the following chapter, which occurred after the re-opening of the University in 2020. Ideally neratinib would be included in experiments alongside the other two inhibitors so that direct comparisons could be made. Using neratinib in a TUNEL experiment would also be ideal if more time were available.

3.9.1   Zebrafish larvae as a model for the study of neutrophilic inflammation

The zebrafish is considered to be a highly suitable model for the investigation of neutrophilic inflammation *in vivo*, due to the transparency of zebrafish larvae and the relative ease of genetic manipulation in this species. Although mammalian models may be considered by some as being more clinically relevant in terms translating the results of these studies relate to humans, some of the genetic work carried out in this chapter would not be possible using models such as mice. For example, murine models genetically deficient in various ErbB family members present with severe developmental abnormalities including hypoplastic development of the sympathetic nervous system (*Erbb2-* and *Erbb3-* deficient), defective cardiac development (*Erbb2* and *Erbb4-* deficient), and death from multi-organ failure shortly after birth (*Egfr-* deficient) (Gassmann *et al.*, 1995; Miettinen *et al.*,

1995; Riethmacher *et al.*, 1997; Britsch *et al.*, 1998). Additionally, the work in this chapter has demonstrated that mutation of both *egfra* and *erbb2* in the zebrafish is required to induce some of the phenotypes measured, and generating double knock-out mice is challenging, particularly as *Egfr* and *Erbb2* are on the same chromosome (11) in mice (Katoh and Katoh, 2003; Du *et al.*, 2004). The use of transient-expression CRISPR/Cas9 to generate mutations in zebrafish larvae was considered ideal to overcome these issues.

3.9.1.1 Use of transient-expression CRISPR/Cas9 to study genetic blockade of ErbB signalling

Pharmacological approaches using chemical inhibitors risk the possibility of off-target effects. Both tyrphostin AG825 and CP-724,714 are selective for ErbB2 over EGFR, with IC50 values of 19 µM (EGFR) and 0.35 µM (ErbB2) for AG825 (Osherov *et al.*, 1993), and 2.2 µM (EGFR) and 11.3 nM (ErbB2) for CP-724,714 (Tang *et al.*, 2018). Neratinib however inhibits these ErbB family members more equally, with IC50 values of 92 nM (EGFR) and 59 nM (ErbB2) (Rabindran *et al.*, 2004). In all cases, the dosage used for experiments in this thesis chapter (10 µM) is likely to be at least partially inhibiting the activity of both receptors. Genetic knock-down of *egfra* and *erbb2*, separately and in combination, was therefore used to confirm a role for ErbBs in the mechanism of action of these inhibitors. This was carried out in zebrafish larvae as human neutrophils are not genetically tractable.

The use of transient-expression CRISPR/Cas9 to mutate ErbB receptors in zebrafish larvae, rather than generation of a traditional stable isogenic mutant line, was employed for several reasons. A number of studies indicate that the CRISPR/Cas9 system can generate biallelic gene disruption to high efficacy in injected embryos, which can result in loss-of-function phenotypes (Jao, Wente and Chen, 2013; Burger *et al.*, 2016; Trubiroha *et al.*, 2018). This allows for rapid analysis of gene function in larvae, resulting in significantly quicker turnaround time for generating data. The use of crispants is exploited by the pharmaceutical industry, as a high-throughput strategy to evaluate the role of candidate genes that may be associated with disease (Cornet, Di Donato and Terriente, 2018). From a 3Rs perspective (the principles of Replacement, Reduction and Refinement to encourage more humane animal research) the use of larval-stage zebrafish only, before they are considered protected under the Animals (Scientific Procedures) Act (ASPA) and EU Directive (2010/63/EU), eliminates the need for licensed procedures to be carried out on adult fish.

Furthermore, others have shown that the various ErbB mutant zebrafish lines have severe defects in normal development and fundamental biological processes. Homozygous *erbb2* mutant zebrafish, in which the resultant protein is truncated and non-functional, die at approximately 12 dpf due to cardiac defects (Liu *et al.*, 2010). Before this stage of development, zebrafish larvae rely on diffused

oxygen rather than a functioning cardiac system, and so their use for research in this thesis, before 5 dpf, may not significantly impact results (Burggren and Pelster, 1995; Sehnert *et al.*, 2002). Generation of an *egfra* knockout allele causes infertility in heterozygous adult female zebrafish, with no offspring surviving beyond 4 dpf; however no other abnormalities were observed in heterozygous adults (Ciano, Kemp, *et al.*, 2019). To determine whether the crispant larvae used in experiments for this thesis show defects, swim bladder development was assessed in *egfra/erbb2* double crispant larvae at 5 dpf. All developed swim bladders, and no other gross developmental defects were seen, indicating that mutation of both genes by transient expression CRISPR/Cas9 does not result in an obvious severe developmental delay before 5 dpf (data not shown).

3.9.2 Genetic compensation and functional redundancy in ErbB family members may explain the lack of phenotypes in single *egfra* and *erbb2* crispant larvae

Research in this chapter used both "single" *egfra* and *erbb2* crispant larvae, and *egfra/erbb2* double crispant larvae. The single crispant larvae had reduced numbers of neutrophils across the whole body, whereas double *egfra/erbb2* crispant larvae additionally had a reduction in neutrophil number at the tail fin injury site, and an increase in the percentage of apoptotic neutrophils. A number of mechanisms could explain the lack of these phenotypes in single crispants.

Research indicates that individual ErbB family members and the dimers they form influences the particular signalling pathways activated, as well as the extent to which activation occurs (Wee and Wang, 2017). However, significant overlap in signalling pathways regulated by different ErbB family members may cause functional redundancy, so that mutation of one ErbB family member is not sufficient to induce a phenotype (Wieduwilt and Moasser, 2008). This lack of phenotype may be further perpetuated by the use of transient-expression CRISPR/Cas9, in which a mosaic pattern of mutation occurs throughout all cells in the larvae, and thus some functional protein may still be produced. The biology of the ErbB family and their ability to form homodimers as well as heterodimers may lead to a level of redundancy when only a single member of the ErbB family is rendered non-functional (Hu *et al.*, 2005).

In addition to compensation at the signal transduction level by other ErbB family members, genetic compensation may be taking place. In zebrafish crispant larvae, the CRISPR/Cas9 induced double-stranded DNA break leads to cellular DNA repair pathways, primarily the non-homologous end joining (NHEJ) pathway, repairing the break by DNA insertions and deletions (indels) (Liu *et al.*, 2019). This may result in a non-functional or unstable protein structure, for example due to a frameshift mutation.

However it may also result in a premature stop codon and truncated protein, the transcript for which may be destroyed by nonsense-mediated decay to prevent aberrant protein production (Popp and Maquat, 2016). Research has shown that nonsense-mediated decay of malformed proteins can result in the upregulation of similar genes. Zebrafish with mutations in genes resulting in a premature stop codon had increased expression of a paralogue or another gene family member; for example *hbegfa* and *vegfaa* mutants had increased expression *hbegfb* and *vegfab*, respectively (El-Brolosy *et al.*, 2019). It is possible that this "transcriptional adaptation" is occurring in ErbB crispant zebrafish larvae, and that the loss of only one ErbB family member can be adequately compensated for, whereas the loss of both *egfra* and *erbb2* cannot.

3.9.3 Temporal factors may play a role in differences between ErbB inhibitor treated and ErbB crispant larvae

Differences were observed in results from larvae treated with pharmacological ErbB inhibitors, and in crispants with genetic mutation of *egfra* and/or *erbb2* genes. For example, neither *egfra, erbb2* or *egfra/erbb2* double crispant larvae had increased numbers of apoptotic neutrophils in the caudal haematopoietic tissue, whereas tyrphostin AG825-treated larvae had significantly more apoptotic neutrophils. Due to only having data from one timepoint, it is difficult to draw conclusions from this but it may reflect the length of time ErbB signalling has been supressed in the larvae.

With ErbB inhibitor treatment, neutrophil production will continue as normal until larvae are exposed to ErbB inhibitors at 2.5 dpf, when (in theory) apoptosis is suddenly induced. Whereas in ErbB crispant larvae, it may be that neutrophils develop at a normal rate but undergo apoptosis at an earlier timepoint, and are subsequently cleared by macrophages; this could potentially explain the reduction in whole body neutrophil count in all ErbB crispant larvae. It is also possible that neutrophil production is impaired by loss of ErbB signalling from the single-cell stage in crispant larvae. Research that suggests EGFR is a co-factor for Wnt9a-Fzd9b signalling, a conserved driver of haematopoietic stem cell development in zebrafish and in human embryonic stem cells (Grainger *et al.*, 2019). Although neutrophil production specifically was not assessed in this research, disrupting WNT9a or FZD9B signalling resulted in decreased numbers of CD45+ cells derived from human embryonic stem cells *in vitro*, indicating a disruption in leukocyte development (Grainger *et al.*, 2019).

It is worth noting that due to the role of the CHT in neutrophil production, the response of neutrophils to ErbB inhibitors in this region cannot be extrapolated to tissue-resident neutrophils in other areas of the larvae. The purpose of this experiment however was to observe neutrophil responses to ErbB

inhibitors in a homeostatic state, and for that the CHT was considered suitable. It is also interesting that no changes in whole body neutrophil numbers were observed in ErbB inhibitor treated zebrafish larvae. As an increase in neutrophil apoptosis was measured in many cases, it would be expected that a reduction in neutrophil number would follow. It may be that 16h treatment with ErbB inhibitors treatment is enough to induce neutrophil apoptosis, but not enough to disrupt neutrophil production at this particular stage. Possibly at a later timepoint, neutrophil numbers would be reduced as apoptotic neutrophils are cleared by macrophages.

3.9.4 *egfra* crispants have increased numbers of neutrophils at the tail fin injury site at 8 hpi

One unexpected result arising from these experiments was the increase in neutrophil number at the injury site of *egfra* crispants at 8 hpi, which opposed the phenotypes observed with ErbB inhibitor treatment and double *egfra/erbb2* crispants. The timing suggests that perhaps neutrophils are being retained at the injury site, or the window for migration is prolonged in *egfra* crispants. Direct comparisons with inhibitor-treated larvae here are not completely appropriate, as the inhibitors used in previous experiments in the zebrafish are selective for ErbB2 (although at the concentrations used, are likely to also be inhibiting EGFR). The knock-down of only one member of the ErbB family may result in a different phenotype compared to knock-down of another (or a combination of two); although ErbBs signal through heterodimerisation, homodimerisation also takes place, and it has been suggested that ErbB agonists have the ability to bias the cell response to one or the other dimer type (Macdonald-Obermann and Pike, 2014).

Mechanisms specific to EGFR, that are not present in other ErbB family members, may be causing this phenotype. Possibly this particular ErbB family member has a specific role in regulating neutrophil migration, directly or indirectly through chemotactic factors released by other tissues, that has an opposing function to other members of the ErbB family. Research indicates that the subcellular localisation of EGFR can alter the cellular phenotype induced: intracellular endosomal accumulation of the ligand-receptor complex (EGF:EGFR), possibly related to high ligand concentration, is associated with increased apoptosis, whereas the activated membrane-bound form of the receptor is linked to cell survival (Hyatt and Ceresa, 2008; Rush *et al.*, 2012). There is evidence suggesting differential signalling pathways are induced by different ErbB family members and their dimers, with heterodimers containing Erbb2 being the most potent inducers of downstream signalling pathways (Muthuswamy, Gilman and Brugge, 1999; Yarden and Sliwkowski, 2001; Holbro *et al.*, 2003). This may be due to the rapid intracellular degradation of EGFR homodimers, whereas heterodimers are recycled to the cell surface (Lenferink *et al.*, 1998). Although many downstream signalling pathways such as

PI3K are common to all dimer types, EGFR homodimers are considered by some to activate the largest number of signalling pathways, although research is still ongoing (Wee and Wang, 2017). This would suggest that some pathways are uniquely activated by EGFR homodimers, and may explain why in the increased number of neutrophils at the injury site is observed with *egfra* mutation or an EGFR-specific inhibitor only.

It is also worth noting that the distribution of neutrophils in control (*tyr*) larvae appears different at the 8-hour timepoint, with a smaller standard deviation than the *tyr* larvae at the same timepoint in the following experiment (Figure 3.6). As these experiments were performed on different batches of larvae some variability is expected. Repeating this experiment would be worthwhile if time permitted, to confirm that the significant increase in the number of neutrophils in *egfra* crispant larvae is not an artifact of an abnormally low number of neutrophils in the control larvae.

3.9.5   Increased neutrophil apoptosis at the injury site suggests ErbB inhibitors can overcome survival signals from the inflammatory environment

The altered phenotype of neutrophils within inflamed tissue can include a prolonged lifespan and increased release of histotoxic factors, increasing the capacity for tissue damage and further perpetuating inflammation (Fortin *et al.*, 2007; Brown *et al.*, 2009). That both tyrphostin AG825 and CP-724,714 were able to induce apoptosis of neutrophils in the inflammatory environment of the tail fin injury site suggests the pro-apoptotic effects of ErbB inhibitors can overcome these survival signals. This correlates with previous *in vitro* research in our group, which demonstrated that the anti-apoptotic effects of cyclic AMP and GM-CSF on human neutrophils could be reversed in the presence of tyrphostin AG825 or Erbstatin analogue (EGFR inhibitor) (Rahman *et al.*, 2019). Research into the signalling pathways regulated by ErbB inhibitors that are inducing neutrophil apoptosis may give further insight into the molecular mechanisms by which these inhibitors are working; this is addressed in Chapter 5.

Although the increase in number of apoptotic neutrophils at the tail fin was not high, it is comparable with other studies in which neutrophil apoptosis in this tail fin injury model was induced via other pharmacological inhibitors (Robertson *et al.*, 2014; Hoodless *et al.*, 2016). In both these studies, this rate of neutrophil apoptosis correlated with increased inflammation resolution. Although other mechanisms that reduce neutrophilic inflammation, such as reverse migration, were shown to also be playing a role in these studies, this does suggest that even a small increase in neutrophil apoptosis may be beneficial for inflammation resolution.

3.9.6 Inhibition of ErbB signalling may be affecting neutrophil migration, in addition to inducing apoptosis

Reduction of the number of neutrophils at 4 hours post-injury in this tail fin transection model is indicative of neutrophil migration to the site of injury being impaired (Renshaw *et al.*, 2006). Apoptotic neutrophils cannot migrate to an injury site due to their decreased functionality and thus are unresponsive to chemotactic agents that may be present at a site of inflammation (Whyte *et al.*, 1993). The increase in neutrophil apoptosis in the CHT of tyrphostin AG825-treated larvae may therefore be contributing to the reduced tail fin injury site neutrophil counts.

ErbBs are known to have a role in migration in cancer cells, with ErbB inhibitors reducing migration in a number of cancer cell lines and patient-derived cells *in vitro* (K. H. Wang *et al.*, 2012; Fichter *et al.*, 2014; Momeny *et al.*, 2017). EGFR was shown to promote tumour metastasis in murine xenograft models, and EGFR, ErbB2 and ErbB3-overexpressing breast cancers are known to correlate with increased metastases (Giltnane *et al.*, 2009; Liang *et al.*, 2017). Overexpression of ErbB signalling leads to a wide variety altered phenotypes in tumour cells, including reduced apoptosis and adhesion, and increased migration, differentiation and cell growth (Yarden and Sliwkowski, 2001). Although *in vitro* studies in this thesis only measured apoptosis, the reduced neutrophil count at the injury site *in vivo* suggests that in this model, inhibition of migratory pathways are also playing a role, and this would be interesting to explore in future experiments.

3.9.7 ErbB inhibitors may not be directly acting on neutrophils in the zebrafish larvae

The induction of neutrophil apoptosis *in vivo* may be by mechanisms other than, or in addition to, direct inhibition of ErbB signalling on neutrophils; it is possible (and likely) that the inhibitors are affecting other cell and tissue types that express ErbBs in the zebrafish. ErbB expression in human and zebrafish tissues is thought to be fairly ubiquitous, and it is likely that other cell types are being affected by the downregulation of ErbB signalling. For example, the inhibition of ErbB signalling in epithelial tissue at the tail fin injury site may result in decreased growth factor production, leading to neutrophil apoptosis due to lack of survival signals. To partially address this, tail fin regeneration was measured in neratinib treatment larvae and was found to be unchanged with treatment, suggesting that the signalling factors regulating tissue regrowth at least are unchanged with neratinib treatment.

This result was interesting as other research suggests that inhibiting ErbB signalling does decrease growth factor production. In human cancer cell lines, treatment with gefitinib, a clinical EGFR-specific

inhibitor, resulted in a dose-dependent inhibition of transforming growth factor alpha (TGFα), vascular endothelial growth factor (VEGF), and basic fibroblast growth factor (bFGF) (Ciardiello *et al.*, 2001). There are of course many differences between these *in vitro* experiments and experiments carried out in the zebrafish larvae for this thesis. It would be interesting to explore in more detail whether neutrophil-specific chemotactic or regulatory factors are deficient in ErbB inhibitor treated larvae, potentially by assessing the cytokine and chemokine levels in tissue that may impact neutrophil growth and development.

If the induction of neutrophil apoptosis in the zebrafish is via indirect mechanisms, this may not significantly impact the potential of these inhibitors to be repurposed for inflammatory disease indications, providing the apoptotic phenotype translates to humans. Further research into the signalling pathways blocked by ErbB inhibitors that are potentially inducing neutrophil apoptosis are investigated further in Chapter 5.

3.9.8   Larval tail fin regeneration is distinctly different to human tissue healing

The ability to repair tissues after injury is a feature conserved across many organisms; however the extent to which damaged tissues are able to regenerate varies widely. Mammals such as humans and mice have a relatively low capacity for tissue regeneration after injury, with only lobes of the liver and the tips of digits able to regenerate, whereas zebrafish have a much higher regenerative capacity, being able to regrow lost fins, up to 20% of the heart, and portions of the eye, brain and spinal cord (Muneoka *et al.*, 2008; Richardson *et al.*, 2017; Beffagna, 2019). The results of the investigations into the impact of neratinib on larval tail fin regrowth therefore cannot be extrapolated to assume that neratinib will not affect human tissue healing after injury. Regrowth of an amputated zebrafish larval tail fin begins with the formation of a blastema, a mass of proliferative stromal cells that differentiate to replace the lost fin (Uemoto, Abe and Tamura, 2020). The wound healing process in humans on the other hand primarily consists of epithelial cell proliferation, and the production of collagen and extracellular matrix by fibroblasts (Guo and Dipietro, 2010). A key similarity between the two models is the infiltration of immune cells to the injured tissue. Macrophages for example are crucial in mediating the repair process in both humans and zebrafish larvae, in part by clearing dead cells and stimulating fibroblasts, and in the zebrafish larvae specifically by contributing to the blastema formation (Guo and Dipietro, 2010; Nguyen-Chi *et al.*, 2017). If this work could be continued it would be interesting to investigate the impact of ErbB inhibition of macrophages specifically, to determine if their role in governing the tissue regeneration process is affected.

3.9.9 Summary

Data collected in these experiments, combined with previous work by other researchers and evidence in the literature, demonstrates the ability of ErbB inhibitors to induce neutrophil apoptosis *in vivo*. Results from genetic mutation of ErbB genes in the form of crispants suggests that this is an ErbB-specific phenotype, rather than an off-target effect of these drugs. It is possible that in this particular zebrafish model, the induction of neutrophil apoptosis is not the only mechanism leading to a reduction in neutrophilic inflammation; inhibition of neutrophil migration is also possibly playing a role. Uncovering these mechanisms is an additional step toward determining whether ErbB inhibitors are likely to be beneficial in human neutrophil-driven inflammatory diseases. Due to the significant unmet need for treatments of chronic inflammatory diseases such as COPD, there is a strong rationale for continuing research that identifies new therapeutics.

4 Neratinib treatment induces anti-inflammatory mechanisms in a mouse model of acute lung injury, but shows less benefit in chronic models of lung disease

4.1 Introduction and aims

Our work in zebrafish larvae and human neutrophils demonstrated the ability of ErbB inhibitors to induce neutrophil apoptosis, and reduce neutrophilic inflammation at the site of injury. One of the aims of this thesis is to determine whether ErbB inhibitors could be repurposed to treat neutrophil driven inflammatory diseases such as COPD in humans, and as the zebrafish model showed the efficacy of ErbB inhibitors *in vivo*, a model of lung inflammation was selected for further experiments. Numerous mouse models of lung inflammation exist in the literature, and two of these were selected for the mouse studies carried out in this thesis chapter.

Neratinib was chosen as the ErbB inhibitor to be used for these studies for a number of reasons. It is the most efficacious ErbB inhibitor at inducing neutrophil apoptosis *in vitro*, and was also shown to reduce neutrophilic inflammation at the site of injury in the zebrafish larvae. Being a clinical ErbB inhibitor, it is known to be safe and tolerated in humans, and importantly numerous mouse studies in cancer research have shown that neratinib is tolerated well in mice, and information on the dosing methods and schedules are published. Oral gavage was the most common administration method found in the literature, and the dose of 20mg/kg was selected as being within the range of tolerated and efficacious doses in numerous cancer studies (Rabindran *et al.*, 2004; Zhao *et al.*, 2012; Canonici *et al.*, 2013; Nagpal *et al.*, 2019). The use of oral gavage, in which the drug is deposited directly into the oesophagus through a tube, ensures the full dose of drug is administered.

Since the aim of these studies was to determine if neratinib can reduce aspects of neutrophilic inflammation in the lungs, much of the analysis was carried out on bronchoalveolar lavage (BAL) fluid collected from mice upon culling. By instilling the lungs of mice with saline solution and recovering it, inflammatory cells within the lungs can be collected for analysis (Van Hoecke *et al.*, 2017). Soluble components of the inflammatory response such as cytokines can similarly be analysed in lavage fluid using techniques such as ELISA. It is important to note however that the saline is unlikely to infiltrate every area of the lungs, and the immune cell infiltrate may be more representative of the inflammation in the airways than the alveoli.

Although there is little literature focusing on the use of ErbB inhibitors on inflammation, published research by my laboratory group showed the efficacy of the ErbB inhibitor tyrphostin AG825 in two

mouse models of acute inflammation: one LPS-induced lung injury, and the other zymosan-induced peritoneal inflammation (Rahman *et al.*, 2019). In the former, increased neutrophil apoptosis and increased rates of efferocytosis by macrophages were observed in tyrphostin AG825 treated mice. The latter study showed reduced cells in the peritoneal lavage, reduced concentrations of the cytokine CXCL1, and reduced IgM in tyrphostin AG825 treated mice (Rahman *et al.*, 2019). Tyrphostin AG825 is for research use only, and so these experiments were continued with neratinib, a clinically used ErbB inhibitor. As neratinib has the same targets as tyrphostin AG825, it was postulated that neratinib would show similar efficacy in inducing apoptosis and supressing aspects of the inflammatory response. Specifically, it was hypothesised that neratinib treated mice would have increased numbers of apoptotic neutrophils and increased rates of efferocytosis of cell bodies by macrophages in comparison to control mice. It was also hypothesised that neratinib would reduce the concentrations of pro-inflammatory cytokines in bronchoalveolar lavage fluid samples, specifically IL-6 and CXCL1. If neratinib were to induce these anti-inflammatory mechanisms, it was considered that this may result in reduced damage to the mouse lung tissue, and so in one study carried out here mouse lungs were collected for histological analysis.

All procedures on live mice, and collection of tissues for analysis, were kindly carried out by Carl Wright, Dr Helen Marriott, and Sam McCaughran. Processing and staining of lung tissue samples for histological analysis was kindly carried out by Fiona Wright and Sam McCaughran.

4.2 Neratinib treatment increases efferocytosis and reduces necrotic neutrophil numbers in a lipopolysaccharide-induced acute lung injury mouse model

The initial mouse model selected to test the efficacy of neratinib against lung inflammation was the lipopolysaccharide-induced acute lung injury model. LPS is one of the most common inducers of lung inflammation in rodent models, and the inflammatory response upon intranasal administration is well-characterised in the literature. An acute influx of inflammatory cells into the lungs is documented, of primarily neutrophils and macrophages (Khadangi *et al.*, 2021). LPS is a known inducer of the NFκB signalling pathway, and an increase in the concentrations of pro-inflammatory cytokines including IL-1β and IL-6 are observed in bronchoalveolar lavage fluid (An *et al.*, 2019). Increased permeability of lung tissue, measured by higher concentrations of proteins such as albumin in bronchoalveolar lavage, is similarly found with the administration of intranasal LPS in mice (Rittirsch *et al.*, 2008). Elevated albumin is a common characteristic of patients with acute lung injury and acute respiratory distress syndrome (Lee and Matthay, 2007). This mouse model was primarily selected as previous work from

my group showed that treatment with another ErbB inhibitor, tyrphostin AG825, resulted in increased neutrophil apoptosis and increased efferocytosis by macrophages in bronchoalveolar lavage fluid (Rahman *et al.*, 2019). It was therefore considered a good initial model to test the efficacy of neratinib, which was hypothesised to have similar outcomes.

4.2.1 Oral gavage neratinib formulation is effective at inducing human neutrophil apoptosis *in vitro*

Although neratinib has not previously been used in this particular mouse model of acute lung injury, there are many examples in the literature of mouse models in which neratinib is given via oral gavage. A number of these papers used a dosing vehicle of 0.5% methylcellulose and 0.4% Tween-80, showing that no toxicity effects were observed with this formulation (Rabindran *et al.*, 2004; Canonici *et al.*, 2013; Nagpal *et al.*, 2019). To check that neratinib was still effective at inducing neutrophil apoptosis in this formulation, the effect of neratinib in vehicle on human neutrophils *in vitro* was assessed. No difference in apoptosis was observed between neutrophils treated with DMSO in standard cell culture media or vehicle. In human neutrophils treated with neratinib in vehicle, a dose-dependent increase in apoptosis was observed, demonstrating that the vehicle does not impede the ability of neratinib to induce neutrophil apoptosis (Figure 4.1). This vehicle was therefore used for all subsequent mouse studies.
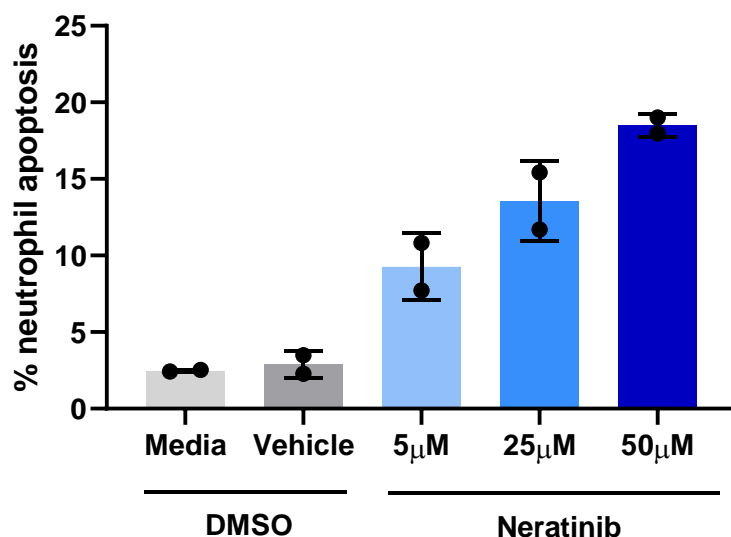
Figure 4.1. The oral gavage formulation of neratinib induces apoptosis of human neutrophils *in vitro*.
Human neutrophils were incubated *in vitro* with DMSO or neratinib in the vehicle formulation to be used for the mouse study, or DMSO in standard neutrophil media. After 5 hours of incubation, apoptosis was assessed based on nuclear morphology. Data from one biological replicate (data points represent technical replicates).

4.2.2 Leukocyte numbers in bronchoalveolar lavage fluid was unchanged with neratinib treatment

For this study, 12 mice were treated with 7μg LPS intranasally, followed by either vehicle only (control) or neratinib via oral gavage (Figure 4.2A). After 48 hours, all mice were culled and bronchoalveolar lavage (BAL) fluid was collected. The number of leukocytes within BAL samples was measured using a haemocytometer. Red blood cells are often identifiable on a haemocytometer chamber, and were excluded from counts where possible so that only leukocytes were counted, although it is possible that some were included in counts. No differences were observed between the two treatment groups, in either the density of leukocytes or in total number of leukocytes in each sample (Figure 4.2B-C).
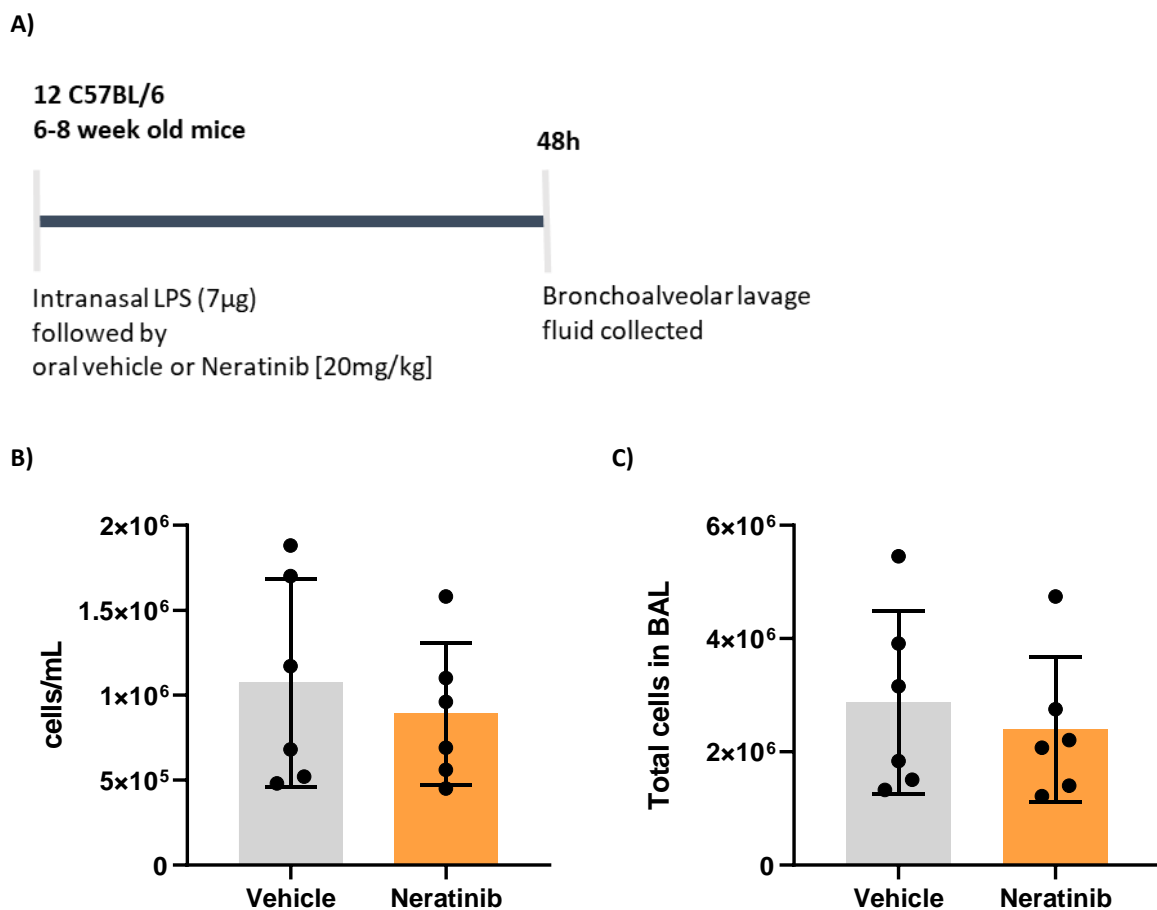
Figure 4.2. No differences in the number of leukocytes in bronchoalveolar lavage fluid were found with neratinib treatment.
Schematic of the treatment protocol (A). After bronchoalveolar lavage fluid was collected, the number of leukocytes was counted using a haemocytometer counting chamber. As there were variations in the volume of BAL from each mouse, data shown as cells/mL BAL (B) and also total cells in BAL (C). Each data point represents data from one mouse. No statistically significant differences between the treatment groups found using unpaired t test.

4.2.3 Distribution of neutrophils, macrophages and lymphocytes in BAL was unchanged with neratinib treatment

Individual cell types in BAL samples were identified by morphology, using cytocentrifuge slide preparations (cytospin slides). Neutrophils, macrophages, lymphocytes, red blood cells and epithelial cells could all be distinguished using this method (Figure 4.3A). The percentage of neutrophils, macrophages and lymphocytes were unchanged with neratinib treatment (Figure 4.3B). Using these percentages and the number of cells in each BAL sample from the haemocytometer counts, the number of each leukocyte type per mL BAL was calculated, and no differences between the two treatment groups were found (Figure 4.3C).
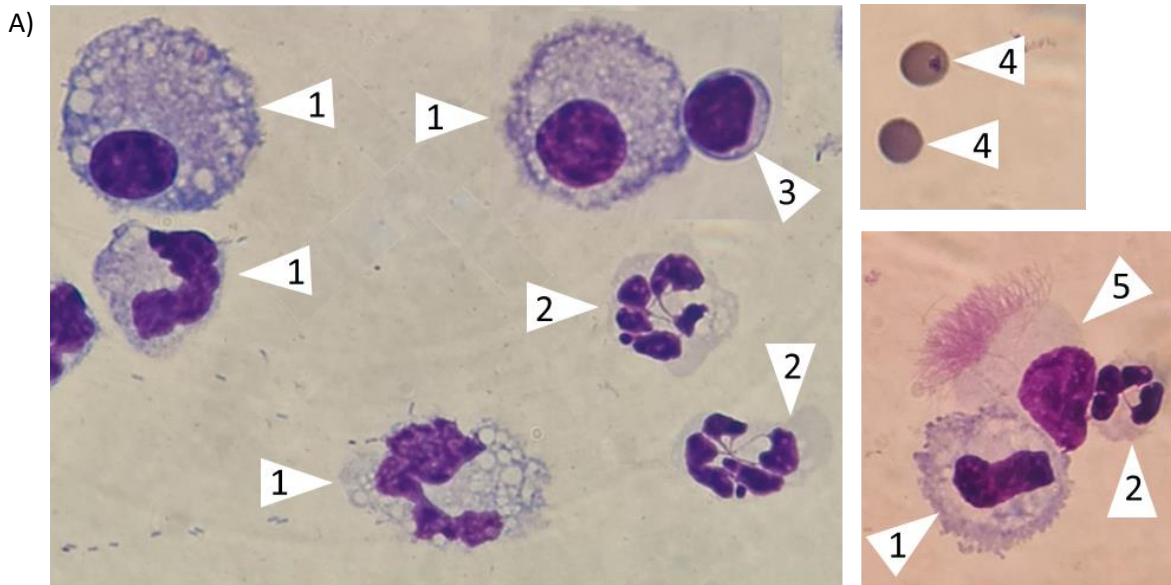
1 – macrophage; 2 – neutrophil; 3 – lymphocyte; 4 – red blood cell; 5 – ciliated epithelial cell
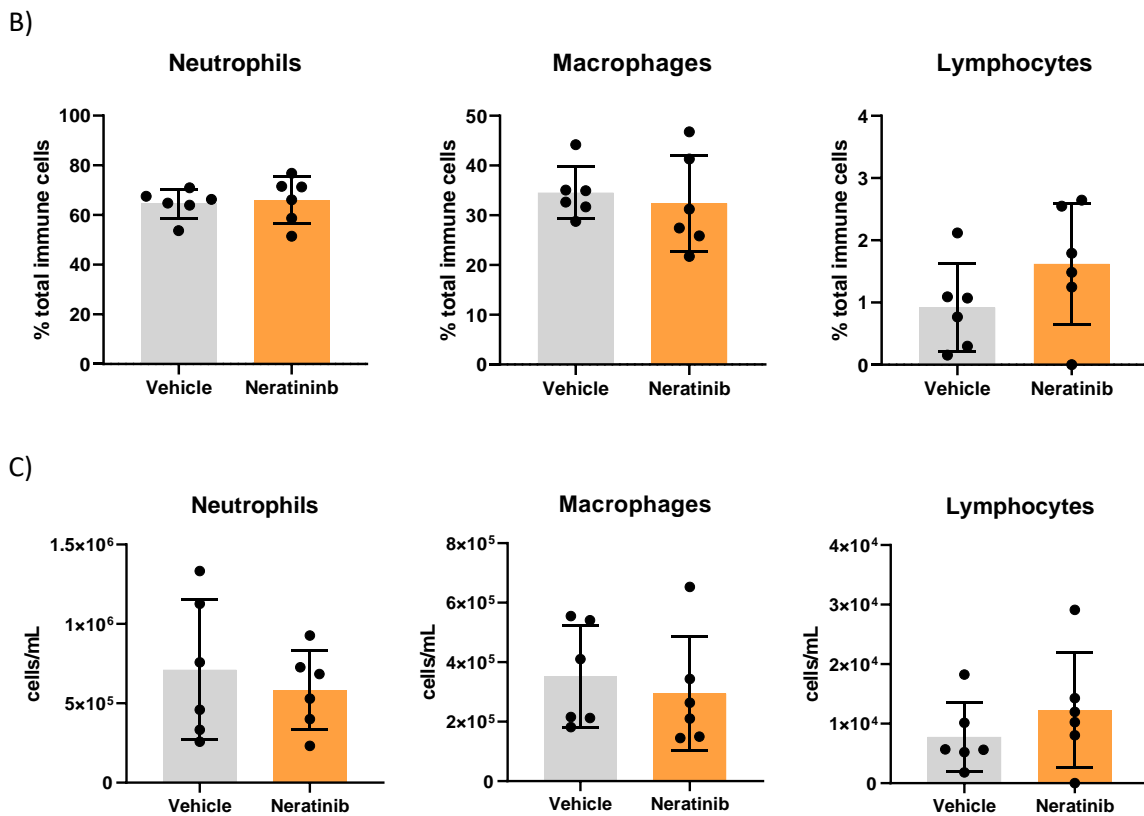
Figure 4.3. Distribution of leukocytes in bronchoalveolar lavage was unchanged with neratinib treatment. Cytospins of BAL were stained with Kwik-Diff, which allows for different blood cells to be identified based on morphology (A). The number of neutrophils, macrophages and lymphocytes per 300 cells on each cytospin slide were counted. Red blood cells and epithelial cells were also identifiable, but not included in analysis. The percentage of each cell type was calculated (B). Based on percentages and the absolute cell numbers from haemocytometer counts, the number of each cell type per mL of BAL was calculated (C). Bars show mean and standard deviation, each data point represents data from one mouse. No significant differences between treatment groups in either percentage or cell number were identified using an unpaired t test.

4.2.4 Flow cytometry analysis of BAL shows fewer dead cells, specifically fewer dead neutrophils, in neratinib treated mice

Flow cytometry was used to identify apoptotic and dead cells within BAL samples, to determine if neratinib treatment upregulates neutrophil apoptosis in mice, as it does with human neutrophils *in vitro*. Flow cytometry was used instead of assessing morphology by light microscopy, as a number of different cell types are present in BAL, and it was not always possible to identify whether a dead cell is a neutrophil, macrophage or another cell type. A FITC-conjugated Ly6G antibody was used to detect neutrophils in BAL samples, and apoptotic cells were detected using PE-conjugated Annexin-V, a protein that that binds to phosphatidylserine. In the early stages of apoptosis, phosphatidylserine is exposed on the outer leaflet of the membrane and thus can be bound by extracellular components such a Annexin V (Fadok *et al.*, 1998; Mariño and Kroemer, 2013). Samples were also stained with TO-PRO-3, which is a cell-impermeable vital dye that binds to DNA, and so can only enter cells in which the membrane is broken (Lee-MacAry *et al.*, 2001). The plasma membrane remains intact during apoptosis, and so Annexin V+ cells are referred to as apoptotic, whereas TO-PRO-3+ cells are referred to as dead. It is possible that TO-PRO-3+ cells underwent apoptosis and are undergoing secondary necrosis, however they may also have undergone a different mechanism of cell death, and so are referred to only as "dead". Cells that are negative for Annexin V and TO-PRO-3 are considered viable. From the single cells, populations of Ly6G+ neutrophils and non-neutrophils were examined for levels of apoptosis and cell death, using the gating strategies shown in Figure 4.4.

The percentage of Ly6G+ neutrophils was unchanged between neratinib treated mice and vehicle treated control mice (Figure 4.5A), which corroborates the cytospin data (Figure 4.3B). Within the single cell population, the levels of viable cells (negative for Annexin V and TO-PRO-3), apoptotic cells (Annexin V+) and dead cells (TO-PRO-3+) were analysed. The only significant difference observed was in the percentage TO-PRO-3+ dead cells, with a mean ± standard deviation of 7.52 ± 3.54 in neratinib treated mice, compared to 15.00 ± 3.32 in vehicle treated mice (Figure 4.5B). The same findings were identified in the Ly6G+ neutrophil population, with significantly fewer TO-PRO-3+ neutrophils present in neratinib treated mice (4.29 ± 2.68) compared to the vehicle treatment group (8.16 ± 2.33) (Figure 4.5C). When non-neutrophils were examined, no significant differences in viability, apoptosis or cell death were found (Figure 4.5D).
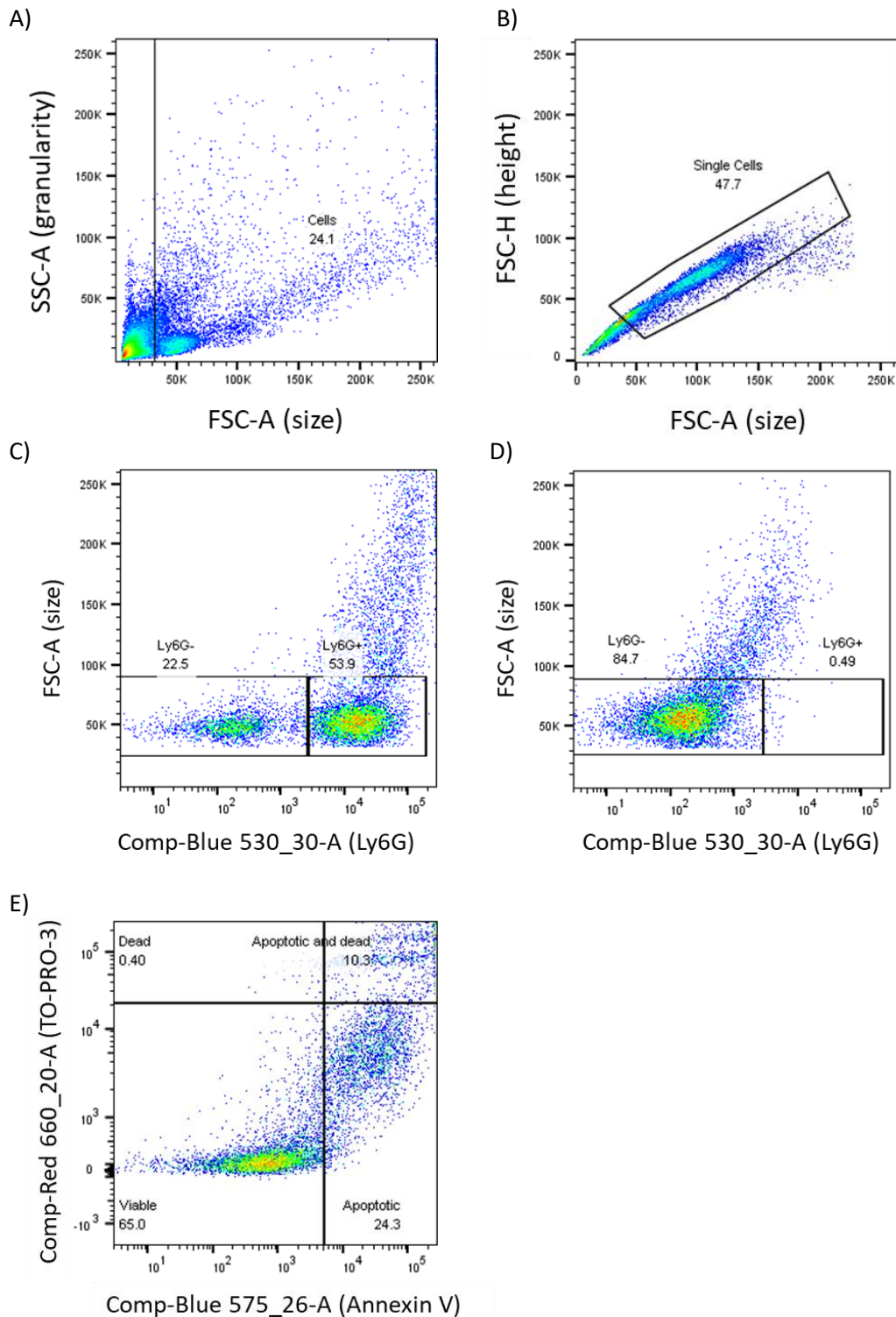
Figure 4.4. Flow cytometry gating strategy for identifying neutrophils, apoptotic cells and dead cells.
Cells were identified based on forward and side scatter plots (A), and single cells identified and debris removed from further analysis (B). The Ly6G+ population of single cells was gated (C), using single stain controls that were not stained with Ly6G (D) to identify the boundary between positive and negative populations. Finally, both the LY6G+ and the Ly6G- populations were analysed for TO-PRO-3 and Annexin V staining (E), to identify cells that were viable (negative for both stains), apoptotic (Annexin V+), dead (TO-PRO-3+) or positive for both stains, i.e. cells that died by apoptosis and are undergoing secondary necrosis.

A)

B)

All cells

All cells

All cells

C)

Ly6G+ cells

Ly6G+ cells

Ly6G+ cells

D)

Ly6G- cells

Ly6G- cells

Ly6G- cells

101
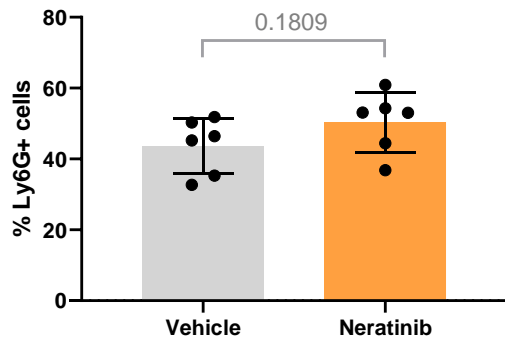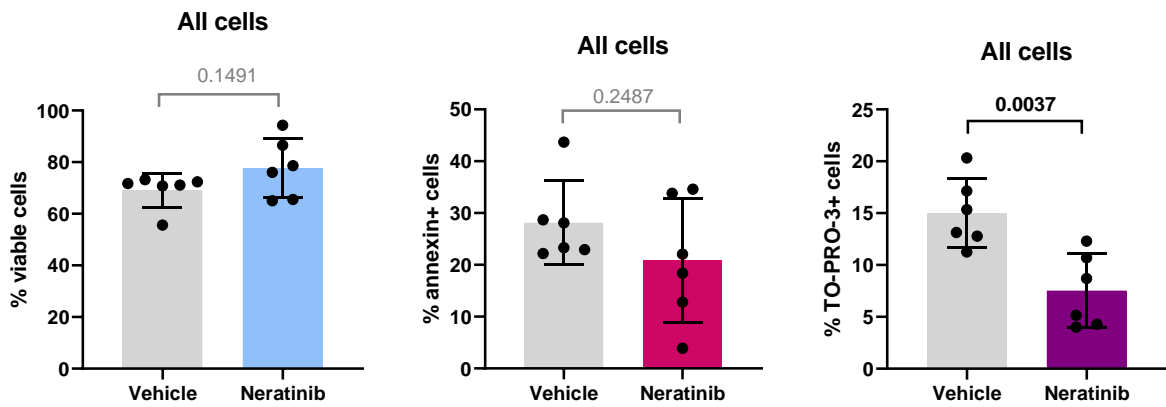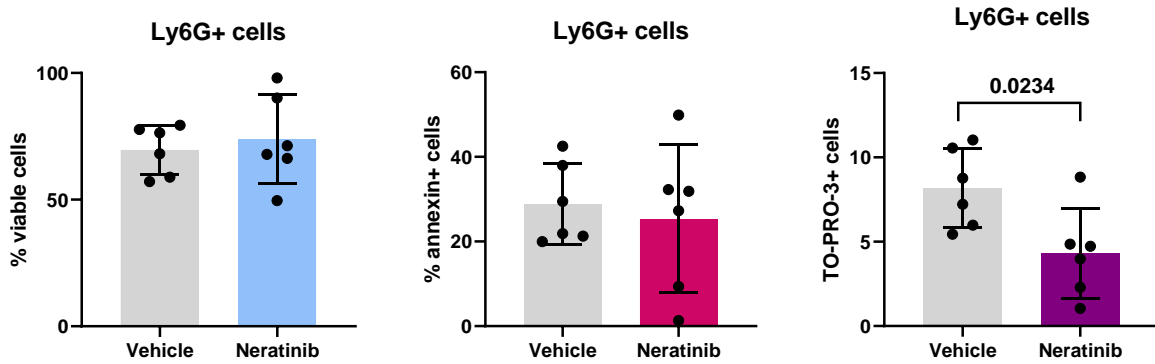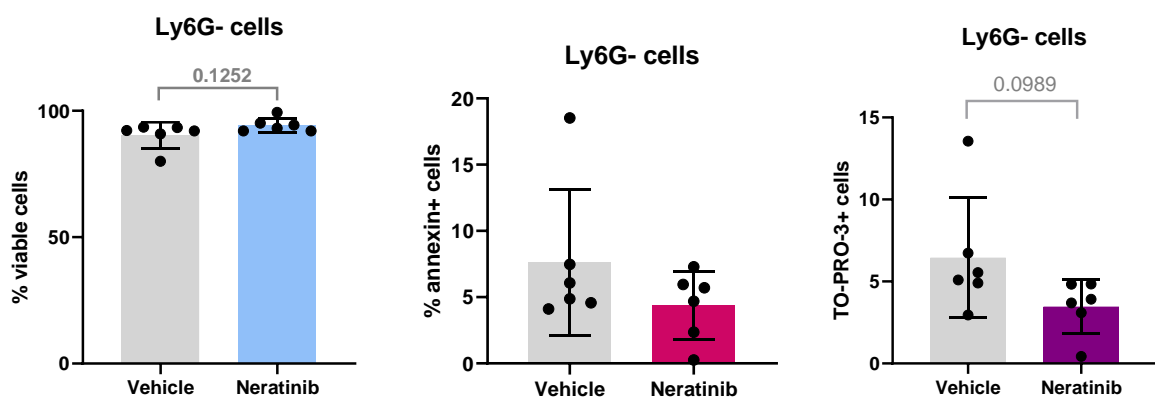
Figure 4.5. Flow cytometry indicates increased numbers of dead cells, including dead neutrophils, in bronchoalveolar lavage fluid with neratinib treatment.

Neutrophils were identified by flow cytometry using Ly6G staining, and the percentage of neutrophils within each mouse BAL sample was calculated (A). Cells were further identified as viable, apoptotic or dead based on Annexin V and TO-PRO-3 staining. These gates were applied to all cells (A), the Ly6G+ population only (B), or non-neutrophils that were negative for Ly6G (C). Bars indicate mean, error bars standard deviation. Each data point represents data from one mouse. P values indicated where appropriate (grey >0.05, black/bold <0.05), calculated using unpaired t test.

This finding was interesting as it was hypothesised that neratinib treatment would upregulate apoptosis, however instead a reduction in cell death was observed instead. The decrease in numbers of dead cells appears to be specific to neutrophils, as no differences in TO-PRO-3 staining in Ly6G- cells were identified.

4.2.5 Efferocytosis is upregulated in neratinib treated mice

Apoptotic and dead cells *in vivo* are rapidly cleared by phagocytes such as macrophages, to prevent inflammatory intracellular components, such as proteases and DAMPs causing further tissue damage (Brostjan and Oehler, 2020). This process of efferocytosis can be identified by morphology on cytospin slides, by looking for cell bodies or inclusions within macrophage vesicles (Figure 4.6A). These can be clearly distinguished from empty vesicles (Figure 4.6A, top left) by the difference in colour between ingested debris and the phagocytic cell. Macrophages may have one apoptotic inclusion, or many, and in cases of many small apoptotic inclusions, these cannot be counted accurately (Figure 4.6A, bottom right). The number of apoptotic inclusions per macrophage was recorded, and if more than 6, this was recorded as 6. The percentage of macrophages containing any number of apoptotic inclusions was significantly increased in neratinib treated mice (mean ± standard deviation of 12.88 ± 3.72) compared to vehicle treated mice (7.87 ± 1.21) (Figure 4.6B). The total number of apoptotic inclusions counted per 100 macrophages was similarly increased in neratinib treated mice (17.75 ± 5.54) compared to vehicle treated mice (11.04 ± 1.87) (Figure 4.6C). This result indicates an increase in efferocytosis in neratinib treated mice.
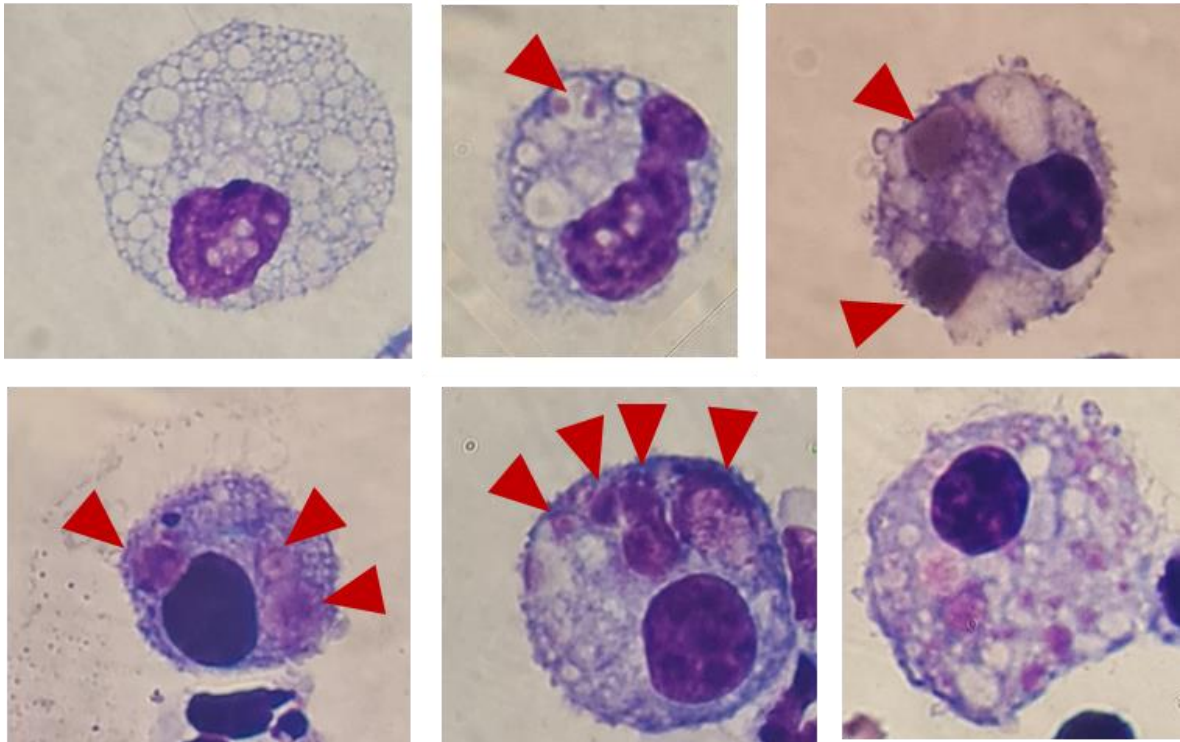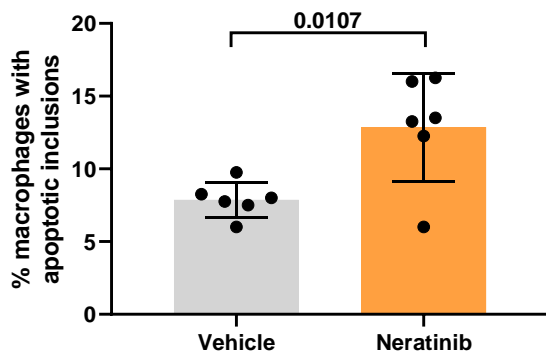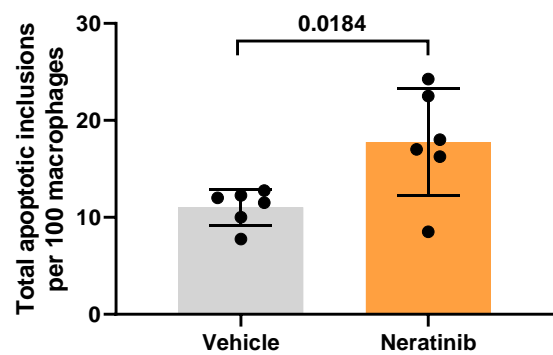
Figure 4.6. Macrophage efferocytosis of dead cells is upregulated with neratinib treatment.

Macrophages ingest dead cell debris in a process called efferocytosis, which can be identified by microscopy as inclusions within macrophage vesicles (A). Top left shows a macrophage with many vesicles, but these do not contain cell debris. Arrowheads in other images indicate vesicles in macrophages containing cell debris. These debris may be broken into several small pieces (top middle) or they may fill the vesicle (top right – in this case, these appear to be ingested red blood cells). Macrophages may contain only one vesicle with apoptotic inclusions, or many; bottom right shows a macrophage with too many apoptotic inclusions to count accurately. If 6 or above, the number of apoptotic inclusions was recorded as 6. Both the percentage of macrophages containing apoptotic inclusions (B) and the total number of apoptotic inclusions counted per 100 macrophages (C) were increased in mice treated with neratinib. 400 macrophages counted on each cytospin slide; two cytospin slides per mouse BAL sample. P values shown on graphs calculated using unpaired t test. Bars indicate mean, error bars standard deviation. Each data point represents data from one mouse.

4.2.6 IL-6 and CXCL1 levels in BAL were unchanged with neratinib treatment

Cytokines are important mediators of the inflammatory response, and can regulate the actions of specific immune cell types through extracellular signalling. The IL-6 family of cytokines regulates a broad range of inflammatory mechanisms including epithelial cell proliferation and apoptosis, the acute phase protein response, B and T lymphocyte stimulation and lineage differentiation, and recruitment of mononuclear cells (Rose-John, 2018). CXCL1, also known as GROα and KC (the latter specific to mice), is a neutrophil chemoattractant that is known to regulate neutrophil recruitment to the lungs in murine models of lung damage (Dunn *et al.*, 2018). Enzyme-linked immunosorbent assay (ELISA) was used to measure the levels of both cytokines in BAL samples. No difference in either IL-6 (Figure 4.7A) or CXCL1 (Figure 4.7B) were found between the two treatment groups.
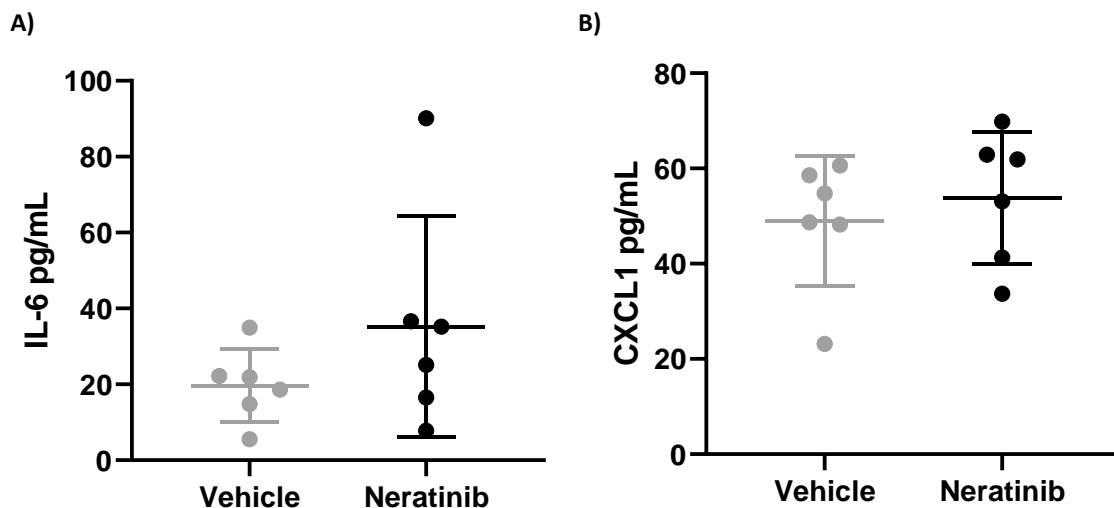
Figure 4.7. Cytokines IL-6 and CXCL1 in bronchoalveolar lavage fluid were unchanged with neratinib treatment.
The concentration of cytokines IL-6 (A) and CXCL1 (B) were measured in the supernatant of bronchoalveolar lavage fluid by ELISA. Bars indicate mean, error bars standard deviation. Each data point represents data from one mouse. No statistically significant differences between the treatment groups found using unpaired t test.

4.2.7 Acute lung injury study summary

The data from this study shows that neratinib treatment of mice has specific effects on LPS-induced acute lung inflammation. No changes were observed in the total number of leukocytes, or in the percentages of macrophages, neutrophils and lymphocytes in the bronchoalveolar lavage fluid. Based

on the decrease in dead neutrophils, and the increase in macrophages containing apoptotic inclusions in neratinib treated mice, it is hypothesised that there are fewer dead neutrophils because they are being taken up by macrophages; however it may also be an upregulation in efferocytosis that is causing the reduction in dead neutrophils. Regardless of which theory is correct, increased efferocytosis and decreased numbers of dead neutrophils are both considered to be anti-inflammatory. This study was therefore followed up with a more chronic murine model of lung disease, to determine if neratinib is similarly efficacious in a chronic inflammation environment.

4.3   Neratinib treatment in a mouse model of chronic lung disease

For the second mouse model of lung disease, a COPD-like model was chosen. Mice given weekly doses of LPS and elastase develop features of COPD within 4 weeks (Ganesan *et al.*, 2012). Elastase is an important proteolytic enzyme known to be upregulated in the lungs of patients with COPD, significantly contributing to tissue damage by breaking down elastin, a component of extracellular matrix and connective tissue (Ohbayashi, 2002; Mecham, 2018). COPD is a disease that develops over decades, and this of course cannot be replicated by a mouse model, however this particular model is well established in the literature and shows similar inflammatory phenotypes to those found in patients with COPD. Studies have shown increases in total leukocytes, and specifically neutrophils, macrophages and lymphocytes, as well as increased levels of pro-inflammatory cytokines such as IFNγ, TNFα and CXCL8 in bronchoalveolar lavage fluid (Ghorani *et al.*, 2017). Airway remodelling, alveolar damage and goblet cell hyperplasia are also observed in this model, replicating the pathophysiological changes observed in patients with COPD (Ghorani *et al.*, 2017). Lung function measurements are also altered, with elastase reducing lung tissue elasticity, and LPS increasing airway resistance, although it was not possible to measure these parameters in work for this thesis (Devos *et al.*, 2017).

For this study, 16 mice were split into two groups of 8, and treated with either neratinib or vehicle immediately after the LPS/elastase doses, with the aim of determining whether neratinib treatment could supress the inflammatory response. In addition to bronchoalveolar lavage fluid, blood samples were also collected, and lungs were harvested for histological analysis (Figure 4.8).

16 C57BL/6
6-8 week old mice

Day 0   Day 7   Day 14   Day 21   Day 28

Weekly dosing of:
• Intranasal LPS (7μg) and elastase (115μg)
followed immediately by
• Oral gavage vehicle or Neratinib [20mg/kg]
For 4 weeks

Cull and harvest:
• Blood
• Bronchoalveolar lavage fluid
• Lungs
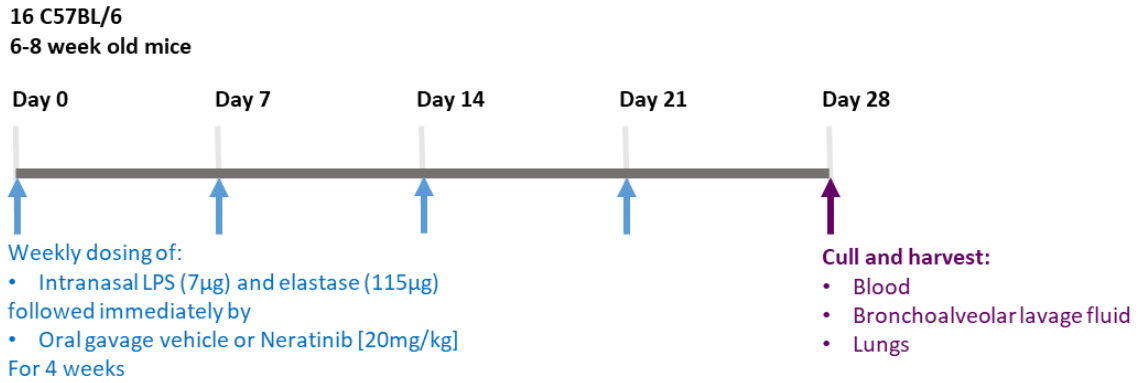
Figure 4.8. Schematic of the treatment protocol.

4.3.1   Leukocyte number in BAL is unchanged with neratinib treatment

Upon the collection of bronchoalveolar lavage fluid, a haemocytometer was used to count the number of cells in lavage fluid from each mouse. As with the previous study, some red blood cells could be identified within the counting chamber, and these were excluded from counts where possible. No differences were found between vehicle and neratinib treated mice, either in the density of cells (Figure 4.9A) or total cells in the lavage fluid (Figure 4.9B).
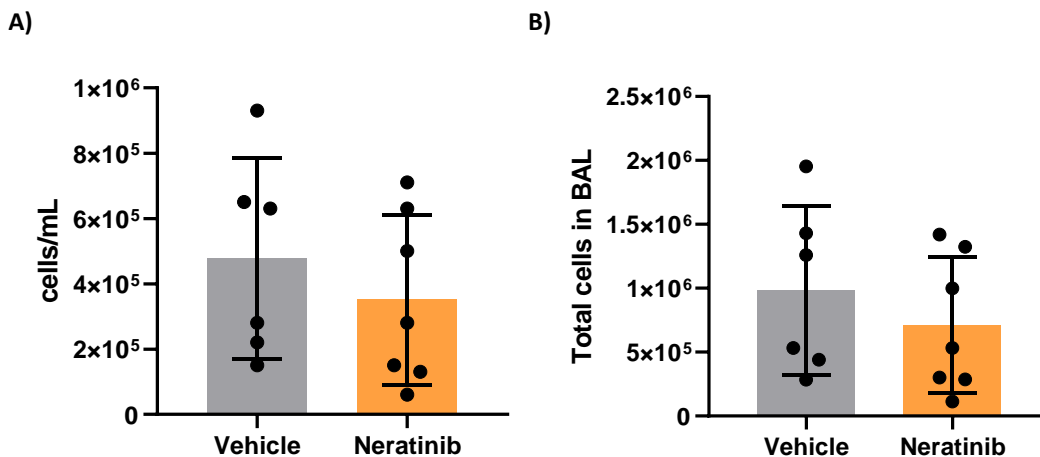
Figure 4.9. No differences in the number of leukocytes in bronchoalveolar lavage fluid between treatment groups were found.
After bronchoalveolar lavage fluid was collected, the number of leukocytes was counted using a haemocytometer counting chamber. As there were variations in the volume of BAL from each mouse, data shown as cells/mL BAL (B) and also total cells in BAL (C). Each data point represents data from one mouse. No statistically significant differences between the treatment groups found using unpaired t test.

106

4.3.2 Distribution of neutrophils, macrophages and lymphocytes is unchanged with neratinib treatment

Cytospin slides of bronchoalveolar lavage fluid were analysed to determine the distribution of macrophages, lymphocytes and neutrophils, based on morphology as shown previously. No differences were observed in either the percentages of these cell types (Figure 4.10A), or the calculated total numbers in each BAL sample based on volumes and haemocytometer counts (Figure 4.10B).

A)
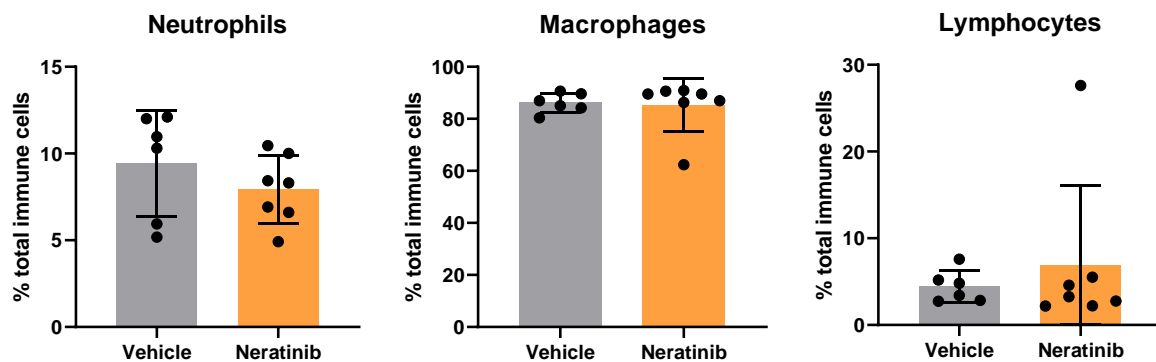
B)
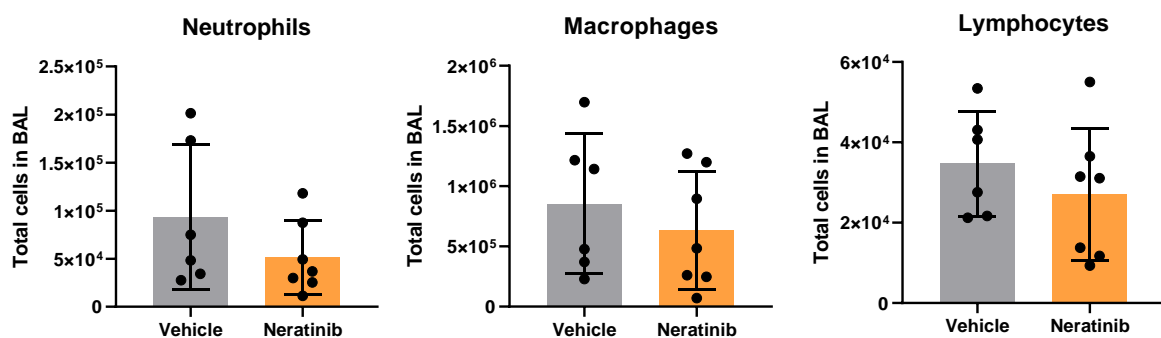
Figure 4.10. Distribution of leukocyte subsets in bronchoalveolar lavage fluid was unchanged with neratinib treatment.

Cytospins of BAL were stained with Kwik-Diff, which allows for different blood cells to be identified based on morphology. The number of neutrophils, macrophages and lymphocytes per 300 cells on each cytospin slide were counted. The percentage of each cell type was calculated (A), showing that macrophages are the predominant cell in the BAL at this timepoint. Based on these percentages and the absolute cell numbers from haemocytometer counts, the total number of each cell type in each BAL was calculated (B). Bars show mean and standard deviation, with each data point representing data from one mouse. No significant differences between treatment groups in either percentage or cell number were identified using an unpaired t test.

It is worth noting that unlike the acute lung injury model in which over half the leukocytes identified in BAL were neutrophils, the cells in this more chronic model were predominantly macrophages (80-90%), with only 5-12% of cells identified as neutrophils (Figure 4.10).

4.3.3 Flow cytometry analysis of BAL showed no difference in viability, apoptosis or cell death between treatment groups

To identify the rates of cell viability, apoptosis and death in BAL samples, analysis by flow cytometry was carried out. The gating strategy used to identify Ly6G+ cells, Annexin+ cells and TO-PRO-3+ cells was as shown previously. The percentage of neutrophils in the lavage fluid, based on Ly6G+ single cells, was between 3-22%. No differences were found between neratinib and vehicle treated mice (Figure 4.11A). No differences in viability (single cells negative for Annexin V or TO-PRO-3), apoptosis (Annexin V+ cells) or cell death (TO-PRO-3+ cells) were found, either when analysing all single cells (Figure 4.11B), neutrophils (Figure 4.11C), or non-neutrophils (Figure 4.11D).
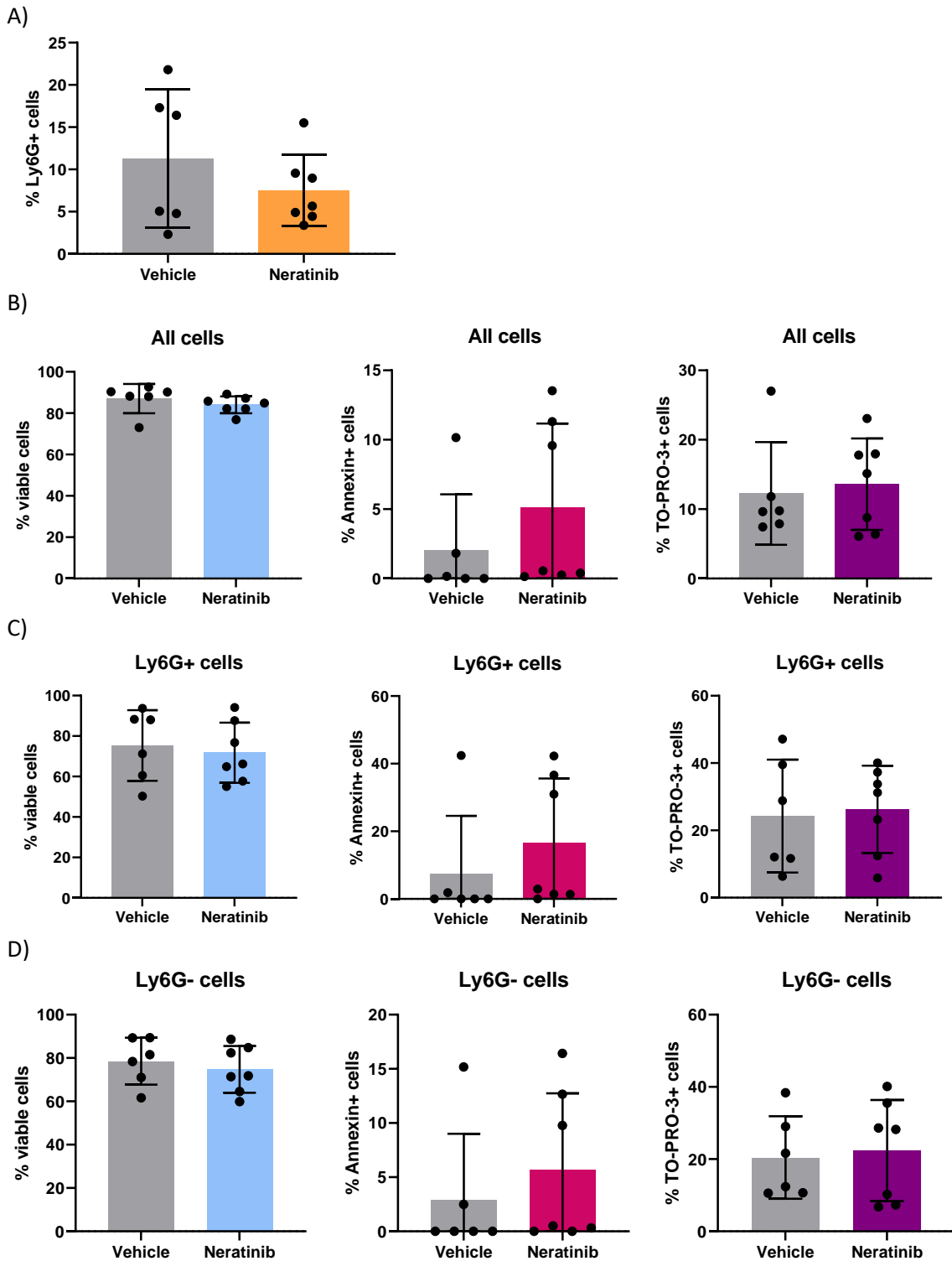
Figure 4.11. Flow cytometry analysis of bronchoalveolar lavage fluid shows no changes in the percentage of viable, apoptotic or dead cells with neratinib treatment.

Neutrophils were identified by flow cytometry using Ly6G staining, and the percentage of neutrophils within each mouse BAL sample was calculated (A). Cells were further identified as viable, apoptotic or dead based on Annexin V and TO-PRO-3 staining. These gates were applied to all cells (B), the Ly6G+ population only (C), and non-neutrophils that were negative for LY6G (D). Bars indicate mean, error bars standard deviation. Each data point represents data from one mouse. No statistically significant differences found between vehicle and neratinib treated mice for any of the cell types, using unpaired t test.

4.3.4 No differences in efferocytosis were found between neratinib and vehicle treated mice

Apoptotic inclusions within macrophages were identified based on cell morphology on cytospin slides, as previously. No differences were observed in the uptake of apoptotic cell debris by macrophages between vehicle and neratinib treated mice (Figure 4.12).
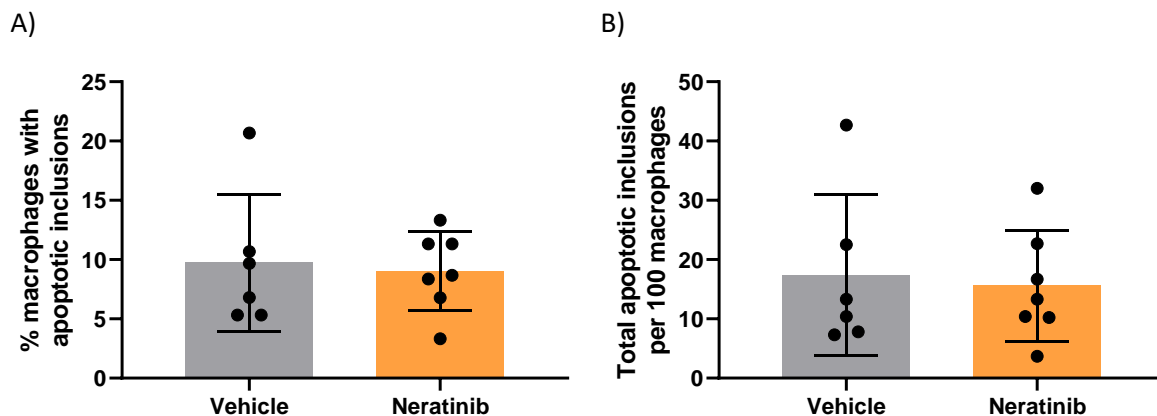
Figure 4.12. Uptake of cell bodies by macrophages was unchanged with neratinib treatment.
Efferocytosis of dead cells and cell debris by macrophages was enumerated by counting inclusions within macrophage vesicles using light microscopy. No differences between vehicle or neratinib treated mice were observed in the percentage of macrophages containing apoptotic inclusions (A) or total number of apoptotic inclusions counted per 100 macrophages(B). 400 macrophages counted on each cytospin slide; two cytospin slides per mouse BAL sample. Unpaired t test used to compare the two groups. Bars indicate mean, error bars standard deviation. Each data point represents data from one mouse.

4.3.5 Levels of CXCL1 is reduced in BAL samples from neratinib treated mice

ELISA was used to measure the levels of the cytokines IL-6 and CXCL1 in the supernatant of BAL samples. The concentration of IL-6 was not significantly different between the treatment groups, with a mean ± standard deviation of 35.64 ± 16.17 pg/mL with neratinib treatment and 35.64 ± 16.17 pg/mL in the vehicle group (Figure 4.13A). CXCL1 however was significantly lower in mice treated with neratinib, at 77.63 ± 31.28 pg/mL, compared to 145.80 ± 69.58 pg/mL in vehicle treated mice (Figure 4.13B). This result is interesting as although no differences in neutrophil number were observed in this study, levels of a key neutrophil chemokine were reduced with neratinib treatment.
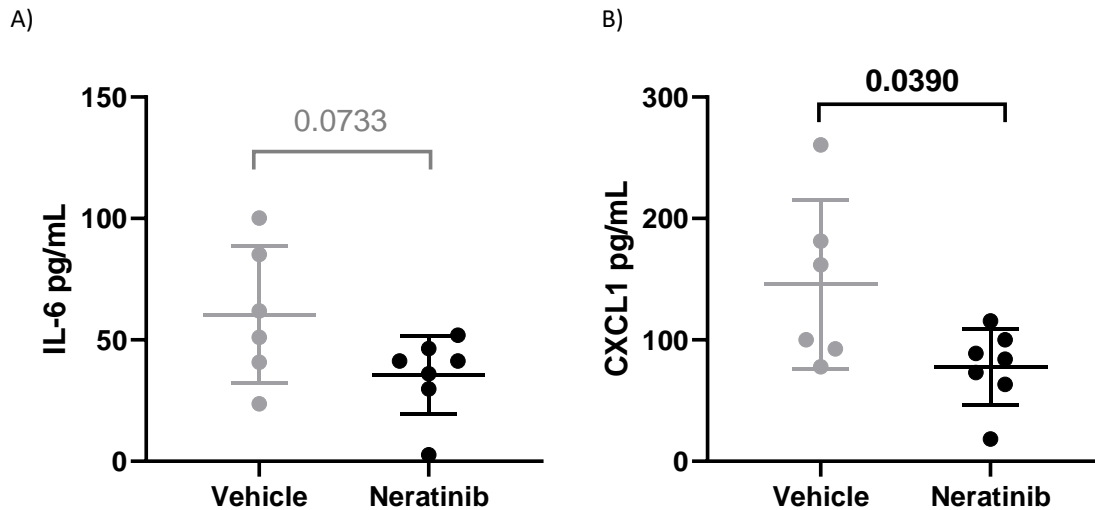
Figure 4.13. The cytokine CXCL1, but not IL-6, in bronchoalveolar lavage fluid was reduced in neratinib treated mice.
ELISA was used to measure the concentration of cytokines IL-6 (A) and KC/CXCL1 (B) in the supernatant of bronchoalveolar lavage fluid from each mouse. A statistically significant reduction in the concentration of KC/CXCL1 was found in mice treated with neratinib. Bars indicate mean, error bars standard deviation. Each data point represents data from one mouse. P values indicated, calculated using unpaired t test.

4.3.6 No differences in circulating leukocytes were observed in neratinib treated mice

In this study, blood samples were collected from mice to analyse the number and distribution of circulating leukocytes. Patients with COPD experience systemic inflammation, and assessing the levels of circulating leukocytes in this study will indicate if neratinib is altering their number and distribution in this particular mouse model. As with bronchoalveolar lavage, blood was collected at the end of the study. An automated haematology analyser (Sysmex) was used to analyse blood samples. The settings for this analyser, which is normally used for human blood, have been modified to detect murine leukocytes, and differentiate between lymphocytes, monocytes and neutrophils. The number of leukocytes detected per microlitre of blood was unchanged between vehicle and neratinib treated mice (Figure 4.14A). The differential leukocyte counts also showed no statistically significant differences between the numbers of lymphocytes, monocytes and neutrophils in the blood samples of mice between the two treatment groups (Figure 4.14B). The percentages of each type of leukocyte were similarly unchanged with neratinib treatment (Figure 4.14C).
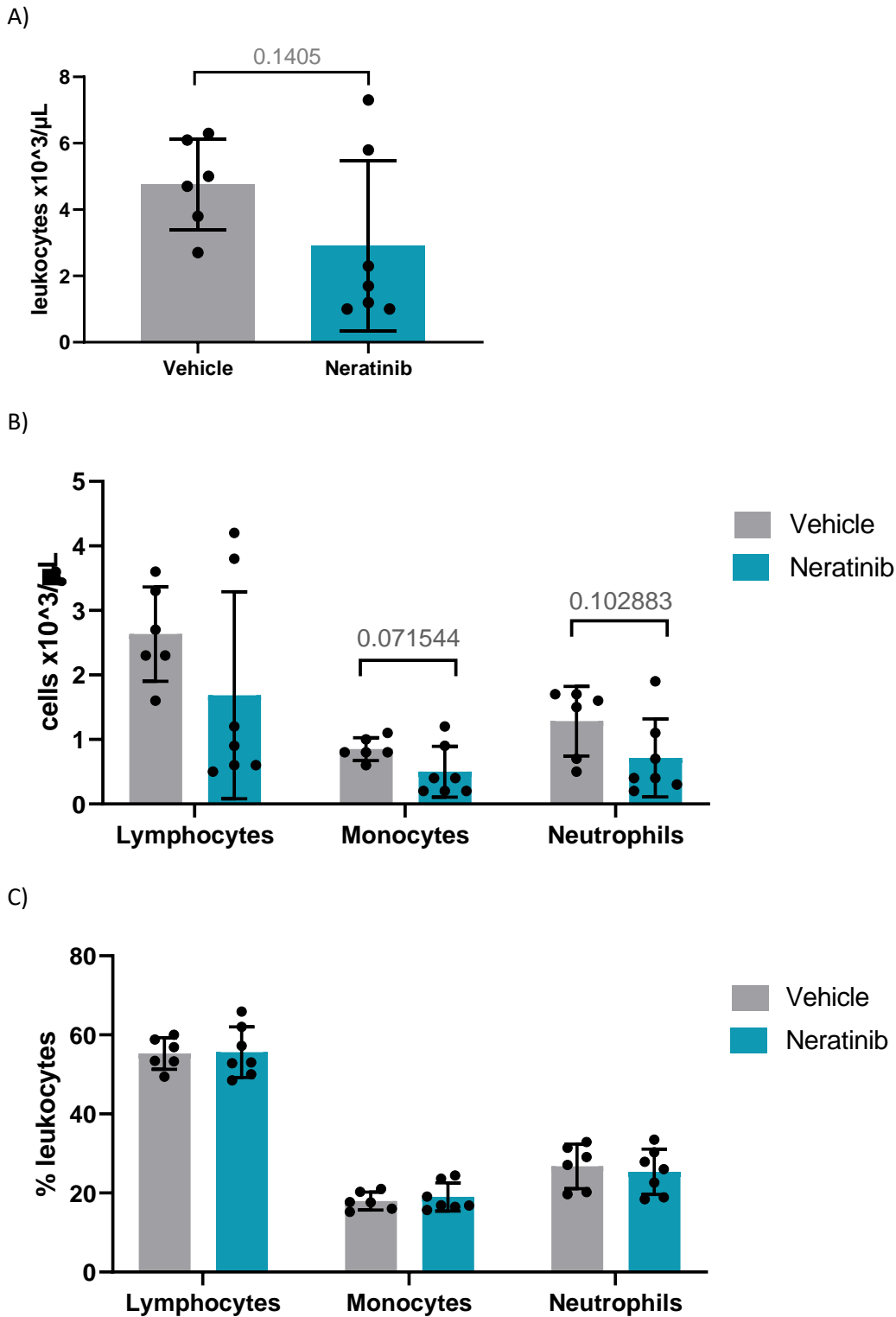
Figure 4.14. The number and distribution of leukocytes in blood was unchanged with neratinib treatment. Blood samples obtained from each mouse were analysed using a Sysmex haematology analyser, which calculates the density of leukocytes in blood (A). Leukocytes are classified as neutrophils, monocytes and lymphocytes. The number of each cell type was not statistically significantly different between the vehicle and neratinib treatment groups (B). The distribution of these neutrophils, monocytes and lymphocytes were similarly unchanged (C). P values shown on graphs calculated using individual unpaired t tests. Bars indicate mean, error bars standard deviation. Each data point represents data from one mouse.

4.3.7 Histological analysis of lung sections shows no difference in alveolar size with neratinib treatment

The final sample type to be analysed as part of this study was the lung tissue itself. Although the focus of work so far has been on the immune cell infiltrate, tissue damage is an important aspect of inflammation and is ultimately the cause of the declining lung function in patients with COPD. After lavage, mouse lungs were harvested, fixed, and sectioned for histological analysis. Some damage to the lung tissue may have occurred during the lavage process, which may affect the histological analysis; however due to the number of mice available it was not possible to use separate mice for histological analysis. Sections were stained using hematoxylin and eosin (H&E), which stains the nuclei of cells purple and the cytoplasm pink, allowing for tissue structure to be analysed. The processing and staining of lung tissue samples was kindly carried out by Fiona Wright and Sam McCaughran.

The focus of this analysis was on alveoli, which were identified by an airspace (lumen) surrounded by characteristically thin squamous epithelial cells (pneumocytes) (Figure 4.15A, stars). Intact alveoli were present (Figure 4.15A, blue stars) as well as damaged alveoli in which the septal tissue had broken, creating larger airspaces characteristic of emphysema (Figure 4.15A, black stars). For analysis, the outline of an alveolus was traced using the polygon tool in NIS elements, generating an area and perimeter measurement (Figure 4.15A, dotted lines). Twenty alveoli per mouse were selected at random to be measured, across two different lung slices. Other structures were present in the lung tissue, and these were important to differentiate to ensure only alveoli were analysed. Blood vessels have a smooth basement membrane surrounding the lumen, which sometimes contained red blood cells (Figure 4.15A, red arrowhead). Bronchioles are clearly identifiable by their thicker wall of oblong epithelial cells (Figure 4.15A, orange arrowhead).

The area (Figure 4.15B) and perimeter (Figure 4.15C) of alveoli were plotted per mouse. As this data did not appear normally distributed, it was decided that analysis would initially be carried out on the median alveolar size per mouse. No significant differences were observed between neratinib and vehicle treated mice, either in the area (Figure 4.15D) or perimeter (Figure 4.15E) of alveoli.

Because of the random selection of alveoli for measurement, many alveoli measured were intact. However the aim of this analysis was to assess the extent of the damage to lung tissue, and it was considered beneficial to also analyse only the damaged alveoli in the mouse lungs. A threshold of $500\mu m^2$ for area, and $75\mu m$ for perimeter, was decided upon as the size of intact alveoli. Any alveoli below these thresholds were removed from analysis, and comparisons of only the larger, damaged alveoli was carried out. The median size per mouse was plotted, and no difference in area (Figure 4.15F) or perimeter (Figure 4.15G) were found between treatment groups.
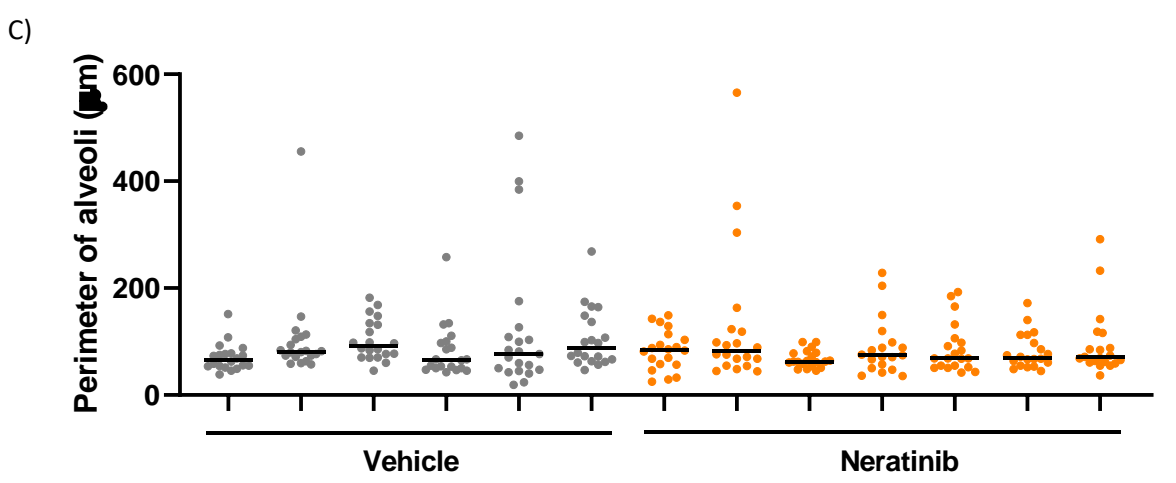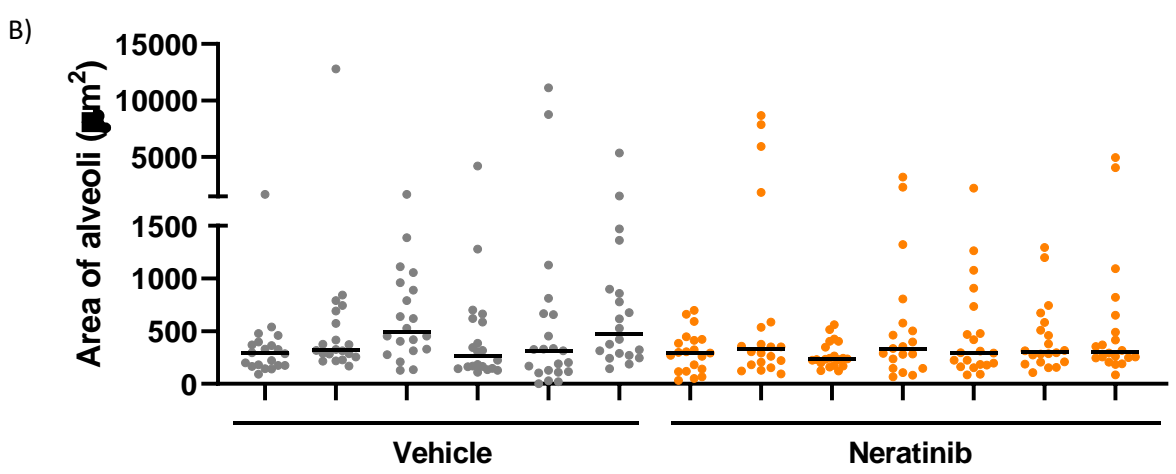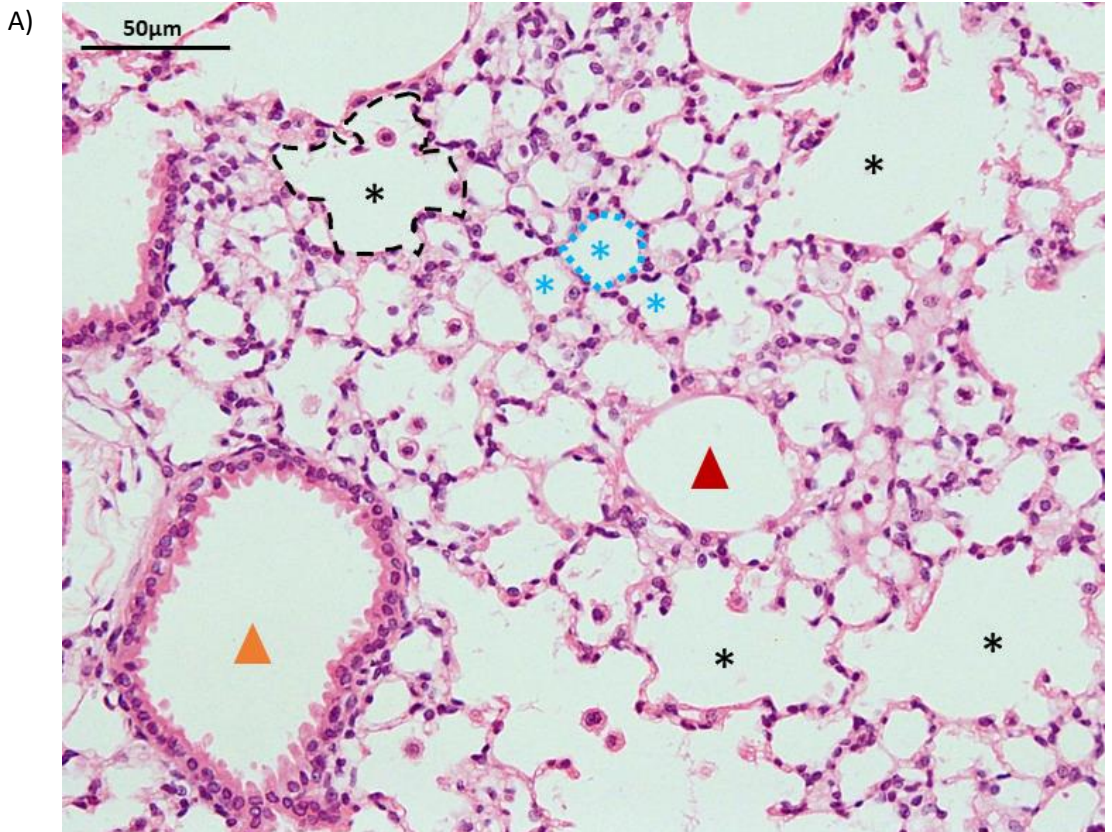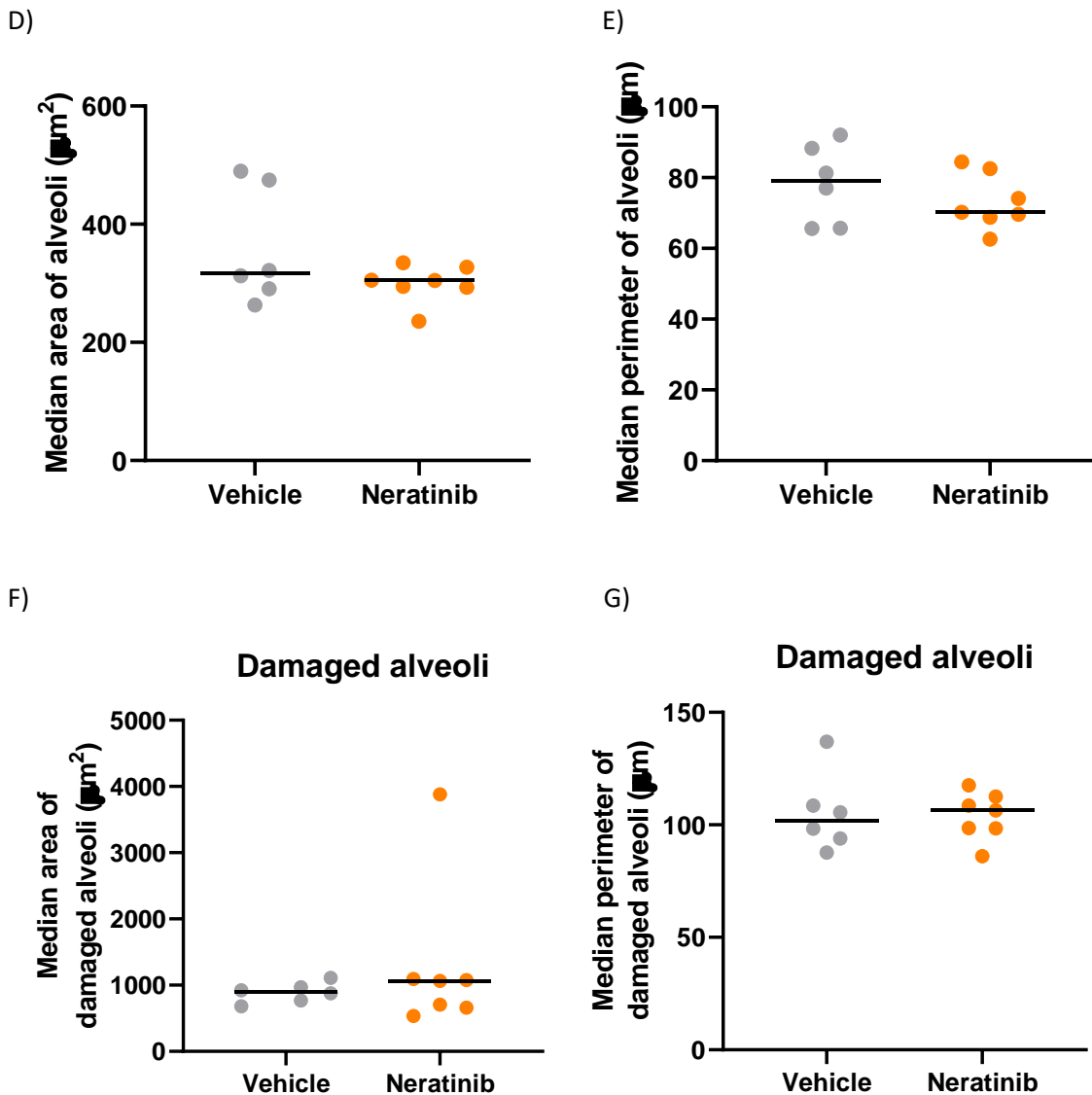
Figure 4.15. Histological analysis of alveolar spaces shows no difference with neratinib treatment.
Lungs from each mouse were harvested, fixed, sectioned and stained with H&E. The alveoli were identified by microscopy, defined by having a single cell thick wall. Blue stars indicate normal, intact alveoli, whereas black stars indicate damaged alveoli. Also identified were bronchioles (orange arrow), which are lined by distinctly larger, oblong epithelial cells. Blood vessels were also identified based on the smooth membrane of the endothelium (red arrow). The outline of individual alveoli was traced using the polygon tool in NIS Elements, which calculated the area and perimeter (blue and black dotted lines) (A). 20 alveoli per mouse lung selected at random for analysis, across two different lung slices. Area (B) and perimeter (C) of individual alveoli for each mouse is shown. Each data point represents measurement for one alveolus, and lines shown median for each mouse. The median area (D) and perimeter (E) of alveoli per mouse was calculated, and no differences between treatment groups were found. To assess alveolar damage, any alveoli with an area below $500\mu m^2$, or perimeter below $75\mu m$, were excluded from analysis, and the median alveolar area (F) and perimeter (G) for each mouse re-calculated. No statistically significant differences found between the two treatment groups. D-G: each data point represents median alveolar measurement for each mouse, line represents median measurement for the treatment group. No statistically significant differences measured using Mann-Whitney test.

4.3.8   COPD study summary

The results of this study show that neratinib treatment in this particular mouse model of COPD does not affect many of the inflammatory parameters measured. The decrease in CXCL1 with neratinib treatment is interesting, as although no changes in the number of neutrophils were observed in the lungs, a decrease in this neutrophil chemokine suggests that some aspects of inflammation are being altered. Similarly although IL-6 was not statistically significantly decreased with neratinib treatment, there is a "trend" towards its decrease. It was considered that the timing of the doses within the model were not optimal to assess differences with neratinib treatment, as mice were culled a full week after the last dose of both LPS/elastase and neratinib/vehicle. Therefore the final mouse model selected for this work incorporated both an increased frequency of drug treatment, as well as a "therapeutic" dosing schedule that better reflects the way patients would receive this treatment.

4.4   Therapeutic treatment with neratinib in a mouse model of chronic lung inflammation

The final mouse study was designed to more closely capture the way neratinib treatment would be used for patients with COPD: after disease onset. Neratinib is known to be safe and tolerated in humans, and numerous mouse studies have used daily doses with no toxicity (Nagpal *et al.*, 2019). The final study therefore used the same inflammatory lung disease model as the previous study, with weekly doses of intranasal LPS and elastase to induce an inflammatory response in the lungs. Neratinib or vehicle was given every weekday for the final two weeks of the study (Figure 4.16), to determine whether neratinib is able to abrogate lung inflammation after the onset of disease. This particular schedule was selected due to its efficacy in a mouse model of liver fibrosis. One study found in the literature demonstrated that daily dosing with neratinib for two weeks, after the onset of liver fibrosis, resulted in a reduction of collagen deposition and fibrotic markers such as IL-6, MCP-1 and TGFβ (Park *et al.*, 2020). As liver fibrosis is induced by chronic inflammation, it was hypothesised that this dosing schedule of neratinib would show similar efficacy in the COPD mouse model.

16 C57BL/6
6-8 week old mice

Day 0   Day 7   Day 14   Day 21   Day 28

Weekly dosing of:
- Intranasal LPS (7µg) and elastase (115µg)
For 4 weeks

Daily weekday dosing of
- Oral gavage vehicle or Neratinib [20mg/kg]
For 10 days

Cull and harvest:
- Blood
- Bronchoalveolar lavage fluid
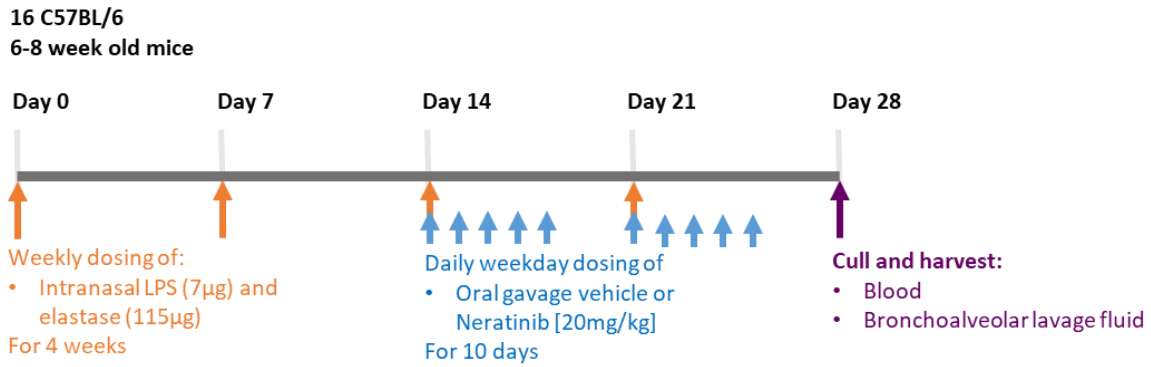
Figure 4.16. Schematic of the treatment protocol.

4.4.1   Leukocyte numbers are unchanged with neratinib treatment in BAL

Leukocytes in bronchoalveolar lavage fluid were counted using a haemocytometer. Red blood cells, where identified, were excluded from counts. No differences in the number of leukocytes were found, either in the density of cells (Figure 4.17A), or the absolute number of cells (Figure 4.17B) between vehicle and neratinib treatment groups. Fewer cells were collected from the lavage fluid in comparison to the previous COPD mouse study, with a mean of ~359,000 cells per BAL sample in this study (Figure 4.17B), in comparison to ~847,000 cells per BAL sample in the previous study (Figure 4.9B). This does not necessarily indicate a difference in the severity of inflammation, as these studies were carried out independently and techniques to collect lavage fluid will vary slightly, but it is worth noting as less cells were available for analysis in this study.
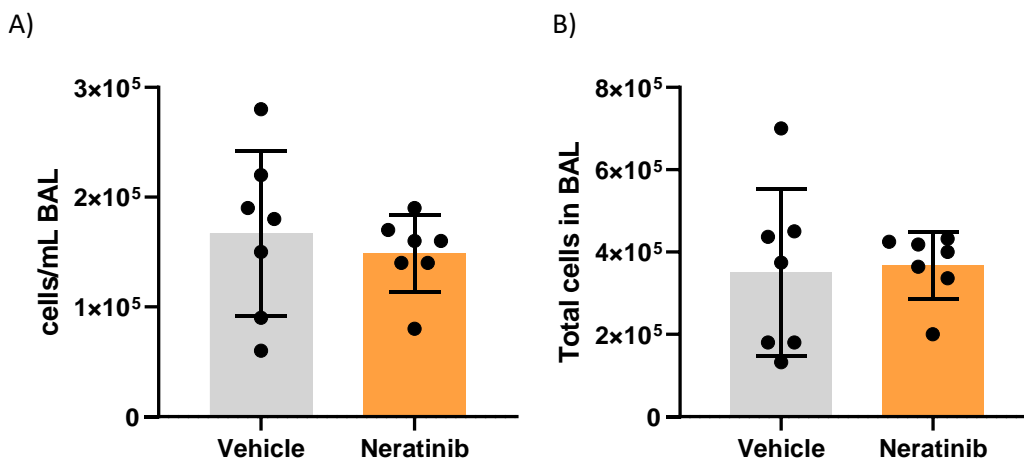
Figure 4.17. No differences in leukocyte numbers in BAL were observed with neratinib treatment.
Haemocytometer counts of the density of cells in each BAL sample (A), and the total number of cells per BAL (B), were unchanged with neratinib treatment. Each data point represents one mouse. Bars show mean, error bars standard deviation. No differences were found between treatment groups using an unpaired t test.

117

4.4.2 Number and distribution of neutrophils, macrophages and lymphocytes in BAL was unchanged between treatment groups

The percentage of neutrophils, macrophages, and lymphocytes were calculated using Kwik-Diff stained cytospin slides, as previously. The percentage of each of these cell types was unchanged between treatment groups (Figure 4.18A). These percentages were also consistent with the previous COPD study, with the prominent leukocyte in the bronchoalveolar lavage sample being macrophages (~90%), with neutrophils and lymphocytes each making up under 10% of the remaining leukocytes in the majority of samples. The total number of each cell type in the bronchoalveolar lavage samples was calculated based on haemocytometer counts, and these were also unchanged with neratinib treatment (Figure 4.18B).

A)
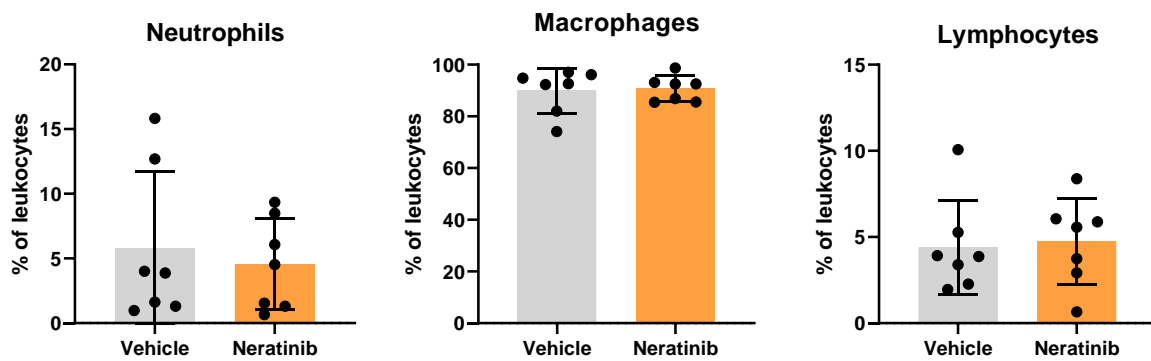
B)
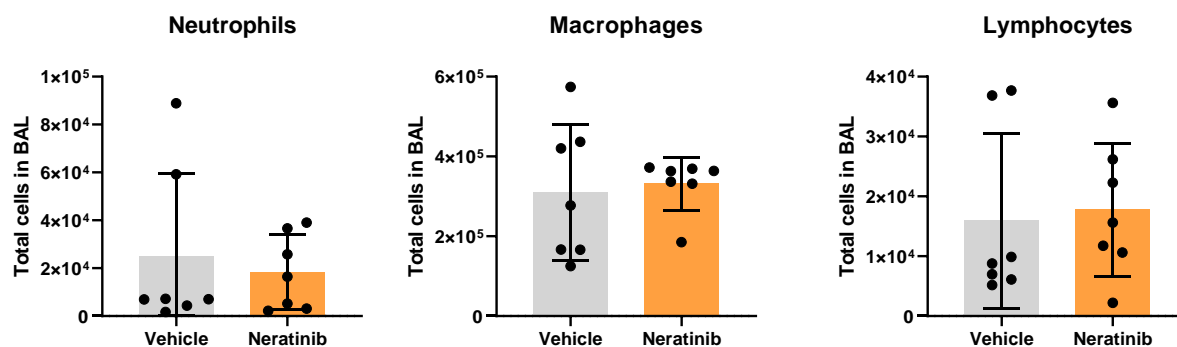
Figure 4.18. No differences in the distribution of neutrophils, macrophages or lymphocytes were found between treatment groups.
Neutrophils, macrophages and lymphocytes in BAL were identified based on morphology. The percentage of each cell type was unchanged with neratinib treatment (A). Using the volume of each lavage fluid sample and the total number of cells in each sample as per the haemocytometer counts, the total number of neutrophils, macrophages and lymphocytes in each lavage fluid sample was calculated (B). Each data point represents one mouse. Bars show mean, error bars standard deviation. No differences were found between treatment groups for any of the datasets, using unpaired t tests.

4.4.3   No differences in apoptosis or cell death were detected between treatment groups

Flow cytometry was carried out on cells within the bronchoalveolar lavage fluid, to identify the percentage of cells that were apoptotic (by Annexin V staining) and dead (by TO-PRO-3 staining). Ly6G was also used to identify neutrophils. Data from one mouse in the vehicle treatment group was excluded as too few cells were available for analysis. The gating strategies used for this analysis were repeated from previous experiments (Figure 4.4). Based on Ly6G staining, the percentage of neutrophils (of all single cells) was found to be unchanged between treatment groups (Figure 4.19A). The percentages of single cells that were viable, apoptotic and dead were also unchanged with neratinib treatment (Figure 4.19B-D).

A)

B)
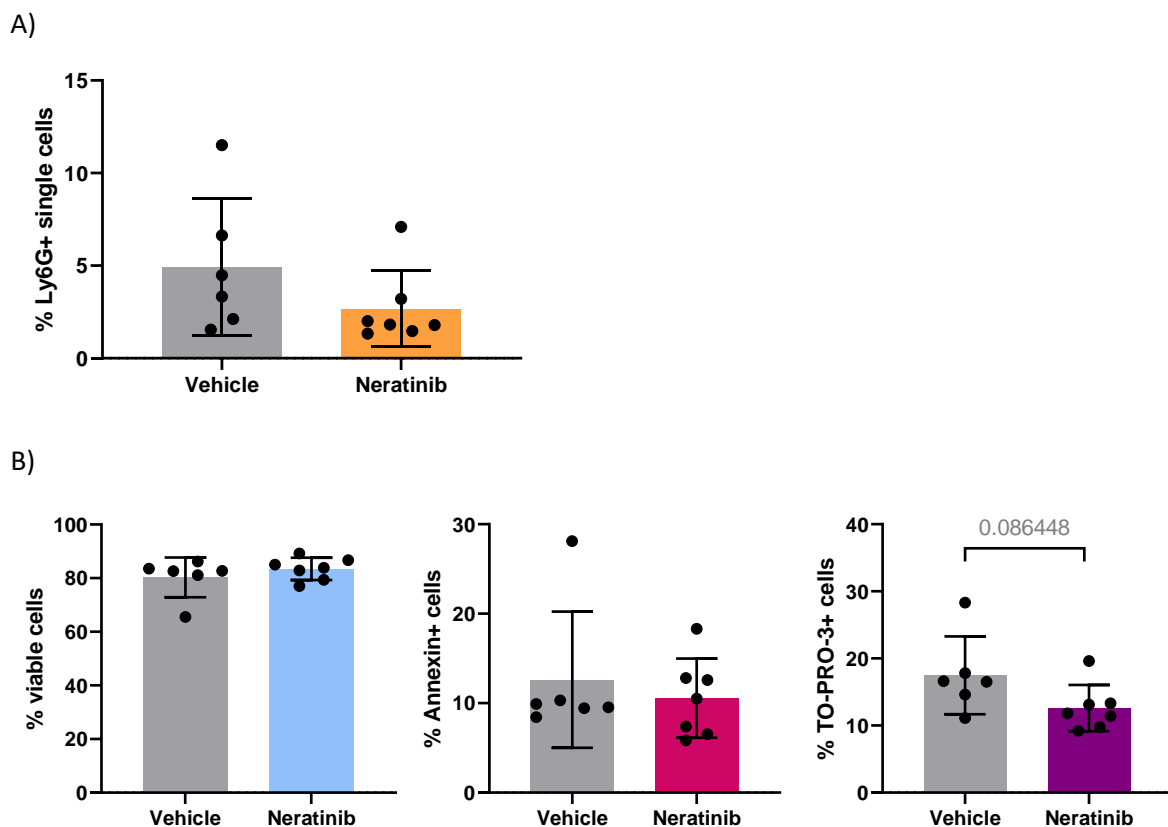
Figure 4.19. Analysis of apoptosis and cell death of cells in BAL by flow cytometry showed no significant differences with neratinib treatment.
Flow cytometry was used for immunophenotyping of cells in bronchoalveolar lavage fluid. The gating strategies were replicated from the previous study. Of all single cells, the percentage of Ly6G+ cells (neutrophils) was not significantly different between mice in vehicle and neratinib treatment groups (A). The percentages of single cells that were viable (negative for Annexin V and TO-PRO-3), apoptotic (Annexin V+) and dead (TO-PRO-3+) were also unchanged between treatment groups (B). Statistical analysis carried out using unpaired t tests. Bars indicate mean, error bars standard deviation. Each data point represents data from one mouse.

Due to the low number of cells obtained from each sample of lavage fluid and the low percentage of neutrophils within each sample, there were not enough cells to reliably calculate percentages of cell viability, apoptosis and death within the neutrophil population.

4.4.4 Efferocytosis is unchanged with neratinib treatment

The rates of efferocytosis were measured by counting the number of macrophages on cytospin slides that contained apoptotic inclusions, as described previously. The percentage of macrophages containing any apoptotic inclusions was unchanged between treatment groups (Figure 4.20A). Of all the macrophages containing apoptotic inclusions, the total number of inclusions was unchanged between the vehicle and neratinib treatment groups (Figure 4.20B).
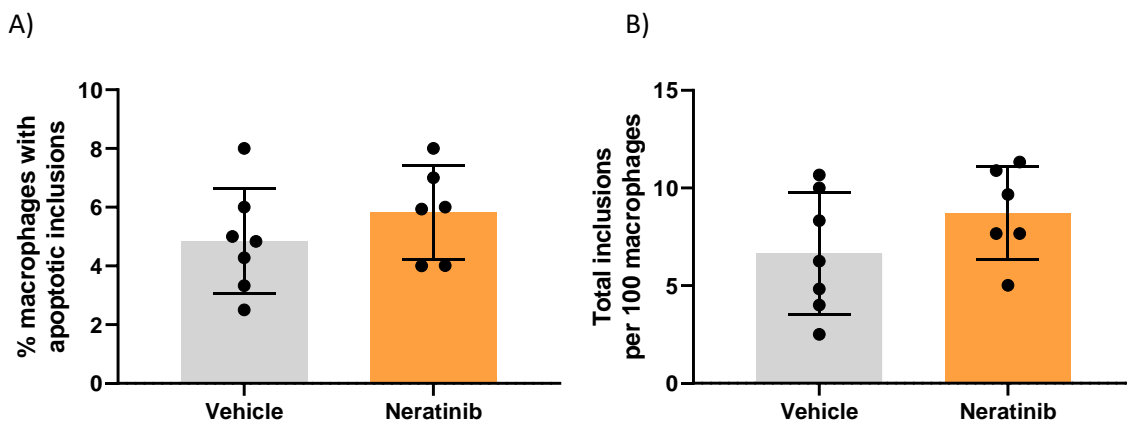
Figure 4.20. Uptake of apoptotic cell debris by macrophages is unchanged between treatment groups. Efferocytosis was assessed by counting the number of macrophages containing vesicles with cell debris (apoptotic inclusions) within BAL samples. As some macrophages contain more than one inclusion, the percentage of macrophages containing any apoptotic inclusions was analysed (A) along with the number of apoptotic inclusions per 100 macrophages that contained any inclusions (B). No differences were found between vehicle and neratinib treated mice. Each data point represents one mouse. Bars show mean, error bars standard deviation. Statistical analysis carried out using unpaired t tests.

4.4.5 Concentrations of IL-6 and CXCL1 in BAL and plasma did not change with neratinib treatment

ELISA was used to measure the concentrations of cytokines IL-6 and CXCL1 in bronchoalveolar lavage samples and plasma samples derived from blood from each mouse. In lavage samples, no differences in either IL-6 (Figure 4.21A) or CXCL1 (Figure 4.21B) were found between treatment groups. Plasma

samples were generated by centrifuging whole blood from each mouse to remove the cell compartment. Due to the small volumes of blood obtained from each mouse, one blood sample from a neratinib treated mouse did not yield enough plasma for analysis by ELISA, and so only 6 data points were available for that group. No difference in the concentration of IL-6 (Figure 4.21C) or CXCL1 (Figure 4.21D) were identified. Three of the samples from neratinib treated mice showed CXCL1 concentrations that were below the lowest standard of the standard curve, and so could not be interpolated. These were entered as having a concentration of 0 for analysis.
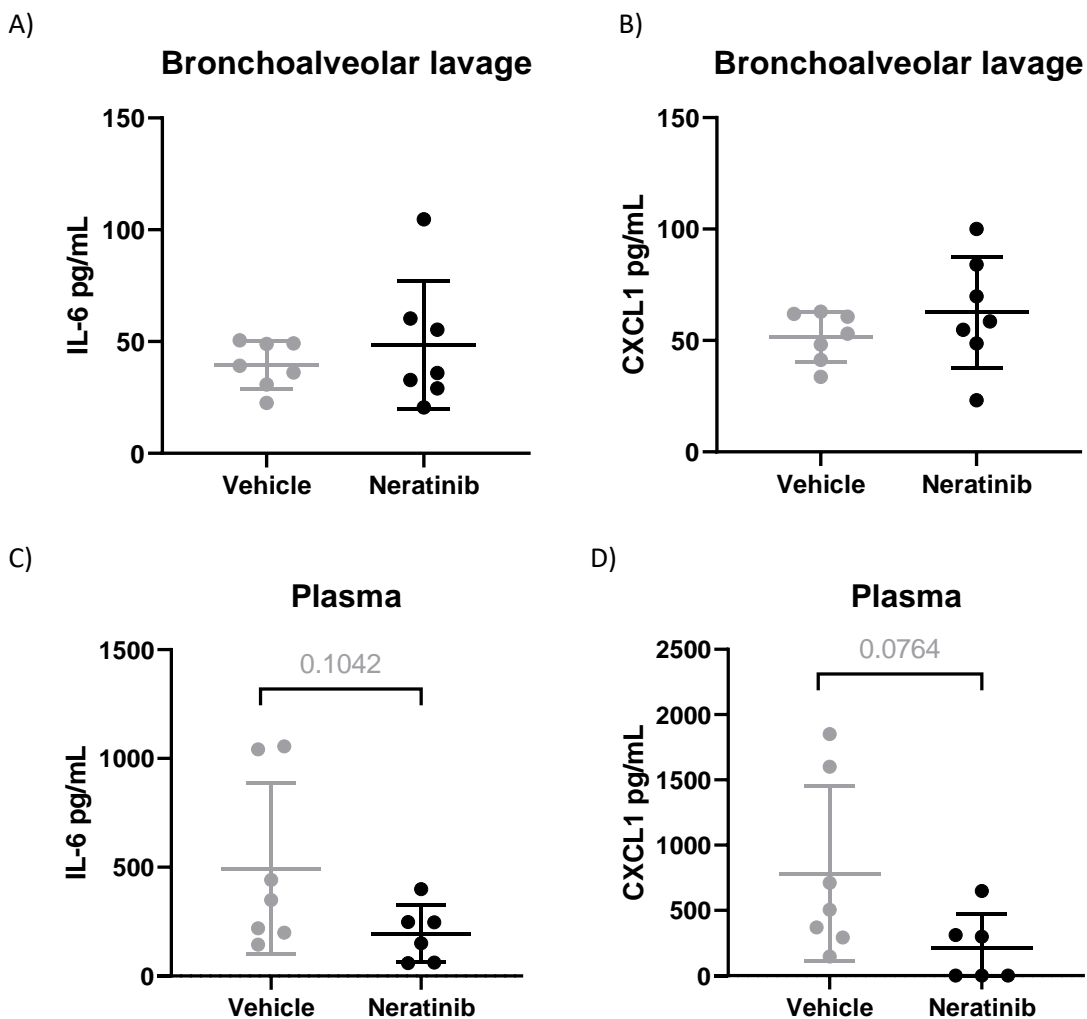
Figure 4.21. IL-6 and CXCL1 in BAL and plasma samples were unchanged with neratinib treatment.
ELISA was used to measure the concentration of cytokines in bronchoalveolar lavage fluid and plasma from mice. In bronchoalveolar lavage fluid samples, IL-6 (A) and CXCL1 (B) were unchanged between treatment groups. Similarly in plasma samples, concentrations of IL-6 (C) and CXCL1 (D) were not statistically different with neratinib treatment. Statistical analysis carried out using unpaired t tests. Bars indicate mean, error bars standard deviation. Each data point represents data from one mouse.

4.4.6 The number and distribution of leukocytes in blood were unchanged between treatment groups

Unlike the previous COPD model, blood samples from each mouse were analysed using a ScilVet ABC Plus™ haematology analyser, which is fully optimised for murine blood. The total number of leukocytes in each mouse sample was found to be unchanged between treatment groups (Figure 4.22A). The differential white blood cell count for this analyser identified monocytes, granulocytes, lymphocytes and eosinophils. Neither the density of each cell type within blood samples (Figure 4.22B) nor the percentage (Figure 4.22C) were found to be different between vehicle and neratinib treated mice.

4.4.7 COPD study II summary

The results of this study demonstrate that neratinib does not significantly reduce inflammatory parameters in this particular mouse model of chronic lung inflammation. There are some cases where a "trend" in the data is observed, for example a reduction in dead cells (as measured by flow cytometry) in bronchoalveolar lavage fluid from neratinib treated mice, and a reduction in CXCL1 concentration in plasma from neratinib treated mice. However as these are not statistically significant, no explicit conclusions can be drawn, and it would not be ethical or humane to repeat this experiment to "chase" a significant p value. As the previous two studies have shown that neratinib does reduce specific aspects of the inflammatory response, these results may indicate that if neratinib were to be used as a treatment, it may only be efficacious if taken early enough into disease onset.
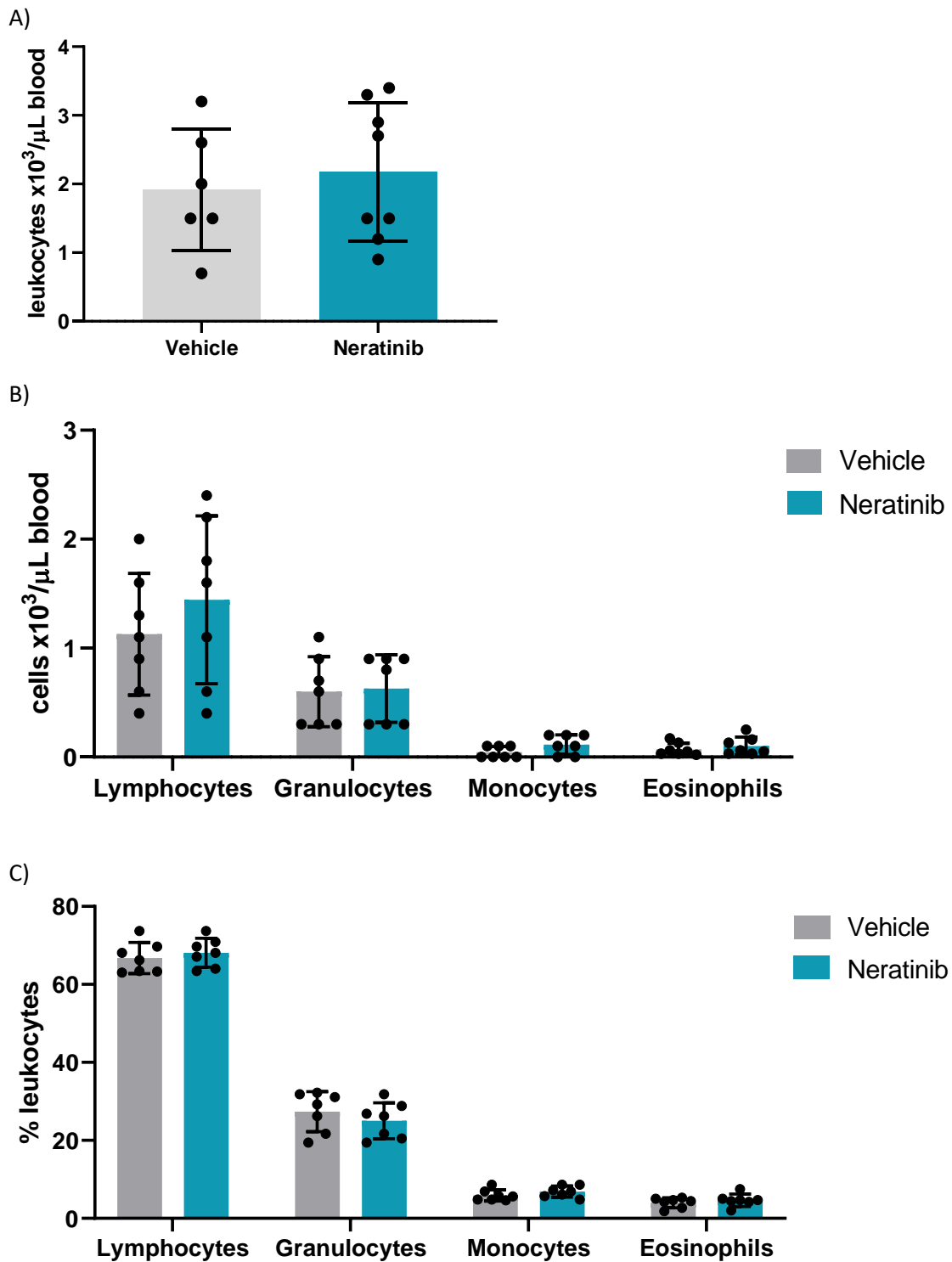
Figure 4.22. The number and distribution of leukocytes in blood was unchanged with neratinib treatment. Blood samples obtained from each mouse were analysed using a ScilVet ABC Plus™ haematology analyser, which detects and counts the number and type of leukocyte in blood samples (A). The density (B) and percentage (C) of monocytes, granulocytes, lymphocytes and eosinophils were also detected. No differences in leukocyte density or distribution were found between mice in vehicle and neratinib treatment groups, using unpaired t tests for individual cell types. Bars indicate mean, error bars standard deviation. Each data point represents data from one mouse.

4.5   Chapter discussion

The results of these studies have yielded some interesting findings into the action of neratinib in an inflammatory lung environment. The most exciting results are perhaps those obtained from the acute LPS-induced lung inflammation model, which showed neratinib-treated mice had reduced numbers of dead neutrophils, and increased rates of efferocytosis in comparison to vehicle treated mice. A reduction in inflammatory cytokine production with neratinib treatment in the chronic inflammation model is also promising. However, no significant differences were observed in the chronic inflammation model in which neratinib was given after disease onset, suggesting that in a clinical setting this drug may be better utilised as a treatment for acute exacerbations of the disease, rather than as a long term therapeutic. Of course much more data would be required to conclude this, including clinical trials in humans with the disease. The data from these mouse studies however give important insights into establishing exactly which aspects of lung inflammation neratinib is be able to attenuate.

4.5.1   Neratinib treatment upregulates efferocytosis in an acute inflammatory model

In the first acute lung injury model, reduced numbers of dead neutrophils were identified in bronchoalveolar lavage fluid from neratinib treated mice. Flow cytometry data showed that the majority of cells (both neutrophils and non-neutrophils) that were positive for TO-PRO-3 were also positive for Annexin V, an apoptotic marker, suggesting that these cells were undergoing secondary necrosis after apoptotic cell death. This finding collaborates with studies in the literature, in which secondary necrosis of neutrophils was demonstrated by transmission electron microscopy in this mouse model, whereas primary necrosis was rare (Rydell-Törmänen, Uller and Erjefält, 2006). Necrotic neutrophils spill their intracellular contents onto tissue, and this release of granule contents includes a number of damage-associated molecular patterns which are known inducers of inflammation (Roth *et al.*, 2015). That this type of cell death is being supressed by neratinib is promising for demonstrating the efficacy of neratinib in reducing pro-inflammatory phenotypes. The mechanism by which it is occurring is unknown, as it was hypothesised that neratinib would upregulate apoptosis, rather than reducing death. It is possible that an upregulation of apoptosis occurred at an earlier timepoint, and at the point at which samples were taken in this study the majority of these apoptotic neutrophils had been cleared by macrophages. This would fit with the increased rates of efferocytosis observed in this study. If further mouse studies were carried out, taking samples at earlier timepoints closer to the induction of inflammation would be useful to assess this.

It is also possible that neratinib is directly regulating pathways involved in efferocytosis by macrophages. There is very little literature regarding the role of ErbB signalling in efferocytosis to support this theory. Work in *Drosophila* showed that in embryos with a constitutively active EGFR ligand (Spitz), macrophages had decreased efficiency of efferocytosis of apoptotic cells (Tardy *et al.*, 2021). However the authors concluded that there may be a number of mechanisms for this finding, including that the additional EGF may be acting as a chemoattractant to "distract" the macrophages from apoptotic clearance, or that EGFR signalling from other tissues may be polarising the macrophages towards phenotype that is less efficient at efferocytosis, rather than directly impacting on pathways that regulate the engulfment of dead cell debris (Tardy *et al.*, 2021). The signalling pathways known to regulate efferocytosis are complex. The release of soluble chemotactic factors by apoptotic cells attracts macrophages, and the presence of phosphatidylserine on the outer membrane leaf indicates a cell is apoptotic (Fadok *et al.*, 1998). The binding of phosphatidylserine to macrophage receptors, primarily BAI, TIM, stabilin and CD300 activates intracellular macrophage signalling pathways that include PI3K-AKT, STAT-SOCS, Rac and RhoA, and supresses NFκB and IFNα/β, resulting in the engulfment of the apoptotic cell (Elliott, Koster and Murphy, 2017). Although it is known that ErbB inhibitors block pathways including PI3K-AKT, there is no evidence in the literature to suggest that in efferocytosis these signalling pathways are activated by the engagement of ErbB receptors. The simplest explanation is that the increase in efferocytosis is not a direct result of inhibiting ErbB signalling, but rather an increase in the availability of apoptotic material to engulf.

If time allowed, this hypothesis would be interesting to follow up experimentally *in vitro*, to identify whether neratinib can directly affect efferocytosis by macrophages. Human monocyte-derived macrophages could be cultured and "fed" apoptotic neutrophils in the presence or absence of neratinib, and the rates of efferocytosis analysed by fluorescent microscopy or immunohistochemistry. Optimisation of this assay was attempted and was unsuccessful, but this would be an important experiment to return to if this project were to be continued. Additionally, immunohistochemical staining of bronchoalveolar lavage samples may be useful to identify whether the increase in apoptotic debris within macrophages is of neutrophil origin – this could be analysed by staining for myeloperoxidase, a commonly used neutrophil marker.

No changes in the rates of cell death or efferocytosis were observed in either of the more chronic models of lung inflammation. This may be due to the timing of these studies: apoptotic and dead cells are rapidly cleared *in vivo*, and in both models of chronic inflammation samples were taken one week after the last treatment with LPS and elastase. Literature indicates that the number of apoptotic neutrophils in the lungs of LPS-treated mice peaks around 60 hours post-treatment, and neutrophils undergoing secondary necrosis peak between 36-60 hours; by 72 hours post-treatment, levels of both

are decreasing (Rydell-Törmänen, Uller and Erjefält, 2006). It is probable that by 8 days post LPS treatment, any excess apoptotic and dead cells have been cleared and levels returned to equilibrium.

4.5.2 Cytokine release in the lungs

From the second mouse model, in which chronic inflammation was treated with a weekly dose of vehicle or neratinib, the most promising result was a reduction in the levels of the cytokine CXCL1 in bronchoalveolar lavage fluid from mice treated with neratinib. CXCL1 (also known as KC in mice) is a key recruiter of neutrophils to sites of inflammation or infection (Sawant *et al.*, 2016). Depletion of CXCL1 in acute lung injury mouse models correlates with decreased early neutrophil recruitment and improved histopathology scores, suggesting a potential therapeutic benefit (Dunn *et al.*, 2018). It is interesting that in our study no changes in the numbers or proportion of neutrophils were detected, as it would follow that reduced levels of a neutrophil chemokine would result in reduced neutrophil numbers. However CXCL1 is not the only neutrophil chemokine in mice, with chemokines including LTB4 and CXCL5 also being known inducers of neutrophil chemotaxis (Grespan *et al.*, 2008; Saiwai *et al.*, 2010), and it appears that other chemotactic factors induced by the inflammatory response in the lungs were sufficient to sustain recruitment.

In humans, CXCL1 is produced by neutrophils, macrophages, epithelial and endothelial cells, and its cognate receptor, CXCR2, is similarly expressed on neutrophils and macrophages amongst other cell types (Miyake *et al.*, 2013; Wu *et al.*, 2021). Macrophage numbers are similarly unchanged in this study with neratinib treatment, suggesting that the reduction in CXCL1 is due to a downregulation in its production or release. One hypothesis is that an increase in neutrophil apoptosis/clearance by macrophages occurred at an earlier timepoint in this model, resulting in a decrease in the production of CXCL1, and that at the timepoint samples were obtained neutrophil numbers may have been replenished but levels of CXCL1 had not. However cytokines have very short half lives *in vivo*, often measured in minutes and hours rather than days (Lotze *et al.*, 1985; Kuribayashi, 2018), which suggests that neratinib may be downregulating other mechanisms relating to cytokine production.

CXCL1 expression by human nasal and bronchial epithelial cells, and human bronchoalveolar macrophages, was found to be upregulated by TNFα (Becker *et al.*, 1994). The PI3K pathway amongst others is known to regulate the TNFα-mediated secretion of CXCL1 into the extracellular space (Shieh *et al.*, 2014), and as PI3K is a key component of ErbB signalling, it is possible that neratinib is reducing CXCL1 release from airway epithelial cells. It would be interesting to measure the concentration of

CXCL1 in isolated neutrophils, macrophages and epithelial cells *in vitro*, to identify whether neratinib is reducing release from any one particular cell type.

Although it did not reach the threshold of statistical significance, a trend towards a decrease in interleukin 6 in bronchoalveolar lavage fluid of neratinib treated mice also occurred in this model, with the p value of 0.0733 indicating that the likelihood of this decrease occurring by chance is only 7.33%. As with CXCL1 it would be interesting to know the origin of this decrease and whether it could be replicated *in vitro*. The measurement of other cytokines in bronchoalveolar lavage fluid samples from mice, including ones specific to macrophages and epithelial cells, would be beneficial, to determine precisely which cells neratinib was regulating in this mouse model. Neither CXCL1 nor IL-6 concentrations were altered by neratinib in the acute LPS-induced inflammation model, suggesting that repeated doses of neratinib, or a longer timeframe, are required to induce this change. No changes in either cytokine were observed in the lavage fluid from mice in the chronic inflammation model in which neratinib was given after the onset of lung inflammation, suggesting that this alterations to CXCL1 production are required from the onset of disease, or possibly a longer length of treatment is required before a difference is observed.

4.5.3   Circulating leukocytes and cytokines

No significant changes were observed in the levels of leukocytes or cytokines in the blood/plasma samples obtained from the chronic mouse models of inflammation, however in the first chronic model, in which neratinib was given weekly at the same time as the inflammatory stimuli, trends towards reductions in circulating leukocyte numbers were observed, particularly in monocyte numbers. It is possible that neratinib is affecting circulating leukocytes in some way, as the drug was given orally in these studies, as it for treating cancer patients, and it is detectable in plasma samples from patients (Keyvanjah *et al.*, 2017). Alterations in whole blood counts are not a known side effect of neratinib treatment in patients (European Medicines Agency, 2018a). If neratinib were affecting circulating leukocyte numbers however, it is interesting that this was not observed in the latter study with ten doses of the drug over two weeks, but is with four doses over four weeks.

Cytokines in plasma samples were only measured with the latter chronic mouse model, and again only a "trend" towards decreased CXCL1 was observed. Blood biomarkers of cytokines such as IL-6 have been shown to correlate with disease severity in patients with COPD (Bradford *et al.*, 2017). As no changes were observed in cytokine levels in bronchoalveolar lavage fluid from this study, it is difficult

to draw any conclusions, as it does not appear that a daily weekday dosing schedule with neratinib is altering inflammatory mechanisms at the site of inflammation.

4.5.4   Limitations of the mouse models

According to the European Medicine Agency report, the plasma half-life of neratinib in mice is 1.4 hours, with a moderate rate of absorption and a peak plasma concentration after oral administration at 2-4 hours (European Medicines Agency, 2018b). In the studies in this chapter, the timepoints at which samples were taken are likely to be after the majority of the drug has cleared, and earlier timepoints may have been beneficial. The dosing protocol for neratinib in the final study in this chapter was based on a paper in which neratinib showed efficacy in attenuating liver fibrosis in a mouse model when given daily for two weeks, 14 days after the onset of disease (Park *et al.*, 2020). The dosing in the study for this thesis however could only be carried out on weekdays, and as the final neratinib dose was given on a Friday, mice were culled and samples collected on the Monday, 72 hours after the final dose of neratinib. Based on the short plasma half-life of neratinib, continuing the administration every 24 hours until culling would be more appropriate to ensure any potential effects of neratinib are not missed, and if any future studies were to be carried out this schedule would be utilised.

4.5.5   Translational relevance for the treatment of lung inflammation in COPD

To assess the relevance of the results of these studies to human disease, differences must be noted between the mouse models selected and the lung inflammation observed in humans with COPD. The percentage of each leukocyte measured in bronchoalveolar lavage fluid samples from the chronic mouse models is roughly on par with those observed in human studies. Human BAL samples from people with COPD showed 14% neutrophils, 65% macrophages, 20% lymphocytes and >1% eosinophils (Vaguliene *et al.*, 2013). In the chronic mouse studies within this chapter, the percentage of neutrophils is similar (~10%), however lymphocytes were generally below 5% and thus macrophages made up the vast majority of the cells in lavage fluid at ~85-90%. As lymphocytes, particularly cytotoxic T cells and NK cells are known to contribute to the pathogenesis of COPD (Rao *et al.*, 2021; Williams, Todd and Fairclough, 2021), it is likely that the mouse models chosen for this work are under-representative of the adaptive immune response in this disease. As the focus of the work in this thesis is on neutrophilic inflammation, this was considered an acceptable limitation, although if this work were to be continued it would be interesting to incorporate immunophenotyping of the lymphocytes

by flow cytometry, to determine if any differences in the T cell subsets are observed with neratinib treatment.

The results from these three mouse models alone are not sufficient to indicate whether neratinib would be effective at reducing inflammation in COPD. The augmentation of specific anti-inflammatory mechanisms and attenuation of pro-inflammatory mediators is promising; however many components of the inflammatory response were not affected by neratinib treatment, and further work would definitely be required to determine a potential benefit for patients. It is also important to note that the mechanisms of action of neratinib may not matter at all if patients find the drug intolerable; reducing inflammation and thus breathlessness, but inducing the side effect of nausea for example may not be beneficial overall for some patients, and tolerance of a side effect in a population of cancer patients is likely to be very different to that in patients with COPD. Ultimately, clinical trials would be required to assess this.

5 Using a multi-omics approach to understand ErbB expression, regulation and signalling in neutrophils and inflammation

5.1 Introduction and aims

ErbB expression in immune cells is not well documented, at either the gene or protein level. I have shown that treatment of human neutrophils with pharmacological ErbB inhibitors *in vitro* induces apoptosis. This suggests that human neutrophils express ErbBs, but the possibility that the inhibitors are having off-target effects and inhibiting other signalling pathways cannot be excluded. This chapter aims to address both of these possibilities, by using a data mining approach to interrogate published datasets for ErbB expression at the gene level, and also using mass spectrometry based phosphoproteomics to elucidate the downstream signalling pathways by which ErbB inhibitors are inducing neutrophil apoptosis.

To address the first aim regarding expression of ErbBs, published RNAseq and transcriptomics microarray datasets were analysed for the levels of ErbB expression in human, mouse and zebrafish neutrophils. This data mining technique was also used to address a different (but related) research question: whether ErbB expression is regulated in inflammation. Since pharmacological inhibition and genetic knock-down (in zebrafish larvae) of particular ErbB family members reduces neutrophilic inflammation in certain disease models, it may be that ErbBs themselves are regulated in inflammatory environments. This was assessed by analysing published datasets generated from samples in both homeostatic and inflammatory environments, including patients with COPD and human neutrophils stimulated *in vitro*.

Many researchers publish complete transcriptomics datasets on open-access databases such as ArrayExpress, where they are freely available for analysis by others. An advantage of these assays is that they are genome-wide, and thus unbiased; using a systems biology approach allows for global changes in gene expression to be observed. These datasets can be used to identify changes in specific subsets of genes, and are useful for researchers analysing the expression of their genes of interest under particular conditions. Exploiting these datasets is an excellent way to generate novel findings, without the time and costs associated with carrying out the assay. This section of work was carried out during University closures due to COVID-19 and was an ideal way of generating data that contributes to the research questions posed by this thesis, while laboratory access was not available.

The second aim of this chapter used a phosphoproteomics approach to attempt to identify the downstream signalling pathways by which ErbB inhibitors, specifically neratinib, are inhibiting to

induce apoptosis in human neutrophils. Phosphoproteomics was chosen specifically as protein phosphorylation is one of the most common the post-translational modifications regulating signalling pathways within cells. The addition or removal of a phosphate group, and the location on the protein at which this occurs, can modify the enzymatic activity, confirmation, and/or binding affinity, regulating interactions with other components within the signalling pathway and enhancing or inhibiting downstream interactions. Similar to the use of RNAseq or microarray datasets, the use of mass spectrometry to identify phosphorylated peptides, or the "phosphoproteome" of neutrophils is unbiased, identifying changes that may be missed by a more targeted approach.

5.2   GeneChip assays reveal no consistent changes in ErbB expression in inflammatory contexts

The first aim addressed in this chapter was to determine whether ErbB expression was regulated in inflammatory environments. This was carried out by mining published datasets, all of which were generated using the Affymetrix GeneChip Human Genome Array, a chip-based assay that allows the expression of genes across the entire human genome to be analysed. This expression is quantified by indirectly measuring the abundance of RNA transcripts in samples. The chip contains oligonucleotide probes complementary to the entire known human genome, including transcript variants. The sample added is complementary DNA (cDNA) generated from RNA isolated from a wide range of samples – *in vitro* cell lines, whole blood, sputum, tissue etc. The cDNA hybridises with the oligonucleotide probes on the chip, which emit a fluorescent signal that correlates with the level of hybridisation, allowing for the abundance of cDNA (and thus RNA) in the original sample to be determined.

The data from studies using the Affymetrix GeneChip Array is often published both as raw data, and "processed" data formats. When a chip is scanned, an image is acquired showing the fluorescence emitted by each hybridised probe. In order to generate data on a scale that directly correlates with transcript abundance, this raw data must be background corrected, normalised and transformed. There are various mathematical algorithms and software packages that can carry out this process, including the Robust Multiarray Average (RMA) and dChip, each with their own advantages and disadvantages. As different methods were used for each published dataset analysed in this chapter, figures in this section contain very different scales and cannot be directly compared. However, each processing method results in data on a scale that correlates linearly with transcript abundance. Therefore, within a dataset, the expression levels of different genes can be directly compared. Although it would have been possible to take the raw data from each dataset analysed here and

process them all using one particular method, it was decided instead that the processed data from these studies would be used. This has the advantage of being able to validate the results obtained in this chapter by extracting data from other genes analysed in the published research articles for these datasets, and determining if the same results are obtained (e.g. a ten-fold increase in a particular gene in one condition).

Affymetrix probes are given designations depending on the uniqueness of the probe sequence to a particular gene, ranging from a probe that: perfectly matches a single transcript; matches multiple transcript variants of the same gene; matches transcript variants for the same gene family; or is identical/highly similar to probes for other genes. In this thesis, only data from probes of the first three types was analysed, and data from probes identical/highly similar to other genes was not included.

In this chapter section, four different datasets were interrogated. Two were samples obtained from patients with COPD (and healthy controls), one blood and one sputum. The other two datasets were obtained from peripheral blood neutrophils from healthy volunteers. The aim of this chapter section is to identify whether ErbB genes are expressed in these sample types, and if so which family members, and whether they are regulated in inflammatory contexts.

5.2.1   Comparison of ErbB expression across human leukocyte subsets in healthy individuals

The evidence for ErbB expression on immune cells is inconsistent, with most research focusing on cancer-related cells or regulation during development. The first dataset analysed in this chapter focused on the expression of ErbB genes across four different leukocyte subsets isolated from the blood of healthy volunteers (Richard *et al.*, 2016). In this study, peripheral blood samples were collected from five healthy donors, and antibody-conjugated magnetic bead selection was used to isolate leukocyte subsets: CD4+ (helper T cells), CD8+ (cytotoxic T cells), CD14+ (monocytes) and CD16+ (neutrophils). Following isolation, RNA was extracted, cDNA synthesised and the Affymetrix GeneChip Array was utilised to measure gene expression. Data was processed using the Robust Multichip Average (RMA) method.

Before assessing the levels of ErbB transcripts, the dataset was validated by analysing the expression of various control genes. The chosen controls in this dataset interrogation were beta actin (*ACTB*) and glyceraldehyde 3-phosphate dehydrogenase (*GAPDH*) as housekeeping genes, and defensin alpha 3 (*DEFA3*) and T cell receptor epsilon chain (*CD3E*) as positive and negative controls. Since neutrophils were the cell of interest, the data were analysed by comparing gene expression in each leukocyte type to that in neutrophils. Both *ACTB* and *GAPDH* appear to have relatively consistent expression between

leukocyte subsets, however when statistical analysis is carried out *GAPDH* expression is increased in monocytes in comparison to neutrophils, and *ACTB* expression is higher in neutrophils than in both T cell subsets (Figure 5.1A). As the differences in expression in neutrophils compared to other leukocyte subsets do not follow the same pattern across the two housekeeping genes, no conclusions were drawn from this.

Defensin alpha 3 (*DEFA3*) is antimicrobial peptide found in the granules of neutrophils, and so expression was expected to be higher in neutrophils than other leukocyte subsets, which was observed here (Figure 5.1A). T cell receptor epsilon chain (*CD3E*) was expressed at much higher levels in both T cells subsets than myeloid cells, as expected. These findings gave confidence to the data analysis approach used. The changes in expression observed for these genes are much more pronounced than the differences in the expression of the housekeeping genes, which suggests that true differences in expression are discernible despite the levels of expression in the housekeeping genes not being completely uniform.

The expression of all ErbB family members was relatively low across all leukocyte subsets when comparing the processed signal values to control genes (Figure 5.1B). Notably, ErbB expression is at similar levels to some of the genes selected as negative controls, such as *CD3E* expression in neutrophils and monocytes, and *DEFA3* expression in all cells except neutrophils. ErbB expression does appear somewhat varied between each leukocyte subset in comparison with the differences observed in the housekeeping genes. Expression of *ERBB3* was found to be significantly higher in neutrophils compared to helper T cells and monocytes, and *ERBB4* expression was significantly higher in neutrophils than helper T cells (Figure 5.1B). It is worth noting that these significant differences in gene expression are less than even half a fold change, and are closer in scale to the fluctuations observed in the housekeeping genes than the positive than negative control genes. Overall, these data suggest that ErbB expression is relatively low across leukocyte subsets, and as any differences in expression are small, the biological impact cannot be inferred from this particular dataset.
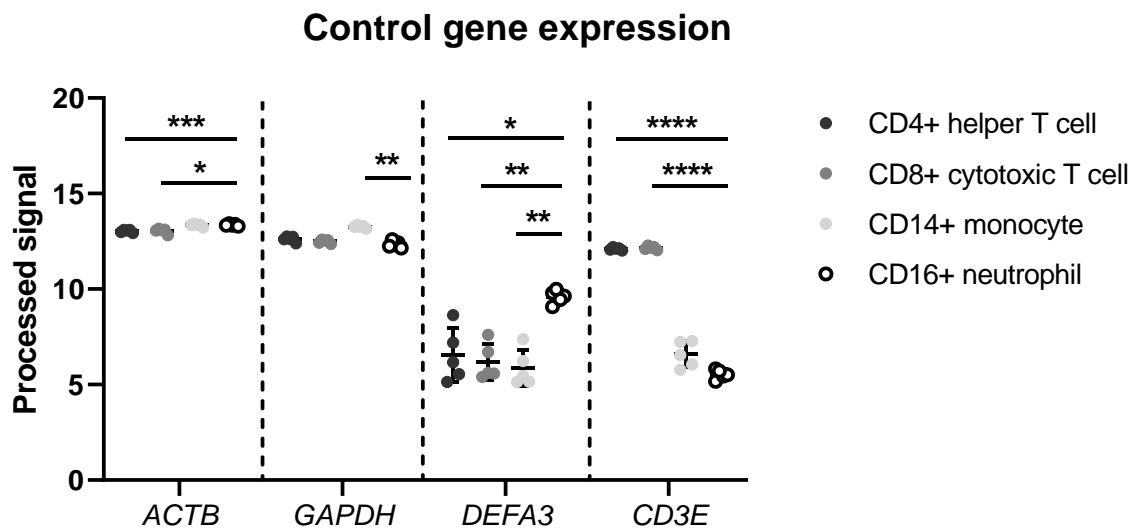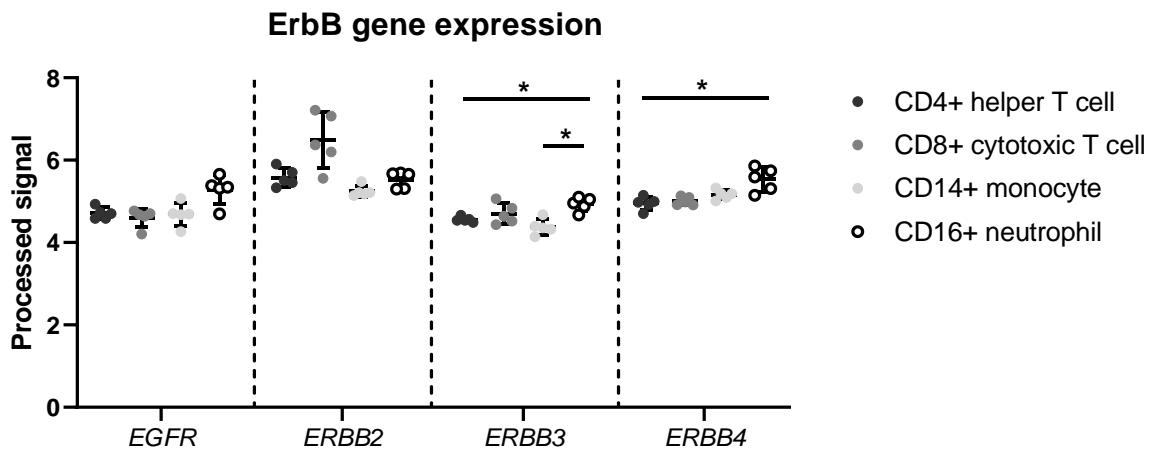
Figure 5.1. ErbB expression changes across leukocyte subsets.
Gene expression was analysed in subsets of leukocytes, isolated from human peripheral blood samples from five healthy donors. CD4+ and CD8+ T cells, and CD14+ monocytes and CD16+ neutrophils were isolated using antibody-conjugated magnetic bead selection, and gene expression measured using the Affymetrix GeneChip assay. Expression of housekeeping genes and positive and negative control genes were assessed to validate the use of this dataset (A). The expression of *ERBB3* and *ERBB4* was significantly increased in neutrophils, in comparison to Helper T cells and monocytes (*ERBB3*) and Helper T cells (*ERBB4*). Each data point represents gene expression from one donor. Bars show mean ± SD. Significance determined two-way ANOVA with multiple comparisons. *p<0.05; **p<0.01; ***p<0.005; ****p<0.0005.

5.2.2 Human neutrophils stimulated *in vitro*

Results from the previous dataset suggest that ErbB expression is low, possibly negligible, across leukocyte subsets. However there are studies in the literature that have detected ErbB expression at the protein level on leukocytes, such as EGFR expression on human neutrophils and ErbB2 and ErbB3 expression on human monocytes by flow cytometry, and EGFR on murine macrophages by western blot (Lewkowicz *et al.*, 2005; Lu *et al.*, 2014; Ryzhov *et al.*, 2017). It was therefore hypothesised that although basal ErbB expression in unstimulated cells is low, stimulation of these immune cells during infection or inflammatory environments may induce expression changes. Various ErbB family members are known to be overexpressed in certain tumours, and ErbB signalling does play a role in inflammation, so this dataset was used to determine whether ErbB genes themselves are upregulated in inflammatory environments.

The aim of this particular published study was to develop a method of isolating neutrophils from whole blood using a microfluidics chip, developed by the authors (Kotz *et al.*, 2010). As part of the testing of this device, a peripheral whole blood sample from a single healthy donor was taken and stimulated for 16 hours with either LPS, GM-CSF and IFNγ, or left unstimulated, followed by an on-chip isolation of neutrophils. Four different chips were tested using blood from one human donor, and thus the four data points for each condition can be considered technical replicates. For this reason, no statistical analysis was carried out on this particular dataset. The isolated neutrophil samples then underwent RNA isolation and cDNA synthesis, followed by use of the Affymetrix Human Genome U133 Plus 2.0 Array to analyse the transcriptome of samples. The dChip Perfect Match method was used to process data.

For this dataset, *GAPDH*, *ACTB* and hypoxanthine phosphoribosyltransferase 1 (*HPRT1*) were selected as housekeeping genes. Their levels do appear to vary somewhat between each treatment condition, particularly *ACTB* and *HPRT1*, but there is no consistent increase or decrease in the levels of these housekeeping genes in one particular condition (Figure 5.2A). The research article in which this dataset is published focused on an increase in *CXCL8* in the LPS stimulated and GM-CSF + IFNγ stimulated conditions, compared to the unstimulated sample, which was also shown here (Figure 5.2A).

This particular array contained several different probes, specific to different transcript variants, of *EGFR*, *ERBB2* and *ERBB3*, which are indicated by the numbers on the x axis of each graph in the figures. Only one probe for *ERBB4* was present in this array. All members of the ErbB family show similar low expression patterns, in comparison to the housekeeping/control genes selected (Figure 5.2B-E). There is some variation in the abundance of transcript variants for each ErbB family member, although this variation would not be greater than a fold change from the highest to the lowest expressed.

The differences in ErbB expression between each treatment condition (unstimulated, LPS stimulated, or GM-CSF + IFNγ stimulated) are also small, and inconsistent between transcript variants. In the *EGFR* family, transcript variant 6 does appear to be increased slightly in the LPS stimulated condition compared to the control, however this pattern is not shown in any of the other transcript variants (Figure 5.2B). *ERBB2* potentially shows the clearest increase in transcript abundance in both LPS and GM-CSF + IFNγ in comparison to the unstimulated condition, for both transcript variants (Figure 5.2C). However the increase is relatively small, and when compared to variation in the control genes looks to be negligible. *ERBB3* expression shows no consistent changes between treatment conditions (Figure 5.2D), nor does *ERBB4* expression (Figure 5.2E). Taken together, this dataset suggests that ErbB expression does not vary in human neutrophils stimulated with either LPS or GM-CSF + IFNγ, using this particular protocol. However it must be noted that as no statistical analysis was carried out on this dataset, due to all data coming from one blood donor, only preliminary conclusions can be drawn.
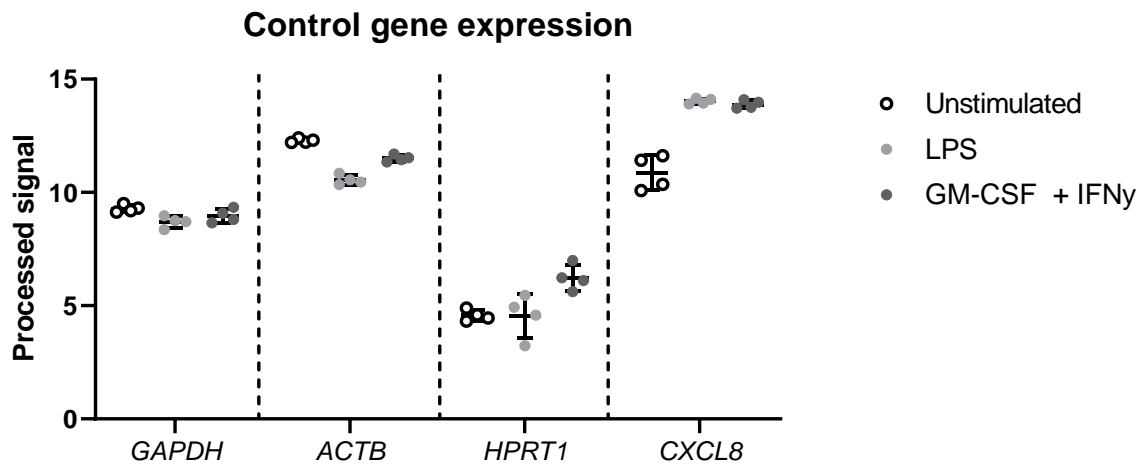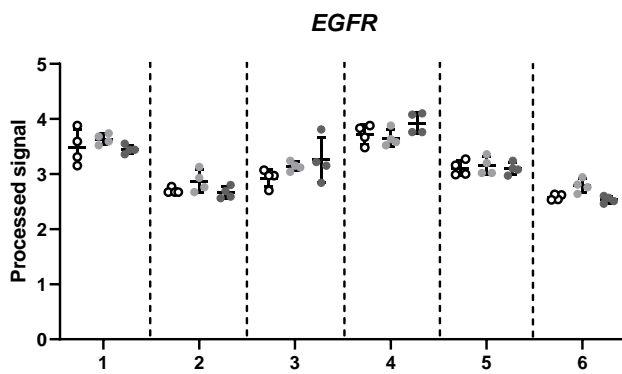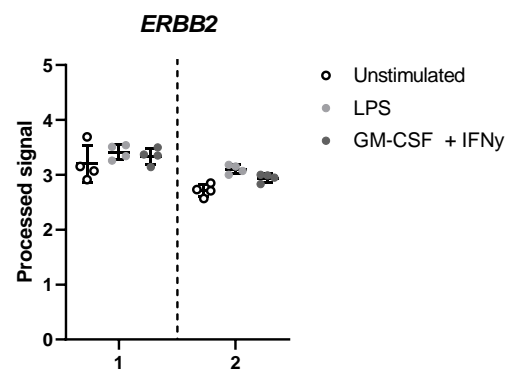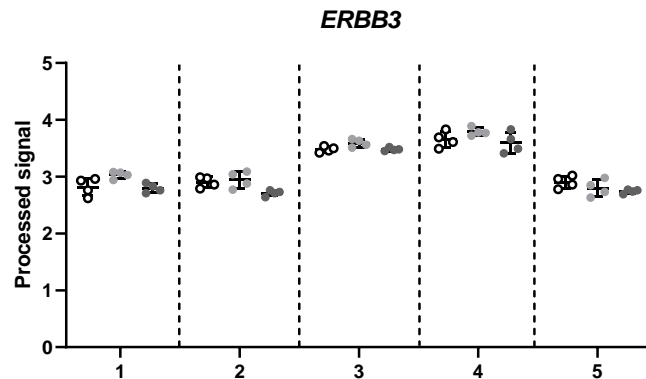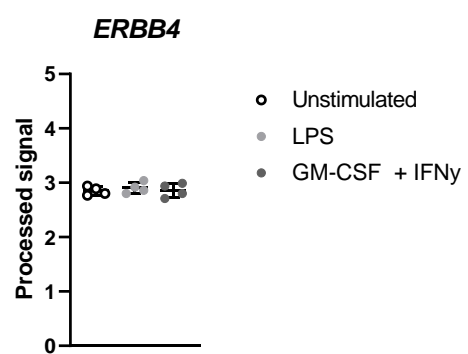
Figure 5.2. Expression of ErbB genes does not differ in neutrophils treated with LPS or GM-CSF + IFNγ. Gene expression, measured as transcript abundance using the Affymetrix GeneChip Array, was analysed in human neutrophils treated with either LPS, GM-CSF + IFNγ, or left unstimulated. The published dataset was interrogated for a number of housekeeping and control genes (A), and the four ErbB family members, *EGFR* (B), *ERBB2* (C), *ERBB3* (D) and *ERBB4* (E). Numbers on the x axis of B-D indicate different transcript variants for that particular gene. No substantial changes were observed in the expression of any ErbB genes between the treatment groups. Each data point represents a technical replicate, all data points are from a single healthy blood donor. Bars indicate mean ± SD.

5.2.3 ErbB expression profile in blood samples from patients with COPD

The previous datasets were used to analyse ErbB expression in single cell populations. It was concluded that ErbB expression is low across leukocyte populations, and any variations in expression are relatively small. Little change in ErbB expression was found in neutrophils when stimulated *in vitro.* However in an inflammatory environment *in vivo*, neutrophils and other immune cell subsets do not exist in isolation; the inflammatory infiltrate in tissues of patients with inflammatory disease is highly complex and dynamic. To determine whether ErbB expression is regulated globally within these tissues, the next datasets analysed were derived from samples taken from patients with COPD, or healthy controls.

In this particular study, the authors analysed whole blood samples taken from 28 patients admitted to hospital with COPD (Almansa *et al.*, 2012). Patients were stratified based on whether they were admitted to the Intensive Care Unit (ICU) for respiratory failure (12 patients), or admitted to non-ICU wards for non-critical exacerbations (16 patients). Blood samples from four healthy donors, who did not have COPD, and were of similar ages were also analysed for comparison. All subjects were tested for fungal, bacterial and viral infections, and this data was also used as a method of stratification. All samples from healthy donors tested negative for infection. The Agilent Whole Human Genome Oligo Microarray Kit, containing 41,000 unique human genes and transcripts, was utilised to measure gene expression from peripheral blood samples. Raw data was processed using the Robust Multichip Average (RMA) algorithm. For this particular dataset, data processing also included normalisation to the gene P75, and baseline transformation of the data using the median of the healthy control samples.

From the processed dataset, the control genes selected for this analysis were *ACTB*, *HPRT1* and *P75*. As the generation of processed data included normalisation to *P75* followed by transformation to the median expression of the healthy controls, the healthy control samples have a median *P75* expression value of 0 (Figure 5.3A). Samples from patients with COPD had a wider range of *P75* expression, however this did not significantly differ from healthy control expression when patient samples were stratified either by type of hospital admission (Figure 5.3A) or the presence of infection (Figure 5.3B). The same was true for the housekeeping genes *HPRT1* and *ACTB*. Again the range of expression was larger in patients with COPD compared to healthy controls, possibly due to the difference in sample size. People with COPD are also likely to have a broad range of co-morbidities and will be undergoing various treatment regimens that may be altering immune cell phenotypes.

Myeloperoxidase (*MPO*) was selected as a positive control gene, as the authors identified this particular gene as being upregulated in patients with COPD admitted to the ICU. Reassuringly, an

upregulation of *MPO* was also observed in this study, with expression being significantly higher in patients admitted to ICU wards, but not non-ICU patients, in comparison to healthy controls (Figure 5.3A). This increase in expression is possibly due to the neutrophilia observed during COPD exacerbations, as neutrophils are the cell that predominantly expresses myeloperoxidase. In this particular study, blood samples were analysed for immune cell counts, and patients admitted to ICU wards had significantly higher neutrophil counts per mm³ blood than non-ICU admissions. The expression of *MPO* does not appear to be dependent on the presence of infection, as there is a statistically significant increase in expression in patients with COPD compared to healthy controls, regardless of whether an infection was detected (Figure 5.3B).

When observing ErbB expression in healthy controls and patients with COPD stratified by their type of hospital admission (ICU vs non-ICU), there is no immediately obvious change in expression across the board. Although there are some trends towards increased or decreased ErbB expression in patients with COPD in comparison to healthy controls, for example *EGFR* and *ERBB4* expression appearing increased in patients admitted to the ICU, no statistically significant differences were found (Figure 5.3C).

ErbB expression was also analysed in the context of whether patients tested positive or negative for infection. Expression patterns when stratifying by the presence of infection were broadly similar to those observed when stratifying by disease severity, with no significant differences in ErbB expression between the different groups of patients (Figure 5.3D). There was one case of a statistically significant change, in the expression of one of the two *ERBB4* genes, which was increased in patients with COPD who tested negative for infection in comparison to both healthy controls and patients who tested positive for infection. When observing this data as it is shown in the graph (Figure 5.3D), the increase in this particular group does not appear particularly different to the variations in expression observed across other genes, and the significance observed here may simply be a by-product of the high number of multiple comparisons carried out in this statistical analysis. In addition, as this significant difference was only found in one of the two probes for *ERBB4*, it is difficult to draw conclusions.

It is important to note that the small size of the healthy control group (4 donors) compared to the COPD group (28 patients) may be skewing the results of this analysis, and an increase in the sample size of the healthy control group would increase the statistical power of this analysis. More neutrophils were present in the blood of patients with COPD admitted to the ICU than non-ICU ward admissions, adding another variable. Based on the data collected however, the results suggest that there is little variation in the global expression of ErbB genes in peripheral blood of patients with COPD, in comparison to healthy controls.

A)

Control gene expression - ICU

- ○ Healthy Control
- ● COPD - non-ICU patient
- ● COPD - ICU patient

B)

Control gene expression - infection

- ○ Healthy Control (no infection)
- ● COPD (no infection)
- ● COPD (infection)

C)

ErbB gene expression - ICU

- ○ Healthy Control
- ● COPD - non-ICU patient
- ● COPD - ICU patient
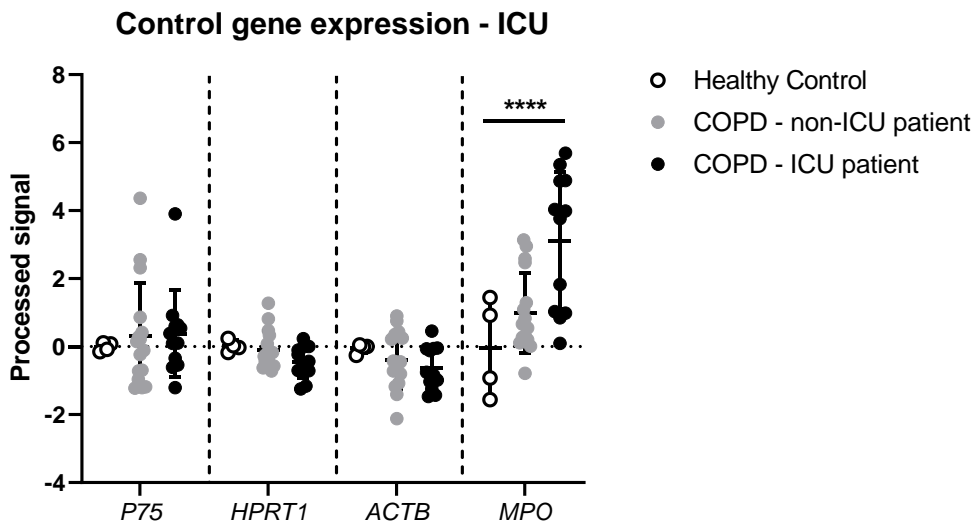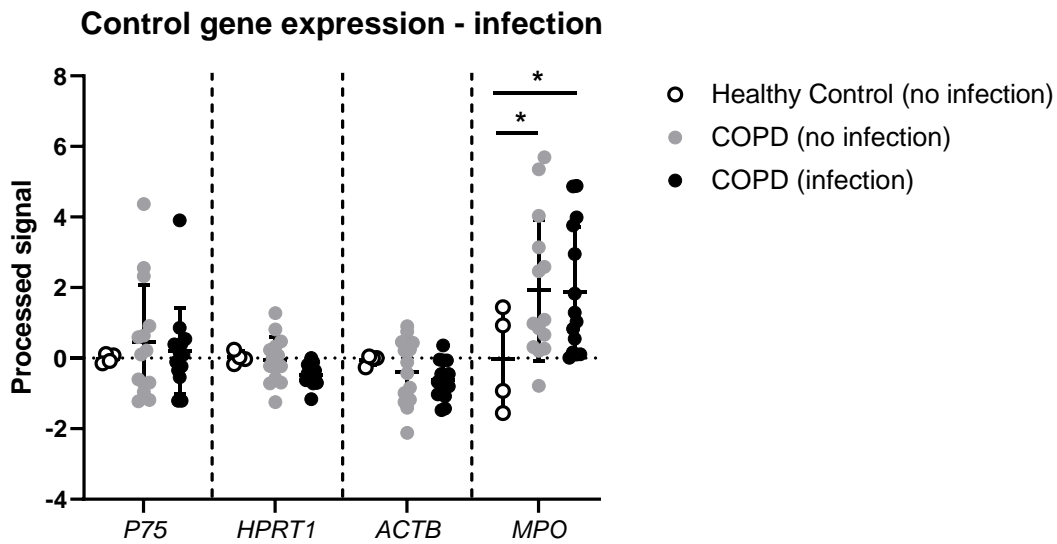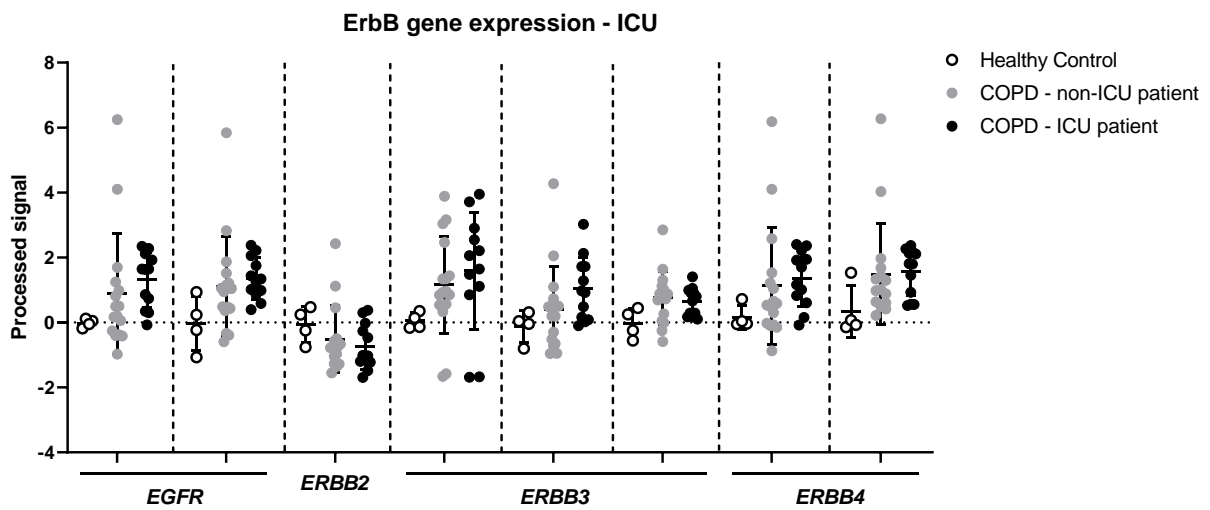
D)
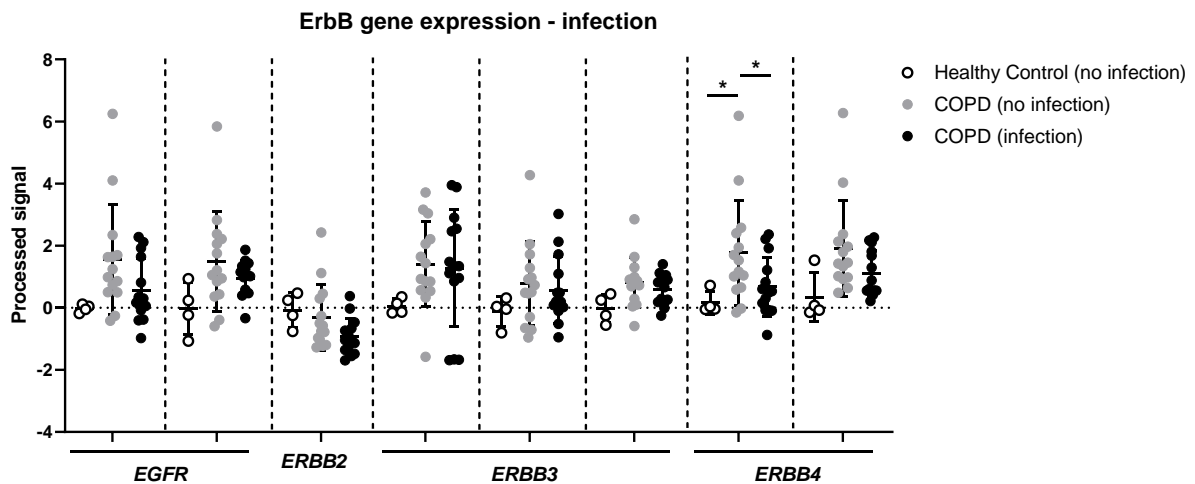
Figure 5.3. Expression of ErbB family members is broadly unchanged in blood samples from patients with COPD.

Gene expression in peripheral blood samples of patients with COPD, or healthy control donors, was measured using the Agilent Whole Human Genome Oligo Microarray Kit. Gene expression was normalised to *P75* gene levels, and data was baseline transformed using the median of the healthy control samples. COPD patients were stratified either based on disease severity (admission to ICU wards or non-ICU wards), or presence of infection. MPO expression increased in COPD patients admitted to ICU (A), and was increased in COPD patients regardless of the presence of infection (B). Housekeeping genes expression levels did not differ either with disease severity (A) or infection (B). ErbB expression did not change in COPD patients when stratified by disease severity (C), and only one statistically significant difference was observed in *ERBB4* expression, in COPD patients negative for infection in comparison to both COPD patients with infection, and healthy controls (D). Each data point represents gene expression from one donor. Bars show mean ± SD. Significance determined two-way ANOVA with multiple comparisons. *$p<0.05$; **$p<0.01$; ***$p<0.005$; ****$p<0.0005$.

5.2.4   ErbB expression in sputum samples from patients with COPD

The previous dataset analysed indicated that ErbB expression in blood cells does not appear to vary in patients with COPD in comparison to healthy control patients, and statistically significant differences that are present are not large. Although inflammation in COPD can be systemic, the lungs are the primary site of the chronic inflammatory environment in this disease. The next dataset therefore analysed induced sputum samples taken from patients with different stages of COPD (Singh *et al.*, 2011). Patients were stratified according to GOLD guidelines, which is based on the severity of dyspnoea (breathing difficulties) and pulmonary function tests (Manian, 2019). Samples were taken from a total of 143 patients in this study and classified as either stage II (moderate COPD; 71 patients), stage III (severe COPD; 59 patients) or stage IV (very severe COPD; 13 patients).

An additional step was carried out when analysing this data for this thesis: the removal of outliers. This particular dataset had a number of apparent outliers, for example in the *ERBB3* group, in which four data points were >1000. The ROUT test for outliers developed by GraphPad Prism, with a false discovery rate of 1% was utilised (Motulsky and Brown, 2006). The cleaned data was then inputted into graphs and statistical tests carried out to identify differences between conditions.

As previously, the expression of housekeeping genes and positive control genes were first analysed to validate the dataset. Levels of *ACTB* were lower in stage III and stage IV patients in comparison to those in stage II; however, the expression of *GAPDH* did not vary between patient stages (Figure 5.4A). The research article that this dataset is published in reported an increase in *IL18R1* expression in stage III and IV patient samples in comparison to samples taken from patients in stage II of the disease, which was also shown here. Expression of *CXCL8* was also increased in patients with stage III and IV of the disease in comparison to stage II. The increase in this neutrophil chemotactic agent correlates with the neutrophilia that is more pronounced in patients in the later stages of COPD.

Initial observations of the expression of ErbB genes in this dataset show that expression is considerably lower than the housekeeping and control genes measured. With the possible exception of *ERBB3*, the expression of which reaches 300 arbitrary units (processed signal), the levels of expression barely register when compared to that of *ACTB*, *GAPDH* and *CXCL8*. However, some statistically significant differences were observed in the expression of ErbB genes between patients with different stages of COPD, although these were not particularly consistent across transcript variants of each family member. *EGFR* expression for example decreases between stage II and III in two of the transcript variants (1 and 4 on the graph), but is another transcript variant (2) this is increased (Figure 5.4B). Similarly, *ERBB2* expression is decreased between stage II and III patients in one of the two transcript variants in this array, but the other shows no statistically significant changes (Figure 5.4C). *ERBB3* has the most consistent pattern; expression is higher in stage IV of the disease in comparison to both stage III and stage II, and this is statistically significant in two of the five transcript variants (Figure 5.4D). *ERBB4* expression was lowest out of all the ErbB family members, and did not vary between the different stages of COPD (Figure 5.4E).

D)

ERBB3

E)

ERBB4
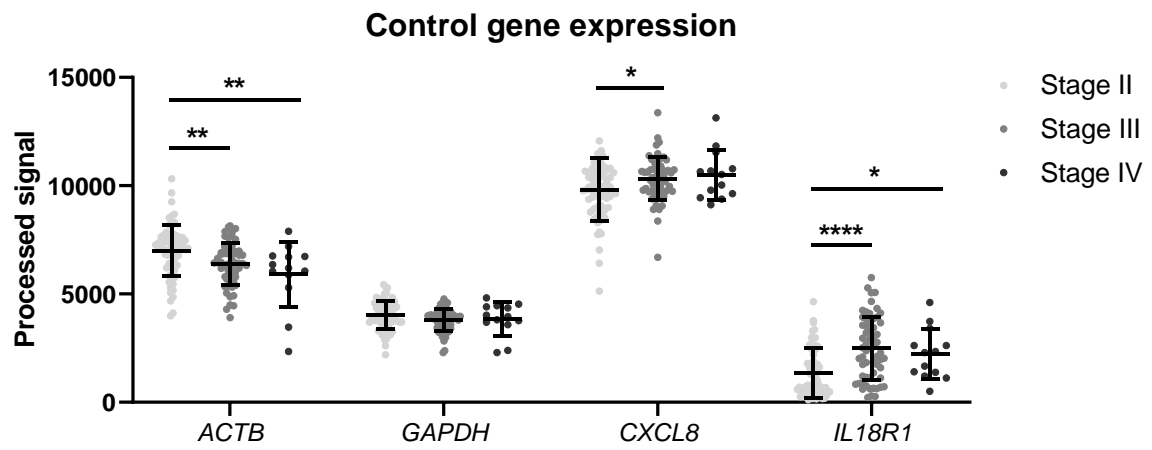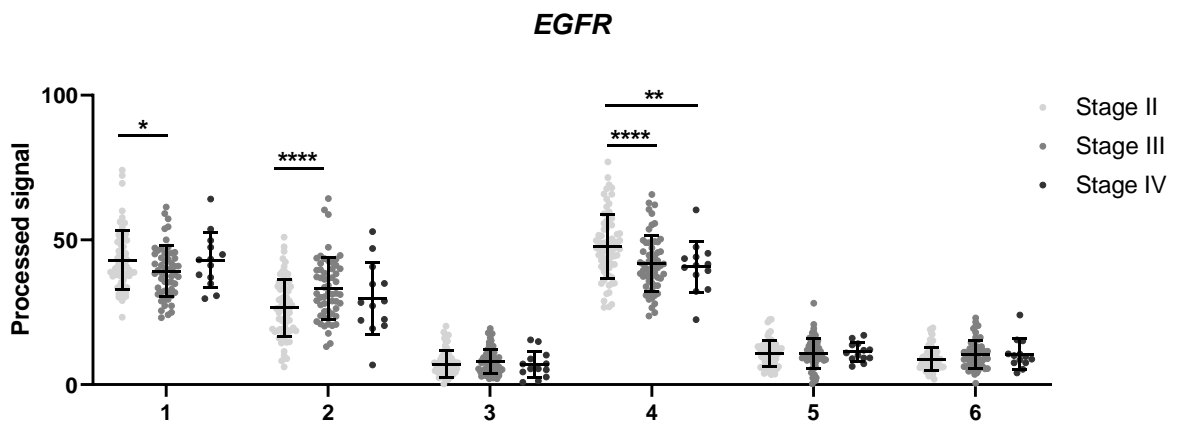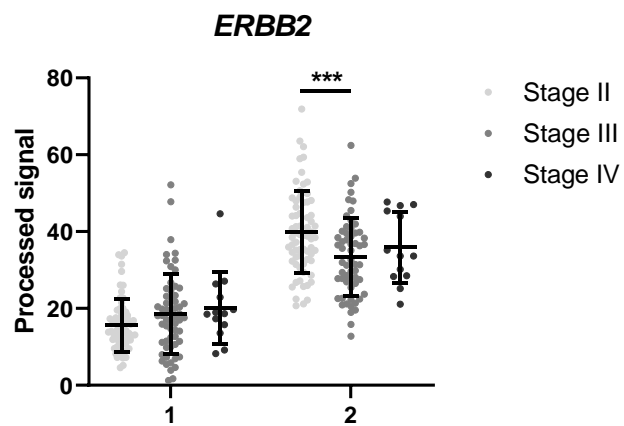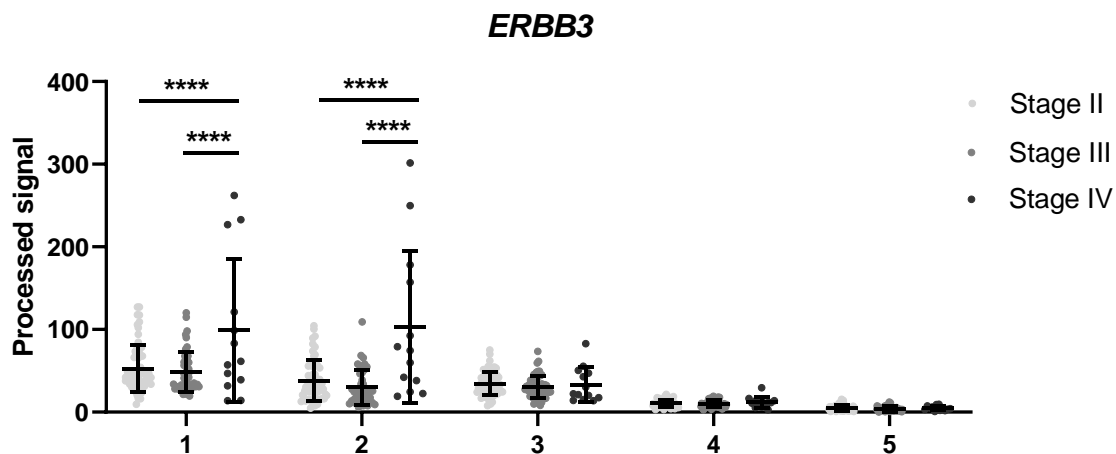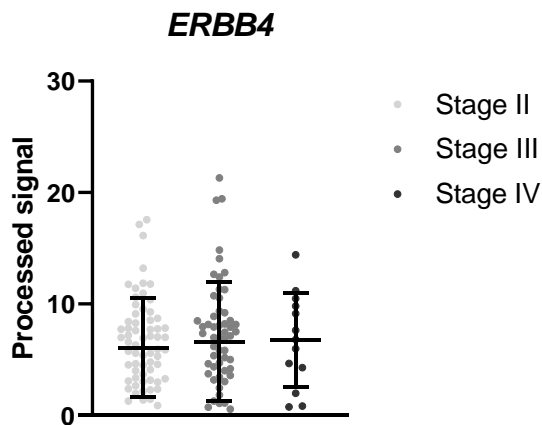
Figure 5.4. Gene expression in sputum samples from patients in various stages of COPD.
Gene expression was assessed in induced sputum samples from patients with COPD, stratified by disease severity into GOLD stages II, III and IV. Expression of two housekeeping genes (*ACTB* and *GAPDH*) and two positive control genes (*CXCL8* and *IL18R*) were analysed to validate the dataset (A). Changes in *EGFR* expression were identified in three of the five transcript variants (B). *ERBB2* expression was also altered in one of the two transcript variants for that gene (C), and *ERBB3* expression in two of the five transcript variants analysed in this array (D). No changes in *ERBB4* expression were identified (E). Each data point represents gene expression from one donor. Bars show mean ± SD. Outliers removed using the ROUT method (Q=1%) (outliers not shown). Significance then determined two-way ANOVA with multiple comparisons (A-D) or one-way ANOVA with multiple comparisons (E). *p<0.05; **p<0.01; ***p<0.005; ****p<0.0005.

The inconsistency in the direction of changes observed in this study, when they are present at all, indicates no clear pattern of change in ErbB expression in sputum samples from patients with different stages of COPD. This particular dataset is limited in that it does not include healthy control patients, and the number of patients in the stage IV group is also considerably lower than the other two stages. However, based on the results obtained, in combination with the previous dataset that analysed ErbB

expression in peripheral blood samples of patients with COPD, it does not appear that ErbB expression is highly regulated in this particular disease.

5.2.5   Discussion of ErbB expression on neutrophils and in inflammation

The results of this analysis indicate that ErbB expression is low across leukocyte subsets including neutrophils, and also in sputum samples taken from patients with COPD. Due to the data processing method for the dataset analysing gene expression in peripheral blood samples of patients with COPD (Almansa *et al.*, 2012), transcript abundance could not be compared between genes and so no conclusions relating to ErbB expression levels can be drawn from this particular dataset. In all datasets, variation was observed in the levels of expression of different ErbB family members, and also transcript variants for each family member, however this was not consistently directional and no clear patterns were found.

This work also aimed to analyse ErbB expression in inflammatory contexts. Although statistically significant differences were observed between various inflammatory contexts in some studies, again these were not consistent, and were often relatively small in comparison to the changes in positive and negative control genes analysed. This indicated that in these particular studies, ErbB expression was not highly regulated in either peripheral blood or sputum samples from patients with COPD, nor neutrophils from healthy volunteers stimulated with pro-inflammatory agents *in vitro*.

It is important to note the differing cell types present in the two studies utilising samples from patients with COPD. Neutrophils are typically the most abundant leukocyte in peripheral blood samples from healthy humans (approximately 50-70% of immune cells), followed by lymphocytes (20-40%), monocytes (2-12%) and eosinophils (0-7%), with basophils (<1%) typically being the least abundant (Hoffbrand and Steensma, 2019). The cells present in induced sputum samples from healthy individuals may also be predominantly neutrophils (approximately 50% of cells present), however macrophages may be present in similar numbers (43%), and lymphocytes (2.6%) and eosinophils (1.4%) are typically less abundant than found in blood samples (Davidson, The and Leigh, 2013). Sputum samples may also contain bronchial epithelial cells (3%) (Belda *et al.*, 2000). Gene expression in bronchial epithelial cells is known to be altered in COPD (Hedström *et al.*, 2018), and it is possible that these cells are contributing to the gene expression observed in the induced sputum study. Sputum samples may also have increased variability in cell numbers and subtypes than peripheral blood samples; this may be the origin of some of the outlying data points observed in this data.

The relatively low expression and lack of regulation of ErbB genes in these studies may not preclude these receptors from playing a role in the inflammatory response, however it does suggest that if so, this is not mediated by changes in gene expression. Neutrophils, which are a key facilitator of the chronic inflammatory environment in the lungs of people with COPD, were initially not considered to be highly transcriptionally active. Although now we know that neutrophils do undergo transcriptional profile changes when responding to an inflammatory stimulus (Lakschevitz *et al.*, 2015), their short half-life and terminally differentiated state necessitates their reliance on other mechanisms in addition to gene transcription to regulate their activity. Neutrophil degranulation for example is receptor-mediated, induced by external ligands binding to and activating a variety of receptors on the cell membrane. The activation of the downstream signalling cascades that ultimately lead to degranulation is mostly dependent upon the phosphorylation of downstream proteins. Analysing the proteome, in particular the phosphoproteome of neutrophils may therefore give further insight into the mechanisms of action of neutrophils that would not be picked up by transcriptomic analysis alone.

5.3 RNAseq reveals low levels of ErbB expression in human and zebrafish neutrophils, but not mouse neutrophils

Microarray-based gene expression assays are incredibly useful for analysing changes in the expression of any known gene within the human genome, in a wide range of sample types. However one disadvantage of this technique is that there is no quantifiable point at which expression should be classed as negligible. Although analysis of data from these assays does include background correction, there are a number of different methods and algorithms used for this that may yield different results, particularly for genes with very low expression. For example, in the datasets analysed above ErbB genes were detected at similar levels to genes selected as negative controls (e.g. T cell receptor chains in myeloid cells). There is always the possibility that myeloid cells do produce very low amounts of transcript for the T cell receptor, or perhaps more likely that the myeloid cell samples contained very low numbers of contaminating T cells. Either way it is difficult to interpret these results, and alternative assays were explored that would more quantifiably determine if ErbB genes are expressed at all in neutrophils.

RNA sequencing (RNAseq) is a next-generation sequencing method used to determine the presence and quantity of RNA transcripts within a sample. RNA is extracted from the sample of interest and converted to a library of cDNA fragments, which are sequenced in a high-throughput manner. These raw sequence "reads" are then mapped to a reference genome or transcripts, or can be assembled *de*

novo into a transcriptome using algorithms to determine which reads overlap and are therefore part of a contiguous sequence (Wang, Gerstein and Snyder, 2009; Stark, Grzelak and Hadfield, 2019). The usefulness of this technique for this particular research question is that if an RNA transcript is not present in a sample, it will not be sequenced, and so there is no "background" to correct.

When carrying out RNAseq, one variable that must be decided upon is the "depth" of sequencing. This equates to the number of reads (cDNA fragments) that are sequenced in each sample, before sequencing is stopped. If a researcher is only interested in a "snapshot" of highly-expressed genes in a sample, less depth will be required, whereas if genes with low expression are of interest, more in depth sequencing will be used. In order to quantify the number of transcripts of a gene in a particular sample, normalisation to the number of reads must be carried out. This is generally done one of two ways (Zhao, Ye and Stanton, 2020). One is to first express the number of reads of each gene per million total reads. These "reads per million" are then divided by the length of the gene in kilobases, giving "reads per kilobase million" or RPKM. If paired-end RNAseq is used, this is instead called fragments per kilobase million (FPKM) and takes into account that two reads can correspond to a single fragment, and so this fragment is not counted twice. Transcripts per million (TPM) is another common way of normalising the number of reads in a sample: this is similar to RPKM/FPKM, except the raw read count is divided by the gene length in kilobases first (generating reads per kilobase) and then divided by the total number of reads per million. RPKM and FPKM are therefore analogous, and proportional to TPM (Zhao, Ye and Stanton, 2020).

For this thesis, published annotated datasets were interrogated for levels of expression of each ErbB family member. In each graph of data, the threshold for negligible expression of 0.3 FPKM/RPKM is shown as a line for reference. In the literature, this threshold is often set between 0.3 – 1. Although anything above 0 indicates a transcript was detected in the sample, an RPKM/FPKM of 1-2 is thought to be equivalent to approximately 1 mRNA molecule of the transcript per cell, hence less than this is considered "negligible" (Hart *et al.*, 2013).

5.3.1 Human neutrophils may express *ERBB2* and *ERBB3* at low levels

In order to assess the transcript levels of ErbB family members, three different datasets in which RNAseq was carried out on neutrophil samples were interrogated. All used neutrophils isolated from peripheral blood samples donated by healthy volunteers. Slightly different methodologies were utilised for these studies, the first being the method of neutrophil isolation: although all used density-gradient centrifugation based techniques, Ficoll-Hypaque (Jiang *et al.*, 2015), Polymorphoprep with

hypotonic lysis of erythrocytes (Wright *et al.*, 2013) and Ficoll-Paque Plus (Chatterjee *et al.*, 2015) were the isolation medias of choice. All studies used TRIzol® to extract RNA, with cleanup kits that included a DNA digest step. Library preparation kits utilised were Illumina TruSeq RNA Sample Preparation Kit (Jiang and Chatterjee) and the Illumina SOLiD kit (Wright). All libraries were sequenced using the Illumina HiSeq 2000 analyser. All researchers aligned reads to the human genome GRCh37 (also known as hg19) using TopHat software, and annotated using the Cufflinks software.

The first dataset by Jiang et al. analysed neutrophil samples from three healthy volunteers. No expression of *EGFR* or *ERBB4* was observed (Figure 5.5A). Two of the three samples showed *ERBB3* expression to be below the 0.3 FPKM threshold, with one sample reading at 0.32, suggesting expression of *ERBB3* is likely negligible. *ERBB2* expression however was higher, with FPKM values of 0.48, 1.68 and 1.98 in each biological sample. Although this is still low expression, in 2/3 samples it is higher than the commonly used threshold of 0.3 – 1 FPKM values.

The second dataset by Wright et al. used neutrophils isolated from one blood donor. This data is presented with error bars showing the upper and lower confidence intervals calculated during analysis. Similarly to the Jiang et al. dataset, no *EGFR* or *ERBB4* transcripts were detected (Figure 5.5B). However in this dataset, *ERBB2* reads were also below the threshold, with a mean FPKM value of 0.0996. Interestingly, *ERBB3* expression is highest of the ErbB family members in this dataset, with a mean value of 1.379 FPKM.

The final human neutrophil dataset by Chatterjee et al. analysed neutrophil samples from four healthy volunteers. Again, no expression of *EGFR* or *ERBB4* were found in any of the samples (Figure 5.5C). *ERBB2* expression was below the 0.3 FPKM threshold in 3 of the 4 samples (although above 0 in all), and one sample had a reading of 0.427 FPKM. Similar to the Wright dataset, *ERBB3* expression appeared the highest, with all four samples ranging from 1.694 to 3.561 FPKM.
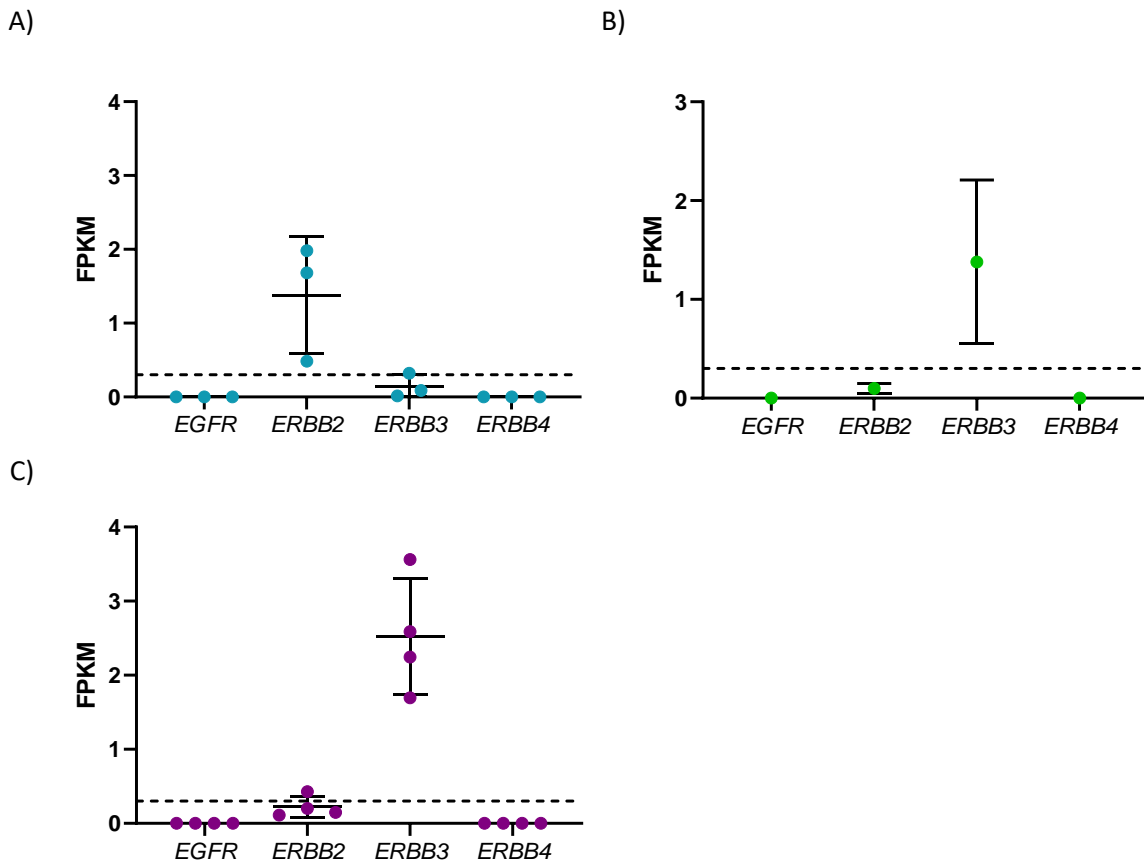
Figure 5.5. RNAseq data of ErbB expression in human neutrophils.

Three different RNAseq datasets generated from healthy human neutrophil samples were interrogated for ErbB expression. The dotted line at 0.3 FPKM is a commonly used threshold to denote negligible expression. The dataset from Jiang et al. (A) indicates *ERBB2* is expressed in human neutrophils (n=3). Datasets from Wright et al. (B) (n=1) and Chatterjee et al. (C) (n=4) show *ERBB3* transcripts are present in human neutrophils. Data points indicate biological replicates, with bars showing the mean and standard deviation (A and C); bars in B indicate upper and lower confidence intervals calculated during data analysis.

These three datasets indicate that *EGFR* and *ERBB4* transcripts are not present in human neutrophils, however the evidence for *ERBB2* and *ERBB3* expression is less conclusive. This may be due to differences in the depth of sequencing carried out between the studies, or possibly the purity of the neutrophil samples. To overcome these limitations, the next datasets interrogated used different isolation protocols and larger sample sizes.

5.3.2 *ERBB2* and *ERBB3* expression was detected at low levels in neutrophils cells using the Human Protein Atlas database

In addition to the considerable number of RNAseq datasets published by individual research groups, there is also an increasing number of searchable "omics" databases available online. These allow researchers to explore large and often multiple datasets in an easily-searchable format. One such database is the Human Protein Atlas, which aims to integrate various omics technologies to map all the human proteins in cells, tissues and organs (Uhlén *et al.*, 2015). The Blood Atlas is one aspect of this database that contains genome-wide RNA expression, proteomics and antibody based protein expression profiles of all human blood cells (Uhlen *et al.*, 2019). When searched for any of the ErbB family members, evidence of expression at the RNA level is shown.

The Blood Atlas displays transcriptomics results as a consensus dataset, which is the summation of data from three different RNAseq datasets. One dataset was generated by the authors of the Human Protein Atlas, in which blood samples were donated by 6 healthy individuals, and sorted into 18 immune cell populations by flow cytometry, and analysed by RNAseq (Uhlen *et al.*, 2019). The second dataset utilised blood samples from 4 healthy donors, which were characterised by flow cytometry and RNAseq into 29 distinct cell types (Monaco *et al.*, 2019). The third dataset only analysed peripheral blood mononuclear cells (monocytes, B cells, NK cells and T cell subsets), separated by flow cytometry from blood samples from 91 healthy subjects (Schmiedel *et al.*, 2018). This last dataset is incorporated into the consensus datasets for those specific blood cell types, but not neutrophils or other granulocytes.

In order to consolidate this data into a consensus dataset, TPM (transcripts per kilobase million) data was used. All TPM values were scaled to a sum of 1 million TPM (pTPM) to compensate for non-coding transcripts, followed by normalisation to remove technical bias and Pareto scaling to remove the relative importance of large values and improve biological interpretability (van den Berg *et al.*, 2006; Robinson and Oshlack, 2010). Batch correction was then used to improve variation caused by technical discrepancies between batches, and the resulting values were denoted normalised TPM (nTPM) (Zhang, Parmigiani and Johnson, 2020).

As with the individual RNAseq datasets analysed in the previous chapter section, the Blood Atlas showed no evidence of *EGFR* or *ERBB4* in human neutrophils at the RNA level (Figure 5.6A, Figure 5.6D). *EGFR* and *ERBB4* transcripts were not detected in any immune cell. *ERBB2* transcripts were detected in all blood cell linages in this database including neutrophils, and are enriched in gamma-delta T cells (Figure 5.6B). *ERBB3* expression was also detected in all blood cell datasets, albeit at low levels for the majority of cell types, the highest being basophils and neutrophils (Figure 5.6C).

A) ***EGFR***

B) ***ERBB2***

C) ***ERBB3***

D)
                                              ERBB4

nTPM
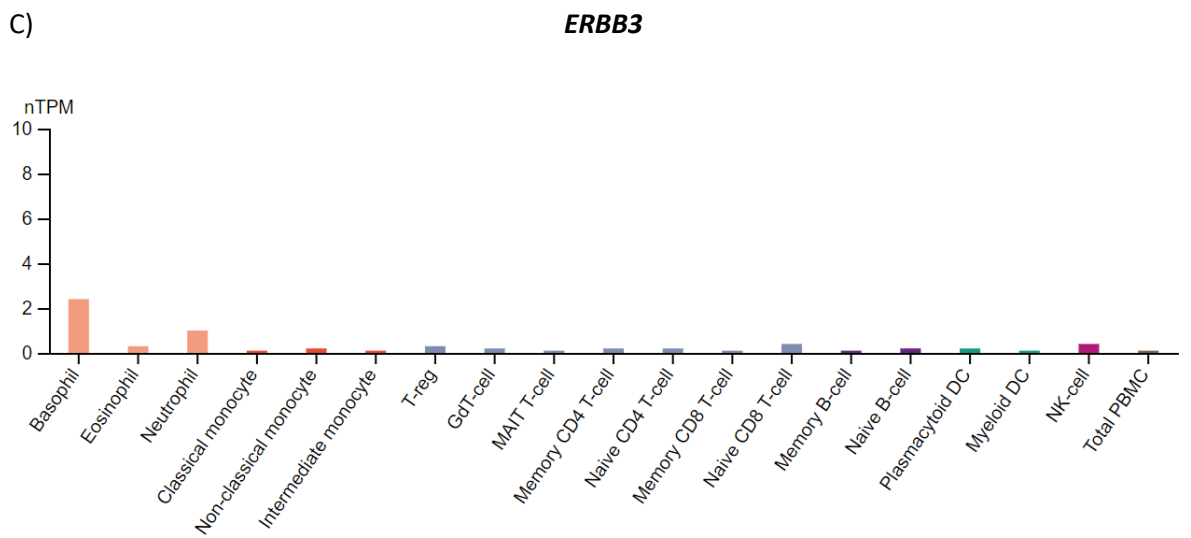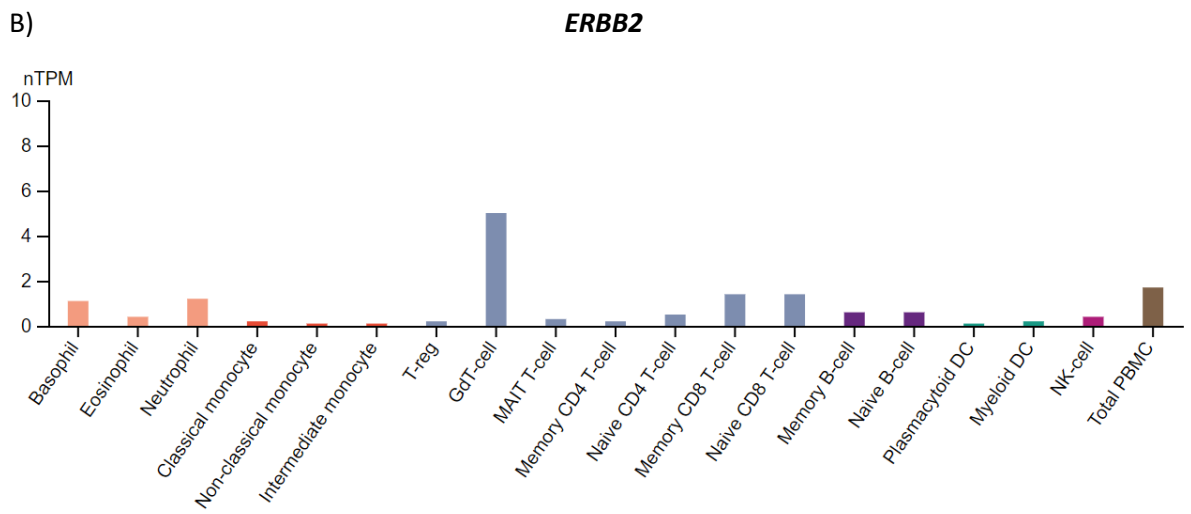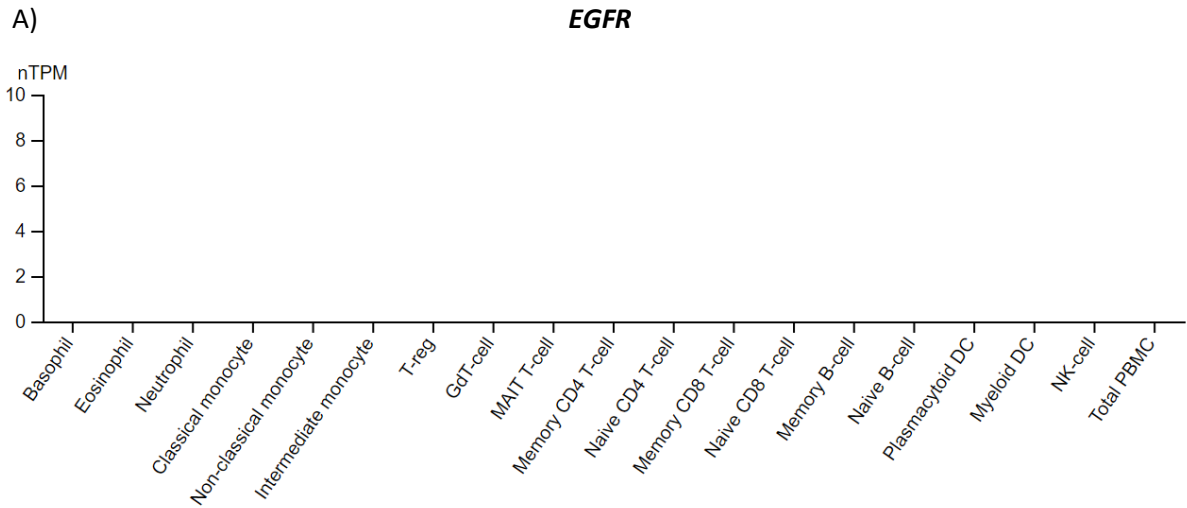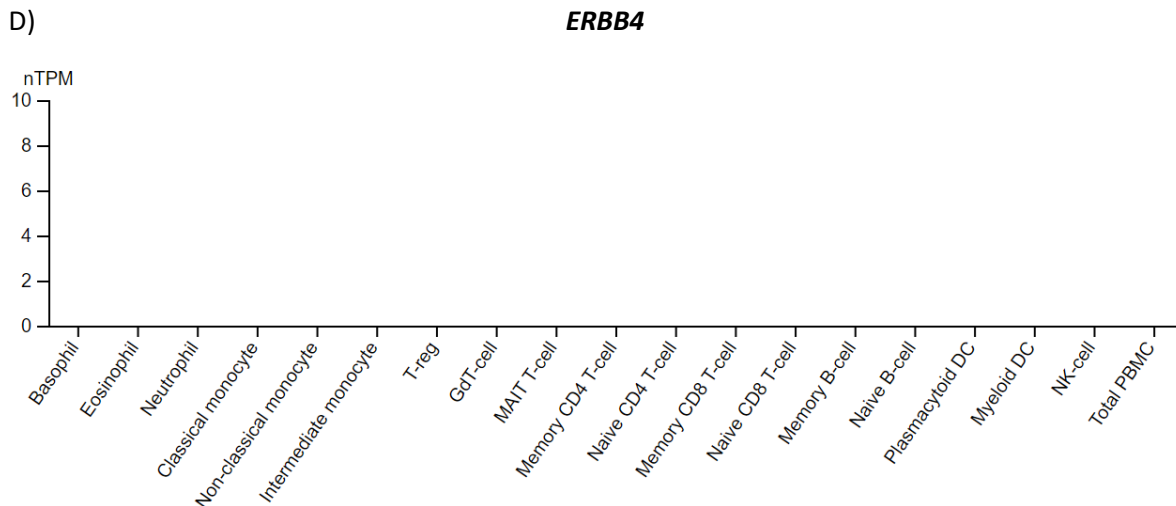
Figure 5.6. ErbB expression in immune cells, from the Blood Atlas database.
The Blood Atlas database, an aspect of the Human Protein Atlas database, was interrogated for the expression of each ErbB family member. The consensus dataset shown is a consolidation of three different RNAseq datasets that have been normalised, scaled and batch corrected to generate normalised TPM (nTPM) values. Cells are organised according to their lineage, as demonstrated by the coloured bars. Expression of *EGFR* (A) and *ERBB4* (D) was not detected in any immune cells. *ERBB2* expression was found in all immune cell subsets including neutrophils, and was highest in gamma-delta T cells (B). *ERBB3* expression was similarly detected in all blood cell subsets, with the highest expression observed in basophils and neutrophils (C).

5.3.3 Zebrafish neutrophils express *egfra* and *erbb2,* whereas mouse neutrophils do not appear to express any ErbB family members

Data produced in this thesis is derived from primary human neutrophils, zebrafish larvae and mouse models. As both ErbB inhibitor treatment and genetic manipulation of ErbB genes was carried out in these models, analysing the expression of ErbB family members in the neutrophils of these species may allow for better interpretation of the results obtained.

To analyse the expression of ErbB genes in mouse neutrophils, a database generated by Rincón, Rocha-Gregg and Collins (2018) was interrogated. This database contained two published RNAseq datasets of mouse neutrophils, configured into an easily-searchable format. One dataset isolated neutrophils from bone marrow of two mice by Percoll gradient centrifugation (Taylor *et al.*, 2014), whereas the second isolated neutrophils from whole blood of four mice using a magnetic separation column containing Ly6G+ coated beads (Coffelt *et al.*, 2015). In both studies, RNA libraries were prepared using the Illumina TruSeq RNA sample preparation kit, and sequenced on an Illumina HiSeq

2000. For compilation of these two datasets into a single searchable database, data was aligned to the GRCm38 genome, and transcript abundance was quantified using Cufflinks (Rincón, Rocha-Gregg and Collins, 2018).

The mouse ErbB family is closely related to the human ErbB family, with each ErbB family member having an orthologous gene in mouse. When this dataset was interrogated for ErbB expression, *Egfr, Erbb2, Erbb3* and *Erbb4* reads were detected in mouse neutrophils from both datasets, however none were above the FPKM threshold of 0.3 (Figure 5.7A).

In order to observe ErbB expression within zebrafish, an RNAseq dataset of larval zebrafish neutrophils was analysed. Three zebrafish larvae of the *TgBAC(mpx:EGFP)i114* transgenic line were digested at 5-6 days post fertilisation, and GFP positive cells (neutrophils) were isolated by fluorescent activated cell sorting (FACS) (Rougeot *et al.*, 2019). RNA extraction and synthesis of cDNA libraries were carried out, followed by single-end Illumina RNA sequencing. Reads were aligned to the Ensembl zebrafish Zv9 genome using the Bowtie and TopHat software. The resulting published dataset was interrogated for ErbB genes. Although the zebrafish paralogue *egfrb* has been described, it has not been mapped, and this RNAseq dataset was aligned to the reference Zv9 genome, precluding *egfrb* from being detected (Reischauer *et al.*, 2009). The human *ERBB3* and *ERBB4* genes also each have two paralogues in zebrafish, named *erbb3a, erbb3b, erbb4a* and *erbb4b*.

Interestingly, *egfra* transcripts were detected in this dataset, making it the first neutrophil dataset to show any expression of the first ErbB family member by RNAseq (Figure 5.7B). *erbb2* transcripts were also detected in neutrophils isolated from all three zebrafish larvae. Both *erbb3a* and *erbb3b* were detected in 2/3 samples, although one of the *erbb3b* RPKM values was bordering the threshold at 0.359 RPKM. *erbb4a* and *erbb4b* were below the threshold in 2/3 and 3/3 samples respectively, indicating negligible expression. This dataset suggests that zebrafish neutrophils express at least the first two members of the ErbB family, potentially the third.

A)

Mouse neutrophils

B)

Zebrafish neutrophils

Figure 5.7. ErbB expression in mouse and zebrafish neutrophils.
Three different RNAseq datasets were interrogated to determine the expression of ErbB genes in mouse and zebrafish neutrophils. RNAseq was carried out on mouse neutrophils, isolated from the bone marrow of two mice (Taylor *et al.,* 2015) or whole blood of four mice (Coffelt *et al.,* 2015). No ErbB expression above the 0.3 FPKM threshold was detected (A). Zebrafish neutrophils isolated from larvae showed consistent expression of *egfra* (*EGFR* homologue) and *erbb2* above the 0.3 RPKM threshold, and *erbb3a* and *erbb3b* in 2/3 larvae (B). *erbb4a* and *erbb4b* expression was below the threshold in 5/6 larvae.

5.3.4   Discussion of RNAseq analysis of ErbB expression on neutrophils

RNA sequencing was chosen as an appropriate method of quantifiably determining whether ErbBs are expressed in neutrophils, from a number of species. The human neutrophil datasets are consistent in their lack of detection of both *EGFR* and *ERBB4* transcripts, and it can be concluded that these family members are not being actively expressed in mature human neutrophils. The expression of *ERBB2* and *ERBB3* genes within the datasets analysed here is less conclusive. Transcripts of *ERBB2* were detected in one of the three RNAseq datasets, whereas transcripts of the *ERBB3* were detected in the other two of three. These discrepancies are possibly due to the depth of sequencing carried out, which would depend on the original aims of the researcher, and it is possible that transcripts with very low expression may be missed. Unfortunately, information relating to the depth of sequencing is not always included in publications. Only the publication relating to one of the Blood Atlas RNAseq datasets noted that a threshold of ten million reads to be sequenced was set, referred to as "deep sequencing" (Uhlen *et al.*, 2019). It would follow that a reduced depth of sequencing in comparison to the Blood Atlas datasets may result in either *ERBB2* or *ERBB3* transcripts being missed, and thus the discrepancies observed between the human neutrophil datasets. If so, this would suggest that both *ERBB2* and *ERBB3* are in fact expressed in human neutrophils, albeit at low levels.

The two datasets obtained from mouse neutrophils do show FPKM values above 0, but none above the 0.3 FPKM threshold of "negligible expression". As there is variation in these values, it may again be that the depth of sequencing was insufficient to identify these low abundance transcripts, or it may be that mouse neutrophils do not express ErbB genes at all. Interestingly the zebrafish neutrophil dataset showed the highest RPKM values for any ErbB family member analysed in this thesis. *egfra* and *erbb2* expression is convincing, whereas *erbb3a* and *erbb3b* is less so, with RPKM values below the threshold of detection in one of the three samples analysed. Similarly, to human neutrophils, *erbb4a* and *erbb4b* do not appear to be expressed at all.

The lack of expression of particular ErbB family members, namely *EGFR* and *ERBB4* in the human neutrophil RNAseq datasets, may not preclude the protein being present in these cells. It is possible that transcription of these genes is carried out in the precursor cells of haematopoietic lineages in the bone marrow, whereas in mature circulating neutrophils the ErbB receptors are fully translated into functional proteins, but are no longer being synthesised. One study that explored the correlation between RNAseq and proteomic data from brain tissue samples found that transcripts have a weak predictive value for the expression of their associated proteins, although interestingly transcripts coding for protein kinases were among the most predictive categories (Bauernfeind and Babbitt, 2017). This correlation between gene expression and protein detection is particularly interesting in

neutrophils due to their short lifespan, and ability to undergo rapid and highly dynamic phenotypic changes within inflammatory environments. A study comparing gene expression and proteomics data from human neutrophils at different stages of differentiation (from pro-myelocytes to mature neutrophils) found that in earlier stages of haematopoiesis, detected proteins often had corresponding transcripts with higher FPKM values, however a significant number of mature neutrophils expressed proteins with corresponding RNA levels below 1 FPKM (Hoogendijk *et al.*, 2019). This supports the idea of gene expression being only one of the many different mechanisms that neutrophils use to respond to an inflammatory stimulus.

There is an interesting contrast between these human RNAseq datasets, which suggest expression of *ERBB2* and *ERBB3*, but not *EGFR* or *ERBB4*, and the microarray datasets, which do not follow the same pattern in terms of transcript abundance detected. The GeneChip assays analysed in Figure 5.1 and Figure 5.2 show very similar levels of the expression of all ErbB family members in human neutrophils. This highlights the shortcoming of microarray data in that it is difficult to differentiate between very low expression and negligible expression, due to the lack of quantifiable threshold for the presence or absence of a transcript. However it can also be said that the limitations of RNA sequencing lies in the depth of sequencing, and that the absence of a transcript does not necessarily preclude it from being present at very low levels.

Analysing proteomics datasets may be considered as a more direct way to identify whether ErbB receptors are present in neutrophils. A popular method of analysing the proteome of a cell or tissue uses high-resolution mass spectrometry to identify peptides, which are mapped to proteins using reference databases in a similar approach to the sequencing of cDNA fragments by RNAseq. These proteomic datasets are also often published in full as part of research papers. Two such datasets analysing the proteome of human neutrophils were interrogated, and no ErbB family members were detected (Rieckmann *et al.*, 2017; Hoogendijk *et al.*, 2019). Similarly to RNAseq, mass spectrometry-based proteomics approaches are limited in that the depth of analysis determines the extent to which low abundance proteins are detected. Analysis of proteins within neutrophils is additionally difficult due to the high concentration of proteases in the cell, which will begin to degrade cytosolic or membrane-bound proteins as soon as sample preparation begins. Protease inhibitors are available and are used as part of this sample preparation process, but it is still not possible to say that because a protein was not detected, it was not present in the cell.

The findings from this data mining somewhat contradict experiments elsewhere in this thesis, which show that pharmacological ErbB inhibitors in a number of systems are able to exert effects specifically on neutrophils. Gefitinib for example is supposedly an EGFR-specific inhibitor, that accelerates

apoptosis of human neutrophils to a statistically significant degree, in a dose-dependent manner; and yet human neutrophils do not express *EGFR* transcripts. Like inhibitors of other kinases, ErbB inhibitors are known to have off-target effects. To address this discrepancy, a phosphoproteomics approach was taken to attempt to identify the downstream signalling pathways by which ErbB inhibitors are working via in human neutrophils.

5.4 Elucidating ErbB signalling pathways in human neutrophils using phosphoproteomics

Mass spectrometry-based phosphoproteomics is a key technique used to research global cellular signal transduction networks. The dysregulation of kinase signalling contributes to numerous diseases including cancer, and so research into the characterisation of phosphorylation events has expanded significantly over the past two decades, furthering the understanding of the mechanisms underpinning these diseases. Interestingly, the EGFR network is one of the most extensively studied in regards to signal transduction, and was one of the first signalling networks in which the temporal dynamics of phosphorylation was elucidated (Blagoev *et al.*, 2004). The extensive knowledge and literature available examining specific phosphorylation events on kinases and other signal transduction enzymes, and the effect this has on their functionality, underpins much of the data interpretation of this chapter. The experiments detailed here aim to elucidate the signalling pathways by which the ErbB inhibitor neratinib induces apoptosis of healthy human neutrophils.

Neratinib, out of a number of available ErbB inhibitors, was selected for these experiments for several reasons. It is the most potent in inducing apoptosis in human neutrophils *in vitro*, and it reduces several inflammatory functions in mouse models of inflammatory lung disease. Furthermore, neratinib binds irreversibly and covalently to its target, and specifically targets EGFR and ErbB2 at similar IC50 values. Being a clinically-used inhibitor, results from this experiment may be considered to have wider applications than if an ErbB inhibitor used only for research were selected.

In addition to neratinib, neutrophil samples for these experiments were treated with cyclic adenosine monophosphate (cAMP), a second messenger derived from the hydrolysis of ATP, and an important inductor of downstream signal transduction pathways in numerous organisms (Sassone-Corsi, 2012). Amongst these is the regulation of apoptosis. The particular cell-permeable analogue of cAMP used for experiments within this chapter, dibutyryl cAMP (db-cAMP), is a known suppressor of apoptosis in human neutrophils (Martin *et al.*, 2001; Rahman *et al.*, 2019). Previous research within our group demonstrated that pharmacological ErbB inhibitors are able to overcome the pro-survival signals of db-cAMP when human neutrophils are treated with both agents (Rahman *et al.*, 2019). In experiments for this chapter, treatment of neutrophils with neratinib induces apoptotic signalling pathways, which would not occur in DMSO treated (control) neutrophils. Subsequent treatment of the cells with cAMP then activates the anti-apoptotic signalling pathways in DMSO treated cells, whereas these remain supressed by neratinib. The differences in protein phosphorylation between the two treatment groups may indicate the signalling pathways inhibited by neratinib.

As phosphorylated proteins make up only a small percentage of the total proteins within the cell, samples were enriched for phosphorylated peptides prior to mass spectrometry. This is a useful technique as phosphorylation events in cell signalling often occurs on proteins expressed at relatively low levels, and the unbiased approach of mass spectrometry means that these may be missed.

After the identification of differentially phosphorylated proteins between the treatment groups, extracting biological relevance from the data is a significant challenge. Literature searches identified a number of specific phosphorylation events on proteins that regulate apoptosis that were also found in the dataset obtained in this chapter. In addition, online tools such as STRING and Reactome were used to identify interactions between proteins within the dataset, and infer biological processes that were altered with neratinib treatment. Using these various types of analysis, potential regulators of apoptosis downstream of neratinib were identified and experiments carried out to validate these findings.

5.4.1 Optimisation of mass spectrometry-based phosphoproteomics analysis of human neutrophils

The initial experimental in this chapter of work aimed to test the protocols used for sample preparation, liquid chromatography and mass spectrometry to identify proteins. The first optimisation run consisted of a single sample of 30 million neutrophils from one healthy donor, from which proteins were isolated and analysed by mass spectrometry. In this run, the sample was not enriched for phosphopeptides. The primary aim of this run was to test the conditions for sample lysis, protein isolation and tryptic digestion into peptides, as neutrophils contain high concentrations of proteases and so a number of different protease and phosphatase inhibitors are required. Neutrophils for this sample were isolated using the standard Dextran/Percoll gradient method, which usually gives a leukocyte purity of >95% neutrophils. However there can also be varying levels of contaminating red blood cells. Within the proteins detected from this optimisation run, haemoglobin subunits alpha and beta were the sixth and tenth most abundant proteins detected, respectively (data not shown). Eosinophil and platelet specific proteins were similarly detected. For all subsequent experiments, neutrophils were isolated using an immunomagnetic negative selection kit, in which all blood cells except neutrophils bind to magnetic beads coated with specific antibody, leaving >99% pure preparation of neutrophils.

Other than the cell contamination issues, the protocols for sample preparation and mass spectrometry were considered to have worked well and were used for all subsequent runs. It was also decided that

300µg of protein would be sufficient for each sample. Protein concentration assays carried out indicated that 15 million neutrophils yielded approximately 500-700µg protein using these particular lysis and extraction conditions. In order to ensure this minimum of 300µg protein was obtained with room for error, all future samples were comprised of 15 million cells each.

The second round of optimisation had two primary aims: one was to test the phosphoenrichment step, and the second to determine whether the treatment of neutrophils with cAMP and neratinib resulted in differential detection of phosphopeptides. Phosphoenrichment isolates peptides which contain a phosphate group by exploiting the negative charge of the phosphate group and using positively charged metal ions to capture phosphorylated peptides. Neratinib was used at 25µM, as this consistently induced neutrophil apoptosis in previous assays (Figure 3.1). Previous research from our group used a Kinexus antibody microarray to determine how treatment of neutrophils with cAMP affected the phosphorylation of kinases. This research found that neutrophils treated with 500µM cAMP for 30 minutes had more phosphorylated kinases in than those treated for 60 minutes, in comparison to untreated neutrophils (Rahman *et al.*, 2019). This concentration of 500µM cAMP was selected.

Literature searches indicated that phosphorylation occurs very quickly, with researchers often treating samples for only a few minutes when assessing whether a treatment alters phosphorylation. It was therefore decided that three samples would be run in a second optimisation round, each consisting of 15 million neutrophils from a single donor. One sample was treated with 500µM cAMP for 10 minutes, and one for 30 minutes. Both these samples would be pre-treated with DMSO for an hour, as a control for neratinib treatment. The third sample would be pre-treated with 25µM neratinib for 1 hour, followed by 500µM cAMP for 30 minutes (Figure 5.8A). At the allocated endpoint for each sample, they would be washed once in PBS and stored immediately at -80°C until sample preparation for mass spectrometry was carried out. Due to COVID-19 related laboratory access restrictions I was unable to carry out the sample preparation for mass spectrometry (Figure 5.8B) as originally intended. Instead, the lead scientist and collaborator in the University of Sheffield Biological Mass Spectrometry Facility, Dr Mark Collins, performed these experiments.

Within the three samples, the number of phosphopeptides detected varied from 1226-1642, which mapped to 951-1245 proteins (Figure 5.8C). The abundance of these phosphopeptides (measured by the mass spectrometer as intensity) appeared similarly distributed between samples, although the neratinib treated sample seemed to have a slight skew towards higher abundances (Figure 5.8C).

The key comparisons within this optimisation step were between samples treated with cAMP for 10 or 30 minutes, and the samples treated with DMSO or neratinib (both followed by cAMP for 30

minutes). To analyse differences in phosphopeptides detected in these samples, the fold change in the intensity of each phosphopeptide between the two treatments was calculated. In 10 vs 30 minute cAMP treatment samples, the abundance of phosphopeptides appeared evenly distributed, with most clustered around a fold change of 1 (no change in intensity between samples), and very few phosphopeptides that were >10 fold higher in either condition (Figure 5.8D). However when comparing the DMSO vs neratinib treated samples, abundance of phosphopeptides appeared to be skewed towards being increased with neratinib treatment (Figure 5.8D). This was interesting as it was initially considered that neratinib would be suppressing signalling pathways, rather than inducing phosphorylation; however as this experiment was from a single donor, no solid conclusions were drawn. As there appeared to be no large differences between the 10- and 30-minute treatment times with cAMP, the latter was chosen for the next set of experiments.

A)

B)

C)

D)

Figure 5.8. Optimising phosphoproteomics analysis of human neutrophils.
Schematic of the treatment protocol used to generate the three samples for the optimisation run (A). Samples were prepared and analysed by liquid chromatography-mass spectrometry and to identify phosphopeptides present in the original samples (B). The number (indicated on the graph) and intensities of phosphopeptides detected across the three different conditions (C). Each dot represents one phosphopeptide; as multiple peptides may map to one protein, number of proteins is also shown. When comparing between treatment groups (D), the intensities of most phosphopeptides do not appear vary widely between the samples treated with cAMP for 10 or 30 minutes, with a median fold change in intensity between the two groups clustered around 1. However in samples pre-treated with either DMSO or Neratinib, the median fold change in intensity of phosphoproteins is shifted towards being increased with Neratinib treatment. All samples from 1 neutrophil donor (n=1).

162

Based on this second optimisation run, the final experiment was designed. Neutrophils from 5 independent donors were treated with DMSO or neratinib for 60 minutes, followed by 30 minutes with cAMP. Samples were prepared as previously, with an additional step of an aliquot of protein from each donor being analysed by mass spectrometry, prior to phosphoenrichment. The remaining samples underwent phosphoenrichment, and were analysed by mass spectrometry to identify both the peptides and also amino acids at which these peptides were phosphorylated.

One method of assessing the quality of samples is to determine how well the abundance of either peptides, or phosphopeptides, correlate between samples. Although the aim is to detect differences between the treatment groups, it was expected that only some proteins would be differentially detected, and the majority should correlate well between samples. This would also assess donor variability. It was found that in both the dataset of peptides, and that of phosphopeptides, abundances from DMSO-treated sample from donor 1 (D1) correlated poorly with the other samples, including the neratinib-treated sample from donor 1 (Figure 5.9). This sample was therefore excluded and analysis was carried out on 4 DMSO treated samples, and 5 neratinib treated samples.

Peptides

intensity D1 DMSO	intensity D2 DMSO	intensity D3 DMSO	intensity D4 DMSO	intensity D5 DMSO	intensity N1 Neratinib	intensity N2 Neratinib	intensity N3 Neratinib	intensity N4 Neratinib	intensity N5 Neratinib	Group1	Name
NaN	0.876914	0.869465	0.875064	0.872291	0.898363	0.865085	0.868983	0.862557	0.87426	DMSO	LFQ intensity D1
0.876914	NaN	0.987485	0.985653	0.982749	0.985308	0.992977	0.985345	0.973715	0.976494	DMSO	LFQ intensity D2
0.869465	0.987485	NaN	0.989059	0.985075	0.983836	0.987792	0.995479	0.974988	0.976536	DMSO	LFQ intensity D3
0.875064	0.985653	0.989059	NaN	0.982224	0.980797	0.985882	0.989499	0.982195	0.972666	DMSO	LFQ intensity D4
0.872291	0.982749	0.985075	0.982224	NaN	0.982965	0.980276	0.985893	0.975527	0.98659	DMSO	LFQ intensity D5
0.898363	0.985308	0.983836	0.980797	0.982965	NaN	0.980529	0.983181	0.970118	0.980071	Neratinib	LFQ intensity N1
0.865085	0.992977	0.987792	0.985882	0.980276	0.980529	NaN	0.986271	0.974456	0.972885	Neratinib	LFQ intensity N2
0.868983	0.985345	0.995479	0.989499	0.985893	0.983181	0.986271	NaN	0.97749	0.978235	Neratinib	LFQ intensity N3
0.862557	0.973715	0.974988	0.982195	0.975527	0.970118	0.974456	0.97749	NaN	0.965815	Neratinib	LFQ intensity N4
0.87426	0.976494	0.976536	0.972666	0.98659	0.980071	0.972885	0.978235	0.965815	NaN	Neratinib	LFQ intensity N5

Phosphopeptides

Intensity D1 DMSO	Intensity D2 DMSO	Intensity D3 DMSO	Intensity D4 DMSO	Intensity D5 DMSO	Intensity N1 Neratinib	Intensity N2 Neratinib	Intensity N3 Neratinib	Intensity N4 Neratinib	Intensity N5 Neratinib	Group1	Name
NaN	0.563973	0.521625	0.525449	0.4084	0.572097	0.48266	0.434751	0.532592	0.517921	DMSO	Intensity D1
0.563973	NaN	0.741009	0.741522	0.618419	0.788882	0.852622	0.747247	0.715284	0.769998	DMSO	Intensity D2
0.521625	0.741009	NaN	0.800505	0.720278	0.838188	0.820424	0.726667	0.685704	0.794674	DMSO	Intensity D3
0.525449	0.741522	0.800505	NaN	0.652922	0.763019	0.778727	0.776102	0.79022	0.776707	DMSO	Intensity D4
0.4084	0.618419	0.720278	0.652922	NaN	0.709654	0.703863	0.660874	0.533951	0.752696	DMSO	Intensity D5
0.572097	0.788882	0.838188	0.763019	0.709654	NaN	0.82503	0.722872	0.674428	0.848565	Neratinib	Intensity N1
0.48266	0.852622	0.820424	0.778727	0.703863	0.82503	NaN	0.823627	0.729956	0.864485	Neratinib	Intensity N2
0.434751	0.747247	0.726667	0.776102	0.660874	0.722872	0.823627	NaN	0.727271	0.807362	Neratinib	Intensity N3
0.532592	0.715284	0.685704	0.79022	0.533951	0.674428	0.729956	0.727271	NaN	0.716894	Neratinib	Intensity N4
0.517921	0.769998	0.794674	0.776707	0.752696	0.848565	0.864485	0.807362	0.716894	NaN	Neratinib	Intensity N5

Figure 5.9. Correlations between the abundances of peptides and phosphopeptides.
Before phosphopeptide enrichment, aliquots of each digested sample were analysed by LC-MS/MS. The average correlation rate of abundance of each peptide were calculated (A). This was also carried out on samples that had been enriched for phosphopeptides (B). As the abundances of both the unenriched peptides, and phosphopeptides, in DMSO sample 1 (D1) correlate poorly in comparison to all other samples, and so this sample was excluded from further analysis.

5.4.2 Validating the dataset by analysing cAMP signalling

The first step in analysis of these samples was to validate the dataset. As all samples in this dataset were treated with db-cAMP, it was expected that phosphorylated peptides would be detected that mapped to proteins downstream of cAMP signalling. The dataset was searched for a number of these proteins, summarised in Figure 5.10A.

Data was analysed by noting the number of samples (out of 4 DMSO, and 5 neratinib treated) in which a particular phosphorylated peptide was identified: i.e. a value of 1 indicates that phosphopeptide was detected in all samples, 0.6 indicates detection in 3/5 neratinib treated samples, 0.25 indicates 1/4 DMSO treated samples (Figure 5.10B). This method was selected over comparing protein abundance for two reasons. The first is that due to the nature of phosphorylation, very few, if any, of one specific phosphopeptide would be detected in each sample, and therefore differences in abundances are more likely to be due to the size of the peptide and number of phosphorylated amino acids than amounts. Secondly since the samples were run through LC-MS/MS separately, background correction had to be calculated in each sample, introducing more variation.

The key pathway activated by cAMP is the protein kinase A (PKA) pathway. Several phosphorylated peptides mapping to different subunits of PKA were identified in the dataset, including the regulatory subunits PRKAR1A, PRKAR2A, and PRKAR2B, and the catalytic subunit PRKACA. PKA directly phosphorylates the transcription factors CREB and AFT2, which were similarly detected in our dataset. A number of other downstream proteins including BRAF, GSK3A and proteins within the MAPK family were identified. Additionally, phosphopeptides mapping to the enzyme PDE, which degrades cAMP into 5' AMP, were similarly detected in the majority of samples. The majority of phosphopeptides mapping to proteins downstream of cAMP signalling were detected at similar levels within the two treatment groups, with the exception of ATF2 and PRKACA (Figure 5.10B). This result was considered an effective validation of the dataset.

Figure 5.10. Validation of the dataset by identifying phosphorylated proteins present in cAMP signalling pathways.

Phosphorylated proteins downstream of cAMP signalling pathways were extracted from the dataset. cAMP binds to the regulatory (R) unit of inactive PKA, resulting in the dissociation and activation of catalytic (C) PKA subunits, which in turn phosphorylate a number of downstream targets, such as RAP1 and BRAF, and transcription factors AFT and CREB in the nucleus. cAMP is also converted to 5' AMP by PDE enzymes. Schematic overview generated in BioRender (A). The number of samples in which a phosphorylated peptide mapping to a protein is detected is shown as a ratio of the number of samples in each treatment group (B). For example, a phosphorylated peptide mapping to CREB1 was detected in 3/4 (0.75) DMSO treated samples and 5/5 (1) Neratinib treated samples. In some cases multiple phosphorylated peptides mapping to the same protein were identified.

5.4.3   Identifying downstream mediators of ErbB signalling

Once the dataset had been validated in part by identifying phosphorylated peptides mapping to proteins downstream of cAMP, the same approach was taken to analyse ErbB signalling. Initially, the dataset was searched for EGFR, ERBB2, ERBB3 and ERBB4, but none were detected in either the protein or phosphopeptide dataset. As ErbB proteins were not detected in other published proteomics datasets, this was not particularly surprising, and may be due to the depth of sequencing carried out.

The dataset was then searched for downstream components of ErbB signalling (Figure 5.11A) and analysed as above. A key downstream mediator of ErbB signalling is the PI3K family. Phosphopeptides mapping to several different subunits of this family were identified (PIK3AP1, PIK3R1, PIK3R5), which were detected in similar numbers of samples in both treatment groups (Figure 5.11B). Similar results were observed for members of the AKT family and several members of the MAPK family.

A)
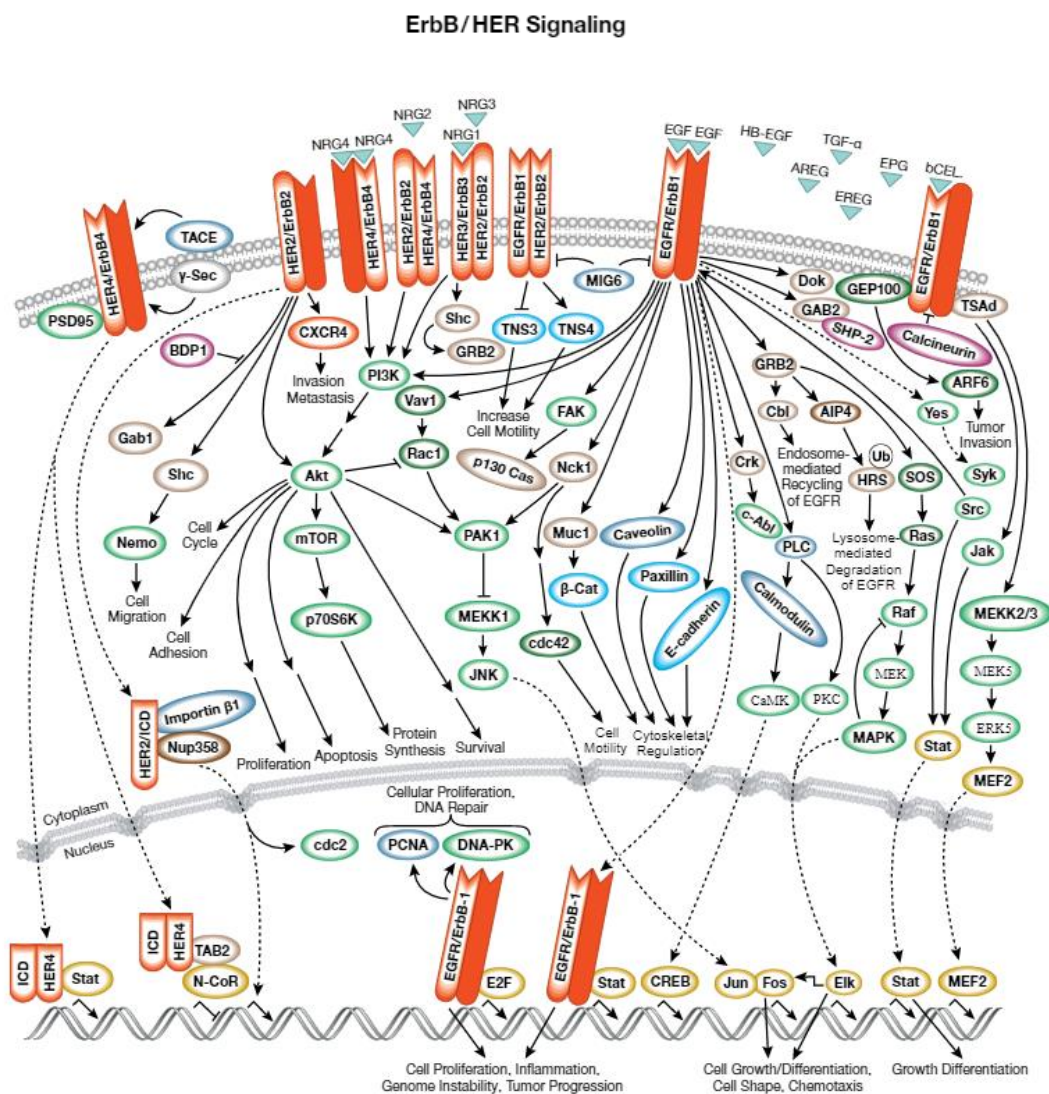
B)
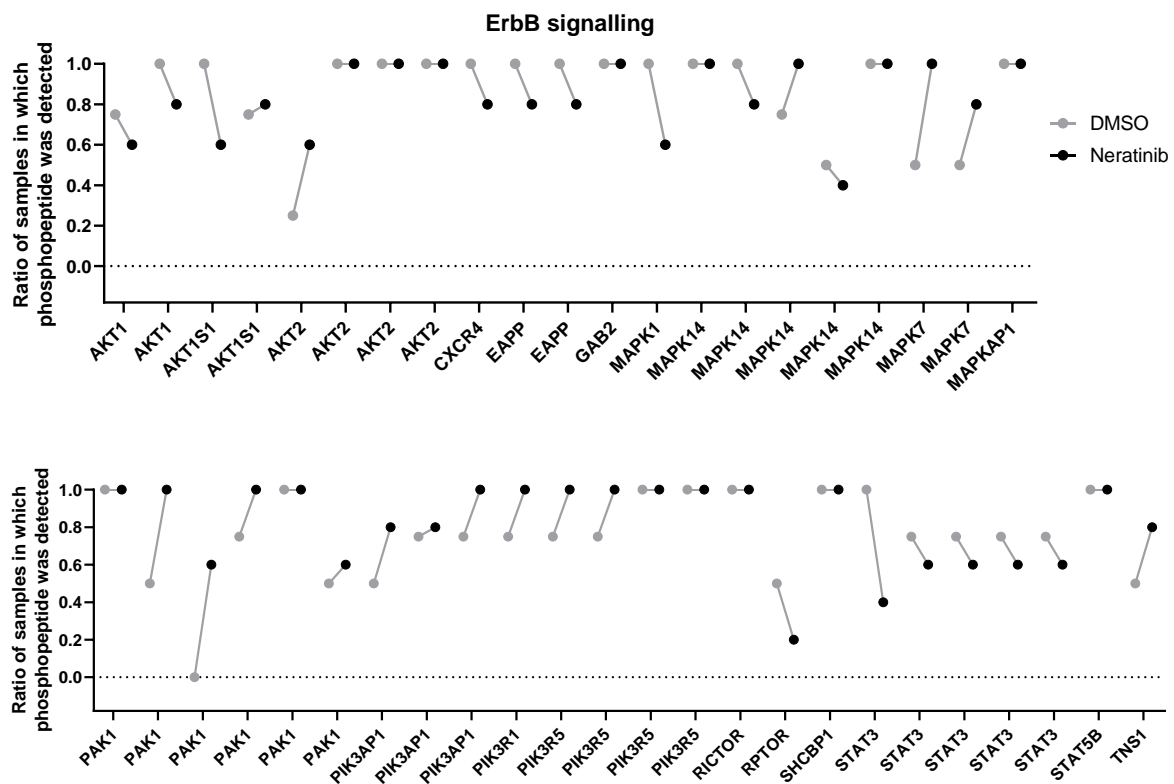
Figure 5.11. Detection of phosphopeptides relating to ErbB signalling pathways.
Schematic overview of ErbB signalling (reproduced courtesy of Cell Signalling Technology, Inc.) (A). Phosphopeptides mapping to proteins downstream of ErbB signalling pathways were identified within the dataset and shown as a ratio of the number of samples in each treatment group it was detected in, out of 4 DMSO treated samples and 5 Neratinib treated samples (B). In some cases multiple phosphorylated peptides mapping to the same protein were identified.

Although there are differences in the detection of some phosphopeptides between the treatment groups, such as STAT3 which was detected in 2/5 neratinib treated samples and all DMSO treated samples, the majority of proteins downstream of ErbB signalling were not differentially detected. At this point it was decided that a definition of "differential detection between treatment groups" would help this analysis, with a threshold for determining when a result should be followed up.

5.4.4 Unbiased analysis of differentially detected phosphorylated peptides between treatment groups

To determine a threshold for differential detection between treatment groups, initially phosphopeptides which were expressed in all DMSO-treated samples ("DMSO specific") and no neratinib-treated samples, and vice versa ("neratinib specific"), were identified. Using this strategy, only four phosphopeptides were counted as specific to DMSO treatment (CCDC88B, EIF3G, TSG101, WASHC2C), and six to the neratinib treatment group (ADD1, ARHGEF2, GLCCI1, PCTP, RGS3, SCAF4). The online database STRING (Szklarczyk *et al.*, 2021) was used to determine if any of these proteins interact, and no interactions, either evidenced or predicted, were found. STRING extracts information from a number of different sources including genomic interaction databases, high throughput experiments, co-expression studies and textmining (searches of the PubMed database for titles or abstracts in which particular proteins appear together).

The parameters used to define "specific" were then expanded and defined as: a phosphopeptide present in at least 4/5 neratinib treated samples, or at least 3/4 DMSO treated samples, and 0-1 samples of the other treatment group. This widened the search to 166 phosphopeptides mapping to 143 proteins specific to either treatment. (Although this no longer falls under the definition of "specific", this word continues to be used in this chapter.)

Rather than analysing the DMSO specific and neratinib specific datasets separately, they were combined for analysis by STRING. As signalling pathways include both the activation and inhibition of downstream enzymes, analysing these datasets separately might result in important interactions being missed. When this data was input into the STRING database, 163 interactions between proteins were detected (Figure 5.12A). For a number of proteins no interactions with others were detected, and for many, more than one interaction was found. STRING also determined that this set of proteins has significantly more interactions than a random set of proteins of the same size and degree of distribution from the genome, indicating that this group of proteins is at least partially biologically connected.

STRING also detects functional enrichments within the protein dataset, i.e. biological processes that one or more proteins within the dataset are involved in. In this dataset, a number of the proteins within a central cluster of interacting proteins were found to be involved in gene expression; that is the regulation of transcription, translation or RNA processing (Figure 5.12B). A second set of related enrichments involved proteins that regulate actin filament assembly and organisation, and cytoskeleton and supramolecular organisation (Figure 5.12C). Although STRING does detect enrichments for specific signalling pathways, none were found within this dataset of proteins specific

to either treatment group. However this does not indicate that no phosphorylated proteins within the same signalling pathway were present, just that they were not significantly enriched, likely due to the large number of proteins within this dataset.

A)
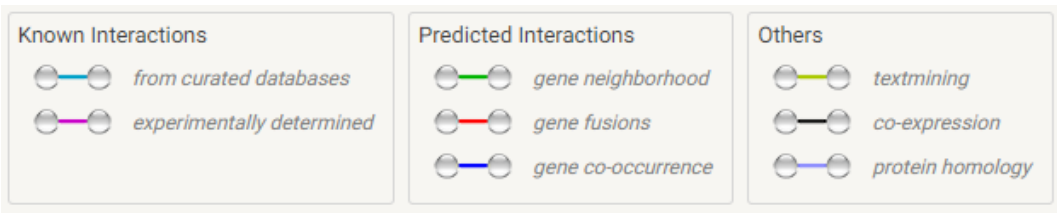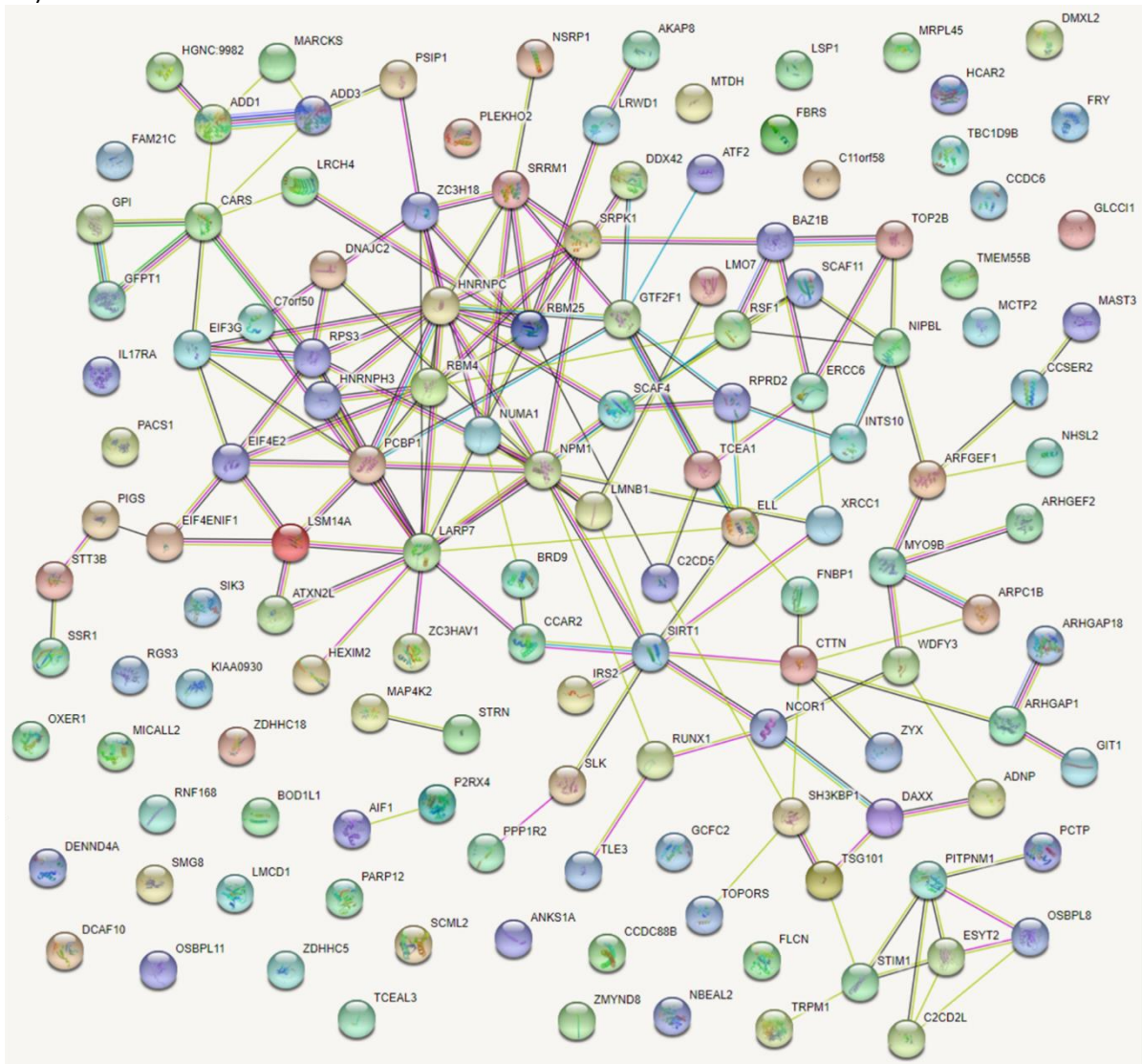
B) Functional enrichments for proteins involved in transcription, translation or RNA processing
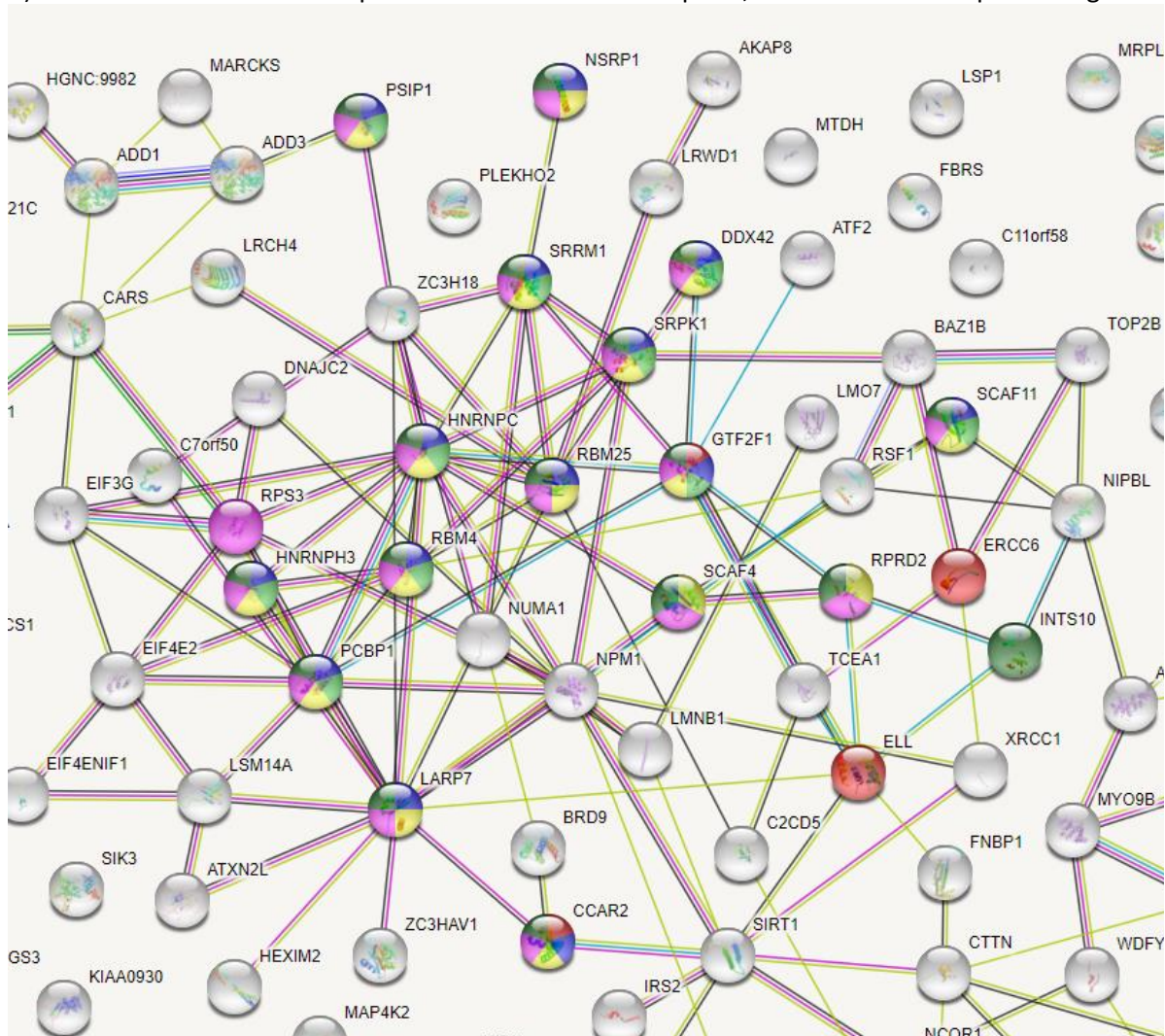
Functional enrichments in your network

explain columns

⌄   **Biological Process (Gene Ontology)**

GO-term	description	count in network	strength	false discovery rate	
GO:0032071	regulation of endodeoxyribonuclease activity	3 of 8	1.74	0.0330	
GO:0000012	single strand break repair	3 of 11	1.6	0.0489	
GO:0032069	regulation of nuclease activity	4 of 22	1.43	0.0316	
GO:0032784	regulation of DNA-templated transcription, elongation	5 of 51	1.16	0.0324	🔴
GO:0051017	actin filament bundle assembly	5 of 55	1.13	0.0342	
GO:2001022	positive regulation of response to DNA damage stimulus	6 of 106	0.92	0.0489	
GO:0007015	actin filament organization	10 of 254	0.76	0.0199	
GO:0032271	regulation of protein polymerization	9 of 232	0.76	0.0324	
GO:0008380	RNA splicing	15 of 396	0.75	0.0011	🔵
GO:0000398	mRNA splicing, via spliceosome	11 of 294	0.74	0.0181	🟢
GO:0006397	mRNA processing	17 of 468	0.73	0.00053	🟡
GO:0016071	mRNA metabolic process	19 of 678	0.62	0.0013	🟣
GO:0097435	supramolecular fiber organization	13 of 480	0.6	0.0316	
GO:0006396	RNA processing	18 of 854	0.49	0.0316	🟢

C) Functional enrichments related to actin filament or cytoskeleton organisation and assembly

GO-term	description	count in network	strength	false discovery rate	
GO:0032071	regulation of endodeoxyribonuclease activity	3 of 8	1.74	0.0330	
GO:0000012	single strand break repair	3 of 11	1.6	0.0489	
GO:0032069	regulation of nuclease activity	4 of 22	1.43	0.0316	
GO:0032784	regulation of DNA-templated transcription, elongation	5 of 51	1.16	0.0324	
GO:0051017	actin filament bundle assembly	5 of 55	1.13	0.0342	🔴
GO:2001022	positive regulation of response to DNA damage stimulus	6 of 106	0.92	0.0489	
GO:0007015	actin filament organization	10 of 254	0.76	0.0199	🔵
GO:0032271	regulation of protein polymerization	9 of 232	0.76	0.0324	
GO:0008380	RNA splicing	15 of 396	0.75	0.0011	
GO:0000398	mRNA splicing, via spliceosome	11 of 294	0.74	0.0181	
GO:0006397	mRNA processing	17 of 468	0.73	0.00053	
GO:0016071	mRNA metabolic process	19 of 678	0.62	0.0013	
GO:0097435	supramolecular fiber organization	13 of 480	0.6	0.0316	🟢
GO:0006396	RNA processing	18 of 854	0.49	0.0316	
GO:0006325	chromatin organization	15 of 713	0.49	0.0489	
GO:0007010	cytoskeleton organization	20 of 1126	0.42	0.0443	🟡

Figure 5.12. Unbiased analysis of differentially detected phosphopeptides mapping to proteins.
All phosphopeptides mapping to proteins that were specific to either treatment group were entered into STRING. Line colour indicates evidence type for interaction (A). STRING shows functional enrichments within the protein dataset. A number of proteins related to gene expression were detected (B), and also relating to actin and cytoskeletal organisation and assembly (C). Columns in tables indicate count in network: number of proteins in dataset, out of total number of proteins involved in that process as per the Gene Ontology database. Strength: how large the enrichment effect is (in comparison to a random network of the same size). False discovery rate: p-values of enrichment, corrected for multiple testing within each category using the Benjamini–Hochberg procedure.

STRING is a very useful tool in determining how proteins interact. However due to the large number of phosphorylated peptides mapping to proteins in this dataset, it was considered that a different tool that related more to biological processes may yield additional information. Data was analysed using the Reactome analysis tool (Fabregat *et al.*, 2017) to attempt to extract pathways or processes in which the differentially phosphorylated proteins may be involved in. Similarly to STRING, Reactome shows pathways that are statistically enriched within the dataset, however Reactome shows these in the context of wider biological processes rather than only the interactions between individual proteins.

Several pathways were found to be statistically enriched within the dataset of phosphopeptides specific to either treatment group. Within the pathways relating to signal transduction, only signalling by Rho GTPases was statistically enriched (Figure 5.13A). Other enriched pathways or processes included the breakdown of the nuclear lamina in apoptosis, circadian clock pathways, transcriptional regulation of DNA repair genes by TP53, and nucleotide excision repair (Figure 5.13B-E).

A)

B)

Apoptotic cleavage of cellular proteins

Apoptotic cleavage of cell adhesion proteins

Caspase-mediated cleavage of cytoskeletal proteins

Breakdown of the nuclear lamina

C)

degradation   metabolism disease events

Scavenging by Class F Receptors

Circadian Clock

Diseases of programmed cell death

Defective pyroptosis

Loss of function of TP53 in cancer due to loss of tetramerization ability

a-Golgi raffic

BMAL1:CLOCK,NPAS2 activates circadian gene expression

Defective Intrinsic Pathway for Apoptosis Due to p14ARF Loss of Function

NR1D1 (REV-ERBA) represses gene expression

RORA activates gene expression

Defective RIPK1-mediated regulated necrosis

D)

Transcriptional Regulation by TP53

regulates transc other transcriptio

TP53 Regulates Transcription of Cell Death Genes

TP53 Regulates Transcription of DNA Repair Genes

TP53 Regulates Metabolic Genes

TP53 Regulates Transcription of Death Receptors and Ligands

TP53 Regulates Transcription of Genes Involved in Cytochrome C Release

TP53 regulates transcription of several additional cell death genes whose specific roles in p53-dependent apoptosis remain uncertain

TP53 Regulates Transcription of Caspase Activators and Caspases

Regulation of TP53 Activity

TP53 Regulates Transcription of Cell Cycle Genes

TP53 Regulates

E)

Figure 5.13. Reactome analysis of the treatment-specific dataset.
Proteins mapping to phosphorylated peptides specific to either treatment group were analysed using the Reactome analysis tool. Enrichment is calculated using the over-representation analysis method, with anything below p=0.05 indicated on a yellow-brown colour scale (pink = not significantly enriched). Statistically enriched pathways include Rho GTPase signalling (A), breakdown of the nuclear lamina (B), circadian clock (C), TP53 regulation translation of DNA repair genes (D), and nucleotide excision repair (E).

Although the aim of this experiment is to determine the signalling pathways by which neratinib is inducing apoptosis, it appears that some of the phosphorylated proteins differentially detected between treatment groups may be identified due to the effects of apoptosis, rather than the upstream signalling pathways. The breakdown of the nuclear lamina is an example of this; it is more likely that this is part of the neutrophil nucleus beginning to condense as part of apoptosis, than being directly downstream of neratinib, although this cannot be concluded for certain.

The next step in the analysis of this data was to attempt to identify differentially phosphorylated proteins that may be upstream of these apoptotic signalling pathways. This approach required literature searches into the function of these proteins, their involvement in cell death pathways, and whether the phosphorylation event detected in this dataset (i.e. phosphorylation of the specific amino acid on that protein) is known to induce cell death. As 166 phosphopeptides mapping to 143 proteins were differentially detected with treatment, it would not be feasible to carry out this level of analysis

for every single one. The data collected from STRING and Reactome was used to narrow down this search – for example more focus was also given to proteins that had interactions with others, and those involved in statistically enriched processes as determined by STRING and Reactome.

5.4.5   Choosing candidates for potential downstream effectors of neratinib

From analysing the dataset of phosphorylated proteins specific to either treatment group, a number of potential pathways by which neratinib may be working were identified. One particularly interesting result from the Reactome analysis was the enrichment of pathways regulating circadian rhythm. Research from a neutrophil group has previously demonstrated the role of cyclin dependant kinases (CDK) in regulating neutrophil apoptosis (K. Q. Wang *et al.*, 2012). Neutrophil apoptosis was upregulated upon treatment with CDK inhibitors, specifically inhibitors of CDK7 and CDK9, with an inhibitor of the latter inducing neutrophil apoptosis and accelerating neutrophilic inflammation resolution in the zebrafish larvae (Leitch *et al.*, 2012; Hoodless *et al.*, 2016). Although neither CDK7 nor CDK9 were detected in this experiment, either as proteins or phosphopeptides, a number of other CDKs and their substrates were, along with several phosphopeptides that were differentially detected between treatment groups.

Phosphorylated peptides mapping to CDK2, CDK11A, CDK12, CDK13, CDK14 and CDK17 were detected in the dataset (Figure 5.14A). Although none were considered specific to either treatment group as per the previous definition, the two phosphopeptides mapping to CDK2 were both present in 2/4 DMSO treated samples and 0 neratinib samples. Phosphopeptides mapping to substrates of CDKs remained mostly unchanged between the treatment groups (Figure 5.14B). Additionally, when the protein dataset (samples run prior to enrichment for phosphopeptides) was interrogated for CDKs, CDK1 and CDK2 were detected (Figure 5.14C). Statistical analysis of the difference in intensity of either CDK1 or CDK2 between the two treatment groups found no significant differences.

Figure 5.14. Analysis of changes in the phosphorylation of cyclin dependant kinases.

Phosphopeptides mapping to CDKs (A) and their substrates (B) were identified within the dataset, and shown as a proportion of the number of samples in each treatment group they were detected in, out of 4 DMSO treated samples and 5 Neratinib treated samples. In some cases multiple phosphorylated peptides mapping to the same CDK were identified. Abundance of CDK1 and CDK2 protein were measured before enrichment for phosphopeptides (C). Data points in C represent data from each donor, with lines joining treatment samples from each biological replicate (n=4).

5.4.5.1 NPM1

Although no major differences were detected between treatment groups of CDKs and related proteins, a number of phosphorylated proteins that regulate CDK activity were found to be specific to either treatment group. Nucleophosmin 1 (NPM1) is a protein involved in a number of pathways including ribosome biogenesis, histone assembly and protein chaperoning, but of interest in this context is that it negatively regulates apoptosis, and regulates the tumour suppressors p53 and ARF. In cancer cells, NPM1 is frequently overexpressed or mutated, and can contribute to oncogenesis (Grisendi *et al.*, 2006).

In this dataset, six phosphopeptides mapping to NPM1 were detected, two of which were phosphorylated in 3/4 DMSO treated samples and 0/5 neratinib treated samples. The phosphorylation of these latter two peptides occurred at Serine 4 and Serine 10. The differential phosphorylation of Serine 4 in NPM1 is interesting, as irradiated basal epithelial cells showed dephosphorylation of this particular amino acid, suggesting a possible link to a damage or stress response (Wiesmann *et al.*, 2019). A research article analysing NPM1 in mutant lymphoblastoid cells found that phosphorylation of Ser10 and Ser70 on NPM1 positively regulated the activity of CDK1 (Du *et al.*, 2010). Simultaneous inactivation of these two phosphorylation sites induced cell cycle arrest in this cell line (Du *et al.*, 2010). Phosphopeptides of NPM1 with phosphorylation at Ser70 were detected in our dataset, however they were present in all samples of both treatment groups.

The role of CDK1 in apoptosis is complex, as it can both induce and suppress apoptosis depending on the cell type and context (Vassilev *et al.*, 2006; Zhou *et al.*, 2014). However research using neutrophils *in vitro* demonstrated CDK1 kinase activity decreased during neutrophil apoptosis (Rossi *et al.*, 2006). One hypothesis may be that in DMSO treated samples in this dataset, NPM1 is phosphorylated and inducing CDK1 activity, whereas in neratinib treated samples CDK1 is inactive. It is unclear at this point whether CDK1 itself is inducing apoptotic effects, as it can directly phosphorylate a number of the BCL-2 family proteins (Zhou *et al.*, 2014).

Although phosphorylation of CDK1 was not detected in this dataset, and protein levels did not change, it is possible that this is related to the timepoint chosen. Additionally, as phosphorylation of NPM1 at Ser70 was not differentially detected between treatment groups in our dataset, it may be that in neutrophils only one phosphorylation event is necessary for CDK1 activity. It is also possible that NPM1 is not regulating CDK signalling at all in these experiments, but is directly inducing apoptosis via its regulation of p53. However further evidence to support the role of cyclin-dependant kinase signalling being regulated by neratinib treatment is evident in this dataset.

5.4.5.2   RPS3

Ribosomal protein S3 (RPS3) is a component of the 40S ribosomal subunit, involved in ribosome maturation and translation initiation by interacting with initiation factors eIF2 and eIF3 (Lee *et al.*, 2010). It has a number of roles throughout the cell, in DNA damage repair, NFκB-mediated transcription, binding and protecting p53 from ubiquitination, and activating caspase-3 and caspase-8 to induce apoptosis (Jang, Lee and Kim, 2004; Yadavilli *et al.*, 2009). In neuronal cells, AKT was found to phosphorylate RPS3 at Threonine 70, which inhibited the pro-apoptotic effect of RPS3 on neurons; when RPS3 was either deleted or overexpressed, apoptosis was induced (Lee *et al.*, 2010). Importantly, RPS3 was shown to be phosphorylated at Threonine 221 by CDK1 in assays using human embryonic kidney cells (Yoon *et al.*, 2011).

In our dataset, one phosphopeptide mapping to RPS3 was detected, phosphorylated at Threonine 95, and detected in 3/4 DMSO treated samples and 1/5 neratinib treated samples. Literature searches yielded no information on phosphorylation on this particular amino acid. Based on research discussed however, it was hypothesised that in this dataset, the phosphorylation of NPM1 was activating CDK1, which was in turn phosphorylating RPS3 in DMSO-treated cells. In neratinib treated cells, the lack of RPS3 phosphorylation may be inducing apoptosis. Although little literature exists on the role of RPS3 in neutrophils specifically, one research group using a mouse model of cigarette smoke induced lung injury found that gene silencing of RPS3 by siRNA in mice suppressed inflammatory mediator and oxidative damage markers, possibly via interruption of the NFκB pathway (Dong *et al.*, 2018). As neratinib also attenuated specific inflammatory markers in mouse models of lung inflammation, RPS3 was considered an interesting candidate to follow up further.

5.4.5.3   SIRT1

Another phosphorylated protein that was differentially detected between treatment groups was Sirtuin 1, also known as NAD-dependant protein deacetylase sirtuin 1 or SIRT1. This deacetylase enzyme has a variety of roles in regulating transcription and intracellular energetics, response to DNA damage, the cell cycle, apoptosis and autophagy (Motta *et al.*, 2004; Vaquero *et al.*, 2004; Lee *et al.*, 2008). It deacetylates histones, modulating chromatin function, and a range of transcription factors, regulating gene expression, and importantly binds to and deacetylates p53, inhibiting apoptosis (Smith, 2002). SIRT1 can be phosphorylated by CDK1, which regulates its activity; when dephosphorylated by phosphatases *in vitro*, the deacetylase activity of SIRT1 was decreased (Sasaki *et al.*, 2008). Although in this particular research article, Threonine 530 and Serine 540 were the key phosphorylation sites that regulated activity, phosphorylation of Serine 14 was also detected and

considered as a possible substrate motif of CDK1 (Sasaki *et al.*, 2008). In the dataset analysed in this thesis chapter, a phosphopeptide of SIRT1 with a phosphosite at Serine 14 was detected in 3/4 DMSO treated samples, and 1/5 neratinib treated samples. It was hypothesised that in DMSO treated cells, SIRT1 phosphorylation was induced by CDK1, which in turn allowed SIRT1 to bind to and inactivate p53, inhibiting apoptosis; whereas in neratinib treated cells, SIRT1 is not phosphorylated, has lower deacetylase activity and does not prevent p53 inducing apoptosis.

5.4.6   Testing inhibitors of candidates for the downstream regulators of apoptosis induced by neratinib

To test whether these candidate proteins regulated apoptosis in response to neratinib treatment, an *in vitro* neutrophil apoptosis assay was designed. Human neutrophils isolated from healthy donors were treated with inhibitors of these candidates, either alone or in combination with neratinib. If the candidates are downstream of neratinib signalling, then theoretically, using the inhibitors in combination should yield levels of apoptosis similar to those with either the inhibitor or neratinib alone, and there should be no additional apoptosis when used in combination. Although this is a relatively indirect assay for analysing signalling pathways, it was considered a good starting point to at least test whether inhibitors of these candidate drugs induce neutrophil apoptosis.

An inhibitor was found for NPM1 (NSC348884), which is known to induce apoptosis of various cancer cell lines (Di Matteo *et al.*, 2016). An SIRT1 inhibitor (EX527) was also selected; this inhibitor was used experimentally to demonstrate that deacetylation of p53 is mediated by SIRT1 (Solomon *et al.*, 2006). Unfortunately no inhibitors of RPS3 were found. However an inhibitor of CDK1 and CDK2 (NU6102) was also selected, due to the potential involvement of these enzymes; inhibitors of these are known to activate p53 and induce apoptosis in tumour cells (Payton *et al.*, 2006).

The concentration of neratinib used in these assays remained the same as that used to treat the samples for phosphoproteomics analysis (25µM). As inhibitors of the candidates had not been used previously in human neutrophils, it was decided that two concentrations of each would be tested; 5µM and 25µM. As in previous *in vitro* neutrophil apoptosis assays, neutrophils were incubated for six hours before apoptosis was assessed by morphology.

The inhibitor of SIRT1 (EX527) did not induce neutrophil apoptosis at either concentration when used alone, with the percentage apoptosis being no higher than the control DMSO-treated cells. When used in combination with neratinib, there was a statistically significant increase in apoptosis to levels

comparable to the neratinib treated cells (Figure 5.15A). This suggests that SIRT1 is not downstream of the signalling pathway neratinib is inhibiting to induce apoptosis.

When used alone, NSC348884 (NPM1 inhibitor) significantly increased the percentage of neutrophil apoptosis at both 5µM and 25µM in comparison to DMSO-treated cells. This level of apoptosis was comparable to the increase observed in neratinib treated neutrophils. When NSC348884 was used in combination with neratinib, there was no statistically significant difference in the levels of apoptosis in comparison to the inhibitor alone, at either 5µM or 25µM (Figure 5.15B). This suggests that NPM1 may be inhibiting the same pathway as neratinib to induce neutrophil apoptosis.

The inhibitor of CDK1/2, NU6102, also induced neutrophil apoptosis at both 5µM and 25µM (Figure 5.15C). There is no statistically significant increase in apoptosis when neratinib is used in combination with the inhibitor, suggesting that they may be inhibiting the same pathways. Interestingly though, the morphology of neutrophils treated with NU6102 was unlike neratinib treated cells, with hypersegmentation of neutrophil nuclei observed (Figure 5.15D). This morphology was observed only with this inhibitor, in all three repetitions of the experiment. This suggests that although NU6102 may be inhibiting the same pathways as neratinib to induce apoptosis, it is affecting other aspects of neutrophil function too.

The results of this experiment suggest that SIRT1 is not a downstream component of neratinib-induced apoptosis, as the SIRT1 inhibitor did not induce apoptosis alone. The effect of inhibiting CDK1 and CDK2 was interesting, as despite the increases in apoptosis that are similar to neratinib treated cells, neutrophil morphology differs from neratinib treated cells. NPM1 remains a possible candidate based on these results.

A)

EX527 (SIRT1 inhibitor)

B)

NSC348884 (NPM1 inhibitor)

181

C)

NU6102 (CDK1/2 inhibitor)
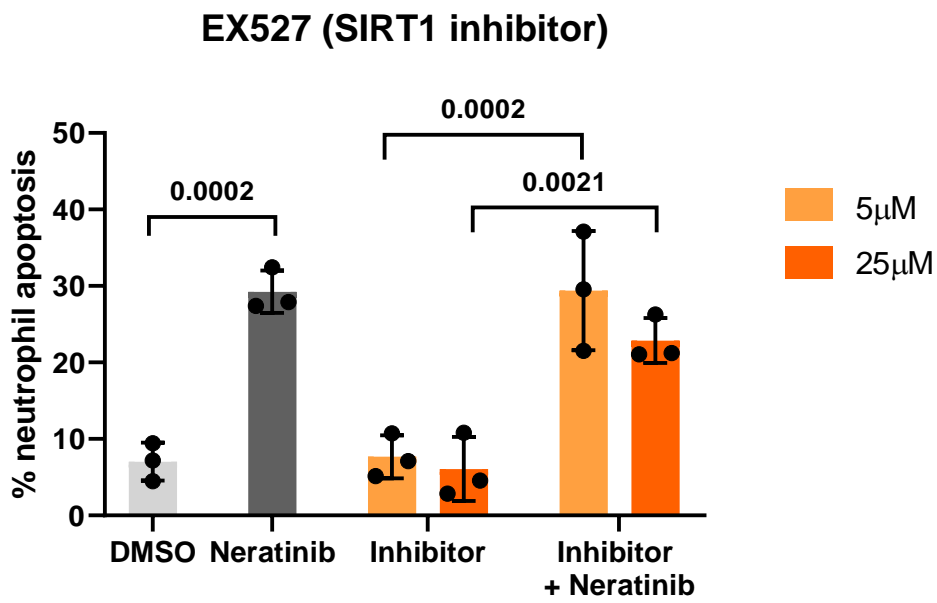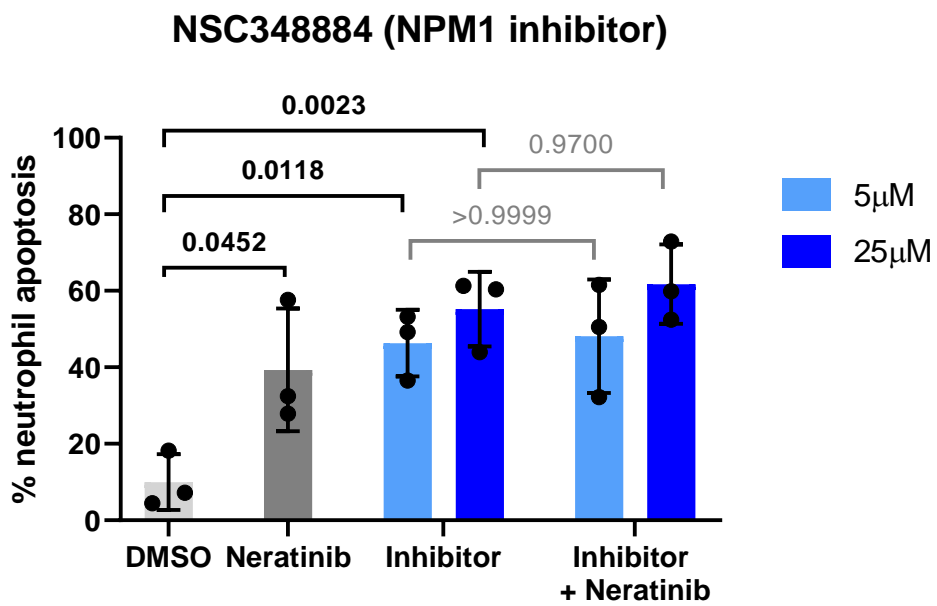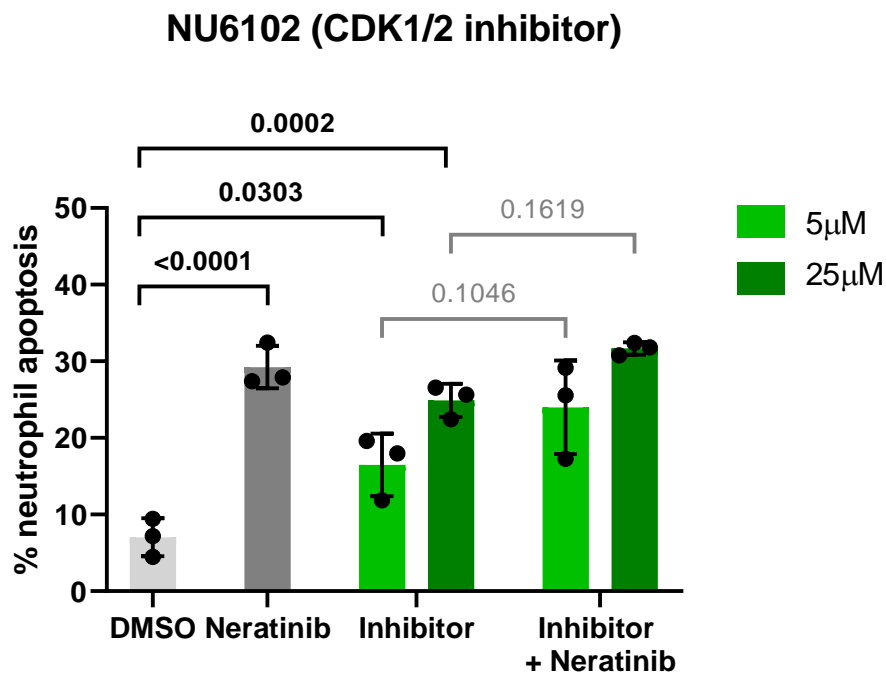
D)
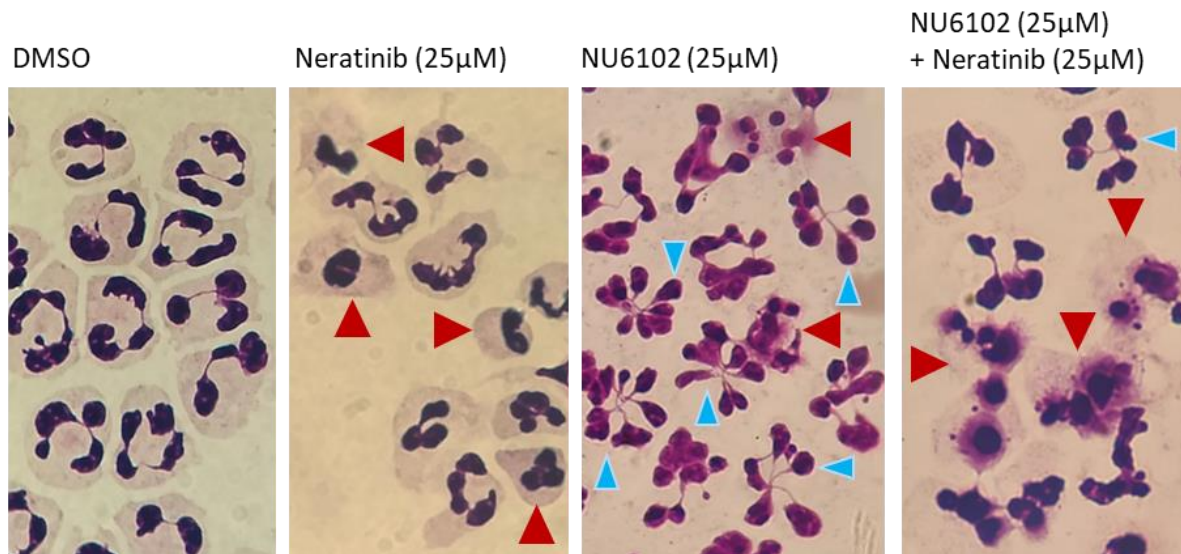
Figure 5.15. Testing inhibitors of candidates for the downstream effectors of neratinib.
Human neutrophils were incubated with inhibitors of candidate proteins, alone or in combination with 25 μM Neratinib, for 6 hours, after which levels of apoptosis were assessed by morphology. Inhibitors of SIRT1 (A), NPM1 (B) and CDK1/2 (C) were tested. The morphology of neutrophils treated with the CDK inhibitor is unlike the typical rounded up nuclear morphology of neratinib treated neutrophils (D, red arrows), with NU6102 also inducing hypersegmentation of nuclei (D, blue arrows). Graphs represent data from 3 individual healthy donors, bars represent mean ± standard deviation. One-way ANOVA with multiple comparisons used to calculate statistical significance, p values indicated where appropriate.

5.4.7 Phosphoproteomics discussion and future work

Analysis of phosphoproteomics data in this chapter, although not conclusive in identifying the downstream signalling pathways by which neratinib is inducing apoptosis, has yielded some interesting results. Firstly, although neratinib is an inhibitor of EGFR and ErbB2, phosphorylated proteins within the known signalling pathways downstream of ErbBs did not appear to be highly regulated by neratinib treatment. This does not completely exclude ErbB signalling from being regulated by neratinib. Phosphorylation, especially in regards to signal transduction, is highly dynamic, and in this experiment a single timepoint was analysed. Ideally multiple timepoints, both earlier and later than that chosen in this experiment would be analysed, however this would have been at the expense of the 5 biological replicates, reducing the power of the analysis.

Originally, plans to optimise the concentrations and timepoints for neratinib and cAMP treatment were to be carried out via western blot. Optimisation of neutrophil western blots that aimed to detect phosphorylated tyrosine residues or phosphorylated AKT were attempted. However after several months of frequently unsuccessful experiments and inconsistent results, this work was halted due to the closure of the University during the first COVID-19 shutdown. When laboratory work could resume four months later, it was decided that there was not enough time to continue with western blot optimisation, and instead the concentration and timepoints at which treatments were given were based on previous research and literature.

In the current experiment, each of the 10 samples were run through the mass spectrometer individually, which is a limitation of this work. Repeating this experiment using isobaric tags and a multiplex system would yield more quantitative data. Isobaric tags are labels of identical masses but with varying heavy isotopes around their structure, which are added to individual samples before they are pooled and analysed together. This multiplexing of samples eliminates variation between runs, allowing quantitative analysis of the abundance of phosphopeptides between samples. Without this technique, comparing the abundance of phosphopeptides between samples was not possible, and analysis was instead carried out based on the proportion of samples in each treatment group within which a phosphopeptide was detected. However the analysis detailed in this chapter has yielded interesting results, and identification of proteins involved in cAMP signalling and apoptosis has demonstrated the validity of this method of analysis.

Analysis by STRING suggested that a number of functionally enriched pathways in the "treatment specific" dataset included those regulating transcription, translation and RNA processing. A number of the proteins involved in these signalling pathways, such as GTP2F1, TCEA1 and ELL, are general transcription factors or parts of the RNA polymerase machinery, and regulate the transcription of a

broad range of genes rather than specific ones. A number of these proteins were phosphorylated in the DMSO treatment group, but not neratinib, and it may be that the induction of apoptosis by neratinib is beginning to shut down general cellular processes. It is possible therefore that differential phosphorylation between treatment groups is as a consequence of apoptosis, rather than them being downstream of neratinib specifically. This may also be the case for the functional enrichment of proteins involved in actin filament assembly and organisation, and cytoskeletal organisation, which were also detected by STRING. Analysis using Reactome also identified breakdown of the nuclear lamina as an enriched process. It is not possible to determine this from this dataset whether these events are directly downstream of neratinib, or are related to apoptosis in general, however repeating this experiment with multiple timepoints may give some answers.

In an attempt to validate some of these findings, I tested inhibitors of pathway components that were most regulated. Ideally a wide range of candidates would be tested, however this was not possible in the time remaining for laboratory work, therefore 3 focused targets were selected. The first, an inhibitor of SIRT1, did not induce neutrophil apoptosis and so could be ruled out as inhibiting the same pathways as neratinib. Inhibitors of both CDK1/2 and NPM1 showed more promising results, as they both induced neutrophil apoptosis, and no additional apoptosis was observed when used in combination with neratinib. NSC348884 (NPM1 inhibitor) is a known inducer of cytotoxicity in other cell types (Šašinková *et al.*, 2021) and so the induction of neutrophil apoptosis was not particularly surprising. There is evidence of interactions between NPM1 and EGFR/EGF signalling in the literature. NPM1 was shown to directly interact with EGFR after ionizing radiation damage of glioma cell lines *in vitro*, using mass spectrometry, however the significance of this has not been investigated (Liccardi, Hartley and Hochhauser, 2014). In prostate cancer cell lines, knockdown of NPM1 results in a decrease in EGF promoter activity, and a decrease in levels of phosphorylated EGFR (Loubeau *et al.*, 2014). The authors demonstrated that NPM1 silencing does not affect the PI3K/AKT arm downstream of EGFR signalling, but is likely required specifically for EGFR-mediated MAPK signalling in these cells. As NPM1 was not found to be a direct transactivator of the EGF promoter in these cells, the authors suggested that NPM1 instead enhances MAPK signalling resulting in increased EGF expression and thus EGFR activity, and so NPM1 regulates the autocrine feedback loop in these tumour cells to promote oncogenesis (Loubeau *et al.*, 2014).

It is important to note that EGFR was not detected in either the proteomic or phosphoproteomic dataset obtained within this thesis, and RNAseq data suggests that the EGFR is not expressed in human neutrophils, and so the relevance of this mechanism to experiments within this thesis are unclear. Numerous phosphorylated MAPK peptides were identified in the dataset from this thesis, however only one was found to be differentially detected between the treatment groups: MAP4K2, present in

4 neratinib-treated samples and 0 DMSO-treated samples. No evidence of interactions between this particular MAPK and NPM1 were found in the literature. This evidence does not rule out NPM1 as being inhibited by neratinib and inducing neutrophil apoptosis, but it suggests that it may not be via MAPK or EGFR signalling.

It was hypothesised that NPM1 may be interacting with cyclin-dependant kinases to induce apoptosis in this dataset. Phosphorylated CDK2 was detected in 2/4 DMSO samples, and 0 neratinib treated samples in this dataset, and a number of phosphorylated proteins that interact with CDKs were differentially detected between treatment groups. In cell-free phosphorylation assays, neratinib did not phosphorylate CDK1, CDK2 or CDK4 (Rabindran *et al.*, 2004). The results of the apoptosis experiment utilising an inhibitor of CDK1/2 demonstrate that although neutrophil apoptosis is induced, this inhibitor also induces hypersegmentation of neutrophil nuclei. This suggests that although this compound may be inhibiting the same pathways as neratinib, it is also affecting other pathways. It is possible that these are off-target effects of the inhibitor and are unrelated to CDK1/2 signalling, and if time allowed this could be tested by using a number of different inhibitors of CDK1/2.

Further experiments to follow up these results would include using Western blotting to determine whether phosphorylated NPM1 and CDK1 or CDK2 could be detected in human neutrophils, and if this was reduced with neratinib treatment. Although this would not yield new data, it would be a useful validation of the phosphoproteomics dataset. It would also be interesting to analyse the temporal aspects of these particular phosphorylation events, using samples treated for different lengths of time.

To further investigate whether neratinib-induced inhibition of NPM1 and CDK1/2 was inducing neutrophil apoptosis, a similar assay to the inhibitor-induced apoptosis experiment could be carried out, but using genetic knockout of the genes rather than pharmacological inhibition. This is difficult to do in human neutrophils due to their short lifespan and terminally differentiated state, but may be possible in cells such as the PLB-985 cell line, derived from an acute myeloid leukaemia and which can be differentiated into neutrophil-like cells (Tucker *et al.*, 1987). The aim of this experiment would firstly be to determine if knock-out of these genes induced apoptosis, and if so, whether treatment with neratinib increases this further. If these candidates were inducing apoptosis in response to neratinib treatment, it would be expected that genetic ablation would render neratinib unable to induce further apoptosis. Using genetic knockout, rather than pharmacological inhibition, would reduce the potential for off-target effects that many pharmacological inhibitors show.

Other pathways of interest that would be interesting to follow up with include the JUN kinase (JNK) pathway, to which four phosphorylated proteins specific to either treatment group were part of: RPS3, MAP4K2, DAXX, and ERCC6. This pathway was of interest as it leads to the activation of transcription

factors of p53, and activation of apoptotic proteins BIM, BAD and BAX, and can inhibit the pro-survival STAT pathway (Dhanasekaran and Reddy, 2008). As a regulator of both mitochondrial (intrinsic) and receptor-mediated (extrinsic) apoptotic pathways, the hypothesis that neratinib is working via this pathway is plausible.

Although the aim of this section of work was to identify the pathways by which neratinib was inducing apoptosis, some of the findings indicated that neratinib may be affecting other cellular functions. An interesting enrichment that came from both the Reactome analysis and STRING was of Rho-GTPases. This highly conserved family regulate a wide range of cellular functions, the best characterised being the regulation of the actin cytoskeleton for migration, but also cell polarity and division, and cell cycle progression (Clayton and Ridley, 2020). In results from the zebrafish larvae, treatment with neratinib and other ErbB inhibitors resulted in reduced migration of neutrophils to the site of injury. Although it was considered that this was due to an increase in neutrophil apoptosis, it may be that inhibition of ErbB signalling is also directly regulating migratory mechanisms. Further assessment of the effect of ErbB inhibition on migration would be interesting to follow up, either using human neutrophils *in vitro* which can migrate towards chemotactic cues, or in the zebrafish larvae by photoconversion techniques to track individual cells in real time.

5.5   Chapter summary

The data mining work in this chapter indicates human neutrophils may only express *ERBB2* and *ERBB3* at low levels, whereas zebrafish neutrophils appear to express *egfra* and *erbb2,* and possibly *erbb3a* and *erbb3b*. In human neutrophils, ErbB gene expression does not appear to be regulated by inflammatory stimuli, either *in vitro* in human neutrophils or in samples from patients with COPD. These results are interesting as they provide context to the results from the phosphoproteomic analysis of human neutrophils: as neratinib is an inhibitor of EGFR and ErbB2, this suggests it may be working via ErbB2 only. However the signalling pathways downstream of ErbBs described in the literature were not particularly regulated by neratinib treatment, and it is possible that neratinib is binding to neutrophil via a different target. The signalling pathways being supressed by neratinib are yet to be fully elucidated, but a number of possible candidates have been identified and further experiments would shed light on the previously undescribed mechanism of action of this drug in human neutrophils.

6   General Discussion

Identifying effective treatment options for patients with chronic inflammatory diseases remains a huge global challenge, and one that urgently needs investment and research. COPD remains one of the leading causes of morbidity and mortality, and as treatments currently focus on reducing symptoms rather than abrogating the underlying inflammatory cause, they do not prevent disease progression. Neutrophils are known to be key drivers of the tissue damage observed in the lungs of patients with COPD, and previous research from my group identified ErbB inhibitors as being able to induce neutrophil apoptosis, which may be beneficial for reducing the chronic inflammatory environment in the lungs (Rahman *et al.*, 2019).

The research in this thesis has demonstrated that ErbB inhibitors are able to induce apoptosis of both human neutrophils *in vitro*, and larval zebrafish neutrophils *in vivo*. No changes in neutrophil apoptosis were observed in the mouse models of lung disease, however an increase in the rate of efferocytosis by macrophages, and decrease in the number of dead neutrophils, suggests that apoptosis may have been upregulated at an earlier timepoint, although this cannot be concluded without further research. Both the upregulation of efferocytosis and decreasing numbers of dead neutrophils observed in the acute lung injury mouse model are pro-resolution mechanisms, suggesting neratinib has potential as an anti-inflammatory agent in this model. The larval zebrafish model also showed a reduction in neutrophils recruited to an injury site with ErbB inhibitor treatment, giving further support to this. On the other hand, a number of inflammatory markers including neutrophil number were unchanged in other mouse models of lung disease, suggesting neratinib is not efficacious in all models.

6.1   Can ErbB inhibitors reduce neutrophil numbers?

When considering whether treatment with ErbB inhibitors would be able to induce neutrophil apoptosis in humans *in vivo*, an important parameter measured in the mouse studies that was not altered by neratinib treatment was neutrophil count. In the latter two studies in which repeated doses of LPS/elastase were given to induce a more chronic inflammatory response in the lungs, it could be hypothesised that neutrophil numbers were initially depleted, but at the time samples were taken (one week after the last dose of LPS/elastase) neutrophil numbers had returned to equilibrium. If this were the case it may be expected that an increase in neutrophil apoptosis would be observed in the acute LPS-induced lung injury model, which it was not, although it is also possible that this 48h

timepoint was similarly too late to observe this; the increased rates of efferocytosis in this model support this hypothesis.

There is an interesting comparison here between the mouse and zebrafish larvae model, in which neutrophil numbers at the tail fin injury site were depleted after ErbB inhibitor treatment and in *egfra/erbb2* double crispant larvae, and rates of neutrophil apoptosis were increased. It may be that the apoptotic neutrophils detected in the zebrafish larvae had actually been engulfed by macrophages; as the transgenic line used for these experiments did not contain a macrophage fluorescent reporter, it was not possible to determine this.

It is also worth analysing the patient population already taking these drugs: people with cancer. Neutropenia is not a common adverse effect of ErbB inhibitor treatment, but it has been reported. In a clinical trial of gefitinib monotherapy as a first-line treatment for pulmonary adenocarcinoma, severe neutropenia was identified in 0.9% (4/607) patients, although it is worth noting that this rate was 65.4% (365/589) patients in the chemotherapy (carboplatin/paclitaxel) treatment arm of the trial (Mok *et al.*, 2009). Another clinical trial of gefitinib showed 7/87 patients developed neutropenia, although all were mild to moderate in severity (Mitsudomi *et al.*, 2010). One case study showed a 77-year-old female with lung adenocarcinoma, who developed a grade 4 (life-threatening) neutropenia after 28 days of gefitinib monotherapy. The patient was switched to erlotinib, and by day 47 neutrophil counts returned to normal without additional intervention (Araya *et al.*, 2013). As both gefitinib and erlotinib inhibit EGFR specifically, it is interesting that the switch resulted in the resolution of neutropenia, suggesting that this may be an off-target effect of gefitinib, or possibly was unrelated to the treatment.

Neratinib has also been observed to induce neutropenia, with the Europeans Medicines Agency listing its incidence as 3.1% with neratinib treatment vs 2.3% in the placebo treatment group (European Medicines Agency, 2018a). Another clinical trial showed only one incidence of neutropenia with neratinib treatment, out of 662 patients (Chan *et al.*, 2021). Studies in which neratinib treatment was used in combination with trastuzumab (ErbB2 monoclonal antibody) and paclitaxel (chemotherapy agent) showed 10% patients developed neutropenia, but as this was a combination therapy it is not possible to determine which drug was responsible (Jankowitz *et al.*, 2013).

These results do suggest that neutropenia is a relatively uncommon adverse effect of ErbB inhibitor treatment, although as the clinical trials described here did not have a disease-free arm it is not possible to determine if this is specific to the treatment or as a result of the cancer. As blood samples from these trials are taken at various timepoints, it is possible that there was an upregulation in

neutrophil apoptosis, but at the time of sampling neutrophil numbers returned to normal, although of course this cannot be determined from the data available.

6.2   Would ErbB inhibitor treatment increase susceptibility to infection?

Although detrimental in chronic inflammatory diseases such as COPD, neutrophils are essential immune cells and patients with chronic neutropenia experience life-threatening infections, particularly in the skin and mouth/gums, which even if cleared can cause permanent damage (Donadieu *et al.*, 2011). Patients with COPD are already increasingly susceptible to infections, and it would be important to establish that a new treatment does not worsen this, particularly one that aims to remove neutrophils, a key defence against pathogens.

There is some evidence that cancer patients using ErbB inhibitors have an increased risk of infection. Urinary tract infection is listed as a common side effect of neratinib (European Medicines Agency, 2018a). A meta-analysis of 25 clinical trials of lung cancer patients treated with either gefitinib or erlotinib showed an overall increased risk of infection of any grade, but this was not statistically significant when stratifying by severe or fatal infections only (Y. Wang *et al.*, 2017). The mechanism leading to this increased rate of infection has not been described, although EGFR signalling is known to regulate inflammation via the NFκB and JAK/STAT pathways. On the other hand, there is evidence that ErbBs may play a role in facilitating the progression of viral infection: a number of pathogens upregulate the surface expression of ErbB receptors, and influenza A virus and respiratory syncytial virus (RSV) can enter host epithelial cells using EGFR (Ho *et al.*, 2017). More recently, a pre-print paper suggested that lapatinib, an inhibitor of EGFR and ErbB2, supresses the replication of viral SARS-CoV-2, and protects against pro-inflammatory cytokine production and epithelial barrier injury in the lungs, although this has not yet been peer-reviewed (Saul *et al.*, 2021).

If time permitted, I would follow up this line of research by investigating whether ErbB inhibitor treatment affected the clearance of pathogens in models used in this thesis. A number of infection models are established in the zebrafish larvae, and phagocytosis assays with various bacteria can be carried out in human neutrophils *in vitro* after treatment with ErbB inhibitors. In COPD, dysregulation of regulatory T cells and exhaustion of effector T cells are considered key mechanisms by which the increased susceptibility to infection arises (Bhat *et al.*, 2015), and so it would also be useful to investigate using models that recapitulate these aspects of the adaptive immune response. The mouse may be the most appropriate for this: although the mouse models used in this paper did not include infectious components, this could be incorporated. Similarly, the adaptive immune response was not

investigated in detail in this work, although lymphocytes were detected in the blood and bronchoalveolar lavage fluid of mouse models of lung inflammation. Using flow cytometry to immunophenotype these cells would be a good starting point to determine whether ErbB inhibitors were affecting the polarisation of T cell subsets.

One promising result from the mouse model of acute lung injury was the upregulation of efferocytosis observed with neratinib treatment. Research has indicated that along with impaired clearance of pathogens, efferocytosis of dead cells may be impaired in the lungs of patients with COPD (Jubrail, Kurian and Niedergang, 2017). As an accumulation of dead cells is highly pro-inflammatory, it is promising that neratinib does not further impair macrophage efferocytosis. If possible, this result could also be further investigated to determine whether the upregulation of efferocytosis is a direct effect of inhibiting ErbB signalling in macrophages. This could be carried out using *in vitro* assays to determine if the uptake of apoptotic neutrophils by cultured human macrophages is altered by ErbB inhibitor treatment.

6.3 Would ErbB inhibitors be suitable for patients with COPD?

The adverse effects of ErbB inhibitors, described in the introduction section 1.4.4, must be carefully considered when determining if these drugs would be suitable for patients with COPD. As neratinib showed the most efficacy in the acute lung inflammation mouse model, it may be that ErbB inhibitor treatment in COPD is reserved for those experiencing exacerbations, rather than as a long-term treatment option. Exacerbations are associated with an influx of neutrophils to the lungs, and being able to induce neutrophil apoptosis could potentially reduce the severity, or duration, of these exacerbations. Avoiding long-term use of ErbB inhibitors would also prevent the prolongation of adverse effects that many patients taking ErbB inhibitors experience. Of course these hypotheses would require further testing in pre-clinical models, followed by clinical trials, to determine whether neratinib or another ErbB inhibitor would be beneficial in this scenario. Repeating the mouse model of acute lung inflammation, but with daily dosing of neratinib and potentially after the onset of inflammation, would be a good model for COPD exacerbations and the way patients could take these drugs to treat them.

Another aspect to consider is the formulation of the ErbB inhibitor. The small-molecule ErbB inhibitors developed for cancer treatment are able to cross cell membranes, and are given as a tablet to be taken orally. Due to their efficacy in treating lung cancer, it is known that they reach the lungs at sufficient concentrations to have therapeutic benefit. To deliver these drugs to the inflamed lungs of patients

with COPD, an inhaled or nebulised version of the drug may be more suitable. A clinical trial of an inhaled antagonist of EGFR (BIBW 2948) showed a dose-related inhibition of EGFR internalisation (reflecting reduced activation of the receptor) in bronchial epithelial cells from patients (Woodruff *et al.*, 2010). The primary outcome of this study was to assess whether this inhibitor could reduce mucus production in the airways of patients with COPD, and although no differences were found between the treatment and control groups, it does demonstrate that a reduction in ErbB signalling in the lungs can be achieved using an inhaled formulation of an ErbB inhibitor.

6.4   Which pathways are ErbB inhibitors blocking to induce neutrophil apoptosis?

The third aim of this thesis was to investigate the signalling pathways that neratinib may be blocking in human neutrophils to induce apoptosis. Although these were not fully elucidated by experiments within this thesis, the results suggest it was not the conventional ErbB signalling pathways described in the literature that were being inhibited by neratinib. It is therefore interesting that in the zebrafish larvae, knockdown of *egfra* and *erbb2*, the family members targeted by neratinib, induces the same increase in apoptosis and reduction in neutrophilic inflammation as the treatment with pharmacological ErbB inhibitors. As the transient CRISPR/Cas9-induced mutation of *egfra* and *erbb2* in these experiments was throughout the whole body of zebrafish larvae, and not specific to neutrophils, the results are less comparable. It would be interesting to use a neutrophil-specific mutation of these genes in the zebrafish larvae to determine whether the same phenotype was observed. The zebrafish could also be used as a model to further validate the results of the phosphoproteomics analysis, if time permitted, by mutating candidates from the phosphoproteomics dataset such as NPM1, and observing whether a similar reduction in neutrophilic inflammation and upregulation of apoptosis was observed. Neutrophil-specific knock-down would be particularly useful for these experiments.

6.5   Are ErbB inhibitors affecting neutrophil migration?

Neutrophil numbers across the whole body of zebrafish larvae were unchanged with ErbB inhibitor treatment, and neutrophil numbers at the site of injury were decreased at both 4 hours post injury (the migration phase of neutrophil recruitment) and 8 hours post injury (the resolution phase), suggesting ErbB inhibitors are supressing neutrophil migration. This is likely, at least partially, due to the upregulation of apoptosis, but other pathways may also be affected. Interestingly pathways

involved in the regulation of migration, specifically the Rho GTPases, were also identified as being supressed in human neutrophils treated with neratinib. ErbBs are known to regulate migration, with research demonstrating that overamplification of ErbB receptors on tumour cells can induce epithelial-mesenchymal transition (leading to metastasis), migration, and tumour invasion (Appert-Collin *et al.*, 2015). Neratinib specifically was shown to reduce the migration of gastric adenocarcinoma cells *in vitro* (Hamzehlou *et al.*, 2019). If ErbB inhibition were reducing neutrophil migration, this would likely be beneficial to patients with COPD, as reducing neutrophil influx into the lungs would possibly reduce further tissue damage. Assessing immune cell migration however is much more difficult in mammals *in vivo* than it is in the transparent zebrafish larvae or neutrophils *in vitro*. If *in vitro* models were used however, co-culture systems could be utilised that incorporate endothelial or epithelial cells, alongside neutrophils or macrophages, to determine if the production of chemokines by the former cell types are affected by ErbB inhibitors. Carrying out these experiments in hypoxic conditions would model an additional characteristic of COPD.

6.6   Future work

If this work were to be continued, a number of different directions could be taken to determine whether ErbB inhibitors might be beneficial for patients with COPD, and also the mechanisms by which this efficacy occurs. As described in 6.2, investigating whether ErbB inhibitor treatment impacts the clearance of pathogens would be a priority, as people with COPD are already more susceptible to respiratory infections. The impact of neratinib on individual cell types in the lung could be analysed using single-cell RNA sequencing of homogenised lung tissue from mouse studies. This could identify global changes in gene expression across the whole lung, as well as in individual cells or tissues such as infiltrating immune cells or the respiratory epithelium. If this work generated sufficient data for clinical trials, using this technique on bronchoalveolar lavage fluid or bronchial brush biopsies from people with COPD would similarly generate an enormous amount of directly clinically relevant data. This could be used alongside techniques such as flow cytometry identifying the phenotypes of neutrophils and macrophages in the lungs, to determine if ErbB inhibitors induce class switching, or result in a shift towards more immature neutrophils being released from the bone marrow to sustain the influx to the lungs. Repeating the phosphoproteomics experiments detailed in this thesis, but with neratinib-treated neutrophils from patients with COPD would add an additional translational aspect to the data, and using isobaric tags to multiplex the samples would allow the dataset to be analysed in a much more quantitative manner.

6.7 Conclusions

Determining the precise signalling pathways and mechanisms of action of ErbB inhibitors will not ultimately affect whether they are beneficial for patients with COPD. This research does however deepen our understanding of why inhibiting ErbB signalling induces the particular phenotypes observed in these experiments, primarily increased apoptosis and potentially reduced migration. This is important because future research may show that ErbB inhibitors are not a suitable treatment for patients with COPD, but another kinase within the pathways regulating neutrophil apoptosis may be a more efficacious target. Similarly, the results from this thesis indicating that neratinib may not be suitable for treating chronic lung inflammation are important, as future research, if it occurs, can focus instead on the use of neratinib where it may be beneficial, such as during acute exacerbations of the disease. Overall this research has demonstrated the ability of ErbB inhibitors to induce neutrophil apoptosis and reduce inflammation in both *in vitro* and *in vivo* models, giving additional evidence to support the prospect of these drugs for repurposing, and in particular narrowing down the inflammatory context in which they may have therapeutic potential.

7 References

Adams, R. A. *et al.* (2016) 'FOCUS4-D: Results from a randomised, placebo controlled trial (RCT) of AZD8931 (an inhibitor of signalling by HER1, 2, and 3) in patients (pts) with advanced or metastatic colorectal cancer (aCRC) in tumours that are wildtype (wt) for BRAF, PIK3CA, KRAS &', *Annals of Oncology*, 27(6), p. vi168. doi: 10.1093/annonc/mdw370.57.

Afonso, P. V *et al.* (2012) 'LTB4 is a signal-relay molecule during neutrophil chemotaxis', *Developmental cell*. 2012/04/26, 22(5), pp. 1079–1091. doi: 10.1016/j.devcel.2012.02.003.

Agustí, A. *et al.* (2003) 'Hypothesis: Does COPD have an autoimmune component?', *Thorax*, 58(10), pp. 832 LP – 834. doi: 10.1136/thorax.58.10.832.

Ahmad, Z. K. *et al.* (2011) 'ErbB Expression, Activation, and Inhibition With Lapatinib and Tyrphostin (AG825) in Human Vestibular Schwannomas', *Otology & Neurotology*, 32(5), pp. 841–847. doi: 10.1097/MAO.0b013e31821f7d88.

Almansa, R. *et al.* (2012) 'Critical COPD respiratory illness is linked to increased transcriptomic activity of neutrophil proteases genes', *BMC research notes*, 5, p. 401. doi: 10.1186/1756-0500-5-401.

Alvarenga, D. M. *et al.* (2018) 'Paradoxical Role of Matrix Metalloproteinases in Liver Injury and Regeneration after Sterile Acute Hepatic Failure', *Cells*, 7(12), pp. 247–263. doi: 10.3390/cells7120247.

Amarante-Mendes, G. P. *et al.* (2018) 'Pattern Recognition Receptors and the Host Cell Death Molecular Machinery', *Frontiers in Immunology*, 9, p. 2379. doi: 10.3389/fimmu.2018.02379.

Amatschek, S. *et al.* (2011) 'CXCL9 induces chemotaxis, chemorepulsion and endothelial barrier disruption through CXCR3-mediated activation of melanoma cells', *British Journal of Cancer*, 104(3), pp. 469–479. doi: 10.1038/sj.bjc.6606056.

An, X. *et al.* (2019) 'Protective effect of oxytocin on LPS-induced acute lung injury in mice', *Scientific Reports*, 9(1), p. 2836. doi: 10.1038/s41598-019-39349-1.

Andrianifahanana, M. *et al.* (2013) 'Profibrotic TGFβ responses require the cooperative action of PDGF and ErbB receptor tyrosine kinases', *The FASEB Journal*, 27(11), pp. 4444–4454. doi: https://doi.org/10.1096/fj.12-224907.

Appert-Collin, A. *et al.* (2015) 'Role of ErbB Receptors in Cancer Cell Migration and Invasion', *Frontiers in pharmacology*, 6, p. 283. doi: 10.3389/fphar.2015.00283.

Araya, T. *et al.* (2013) 'Successful treatment with erlotinib of severe neutropenia induced by gefitinib

in a patient with advanced non-small cell lung cancer', *Lung Cancer*, 80(3), pp. 344–346. doi: 10.1016/j.lungcan.2013.02.014.

Asehnoune, K. *et al.* (2004) 'Involvement of Reactive Oxygen Species in Toll-Like Receptor 4-Dependent Activation of NF-κB', *The Journal of Immunology*, 172(4), pp. 2522 LP – 2529. doi: 10.4049/jimmunol.172.4.2522.

Auner, H. W. *et al.* (2010) 'The life span of short-lived plasma cells is partly determined by a block on activation of apoptotic caspases acting in combination with endoplasmic reticulum stress', *Blood*, 116(18), pp. 3445–3455. doi: 10.1182/blood-2009-10-250423.

Ballesteros, I. *et al.* (2020) 'Co-option of Neutrophil Fates by Tissue Environments.', *Cell*, 183(5), pp. 1282-1297.e18. doi: 10.1016/j.cell.2020.10.003.

Bang, Y.-J. *et al.* (2010) 'Trastuzumab in combination with chemotherapy versus chemotherapy alone for treatment of HER2-positive advanced gastric or gastro-oesophageal junction cancer (ToGA): a phase 3, open-label, randomised controlled trial', *The Lancet*, 376(9742), pp. 687–697. doi: 10.1016/S0140-6736(10)61121-X.

Barceló, B. *et al.* (2008) 'Phenotypic characterisation of T-lymphocytes in COPD: abnormal CD4+CD25+ regulatory T-lymphocyte response to tobacco smoking.', *The European respiratory journal*, 31(3), pp. 555–562. doi: 10.1183/09031936.00010407.

Barnes, P. J. *et al.* (2015) 'Chronic obstructive pulmonary disease', *Nature Reviews Disease Primers*, 1(1), p. 15076. doi: 10.1038/nrdp.2015.76.

Barnes, P. J. (2019) 'Small airway fibrosis in COPD', *The International Journal of Biochemistry & Cell Biology*, 116, p. 105598. doi: https://doi.org/10.1016/j.biocel.2019.105598.

Barnes, P. J. and Celli, B. R. (2009) 'Systemic manifestations and comorbidities of COPD', *European Respiratory Journal*, 33(5), pp. 1165–1185. doi: 10.1183/09031936.00128008.

Bauernfeind, A. L. and Babbitt, C. C. (2017) 'The predictive nature of transcript expression levels on protein expression in adult human brain', *BMC Genomics*, 18(1), p. 322. doi: 10.1186/s12864-017-3674-x.

Becker, S. *et al.* (1994) 'Constitutive and stimulated MCP-1, GRO alpha, beta, and gamma expression in human airway epithelium and bronchoalveolar macrophages.', *The American journal of physiology*, 266(3 Pt 1), pp. L278-86. doi: 10.1152/ajplung.1994.266.3.L278.

Beffagna, G. (2019) 'Zebrafish as a Smart Model to Understand Regeneration After Heart Injury: How

Fish Could Help Humans', *Frontiers in Cardiovascular Medicine*, 6. doi: 10.3389/fcvm.2019.00107.

Bekes, E. M. *et al.* (2011) 'Tumor-recruited neutrophils and neutrophil TIMP-free MMP-9 regulate coordinately the levels of tumor angiogenesis and efficiency of malignant cell intravasation', *The American journal of pathology*. 2011/07/08, 179(3), pp. 1455–1470. doi: 10.1016/j.ajpath.2011.05.031.

Belda, J. *et al.* (2000) 'Induced sputum cell counts in healthy adults.', *American journal of respiratory and critical care medicine*, 161(2 Pt 1), pp. 475–478. doi: 10.1164/ajrccm.161.2.9903097.

van den Berg, R. A. *et al.* (2006) 'Centering, scaling, and transformations: improving the biological information content of metabolomics data.', *BMC genomics*, 7, p. 142. doi: 10.1186/1471-2164-7-142.

Berk, J. L. *et al.* (2005) 'Hypoxia suppresses elastin repair by rat lung fibroblasts', *American Journal of Physiology-Lung Cellular and Molecular Physiology*, 289(6), pp. L931–L936. doi: 10.1152/ajplung.00037.2005.

Bertrand, J. Y. *et al.* (2007) 'Definitive hematopoiesis initiates through a committed erythromyeloid progenitor in the zebrafish embryo', *Development*, 134(23), pp. 4147–4156. doi: 10.1242/dev.012385.

Bhat, T. A. *et al.* (2015) 'Immune Dysfunction in Patients with Chronic Obstructive Pulmonary Disease', *Annals of the American Thoracic Society*, 12 Suppl 2(Suppl 2), pp. S169–S175. doi: 10.1513/AnnalsATS.201503-126AW.

Bhullar, K. S. *et al.* (2018) 'Kinase-targeted cancer therapies: progress, challenges and future directions', *Molecular Cancer*, 17, p. 20. doi: 10.1186/s12943-018-0804-2.

Blagoev, B. *et al.* (2004) 'Temporal analysis of phosphotyrosine-dependent signaling networks by quantitative proteomics', *Nature Biotechnology*, 22(9), pp. 1139–1145. doi: 10.1038/nbt1005.

Boada-Romero, E. *et al.* (2020) 'The clearance of dead cells by efferocytosis', *Nature reviews. Molecular cell biology*. 2020/04/06, 21(7), pp. 398–414. doi: 10.1038/s41580-020-0232-1.

Boehrer, S. *et al.* (2008) 'Erlotinib and gefitinib for the treatment of myelodysplastic syndrome and acute myeloid leukemia: A preclinical comparison', *Biochemical Pharmacology*, 76(11), pp. 1417–1425. doi: 10.1016/j.bcp.2008.05.024.

Bose, P. and Verstovsek, S. (2017) 'JAK2 inhibitors for myeloproliferative neoplasms: what is next?', *Blood*, 130(2), pp. 115–125. doi: 10.1182/blood-2017-04-742288.

Bosmann, M. and Ward, P. A. (2014) 'Protein-based therapies for acute lung injury: targeting

neutrophil extracellular traps', *Expert Opinion on Therapeutic Targets*, 18(6), pp. 703–714. doi: 10.1517/14728222.2014.902938.

Bradford, E. *et al.* (2017) 'The value of blood cytokines and chemokines in assessing COPD', *Respiratory research*, 18(1), p. 180. doi: 10.1186/s12931-017-0662-2.

Branzk, N. *et al.* (2014) 'Neutrophils sense microbe size and selectively release neutrophil extracellular traps in response to large pathogens.', *Nature immunology*, 15(11), pp. 1017–1025. doi: 10.1038/ni.2987.

Breen, M. E. and Soellner, M. B. (2015) '6 Small Molecule Substrate Phosphorylation Site Inhibitors of Protein Kinases: Approaches and Challenges', *Acs Chemical Biology*, 10(1), pp. 175–189. doi: 10.1021/cb5008376.

Britsch, S. *et al.* (1998) 'The ErbB2 and ErbB3 receptors and their ligand, neuregulin-1, are essential for development of the sympathetic nervous system', *Genes & Development*, 12(12), pp. 1825–1836. doi: 10.1101/gad.12.12.1825.

Brostjan, C. and Oehler, R. (2020) 'The role of neutrophil death in chronic inflammation and cancer', *Cell Death Discovery*, 6(1), p. 26. doi: 10.1038/s41420-020-0255-6.

Brown, D. M. *et al.* (2004) 'Calcium and ROS-mediated activation of transcription factors and TNF-alpha cytokine gene expression in macrophages exposed to ultrafine particles', *American Journal of Physiology-Lung Cellular and Molecular Physiology*, 286(2), pp. L344–L353. doi: 10.1152/ajplung.00139.2003.

Brown, V. *et al.* (2009) 'Dysregulated apoptosis and NF kappa B expression in COPD subjects', *Respiratory Research*, 10, p. 12. doi: 10.1186/1465-9921-10-24.

Brusselle, G. G. *et al.* (2009) 'Lymphoid follicles in (very) severe COPD: beneficial or harmful?', *European Respiratory Journal*, 34(1), pp. 219 LP – 230. doi: 10.1183/09031936.00150208.

Buckley, C. D. *et al.* (2006) 'Identification of a phenotypically and functionally distinct population of long-lived neutrophils in a model of reverse endothelial migration', *Journal of Leukocyte Biology*, 79(2), pp. 303–311. doi: https://doi.org/10.1189/jlb.0905496.

Burger, A. *et al.* (2016) 'Maximizing mutagenesis with solubilized CRISPR-Cas9 ribonucleoprotein complexes', *Development*, 143(11), pp. 2025–2037. doi: 10.1242/dev.134809.

Burggren, W. and Pelster, B. (1995) 'Disruption of Hb-O-2 transport does not diminish O-2-dependent physiological processes in developing embryos of the zebrafish (Brachydanio rerio)', *American*

Zoologist, 35(5), p. 35A. Available at: %3CGo.

Butler, A., Walton, G. M. and Sapey, E. (2018) 'Neutrophilic Inflammation in the Pathogenesis of Chronic Obstructive Pulmonary Disease', *Copd*, pp. 1–13. doi: 10.1080/15412555.2018.1476475.

Calverley, P. M. A. *et al.* (2017) 'A randomised, placebo-controlled trial of anti-interleukin-1 receptor 1 monoclonal antibody MEDI8968 in chronic obstructive pulmonary disease', *Respiratory Research*, 18, p. 12. doi: 10.1186/s12931-017-0633-7.

Canfield, K. *et al.* (2015) 'Receptor tyrosine kinase ERBB4 mediates acquired resistance to ERBB2 inhibitors in breast cancer cells (vol 14, pg 648, 2015)', *Cell Cycle*, 14(8), pp. 1339–1341. doi: 10.1080/15384101.2015.1029377.

Cano, R. L. E. and Lopera, H. D. E. (2013) 'Introduction to T and B lymphocytes', in *Autoimmunity: From Bench to Bedside*. Bogota, Colombia: El Rosario University Press.

Canonici, A. *et al.* (2013) 'Neratinib overcomes trastuzumab resistance in HER2 amplified breast cancer', *Oncotarget*, 4(10), pp. 1592–1605. doi: 10.18632/oncotarget.1148.

Capucetti, A., Albano, F. and Bonecchi, R. (2020) 'Multiple Roles for Chemokines in Neutrophil Biology', *Frontiers in Immunology*, 11, p. 1259. doi: 10.3389/fimmu.2020.01259.

Castro-Alcaraz, S. *et al.* (2002) 'NF-kappa B regulation in human neutrophils by nuclear I kappa B alpha: correlation to apoptosis.', *Journal of immunology (Baltimore, Md. : 1950)*, 169(7), pp. 3947–3953. doi: 10.4049/jimmunol.169.7.3947.

Chan, A. *et al.* (2021) 'Final Efficacy Results of Neratinib in HER2-positive Hormone Receptor-positive Early-stage Breast Cancer From the Phase III ExteNET Trial', *Clinical Breast Cancer*, 21(1), pp. 80-91.e7. doi: https://doi.org/10.1016/j.clbc.2020.09.014.

Chatterjee, A. *et al.* (2015) 'Genome-wide DNA methylation map of human neutrophils reveals widespread inter-individual epigenetic variation', *Scientific reports*, 5, p. 17328. doi: 10.1038/srep17328.

Chen, L. *et al.* (2017) 'Inflammatory responses and inflammation-associated diseases in organs', *Oncotarget*, 9(6), pp. 7204–7218. doi: 10.18632/oncotarget.23208.

Chen, Z. H. *et al.* (2008) 'Egr-1 Regulates Autophagy in Cigarette Smoke-Induced Chronic Obstructive Pulmonary Disease', *Plos One*, 3(10), p. 13. doi: 10.1371/journal.pone.0003316.

Chilà, G. *et al.* (2021) 'The Clinical Efficacy and Safety of Neratinib in Combination with Capecitabine for the Treatment of Adult Patients with Advanced or Metastatic HER2-Positive Breast Cancer', *Drug*

design, development and therapy, 15, pp. 2711–2720. doi: 10.2147/DDDT.S281599.

Cho, J. H. *et al.* (2010) 'The Effect of Gefitinib on Immune Response of Human Peripheral Blood Monocyte-Derived Dendritic Cells', *Tuberculosis and Respiratory Diseases*, 69(6), pp. 456–464. Available at: %3CGo.

Christoffersson, G. *et al.* (2012) 'VEGF-A recruits a proangiogenic MMP-9-delivering neutrophil subset that induces angiogenesis in transplanted hypoxic tissue', *Blood*. 2012/09/10, 120(23), pp. 4653–4662. doi: 10.1182/blood-2012-04-421040.

Churg, A. *et al.* (2004) 'Tumor necrosis factor-alpha drives 70% of cigarette smoke-induced emphysema in the mouse', *American Journal of Respiratory and Critical Care Medicine*, 170(5), pp. 492–498. doi: 10.1164/rccm.200404-5110C.

Churg, A., Zhou, S. and Wright, J. L. (2012) 'Matrix metalloproteinases in COPD', *European Respiratory Journal*, 39(1), pp. 197–209. doi: 10.1183/09031936.00121611.

Ciano, M., Mantellato, G., *et al.* (2019) 'EGF receptor (EGFR) inhibition promotes a slow-twitch oxidative, over a fast-twitch, muscle phenotype', *Scientific reports*, 9(1), p. 9218. doi: 10.1038/s41598-019-45567-4.

Ciano, M., Kemp, P. R., *et al.* (2019) 'Haploinsufficient maternal effect of Epidermal Growth Factor Receptor A mutation in zebrafish', *bioRxiv*, p. 745018. doi: 10.1101/745018.

Ciardiello, F. *et al.* (2001) 'Inhibition of growth factor production and angiogenesis in human cancer cells by ZD1839 (Iressa), a selective epidermal growth factor receptor tyrosine kinase inhibitor', *Clinical Cancer Research*, 7(5), pp. 1459–1465. Available at: %3CGo.

Clayton, N. S. and Ridley, A. J. (2020) 'Targeting Rho GTPase Signaling Networks in Cancer ', *Frontiers in Cell and Developmental Biology* , p. 222. Available at: https://www.frontiersin.org/article/10.3389/fcell.2020.00222.

Coffelt, S. B. *et al.* (2015) 'IL-17-producing γδ T cells and neutrophils conspire to promote breast cancer metastasis.', *Nature*, 522(7556), pp. 345–348. doi: 10.1038/nature14282.

Cornet, C., Di Donato, V. and Terriente, J. (2018) 'Combining Zebrafish and CRISPR/Cas9: Toward a More Efficient Drug Discovery Pipeline', *Frontiers in Pharmacology*, 9, p. 11. doi: 10.3389/fphar.2018.00703.

Cowland, J. B. and Borregaard, N. (2016) 'Granulopoiesis and granules of human neutrophils.', *Immunological reviews*, 273(1), pp. 11–28. doi: 10.1111/imr.12440.

Craig, J. M., Scott, A. L. and Mitzner, W. (2017) 'Immune-mediated inflammation in the pathogenesis of emphysema: insights from mouse models', *Cell and tissue research*. 2017/02/06, 367(3), pp. 591–605. doi: 10.1007/s00441-016-2567-7.

Croker, B. A. *et al.* (2011) 'Fas-mediated neutrophil apoptosis is accelerated by Bid, Bak, and Bax and inhibited by Bcl-2 and Mcl-1', *Proceedings of the National Academy of Sciences*, 108(32), pp. 13135 LP – 13140. doi: 10.1073/pnas.1110358108.

da Cruz Nizer, W. S., Inkovskiy, V. and Overhage, J. (2020) 'Surviving Reactive Chlorine Stress: Responses of Gram-Negative Bacteria to Hypochlorous Acid', *Microorganisms*, 8(8), p. 1220. doi: 10.3390/microorganisms8081220.

Dahlhoff, M. *et al.* (2017) 'CRISPR-assisted receptor deletion reveals distinct roles for ERBB2 and ERBB3 in skin keratinocytes', *Febs Journal*, 284(19), pp. 3339–3349. doi: 10.1111/febs.14196.

Daniel, C. *et al.* (2019) 'Extracellular DNA traps in inflammation, injury and healing', *Nature Reviews Nephrology*, 15(9), pp. 559–575. doi: 10.1038/s41581-019-0163-2.

Davidson, W. J., The, S. and Leigh, R. (2013) 'Establishing a normal range for induced sputum cell counts in Western Canada', *Canadian respiratory journal*. 2013/09/30, 20(6), pp. 424–425. doi: 10.1155/2013/547309.

Day, A., Barnes, P. and Donnelly, L. (2014) 'Elevated GM-CSF in COPD may drive defective macrophage phenotype', *European Respiratory Journal*, 44, p. 4. Available at: %3CGo.

Denburg, J. A. (1998) 'The origins of basophils and eosinophils in allergic inflammation', *Journal of Allergy and Clinical Immunology*, 102(5), pp. S74–S76. doi: 10.1016/S0091-6749(98)70034-X.

Deng, Y. *et al.* (2018) 'An in vitro transepithelial migration assay to evaluate the role of neutrophils in Respiratory Syncytial Virus (RSV) induced epithelial damage', *Scientific Reports*, 8(1), p. 6777. doi: 10.1038/s41598-018-25167-4.

Derouet, M. *et al.* (2004) 'Granulocyte macrophage colony-stimulating factor signaling and proteasome inhibition delay neutrophil apoptosis by increasing the stability of Mcl-1.', *The Journal of biological chemistry*, 279(26), pp. 26915–26921. doi: 10.1074/jbc.M313875200.

Devos, F. C. *et al.* (2017) 'Forced expiration measurements in mouse models of obstructive and restrictive lung diseases', *Respiratory Research*, 18(1), p. 123. doi: 10.1186/s12931-017-0610-1.

Dhanasekaran, D. N. and Reddy, E. P. (2008) 'JNK signaling in apoptosis', *Oncogene*, 27(48), pp. 6245–6251. doi: 10.1038/onc.2008.301.

Dicker, A. J. *et al.* (2018) 'Neutrophil extracellular traps are associated with disease severity and microbiota diversity in patients with chronic obstructive pulmonary disease.', *The Journal of allergy and clinical immunology*, 141(1), pp. 117–127. doi: 10.1016/j.jaci.2017.04.022.

Doeing, D. C., Borowicz, J. L. and Crockett, E. T. (2003) 'Gender dimorphism in differential peripheral blood leukocyte counts in mice using cardiac, tail, foot, and saphenous vein puncture methods.', *BMC clinical pathology*, 3(1), p. 3. doi: 10.1186/1472-6890-3-3.

Donadieu, J. *et al.* (2011) 'Congenital neutropenia: diagnosis, molecular bases and patient management', *Orphanet Journal of Rare Diseases*, 6(1), p. 26. doi: 10.1186/1750-1172-6-26.

Donaldson, G. C. *et al.* (2005) 'Airway and systemic inflammation and decline in lung function in patients with COPD', *Chest*, 128(4), pp. 1995–2004. doi: 10.1378/chest.128.4.1995.

Dong, J. *et al.* (2018) 'Ribosomal Protein S3 Gene Silencing Protects Against Cigarette Smoke-Induced Acute Lung Injury', *Molecular Therapy. Nucleic Acids*, 12, pp. 370–380. doi: 10.1016/j.omtn.2018.05.027.

Doukas, J. *et al.* (2009) 'Aerosolized Phosphoinositide 3-Kinase gamma/delta Inhibitor TG100-115 3-2,4-Diamino-6-(3-hydroxyphenyl)pteridin-7-yl phenol as a Therapeutic Candidate for Asthma and Chronic Obstructive Pulmonary Disease', *Journal of Pharmacology and Experimental Therapeutics*, 328(3), pp. 758–765. doi: 10.1124/jpet.108.144311.

Du, W. *et al.* (2010) 'NPM phosphorylation stimulates Cdk1, overrides G2/M checkpoint and increases leukemic blasts in mice', *Carcinogenesis*. 2009/11/23, 31(2), pp. 302–310. doi: 10.1093/carcin/bgp270.

Du, X. *et al.* (2004) 'Velvet, a Dominant Egfr Mutation That Causes Wavy Hair and Defective Eyelid Development in Mice', *Genetics*, 166(1), pp. 331–340. doi: 10.1534/genetics.166.1.331.

Dunn, J. L. M. *et al.* (2018) 'Blocking CXCL1-dependent neutrophil recruitment prevents immune damage and reduces pulmonary bacterial infection after inhalation injury', *American Journal of Physiology-Lung Cellular and Molecular Physiology*, 314(5), pp. L822–L834. doi: 10.1152/ajplung.00272.2017.

Dupont, P. J. and Warrens, A. N. (2007) 'Fas ligand exerts its pro-inflammatory effects via neutrophil recruitment but not activation', *Immunology*, 120(1), pp. 133–139. doi: 10.1111/j.1365-2567.2006.02504.x.

Duthie, M. S. *et al.* (2007) 'Parasite-induced chronic inflammation is not exacerbated by immunotherapy before or during Trypanosoma cruzi Infection.', *Clinical and vaccine immunology :*

CVI, 14(8), pp. 1005–1012. doi: 10.1128/CVI.00087-07.

van Eerd, E. A. M. *et al.* (2016) 'Smoking cessation for people with chronic obstructive pulmonary disease', *Cochrane Database of Systematic Reviews*, (8), p. 93. doi: 10.1002/14651858.CD010744.pub2.

van Eerd, E. A. M. *et al.* (2017) 'Predictors of long-term smoking cessation in patients with COPD: results from a randomised controlled trial', *European Respiratory Journal*, 49(6), p. 1700561. doi: 10.1183/13993003.00561-2017.

El-Brolosy, M. A. *et al.* (2019) 'Genetic compensation triggered by mutant mRNA degradation', *NATURE*, 568(7751), p. 193+. doi: 10.1038/s41586-019-1064-z.

Elliott, M. R., Koster, K. M. and Murphy, P. S. (2017) 'Efferocytosis Signaling in the Regulation of Macrophage Inflammatory Responses', *The Journal of Immunology*, 198(4), pp. 1387 LP – 1394. doi: 10.4049/jimmunol.1601520.

European Medicines Agency (2018a) *Nerlynx : EPAR - Product Information*. Available at: https://www.ema.europa.eu/en/medicines/human/EPAR/nerlynx.

European Medicines Agency (2018b) *Nerlynx : EPAR - Public Assessment Report*. Available at: https://www.ema.europa.eu/en/medicines/human/EPAR/nerlynx#product-information-section.

Fabregat, A. *et al.* (2017) 'Reactome pathway analysis: a high-performance in-memory approach.', *BMC bioinformatics*, 18(1), p. 142. doi: 10.1186/s12859-017-1559-2.

Fadok, V. A. *et al.* (1998) 'The role of phosphatidylserine in recognition of apoptotic cells by phagocytes', *Cell Death & Differentiation*, 5(7), pp. 551–562. doi: 10.1038/sj.cdd.4400404.

Fahy, W. A. *et al.* (2021) 'Nemiralisib in Patients with an Acute Exacerbation of COPD: Placebo-Controlled, Dose-Ranging Study.', *International journal of chronic obstructive pulmonary disease*, 16, pp. 1637–1646. doi: 10.2147/COPD.S309320.

Feghali-Bostwick, C. A. *et al.* (2008) 'Autoantibodies in patients with chronic obstructive pulmonary disease', *American Journal of Respiratory and Critical Care Medicine*, 177(2), pp. 156–163. doi: 10.1164/rccm.200701-014OC.

Fialkow, L. *et al.* (2006) 'Neutrophil apoptosis: a marker of disease severity in sepsis and sepsis-induced acute respiratory distress syndrome', *Critical Care*, 10(6), p. 14. doi: 10.1186/cc5090.

Fichter, C. D. *et al.* (2014) 'ErbB targeting inhibitors repress cell migration of esophageal squamous cell carcinoma and adenocarcinoma cells by distinct signaling pathways', *Journal of Molecular*

Medicine-Jmm, 92(11), pp. 1209–1223. doi: 10.1007/s00109-014-1187-5.

De Filippo, K. and Rankin, S. M. (2018) 'CXCR4, the master regulator of neutrophil trafficking in homeostasis and disease', *European Journal of Clinical Investigation*, 48(S2), p. e12949. doi: https://doi.org/10.1111/eci.12949.

Fock, V. *et al.* (2015) 'Neuregulin-1-mediated ErbB2-ErbB3 signalling protects human trophoblasts against apoptosis to preserve differentiation', *Journal of Cell Science*, 128(23), pp. 4306–4316. doi: 10.1242/jcs.176933.

Fortin, C. F. *et al.* (2007) 'GM-CSF activates the Jak/STAT pathway to rescue polymorphonuclear neutrophils from spontaneous apoptosis in young but not elderly individuals', 8(2), pp. 173–187. doi: 10.1007/s10522-006-9067-1.

Foster, J. G. *et al.* (2012) 'Inhibition of PI3K Signaling Spurs New Therapeutic Opportunities in Inflammatory/Autoimmune Diseases and Hematological Malignancies', *Pharmacological Reviews*, 64(4), pp. 1027–1054. doi: 10.1124/pr.110.004051.

Fox, S. *et al.* (2010) 'Neutrophil apoptosis: relevance to the innate immune response and inflammatory disease', *Journal of innate immunity*. 2010/02/11, 2(3), pp. 216–227. doi: 10.1159/000284367.

Freeman, C. M. *et al.* (2010) 'Cytotoxic potential of lung CD8(+) T cells increases with chronic obstructive pulmonary disease severity and with in vitro stimulation by IL-18 or IL-15', *Journal of immunology (Baltimore, Md. : 1950)*. 2010/04/28, 184(11), pp. 6504–6513. doi: 10.4049/jimmunol.1000006.

Freeman, C. M., Curtis, J. L. and Chensue, S. W. (2007) 'CC chemokine receptor 5 and CXC chemokine receptor 6 expression by lung CD8+ cells correlates with chronic obstructive pulmonary disease severity.', *The American journal of pathology*, 171(3), pp. 767–776. doi: 10.2353/ajpath.2007.061177.

Fung-Leung, W.-P. (2011) 'Phosphoinositide 3-kinase delta (PI3Kδ) in leukocyte signaling and function', *Cellular Signalling*, 23(4), pp. 603–608. doi: https://doi.org/10.1016/j.cellsig.2010.10.002.

Furman, D. *et al.* (2019) 'Chronic inflammation in the etiology of disease across the life span', *Nature medicine*. 2019/12/05, 25(12), pp. 1822–1832. doi: 10.1038/s41591-019-0675-0.

Gadgil, A. and Duncan, S. R. (2008) 'Role of T-lymphocytes and pro-inflammatory mediators in the pathogenesis of chronic obstructive pulmonary disease', *International journal of chronic obstructive pulmonary disease*, 3(4), pp. 531–541. doi: 10.2147/copd.s1759.

Gahring, L. C. *et al.* (2017) 'Lung epithelial response to cigarette smoke and modulation by the nicotinic

alpha 7 receptor', *PLoS ONE*, 12.

Galbán, C. J. *et al.* (2012) 'Computed tomography–based biomarker provides unique signature for diagnosis of COPD phenotypes and disease progression', *Nature Medicine*, 18(11), pp. 1711–1715. doi: 10.1038/nm.2971.

Ganesan, S. *et al.* (2012) 'Elastase/LPS-Exposed Mice Exhibit Impaired Innate Immune Responses to Bacterial Challenge Role of Scavenger Receptor A', *American Journal of Pathology*, 180(1), pp. 61–72. doi: 10.1016/j.ajpath.2011.09.029.

Ganesan, S. *et al.* (2013) 'Aberrantly activated EGFR contributes to enhanced IL-8 expression in COPD airways epithelial cells via regulation of nuclear FoxO3A', *Thorax*, 68(2), pp. 131 LP – 141. doi: 10.1136/thoraxjnl-2012-201719.

Gao, W. *et al.* (2015) 'Bronchial epithelial cells: The key effector cells in the pathogenesis of chronic obstructive pulmonary disease?', *Respirology*, 20(5), pp. 722–729. doi: 10.1111/resp.12542.

Gassmann, M. *et al.* (1995) 'ABERRANT NEURAL AND CARDIAC DEVELOPMENT IN MICE LACKING THE ERBB4 NEUREGULIN RECEPTOR', *Nature*, 378(6555), pp. 390–394. doi: 10.1038/378390a0.

Geering, B. and Simon, H. U. (2011) 'Peculiarities of cell death mechanisms in neutrophils', *Cell Death and Differentiation*, 18(9), pp. 1457–1469. doi: 10.1038/cdd.2011.75.

Geto, Z. *et al.* (2020) 'Mitochondrial Dynamic Dysfunction as a Main Triggering Factor for Inflammation Associated Chronic Non-Communicable Diseases', *Journal of inflammation research*, 13, pp. 97–107. doi: 10.2147/JIR.S232009.

Ghorani, V. *et al.* (2017) 'Experimental animal models for COPD: a methodological review', *Tobacco Induced Diseases*, 15(1), p. 25. doi: 10.1186/s12971-017-0130-2.

Giltnane, J. M. *et al.* (2009) 'Quantitative Multiplexed Analysis of ErbB Family Coexpression for Primary Breast Cancer Prognosis in a Large Retrospective Cohort', *Cancer*, 115(11), pp. 2400–2409. doi: 10.1002/cncr.24277.

Gindele, J. A. *et al.* (2020) 'Intermittent exposure to whole cigarette smoke alters the differentiation of primary small airway epithelial cells in the air-liquid interface culture', *Scientific Reports*, 10(1), p. 6257. doi: 10.1038/s41598-020-63345-5.

Grainger, S. *et al.* (2019) 'EGFR is required for Wnt9a-Fzd9b signalling specificity in haematopoietic stem cells', *Nature Cell Biology*, 21(6), p. 721. doi: 10.1038/s41556-019-0330-5.

Graus-Porta, D. *et al.* (1997) 'ErbB-2, the preferred heterodimerization partner of all ErbB receptors,

is a mediator of lateral signaling.', *The EMBO journal*, 16(7), pp. 1647–1655. doi: 10.1093/emboj/16.7.1647.

Gray, C. *et al.* (2011) 'Simultaneous intravital imaging of macrophage and neutrophil behaviour during inflammation using a novel transgenic zebrafish', *Thrombosis and Haemostasis*, 105(5), pp. 811–819. doi: 10.1160/th10-08-0525.

Green, S. R. *et al.* (2006) 'The CC chemokine MCP-1 stimulates surface expression of CX3CR1 and enhances the adhesion of monocytes to fractalkine/CX3CL1 via p38 MAPK', *Journal of Immunology*, 176(12), pp. 7412–7420. doi: 10.4049/jimmunol.176.12.7412.

Grespan, R. *et al.* (2008) 'CXCR2-specific chemokines mediate leukotriene B4-dependent recruitment of neutrophils to inflamed joints in mice with antigen-induced arthritis.', *Arthritis and rheumatism*, 58(7), pp. 2030–2040. doi: 10.1002/art.23597.

van Grinsven, E. *et al.* (2018) 'A comprehensive three-dimensional assay to assess neutrophil defense against bacteria', *Journal of Immunological Methods*, 462, pp. 83–90. doi: https://doi.org/10.1016/j.jim.2018.09.001.

Grisendi, S. *et al.* (2006) 'Nucleophosmin and cancer.', *Nature reviews. Cancer*, 6(7), pp. 493–505. doi: 10.1038/nrc1885.

Guo, S. and Dipietro, L. A. (2010) 'Factors affecting wound healing', *Journal of dental research*. 2010/02/05, 89(3), pp. 219–229. doi: 10.1177/0022034509359125.

Guo, Y. *et al.* (2016) 'Neutrophil elastase ameliorates matrix metalloproteinase-9 to promote lipopolysaccharide-induced acute lung injury in mice 1.', *Acta cirurgica brasileira*, 31(6), pp. 382–388. doi: 10.1590/S0102-865020160060000004.

Hamzehlou, S. *et al.* (2019) 'Anti-tumor activity of neratinib, a pan-HER inhibitor, in gastric adenocarcinoma cells', *European Journal of Pharmacology*, 863, p. 172705. doi: https://doi.org/10.1016/j.ejphar.2019.172705.

Hannah, S. *et al.* (1995) 'Hypoxia prolongs neutrophil survival in vitro.', *FEBS letters*, 372(2–3), pp. 233–237. doi: 10.1016/0014-5793(95)00986-j.

Harrington, R., Al Nokhatha, S. A. and Conway, R. (2020) 'JAK Inhibitors in Rheumatoid Arthritis: An Evidence-Based Review on the Emerging Clinical Data', *Journal of inflammation research*, 13, pp. 519–531. doi: 10.2147/JIR.S219586.

Hart, T. *et al.* (2013) 'Finding the active genes in deep RNA-seq gene expression studies', *BMC*

genomics, 14, p. 778. doi: 10.1186/1471-2164-14-778.

Harvie, E. A. and Huttenlocher, A. (2015) 'Neutrophils in host defense: new insights from zebrafish', *Journal of Leukocyte Biology*, 98(4), pp. 523–537. doi: https://doi.org/10.1189/jlb.4MR1114-524R.

Hasenberg, M. *et al.* (2011) 'Rapid immunomagnetic negative enrichment of neutrophil granulocytes from murine bone marrow for functional studies in vitro and in vivo', *PloS one*, 6(2), pp. e17314–e17314. doi: 10.1371/journal.pone.0017314.

Haslett, C. *et al.* (1985) 'MODULATION OF MULTIPLE NEUTROPHIL FUNCTIONS BY PREPARATIVE METHODS OR TRACE CONCENTRATIONS OF BACTERIAL LIPOPOLYSACCHARIDE', *American Journal of Pathology*, 119(1), pp. 101–110. Available at: %3CGo.

Haslett, C. *et al.* (1991) 'Apoptosis (programmed cell death) and functional changes in aging neutrophils. Modulation by inflammatory mediators.', *Chest*, 99(3 Suppl), p. 6S.

Headland, S. E. and Norling, L. V (2015) 'The resolution of inflammation: Principles and challenges', *Seminars in Immunology*, 27(3), pp. 149–160. doi: https://doi.org/10.1016/j.smim.2015.03.014.

Hedström, U. *et al.* (2018) 'Bronchial extracellular matrix from COPD patients induces altered gene expression in repopulated primary human bronchial epithelial cells', *Scientific Reports*, 8(1), p. 3502. doi: 10.1038/s41598-018-21727-w.

Hein, A. L., Ouellette, M. M. and Yan, Y. (2014) 'Radiation-induced signaling pathways that promote cancer cell survival (Review)', *International Journal of Oncology*, 45(5), pp. 1813–1819. doi: 10.3892/ijo.2014.2614.

Henry, K. M. *et al.* (2013) 'Zebrafish as a model for the study of neutrophil biology', *Journal of Leukocyte Biology*, 94(4), pp. 633–642. doi: https://doi.org/10.1189/jlb.1112594.

Herbomel, P., Thisse, B. and Thisse, C. (1999) 'Ontogeny and behaviour of early macrophages in the zebrafish embryo', *Development*, 126(17), pp. 3735 LP – 3745. Available at: http://dev.biologists.org/content/126/17/3735.abstract.

Herbomel, P., Thisse, B. and Thisse, C. (2001) 'Zebrafish Early Macrophages Colonize Cephalic Mesenchyme and Developing Brain, Retina, and Epidermis through a M-CSF Receptor-Dependent Invasive Process', *Developmental Biology*, 238(2), pp. 274–288. doi: https://doi.org/10.1006/dbio.2001.0393.

Herman, K. D., Rahman, A. and Prince, L. R. (2020) 'Isolation and High Throughput Flow Cytometric Apoptosis Assay of Human Neutrophils to Enable Compound Library Screening', *Bio-protocol*, 10(11),

p. e3640. doi: 10.21769/BioProtoc.3640.

Hessel, E. *et al.* (2018) 'Inhaled PI3K delta Inhibitor Nemiralisib Improves Lung Function and Reduces Re-Exacerbations in Exacerbating Chronic Obstructive Pulmonary Disease (COPD) Patients (PII116678)', *American Journal of Respiratory and Critical Care Medicine*, 197, p. 2. Available at: %3CGo.

Hickinson, D. M. *et al.* (2010) 'AZD8931, an Equipotent, Reversible Inhibitor of Signaling by Epidermal Growth Factor Receptor, ERBB2 (HER2), and ERBB3: A Unique Agent for Simultaneous ERBB Receptor Blockade in Cancer', *Clinical Cancer Research*, 16(4), pp. 1159–1169. doi: 10.1158/1078-0432.ccr-09-2353.

Higham, A. *et al.* (2019) 'The pathology of small airways disease in COPD: historical aspects and future directions', *Respiratory Research*, 20(1), p. 49. doi: 10.1186/s12931-019-1017-y.

Ho, J. *et al.* (2017) 'The Role of ErbB Receptors in Infection', *Trends in Microbiology*, 25(11), pp. 942–952. doi: 10.1016/j.tim.2017.04.009.

Hodge, S. *et al.* (2007) 'Smoking alters alveolar macrophage recognition and phagocytic ability: implications in chronic obstructive pulmonary disease.', *American journal of respiratory cell and molecular biology*, 37(6), pp. 748–755. doi: 10.1165/rcmb.2007-0025OC.

Van Hoecke, L. *et al.* (2017) 'Bronchoalveolar Lavage of Murine Lungs to Analyze Inflammatory Cell Infiltration', *Journal of visualized experiments : JoVE*, (123), p. 55398. doi: 10.3791/55398.

Hoenderdos, K. and Condliffe, A. (2013) 'The Neutrophil in Chronic Obstructive Pulmonary Disease Too Little, Too Late or Too Much, Too Soon?', *American Journal of Respiratory Cell and Molecular Biology*, 48(5), pp. 531–539. doi: 10.1165/rcmb.2012-0492TR.

Hoffbrand, A. V. and Steensma, D. P. (2019) *Hoffbrand's Essential Haematology*. 8th edn. John Wiley & Sons, Ltd.

Hogg, J. C. *et al.* (2004) 'The nature of small-airway obstruction in chronic obstructive pulmonary disease', *New England Journal of Medicine*, 350(26), pp. 2645–2653. doi: 10.1056/NEJMoa032158.

Holbro, T. *et al.* (2003) 'The ErbB2/ErbB3 heterodimer functions as an oncogenic unit: ErbB2 requires ErbB3 to drive breast tumor cell proliferation', *Proceedings of the National Academy of Sciences of the United States of America*, 100(15), pp. 8933–8938. doi: 10.1073/pnas.1537685100.

Hoodless, L. J. *et al.* (2016) 'Genetic and pharmacological inhibition of CDK9 drives neutrophil apoptosis to resolve inflammation in zebrafish in vivo', *Scientific Reports*, 6, p. 14. doi:

10.1038/srep36980.

Hoogendijk, A. J. *et al.* (2019) 'Dynamic Transcriptome-Proteome Correlation Networks Reveal Human Myeloid Differentiation and Neutrophil-Specific Programming.', *Cell reports*, 29(8), pp. 2505-2519.e4. doi: 10.1016/j.celrep.2019.10.082.

Hoppenbrouwers, T. *et al.* (2017) 'In vitro induction of NETosis: Comprehensive live imaging comparison and systematic review', *PLOS ONE*, 12(5), p. e0176472. Available at: https://doi.org/10.1371/journal.pone.0176472.

Horiguchi, M. *et al.* (2015) 'Pulmonary administration of phosphoinositide 3-kinase inhibitor is a curative treatment for chronic obstructive pulmonary disease by alveolar regeneration', *Journal of Controlled Release*, 213, pp. 112–119. doi: 10.1016/j.jconrel.2015.07.004.

Howe, K. *et al.* (2013) 'The zebrafish reference genome sequence and its relationship to the human genome', *Nature*, 496(7446), pp. 498–503. doi: 10.1038/nature12111.

Hu, Y. P. *et al.* (2005) 'Reorganization of ErbB family and cell survival signaling after knock-down of ErbB2 in colon cancer cells', *Journal of Biological Chemistry*, 280(29), pp. 27383–27392. doi: 10.1074/jbc.M414238200.

Hussain, A. R. *et al.* (2012) 'Cross-talk between NFkB and the PI3-kinase/AKT pathway can be targeted in primary effusion lymphoma (PEL) cell lines for efficient apoptosis', *PloS one*. 2012/06/29, 7(6), pp. e39945–e39945. doi: 10.1371/journal.pone.0039945.

Hyatt, D. C. and Ceresa, B. P. (2008) 'Cellular localization of the activated EGFR determines its effect on cell growth in MDA-MB-468 cells', *Experimental Cell Research*, 314(18), pp. 3415–3425. doi: 10.1016/j.yexcr.2008.08.020.

Isles, H. M. *et al.* (2019) 'The CXCL12/CXCR4 Signaling Axis Retains Neutrophils at Inflammatory Sites in Zebrafish', *FRONTIERS IN IMMUNOLOGY*, 10. doi: 10.3389/fimmu.2019.01784.

Isles, H. M. *et al.* (2021) 'Pioneer neutrophils release chromatin within in vivo swarms.', *eLife*, 10. doi: 10.7554/eLife.68755.

Jackson, N. M. and Ceresa, B. P. (2017) 'EGFR-mediated apoptosis via STAT3', *Experimental Cell Research*, 356(1), pp. 93–103. doi: 10.1016/j.yexcr.2017.04.016.

Jang, C.-Y., Lee, J. Y. and Kim, J. (2004) 'RpS3, a DNA repair endonuclease and ribosomal protein, is involved in apoptosis.', *FEBS letters*, 560(1–3), pp. 81–85. doi: 10.1016/S0014-5793(04)00074-2.

Jani, J. P. *et al.* (2007) 'Discovery and pharmacologic characterization of CP-724,714, a selective ErbB2

tyrosine kinase inhibitor', *Cancer Research*, 67(20), pp. 9887–9893. doi: 10.1158/0008-5472.can-06-3559.

Jankowitz, R. C. *et al.* (2013) 'Safety and efficacy of neratinib in combination with weekly paclitaxel and trastuzumab in women with metastatic HER2-positive breast cancer: an NSABP Foundation Research Program phase I study', *Cancer Chemotherapy and Pharmacology*, 72(6), pp. 1205–1212. doi: 10.1007/s00280-013-2262-2.

Jao, L. E., Wente, S. R. and Chen, W. B. (2013) 'Efficient multiplex biallelic zebrafish genome editing using a CRISPR nuclease system', *Proceedings of the National Academy of Sciences of the United States of America*, 110(34), pp. 13904–13909. doi: 10.1073/pnas.1308335110.

Jhunjhunwala, S. *et al.* (2015) 'Neutrophil Responses to Sterile Implant Materials', *Plos One*, 10(9), p. 16. doi: 10.1371/journal.pone.0137550.

Jiang, G.-M. *et al.* (2019) 'The relationship between autophagy and the immune system and its applications for tumor immunotherapy', *Molecular Cancer*, 18(1), p. 17. doi: 10.1186/s12943-019-0944-z.

Jiang, K. *et al.* (2015) 'Disease-Associated Single-Nucleotide Polymorphisms From Noncoding Regions in Juvenile Idiopathic Arthritis Are Located Within or Adjacent to Functional Genomic Elements of Human Neutrophils and CD4+ T Cells.', *Arthritis & rheumatology (Hoboken, N.J.)*, 67(7), pp. 1966–1977. doi: 10.1002/art.39135.

Jubrail, J., Kurian, N. and Niedergang, F. (2017) 'Macrophage phagocytosis cracking the defect code in COPD', *Biomedical journal*. 2017/12/26, 40(6), pp. 305–312. doi: 10.1016/j.bj.2017.09.004.

Kaplan, M. J. and Radic, M. (2012) 'Neutrophil extracellular traps: double-edged swords of innate immunity', *Journal of immunology (Baltimore, Md. : 1950)*, 189(6), pp. 2689–2695. doi: 10.4049/jimmunol.1201719.

Karayama, M. *et al.* (2010) 'Antiendothelial Cell Antibodies in Patients With COPD', *Chest*, 138(6), pp. 1303–1308. doi: 10.1378/chest.10-0863.

Katoh, Masuko and Katoh, Masaru (2003) 'Identification and characterization of mouse Erbb2 gene in silico.', *International journal of oncology*, 23(3), pp. 831–835.

Kaur, B. P. and Secord, E. (2019) 'Innate Immunity.', *Pediatric clinics of North America*, 66(5), pp. 905–911. doi: 10.1016/j.pcl.2019.06.011.

Kaveh, A. *et al.* (2020) 'Live Imaging of Heart Injury in Larval Zebrafish Reveals a Multi-Stage Model of

Neutrophil and Macrophage Migration', *Frontiers in Cell and Developmental Biology*, 8, p. 1048. doi: 10.3389/fcell.2020.579943.

Kaźmierczak, M. *et al.* (2015) 'Evaluation of Markers of Inflammation and Oxidative Stress in COPD Patients with or without Cardiovascular Comorbidities.', *Heart, lung & circulation*, 24(8), pp. 817–823. doi: 10.1016/j.hlc.2015.01.019.

El Kebir, D. and Filep, J. G. (2013) 'Modulation of neutrophil apoptosis and the resolution of inflammation through beta(2) integrins', *Frontiers in Immunology*, 4, p. 15. doi: 10.3389/fimmu.2013.00060.

Kent, B. D., Mitchell, P. D. and McNicholas, W. T. (2011) 'Hypoxemia in patients with COPD: cause, effects, and disease progression', *International journal of chronic obstructive pulmonary disease*. 2011/03/14, 6, pp. 199–208. doi: 10.2147/COPD.S10611.

Keyvanjah, K. *et al.* (2017) 'Pharmacokinetics of neratinib during coadministration with lansoprazole in healthy subjects', *British journal of clinical pharmacology*. 2016/10/16, 83(3), pp. 554–561. doi: 10.1111/bcp.13132.

Khadangi, F. *et al.* (2021) 'Intranasal versus intratracheal exposure to lipopolysaccharides in a murine model of acute respiratory distress syndrome', *Scientific Reports*, 11(1), p. 7777. doi: 10.1038/s41598-021-87462-x.

Kim, T.-H. (2017) 'Systemic White Blood Cell Count as a Biomarker for Chronic Obstructive Pulmonary Disease: Utility and Limitations', *Tuberculosis and respiratory diseases*. 2017/07/03, 80(3), pp. 313–315. doi: 10.4046/trd.2017.80.3.313.

Kim, V. and Criner, G. J. (2013) 'Chronic bronchitis and chronic obstructive pulmonary disease.', *American journal of respiratory and critical care medicine*, 187(3), pp. 228–237. doi: 10.1164/rccm.201210-1843CI.

King, P. T. (2015) 'Inflammation in chronic obstructive pulmonary disease and its role in cardiovascular disease and lung cancer', *Clinical and Translational Medicine*, 4, p. 13. doi: 10.1186/s40169-015-0068-z.

Klein, J. B. *et al.* (2000) 'Granulocyte-macrophage colony-stimulating factor delays neutrophil constitutive apoptosis through phosphoinositide 3-kinase and extracellular signal-regulated kinase pathways', *Journal of Immunology*, 164(8), pp. 4286–4291. doi: 10.4049/jimmunol.164.8.4286.

Ko, Y.-P. *et al.* (2013) 'Phagocytosis Escape by a Staphylococcus aureus Protein That Connects Complement and Coagulation Proteins at the Bacterial Surface', *PLOS Pathogens*, 9(12), p. e1003816.

Available at: https://doi.org/10.1371/journal.ppat.1003816.

Kobayashi, S. D. *et al.* (2005) 'Spontaneous neutrophil apoptosis and regulation of cell survival by granulocyte macrophage-colony stimulating factor', *Journal of Leukocyte Biology*, 78(6), pp. 1408–1418. doi: 10.1189/jlb.0605289.

Kolaczkowska, E. and Kubes, P. (2013) 'Neutrophil recruitment and function in health and inflammation', *Nature Reviews Immunology*, 13(3), pp. 159–175. doi: 10.1038/nri3399.

Kong, T. *et al.* (2004) 'Leukocyte adhesion during hypoxia is mediated by HIF-1-dependent induction of beta-2 integrin gene expression', *Proceedings of the National Academy of Sciences*, 101(28), pp. 10440–10445. doi: 10.1073/pnas.0401339101.

Koo, H.-K. *et al.* (2017) 'Systemic White Blood Cell Count as a Biomarker Associated with Severity of Chronic Obstructive Lung Disease', *Tuberculosis and respiratory diseases*. 2017/07/03, 80(3), pp. 304–310. doi: 10.4046/trd.2017.80.3.304.

Kotz, K. T. *et al.* (2010) 'Clinical microfluidics for neutrophil genomics and proteomics', *Nature medicine*, 16(9), p. 1042—1047. doi: 10.1038/nm.2205.

Krammer, P. H., Arnold, R. and Lavrik, I. N. (2007) 'Life and death in peripheral T cells', *Nature Reviews Immunology*, 7(7), pp. 532–542. doi: 10.1038/nri2115.

Krysko, D. V *et al.* (2008) 'Apoptosis and necrosis: detection, discrimination and phagocytosis.', *Methods (San Diego, Calif.)*, 44(3), pp. 205–221. doi: 10.1016/j.ymeth.2007.12.001.

Kuribayashi, T. (2018) 'Elimination half-lives of interleukin-6 and cytokine-induced neutrophil chemoattractant-1 synthesized in response to inflammatory stimulation in rats', *Laboratory animal research*. 2018/06/18, 34(2), pp. 80–83. doi: 10.5625/lar.2018.34.2.80.

Kuwahara, I. *et al.* (2007) 'The signaling pathway involved in neutrophil elastase-stimulated MUC1 transcription', *American Journal of Respiratory Cell and Molecular Biology*, 37(6), pp. 691–698. doi: 10.1165/rcmb.2007-00720C.

Laisney, J. A. G. C. *et al.* (2010) 'Lineage-specific co-evolution of the Egf receptor/ligand signaling system', *BMC Evolutionary Biology*, 10(1), p. 27. doi: 10.1186/1471-2148-10-27.

Lakschevitz, F. S. *et al.* (2015) 'Neutrophil transcriptional profile changes during transit from bone marrow to sites of inflammation', *Cellular & Molecular Immunology*, 12(1), pp. 53–65. doi: 10.1038/cmi.2014.37.

Lawrence, S. M., Corriden, R. and Nizet, V. (2018) 'The Ontogeny of a Neutrophil: Mechanisms of

Granulopoiesis and Homeostasis', *Microbiology and Molecular Biology Reviews*, 82(1), pp. e00057-17. doi: 10.1128/MMBR.00057-17.

Lawrence, S. M., Corriden, R. and Nizet, V. (2020) 'How Neutrophils Meet Their End.', *Trends in immunology*, 41(6), pp. 531–544. doi: 10.1016/j.it.2020.03.008.

Lee-MacAry, A. E. *et al.* (2001) 'Development of a novel flow cytometric cell-mediated cytotoxicity assay using the fluorophores PKH-26 and TO-PRO-3 iodide', *Journal of Immunological Methods*, 252(1), pp. 83–92. doi: https://doi.org/10.1016/S0022-1759(01)00336-2.

Lee, I. H. *et al.* (2008) 'A role for the NAD-dependent deacetylase Sirt1 in the regulation of autophagy.', *Proceedings of the National Academy of Sciences of the United States of America*, 105(9), pp. 3374–3379. doi: 10.1073/pnas.0712145105.

Lee, J. W. and Matthay, M. A. (2007) 'Protein permeability in lung injury: now in real time again?', *Journal of Applied Physiology*, 102(2), pp. 508–509. doi: 10.1152/japplphysiol.01180.2006.

Lee, K. F. *et al.* (1995) 'REQUIREMENT FOR NEUREGULIN RECEPTOR ERBB2 IN NEURAL AND CARDIAC DEVELOPMENT', *Nature*, 378(6555), pp. 394–398. doi: 10.1038/378394a0.

Lee, M. and Chang, E. B. (2021) 'Inflammatory Bowel Diseases (IBD) and the Microbiome - Searching the Crime Scene for Clues', *Gastroenterology*, 160(2), pp. 524–537. doi: 10.1053/j.gastro.2020.09.056.

Lee, S. B. *et al.* (2010) 'Ribosomal protein S3, a new substrate of Akt, serves as a signal mediator between neuronal apoptosis and DNA repair.', *The Journal of biological chemistry*, 285(38), pp. 29457–29468. doi: 10.1074/jbc.M110.131367.

Leitch, A. E. *et al.* (2012) 'Cyclin-dependent kinases 7 and 9 specifically regulate neutrophil transcription and their inhibition drives apoptosis to promote resolution of inflammation', *Cell Death and Differentiation*, 19(12), pp. 1950–1961. doi: 10.1038/cdd.2012.80.

Leliefeld, P. H. C. *et al.* (2018) 'Differential antibacterial control by neutrophil subsets', *Blood Advances*, 2(11), pp. 1344–1355. doi: 10.1182/bloodadvances.2017015578.

Lenferink, A. E. G. *et al.* (1998) 'Differential endocytic routing of homo- and hetero-dimeric ErbB tyrosine kinases confers signaling superiority to receptor heterodimers', *Embo Journal*, 17(12), pp. 3385–3397. doi: 10.1093/emboj/17.12.3385.

Lewkowicz, N. *et al.* (2013) 'Neutrophil--CD4+CD25+ T regulatory cell interactions: a possible new mechanism of infectious tolerance.', *Immunobiology*, 218(4), pp. 455–464. doi: 10.1016/j.imbio.2012.05.029.

Lewkowicz, P. *et al.* (2005) 'Epidermal growth factor enhances TNF-alpha-induced priming of human neutrophils', *Immunology Letters*, 96(2), pp. 203–210. doi: 10.1016/j.imlet.2004.08.012.

Li, M. *et al.* (2001) 'An essential role of the NF-kappa B/Toll-like receptor pathway in induction of inflammatory and tissue-repair gene expression by necrotic cells.', *Journal of immunology (Baltimore, Md. : 1950)*, 166(12), pp. 7128–7135. doi: 10.4049/jimmunol.166.12.7128.

Liang, X. *et al.* (2020) 'Autophagy-driven NETosis is a double-edged sword – Review', *Biomedicine & Pharmacotherapy*, 126, p. 110065. doi: https://doi.org/10.1016/j.biopha.2020.110065.

Liang, Y. C. *et al.* (2017) 'The EGFR/miR-338-3p/EYA2 axis controls breast tumor growth and lung metastasis', *Cell Death & Disease*, 8, p. 12. doi: 10.1038/cddis.2017.325.

Liccardi, G., Hartley, J. A. and Hochhauser, D. (2014) 'Importance of EGFR/ERCC1 interaction following radiation-induced DNA damage.', *Clinical cancer research : an official journal of the American Association for Cancer Research*, 20(13), pp. 3496–3506. doi: 10.1158/1078-0432.CCR-13-2695.

Lieschke, G. J. *et al.* (2001) 'Morphologic and functional characterization of granulocytes and macrophages in embryonic and adult zebrafish', *Blood*, 98(10), pp. 3087–3096. doi: 10.1182/blood.V98.10.3087.

Lin, W.-C. and Fessler, M. B. (2021) 'Regulatory mechanisms of neutrophil migration from the circulation to the airspace', *Cellular and Molecular Life Sciences*, 78(9), pp. 4095–4124. doi: 10.1007/s00018-021-03768-z.

Liu, J. *et al.* (2021) 'Dendritic cell migration in inflammation and immunity', *Cellular & Molecular Immunology*, 18(11), pp. 2461–2471. doi: 10.1038/s41423-021-00726-4.

Liu, J. D. *et al.* (2010) 'A dual role for ErbB2 signaling in cardiac trabeculation', *Development*, 137(22), pp. 3867–3875. doi: 10.1242/dev.053736.

Liu, J. Q. *et al.* (2017) 'CRISPR/Cas9 in zebrafish: an efficient combination for human genetic diseases modeling', *Human Genetics*, 136(1), pp. 1–12. doi: 10.1007/s00439-016-1739-6.

Liu, K. L. *et al.* (2019) 'Expanding the CRISPR Toolbox in Zebrafish for Studying Development and Disease', *Frontiers in Cell and Developmental Biology*, 7, p. 15. doi: 10.3389/fcell.2019.00013.

Lodge, K. M. *et al.* (2020) 'The Impact of Hypoxia on Neutrophil Degranulation and Consequences for the Host', *International journal of molecular sciences*, 21(4), p. 1183. doi: 10.3390/ijms21041183.

Lok, L. S. C. *et al.* (2019) 'Phenotypically distinct neutrophils patrol uninfected human and mouse lymph nodes', *Proceedings of the National Academy of Sciences of the United States of America*.

2019/09/04, 116(38), pp. 19083–19089. doi: 10.1073/pnas.1905054116.

Lok, L. S. C. and Clatworthy, M. R. (2021) 'Neutrophils in secondary lymphoid organs', *Immunology*, 164(4), pp. 677–688. doi: https://doi.org/10.1111/imm.13406.

Lokwani, R. *et al.* (2019) 'Blood Neutrophils In COPD But Not Asthma Exhibit A Primed Phenotype With Downregulated CD62L Expression', *International journal of chronic obstructive pulmonary disease*, 14, pp. 2517–2525. doi: 10.2147/COPD.S222486.

López-Boado, Y. S. *et al.* (2004) 'Neutrophil Serine Proteinases Cleave Bacterial Flagellin, Abrogating Its Host Response-Inducing Activity', *The Journal of Immunology*, 172(1), pp. 509 LP – 515. doi: 10.4049/jimmunol.172.1.509.

Lotze, M. T. *et al.* (1985) 'In vivo administration of purified human interleukin 2. II. Half life, immunologic effects, and expansion of peripheral lymphoid cells in vivo with recombinant IL 2.', *Journal of immunology (Baltimore, Md. : 1950)*, 135(4), pp. 2865–2875.

Loubeau, G. *et al.* (2014) 'NPM1 Silencing Reduces Tumour Growth and MAPK Signalling in Prostate Cancer Cells', *PLOS ONE*, 9(5), p. e96293. Available at: https://doi.org/10.1371/journal.pone.0096293.

Loynes, C. A. *et al.* (2018) 'PGE2 production at sites of tissue injury promotes an anti-inflammatory neutrophil phenotype and determines the outcome of inflammation resolution in vivo', *Science Advances*, 4(9), p. eaar8320. doi: 10.1126/sciadv.aar8320.

Lu, N. *et al.* (2014) 'Activation of the Epidermal Growth Factor Receptor in Macrophages Regulates Cytokine Production and Experimental Colitis', *Journal of Immunology*, 192(3), pp. 1013–1023. doi: 10.4049/jimmunol.1300133.

Luo, H. R. and Loison, F. (2008) 'Constitutive neutrophil apoptosis: mechanisms and regulation.', *American journal of hematology*, 83(4), pp. 288–295. doi: 10.1002/ajh.21078.

Luster, A. D., Alon, R. and von Andrian, U. H. (2005) 'Immune cell migration in inflammation: present and future therapeutic targets', *Nature Immunology*, 6(12), pp. 1182–1190. doi: 10.1038/ni1275.

Macdonald-Obermann, J. L. and Pike, L. J. (2014) 'Different Epidermal Growth Factor (EGF) Receptor Ligands Show Distinct Kinetics and Biased or Partial Agonism for Homodimer and Heterodimer Formation', *Journal of Biological Chemistry*, 289(38), pp. 26178–26188. doi: 10.1074/jbc.M114.586826.

Makris, D. *et al.* (2009) 'Increased apoptosis of neutrophils in induced sputum of COPD patients', *Respiratory Medicine*, 103(8), pp. 1130–1135. doi: 10.1016/j.rmed.2009.03.002.

Makurvet, F. D. (2021) 'Biologics vs. small molecules: Drug costs and patient access', *Medicine in Drug Discovery*, 9, p. 100075. doi: https://doi.org/10.1016/j.medidd.2020.100075.

Manian, P. (2019) 'Chronic obstructive pulmonary disease classification, phenotypes and risk assessment', *Journal of thoracic disease*, 11(Suppl 14), pp. S1761–S1766. doi: 10.21037/jtd.2019.05.10.

Manley, H. R. *et al.* (2020) 'Frontline Science: Dynamic cellular and subcellular features of migrating leukocytes revealed by in vivo lattice lightsheet microscopy', *J Leukoc Biol*, 108(2), pp. 455–468. doi: 10.1002/JLB.3HI0120-589R.

Manz, M. G. and Boettcher, S. (2014) 'Emergency granulopoiesis', *Nature Reviews Immunology*, 14(5), pp. 302–314. doi: 10.1038/nri3660.

Marchi, L. F. *et al.* (2014) 'Comparison of four methods for the isolation of murine blood neutrophils with respect to the release of reactive oxygen and nitrogen species and the expression of immunological receptors', *Comparative Clinical Pathology*, 23(5), pp. 1469–1476. doi: 10.1007/s00580-013-1808-3.

Mariño, G. and Kroemer, G. (2013) 'Mechanisms of apoptotic phosphatidylserine exposure', *Cell research*. 2013/08/27, 23(11), pp. 1247–1248. doi: 10.1038/cr.2013.115.

Marmor, M. D., Skaria, K. B. and Yarden, Y. (2004) 'Signal transduction and oncogenesis by ErbB/HER receptors', *International Journal of Radiation Oncology Biology Physics*, 58(3), pp. 903–913. doi: 10.1016/j.ijrobp.2003.06.002.

Martí-Lliteras, P. *et al.* (2009) 'Nontypeable Haemophilus influenzae clearance by alveolar macrophages is impaired by exposure to cigarette smoke.', *Infection and immunity*, 77(10), pp. 4232–4242. doi: 10.1128/IAI.00305-09.

Martin, M. C. *et al.* (2001) 'Cyclic AMP Regulation of Neutrophil Apoptosis Occurs via a Novel Protein Kinase A-independent Signaling Pathway *', *Journal of Biological Chemistry*, 276(48), pp. 45041–45050. doi: 10.1074/jbc.M105197200.

Martinez, F. J. *et al.* (2016) 'Effect of Roflumilast and Inhaled Corticosteroid/Long-Acting β2-Agonist on Chronic Obstructive Pulmonary Disease Exacerbations (RE(2)SPOND). A Randomized Clinical Trial.', *American journal of respiratory and critical care medicine*, 194 5, pp. 559–567.

Mathias, J. R. *et al.* (2006) 'Resolution of inflammation by retrograde chemotaxis of neutrophils in transgenic zebrafish', *Journal of Leukocyte Biology*, 80(6), pp. 1281–1288. doi: https://doi.org/10.1189/jlb.0506346.

Di Matteo, A. *et al.* (2016) 'Molecules that target nucleophosmin for cancer treatment: an update', *Oncotarget*, 7(28), pp. 44821–44840. doi: 10.18632/oncotarget.8599.

Matute-Bello, G., Frevert, C. W. and Martin, T. R. (2008) 'Animal models of acute lung injury', *American journal of physiology. Lung cellular and molecular physiology*. 2008/07/11, 295(3), pp. L379–L399. doi: 10.1152/ajplung.00010.2008.

McGovern, N. N. *et al.* (2011) 'Hypoxia Selectively Inhibits Respiratory Burst Activity and Killing of Staphylococcus aureus in Human Neutrophils', *The Journal of Immunology*, 186(1), pp. 453 LP – 463. doi: 10.4049/jimmunol.1002213.

Mecham, R. P. (2018) 'Elastin in lung development and disease pathogenesis.', *Matrix biology : journal of the International Society for Matrix Biology*, 73, pp. 6–20. doi: 10.1016/j.matbio.2018.01.005.

Mestas, J. and Hughes, C. C. W. (2004) 'Of Mice and Not Men: Differences between Mouse and Human Immunology', *The Journal of Immunology*, 172(5), pp. 2731 LP – 2738. doi: 10.4049/jimmunol.172.5.2731.

Miettinen, P. J. *et al.* (1995) 'EPITHELIAL IMMATURITY AND MULTIORGAN FAILURE IN MICE LACKING EPIDERMAL GROWTH-FACTOR RECEPTOR', *Nature*, 376(6538), pp. 337–341. doi: 10.1038/376337a0.

Milot, E. and Filep, J. G. (2011) 'Regulation of neutrophil survival/apoptosis by Mcl-1', *TheScientificWorldJournal*. 2011/10/26, 11, pp. 1948–1962. doi: 10.1100/2011/131539.

Miralda, I., Uriarte, S. M. and McLeish, K. R. (2017) 'Multiple Phenotypic Changes Define Neutrophil Priming', *Frontiers in Cellular and Infection Microbiology*, 7, p. 13. doi: 10.3389/fcimb.2017.00217.

Mitra, A. *et al.* (2018) 'Association of Elevated Serum GM-CSF, IFN-gamma, IL-4, and TNF-alpha Concentration with Tobacco Smoke Induced Chronic Obstructive Pulmonary Disease in a South Indian Population', *International Journal of Inflammation*, p. 10. doi: 10.1155/2018/2027856.

Mitsudomi, T. *et al.* (2010) 'Gefitinib versus cisplatin plus docetaxel in patients with non-small-cell lung cancer harbouring mutations of the epidermal growth factor receptor (WJTOG3405): an open label, randomised phase 3 trial', *The Lancet Oncology*, 11(2), pp. 121–128. doi: https://doi.org/10.1016/S1470-2045(09)70364-X.

Miyake, M. *et al.* (2013) 'Expression of CXCL1 in human endothelial cells induces angiogenesis through the CXCR2 receptor and the ERK1/2 and EGF pathways', *Laboratory Investigation*, 93(7), pp. 768–778. doi: 10.1038/labinvest.2013.71.

Mok, T. S. *et al.* (2009) 'Gefitinib or Carboplatin–Paclitaxel in Pulmonary Adenocarcinoma', *New

England Journal of Medicine, 361(10), pp. 947–957. doi: 10.1056/NEJMoa0810699.

Momeny, M. *et al.* (2017) 'Dacomitinib, a pan-inhibitor of ErbB receptors, suppresses growth and invasive capacity of chemoresistant ovarian carcinoma cells', *Scientific Reports*, 7, p. 12. doi: 10.1038/s41598-017-04147-0.

Monaco, G. *et al.* (2019) 'RNA-Seq Signatures Normalized by mRNA Abundance Allow Absolute Deconvolution of Human Immune Cell Types', *Cell Reports*, 26(6), pp. 1627-1640.e7. doi: https://doi.org/10.1016/j.celrep.2019.01.041.

Moran, C. J. *et al.* (2013) 'IL-10R polymorphisms are associated with very-early-onset ulcerative colitis.', *Inflammatory bowel diseases*, 19(1), pp. 115–123. doi: 10.1002/ibd.22974.

Moret, I. *et al.* (2011) 'Increased lung neutrophil apoptosis and inflammation resolution in nonresponding pneumonia', *European Respiratory Journal*, 38(5), pp. 1158–1164. doi: 10.1183/09031936.00190410.

Morikis, V. A. and Simon, S. I. (2018) 'Neutrophil Mechanosignaling Promotes Integrin Engagement With Endothelial Cells and Motility Within Inflamed Vessels', *Frontiers in Immunology*, 9. doi: 10.3389/fimmu.2018.02774.

Mortimer, J. *et al.* (2019) 'Patterns of occurrence and implications of neratinib-associated diarrhea in patients with HER2-positive breast cancer: analyses from the randomized phase III ExteNET trial', *Breast Cancer Research*, 21(1), p. 32. doi: 10.1186/s13058-019-1112-5.

Mosca, T. and Forte, W. C. N. (2016) 'Comparative Efficiency and Impact on the Activity of Blood Neutrophils Isolated by Percoll, Ficoll and Spontaneous Sedimentation Methods', *Immunological Investigations*, 45(1), pp. 29–37. doi: 10.3109/08820139.2015.1085393.

Motta, M. C. *et al.* (2004) 'Mammalian SIRT1 represses forkhead transcription factors.', *Cell*, 116(4), pp. 551–563. doi: 10.1016/s0092-8674(04)00126-6.

Motulsky, H. J. and Brown, R. E. (2006) 'Detecting outliers when fitting data with nonlinear regression – a new method based on robust nonlinear regression and the false discovery rate', *BMC Bioinformatics*, 7(1), p. 123. doi: 10.1186/1471-2105-7-123.

Moy, B. and Goss, P. E. (2007) 'Lapatinib-associated toxicity and practical management recommendations', *Oncologist*, 12(7), pp. 756–765. doi: 10.1634/theoncologist.12-7-756.

Muefong, C. N. and Sutherland, J. S. (2020) 'Neutrophils in Tuberculosis-Associated Inflammation and Lung Pathology', *Frontiers in Immunology*, 11, p. 962. doi: 10.3389/fimmu.2020.00962.

Mukhopadhyay, S., Hoidal, J. R. and Mukherjee, T. K. (2006) 'Role of TNFα in pulmonary pathophysiology', *Respiratory Research*, 7(1), p. 125. doi: 10.1186/1465-9921-7-125.

Muller, W. A. (2013) 'Getting leukocytes to the site of inflammation', *Veterinary pathology*, 50(1), pp. 7–22. doi: 10.1177/0300985812469883.

Muneoka, K. *et al.* (2008) 'Mammalian regeneration and regenerative medicine', *Birth Defects Research Part C: Embryo Today: Reviews*, 84(4), pp. 265–280. doi: https://doi.org/10.1002/bdrc.20137.

Muñoz, L. E. *et al.* (2010) 'Autoimmunity and chronic inflammation - two clearance-related steps in the etiopathogenesis of SLE.', *Autoimmunity reviews*, 10(1), pp. 38–42. doi: 10.1016/j.autrev.2010.08.015.

Murayama, E. *et al.* (2006) 'Tracing Hematopoietic Precursor Migration to Successive Hematopoietic Organs during Zebrafish Development', *Immunity*, 25(6), pp. 963–975. doi: https://doi.org/10.1016/j.immuni.2006.10.015.

Murayama, E. *et al.* (2015) 'NACA deficiency reveals the crucial role of somite-derived stromal cells in haematopoietic niche formation', *Nature Communications*, 6, p. 14. doi: 10.1038/ncomms9375.

Muthuswamy, S. K., Gilman, M. and Brugge, J. S. (1999) 'Controlled dimerization of ErbB receptors provides evidence for differential signaling by homo- and heterodimers', *Molecular and Cellular Biology*, 19(10), pp. 6845–6857. Available at: %3CGo.

Naegelen, I. *et al.* (2015) 'Regulation of Neutrophil Degranulation and Cytokine Secretion: A Novel Model Approach Based on Linear Fitting', *Journal of Immunology Research*. Edited by E. Uribe-Querol, 2015, p. 817038. doi: 10.1155/2015/817038.

Naeini, M. B. *et al.* (2020) 'The role of phosphatidylserine recognition receptors in multiple biological functions', *Cellular & molecular biology letters*, 25, p. 23. doi: 10.1186/s11658-020-00214-z.

Nagpal, A. *et al.* (2019) 'Neoadjuvant neratinib promotes ferroptosis and inhibits brain metastasis in a novel syngeneic model of spontaneous HER2+ve breast cancer metastasis', *Breast Cancer Research*, 21(1), p. 94. doi: 10.1186/s13058-019-1177-1.

Narasaraju, T. *et al.* (2011) 'Excessive Neutrophils and Neutrophil Extracellular Traps Contribute to Acute Lung Injury of Influenza Pneumonitis', *American Journal of Pathology*, 179(1), pp. 199–210. doi: 10.1016/j.ajpath.2011.03.013.

Nguyen-Chi, M. *et al.* (2017) 'TNF signaling and macrophages govern fin regeneration in zebrafish

larvae', *Cell Death & Disease*, 8(8), pp. e2979–e2979. doi: 10.1038/cddis.2017.374.

Ningappa, M. *et al.* (2015) 'The Role of ARF6 in Biliary Atresia', *PLOS ONE*, 10(9), p. e0138381. Available at: https://doi.org/10.1371/journal.pone.0138381.

Nita, M. and Grzybowski, A. (2016) 'The Role of the Reactive Oxygen Species and Oxidative Stress in the Pathomechanism of the Age-Related Ocular Diseases and Other Pathologies of the Anterior and Posterior Eye Segments in Adults', *Oxidative Medicine and Cellular Longevity*, p. 23. doi: 10.1155/2016/3164734.

Noguera, A. *et al.* (2004) 'Expression of adhesion molecules during apoptosis of circulating neutrophils in COPD', *Chest*, 125(5), pp. 1837–1842. doi: 10.1378/chest.125.5.1837.

Nordenfelt, P. and Tapper, H. (2011) 'Phagosome dynamics during phagocytosis by neutrophils', *Journal of Leukocyte Biology*, 90(2), pp. 271–284. doi: 10.1189/jlb.0810457.

Nourshargh, S., Renshaw, S. A. and Imhof, B. A. (2016) 'Reverse Migration of Neutrophils: Where, When, How, and Why?', *Trends in immunology*, 37(5), pp. 273–286. doi: 10.1016/j.it.2016.03.006.

Núñez, B. *et al.* (2011) 'Anti-Tissue Antibodies Are Related to Lung Function in Chronic Obstructive Pulmonary Disease', *American Journal of Respiratory and Critical Care Medicine*, 183(8), pp. 1025–1031. doi: 10.1164/rccm.201001-0029OC.

Nüsslein-Volhard, C. and Dahm, R. (2002) 'Zebrafish: a practical approach.' New York: Oxford University Press.

Ohbayashi, H. (2002) 'Neutrophil elastase inhibitors as treatment for COPD.', *Expert opinion on investigational drugs*, 11(7), pp. 965–980. doi: 10.1517/13543784.11.7.965.

Osherov, N. *et al.* (1993) 'Selective inhibition of the epidermal growth factor and HER2/neu receptors by tyrphostins.', *The Journal of biological chemistry*, 268(15), pp. 11134–11142.

Oudijk, E. D., Lammers, J. J. and Koenderman, L. (2003) 'Systemic inflammation in chronic obstructive pulmonary disease', *European Respiratory Journal*, 22(46 suppl), pp. 5s LP-13s. doi: 10.1183/09031936.03.00004603a.

Page, T. H. *et al.* (2009) 'Tyrosine kinases and inflammatory signalling.', *Current molecular medicine*, 9(1), pp. 69–85. doi: 10.2174/156652409787314507.

Pahwa, R. *et al.* (2021) 'Chronic Inflammation', in *StatPearls*. StatPearls Publishing.

Palić, D. *et al.* (2007) 'Zebrafish (Danio rerio) whole kidney assays to measure neutrophil extracellular

trap release and degranulation of primary granules', *Journal of Immunological Methods*, 319(1–2), pp. 87–97. doi: 10.1016/j.jim.2006.11.003.

Panday, A. *et al.* (2015) 'NADPH oxidases: an overview from structure to innate immunity-associated pathologies', *Cellular & Molecular Immunology*, 12(1), pp. 5–23. doi: 10.1038/cmi.2014.89.

Pandey, K. C., De, S. and Mishra, P. K. (2017) 'Role of Proteases in Chronic Obstructive Pulmonary Disease', *Frontiers in Pharmacology*, 8, p. 512. doi: 10.3389/fphar.2017.00512.

Papayannopoulos, V. *et al.* (2010) 'Neutrophil elastase and myeloperoxidase regulate the formation of neutrophil extracellular traps', *The Journal of cell biology*. 2010/10/25, 191(3), pp. 677–691. doi: 10.1083/jcb.201006052.

Park, J. H. *et al.* (2012) 'Erlotinib binds both inactive and active conformations of the EGFR tyrosine kinase domain', *Biochemical Journal*, 448, pp. 417–423. doi: 10.1042/bj20121513.

Park, S.-Y. and Kim, I.-S. (2017) 'Engulfment signals and the phagocytic machinery for apoptotic cell clearance.', *Experimental & molecular medicine*, 49(5), p. e331. doi: 10.1038/emm.2017.52.

Park, Y. J. *et al.* (2020) 'Tyrosine kinase inhibitor neratinib attenuates liver fibrosis by targeting activated hepatic stellate cells', *Scientific Reports*, 10(1), p. 14756. doi: 10.1038/s41598-020-71688-2.

Pauwels, N. S. *et al.* (2011) 'Role of IL-1 alpha and the Nlrp3/caspase-1/IL-1 beta axis in cigarette smoke-induced pulmonary inflammation and COPD', *European Respiratory Journal*, 38(5), pp. 1019–1028. doi: 10.1183/09031936.00158110.

Payton, M. *et al.* (2006) 'Discovery and evaluation of dual CDK1 and CDK2 inhibitors.', *Cancer research*, 66(8), pp. 4299–4308. doi: 10.1158/0008-5472.CAN-05-2507.

Pennock, N. D. *et al.* (2013) 'T cell responses: naive to memory and everything in between', *Advances in physiology education*, 37(4), pp. 273–283. doi: 10.1152/advan.00066.2013.

Perciavalle, R. M. *et al.* (2012) 'Anti-apoptotic MCL-1 localizes to the mitochondrial matrix and couples mitochondrial fusion to respiration', *Nature Cell Biology*, 14(6), pp. 575-+. doi: 10.1038/ncb2488.

Pérez-Figueroa, E. *et al.* (2021) 'Neutrophils: Many Ways to Die', *Frontiers in Immunology*, 12, p. 509. doi: 10.3389/fimmu.2021.631821.

Pillay, J. *et al.* (2010) 'In vivo labeling with 2H2O reveals a human neutrophil lifespan of 5.4 days.', *Blood*, 116 4, pp. 625–627.

Pinder, E. M. *et al.* (2018) 'Randomised controlled trial of GM-CSF in critically ill patients with impaired

neutrophil phagocytosis', *Thorax*, 73(10), pp. 918–925. doi: 10.1136/thoraxjnl-2017-211323.

Pletz, M. W. R. *et al.* (2004) 'Reduced spontaneous apoptosis in peripheral blood neutrophils during exacerbation of COPD', *Respiratory Medicine*, 23(4), pp. 639–647. doi: 10.1016/j.rmed.2005.08.011.

Plowman, G. D. *et al.* (1990) 'Molecular cloning and expression of an additional epidermal growth-factor receptor-related gene', *Proceedings of the National Academy of Sciences of the United States of America*, 87(13), pp. 4905–4909. doi: 10.1073/pnas.87.13.4905.

Pober, J. S. and Sessa, W. C. (2014) 'Inflammation and the blood microvascular system', *Cold Spring Harbor perspectives in biology*, 7(1), pp. a016345–a016345. doi: 10.1101/cshperspect.a016345.

Polosukhin, V. V *et al.* (2007) 'Association of progressive structural changes in the bronchial epithelium with subepithelial fibrous remodeling: a potential role for hypoxia.', *Virchows Archiv : an international journal of pathology*, 451(4), pp. 793–803. doi: 10.1007/s00428-007-0469-5.

Polverino, F. *et al.* (2014) 'A novel non-human primate model of cigarette smoke-induced chronic obstructive pulmonary disease', *European Respiratory Journal*, 44(Suppl 58). Available at: https://erj.ersjournals.com/content/44/Suppl_58/P864.

Poplimont, H. *et al.* (2020) 'Neutrophil Swarming in Damaged Tissue Is Orchestrated by Connexins and Cooperative Calcium Alarm Signals', *Current Biology*, 30(14), pp. 2761-2776.e7. doi: https://doi.org/10.1016/j.cub.2020.05.030.

Popp, M. W. and Maquat, L. E. (2016) 'Leveraging Rules of Nonsense-Mediated mRNA Decay for Genome Engineering and Personalized Medicine', *Cell*, 165(6), pp. 1319–1322. doi: 10.1016/j.cell.2016.05.053.

Procter, M. *et al.* (2007) 'P110 Cardiac side effects in the HERceptin Adjuvant, (HERA) trial', *The Breast : official journal of the European Society of Mastology.* [Amsterdam] :, pp. S44–S44. doi: 10.1016/s0960-9776(07)70170-4.

Proto, J. D. *et al.* (2018) 'Regulatory T Cells Promote Macrophage Efferocytosis during Inflammation Resolution.', *Immunity*, 49(4), pp. 666-677.e6. doi: 10.1016/j.immuni.2018.07.015.

Puljic, R. *et al.* (2007) 'Lipopolysaccharide-induced lung inflammation is inhibited by neutralization of GM-CSF', *European Journal of Pharmacology*, 557(2), pp. 230–235. doi: https://doi.org/10.1016/j.ejphar.2006.11.023.

Qiu, Y. S. *et al.* (2003) 'Biopsy neutrophilia, neutrophil chemokine and receptor gene expression in severe exacerbations of chronic obstructive pulmonary disease', *American Journal of Respiratory and*

Critical Care Medicine, 168(8), pp. 968–975. doi: 10.1164/rccm.200208-794OC.

Rabindran, S. K. *et al.* (2004) 'Antitumor activity of HKI-272, an orally active, irreversible inhibitor of the HER-2 tyrosine kinase.', *Cancer research*, 64(11), pp. 3958–3965. doi: 10.1158/0008-5472.CAN-03-2868.

Ragab, G., Elshahaly, M. and Bardin, T. (2017) 'Gout: An old disease in new perspective – A review', *Journal of Advanced Research*, 8(5), pp. 495–511. doi: https://doi.org/10.1016/j.jare.2017.04.008.

Rahman, A. *et al.* (2019) 'Inhibition of ErbB kinase signalling promotes resolution of neutrophilic inflammation', *eLife*, 8, p. e50990. doi: 10.7554/eLife.50990.

Rao, Y. *et al.* (2021) 'NK Cells in the Pathogenesis of Chronic Obstructive Pulmonary Disease', *Frontiers in immunology*, 12, p. 666045. doi: 10.3389/fimmu.2021.666045.

Ratajczak-Wrona, W. *et al.* (2014) 'PI3K-Akt/PKB signaling pathway in neutrophils and mononuclear cells exposed to N-nitrosodimethylamine.', *Journal of immunotoxicology*, 11(3), pp. 231–237. doi: 10.3109/1547691X.2013.826307.

Rauf, F. *et al.* (2018) 'Ibrutinib inhibition of ERBB4 reduces cell growth in a WNT5A-dependent manner', *Oncogene*, 37(17), pp. 2237–2250. doi: 10.1038/s41388-017-0079-x.

Rawat, K., Syeda, S. and Shrivastava, A. (2021) 'Neutrophil-derived granule cargoes: paving the way for tumor growth and progression', *Cancer and Metastasis Reviews*, 40(1), pp. 221–244. doi: 10.1007/s10555-020-09951-1.

Reischauer, S. *et al.* (2009) 'Lgl2 Executes Its Function as a Tumor Suppressor by Regulating ErbB Signaling in the Zebrafish Epidermis', *PLOS Genetics*, 5(11), p. e1000720. Available at: https://doi.org/10.1371/journal.pgen.1000720.

Rennard, S. I. *et al.* (2007) 'The safety and efficacy of infliximab in moderate to severe chronic obstructive pulmonary disease', *American Journal of Respiratory and Critical Care Medicine*, 175(9), pp. 926–934. doi: 10.1164/rccm.200607-995OC.

Renshaw, S. A. *et al.* (2006) 'A transgenic zebrafish model of neutrophilic inflammation', *Blood*, 108(13), pp. 3976–3978. doi: 10.1182/blood-2006-05-024075.

Reutershan, J. *et al.* (2010) 'Phosphoinositide 3-kinase γ required for lipopolysaccharide-induced transepithelial neutrophil trafficking in the lung', *European Respiratory Journal*, 35(5), pp. 1137–1147. doi: 10.1183/09031936.00085509.

Richard, A. C. *et al.* (2016) 'Targeted genomic analysis reveals widespread autoimmune disease

association with regulatory variants in the TNF superfamily cytokine signalling network', *Genome Medicine*, 8(1), p. 76. doi: 10.1186/s13073-016-0329-5.

Richards, H. *et al.* (2010) 'Novel role of regulatory T cells in limiting early neutrophil responses in skin.', *Immunology*, 131(4), pp. 583–592. doi: 10.1111/j.1365-2567.2010.03333.x.

Richardson, R. *et al.* (2017) 'The zebrafish eye—a paradigm for investigating human ocular genetics', *Eye*, 31(1), pp. 68–86. doi: 10.1038/eye.2016.198.

Rieckmann, J. C. *et al.* (2017) 'Social network architecture of human immune cells unveiled by quantitative proteomics', *Nature Immunology*, 18(5), pp. 583–593. doi: 10.1038/ni.3693.

Riethmacher, D. *et al.* (1997) 'Severe neuropathies in mice with targeted mutations in the ErbB3 receptor', *Nature*, 389(6652), pp. 725–730. doi: 10.1038/39593.

Rimawi, M. F. *et al.* (2010) 'Epidermal Growth Factor Receptor Expression in Breast Cancer Association With Biologic Phenotype and Clinical Outcomes', *Cancer*, 116(5), pp. 1234–1242. doi: 10.1002/cncr.24816.

Rincón, E., Rocha-Gregg, B. L. and Collins, S. R. (2018) 'A map of gene expression in neutrophil-like cell lines', *BMC genomics*, 19(1), p. 573. doi: 10.1186/s12864-018-4957-6.

Rittirsch, D. *et al.* (2008) 'Acute lung injury induced by lipopolysaccharide is independent of complement activation', *Journal of immunology (Baltimore, Md. : 1950)*, 180(11), pp. 7664–7672. doi: 10.4049/jimmunol.180.11.7664.

Robertson, A. L. *et al.* (2014) 'A Zebrafish Compound Screen Reveals Modulation of Neutrophil Reverse Migration as an Anti-Inflammatory Mechanism', *Science Translational Medicine*, 6(225), p. 10. doi: 10.1126/scitranslmed.3007672.

Robinson, M. D. and Oshlack, A. (2010) 'A scaling normalization method for differential expression analysis of RNA-seq data', *Genome Biology*, 11(3), p. R25. doi: 10.1186/gb-2010-11-3-r25.

Rose-John, S. (2018) 'Interleukin-6 Family Cytokines.', *Cold Spring Harbor perspectives in biology*, 10(2). doi: 10.1101/cshperspect.a028415.

Roskoski, R. J. (2014) 'The ErbB/HER family of protein-tyrosine kinases and cancer', *Pharmacological Research*, 79, pp. 34–74. doi: 10.1016/j.phrs.2013.11.002.

Rossi, A. G. *et al.* (2006) 'Cyclin-dependent kinase inhibitors enhance the resolution of inflammation by promoting inflammatory cell apoptosis', *Nature Medicine*, 12(9), pp. 1056–1064. doi: 10.1038/nm1468.

Le Rossignol, S., Ketheesan, N. and Haleagrahara, N. (2018) 'Redox-sensitive transcription factors play a significant role in the development of rheumatoid arthritis', *International Reviews of Immunology*, 37(3), pp. 129–143. doi: 10.1080/08830185.2017.1363198.

Roth, S. *et al.* (2015) 'Secondary necrotic neutrophils release interleukin-16C and macrophage migration inhibitory factor from stores in the cytosol', *Cell Death Discovery*, 1(1), p. 15056. doi: 10.1038/cddiscovery.2015.56.

Rougeot, J. *et al.* (2019) 'RNAseq Profiling of Leukocyte Populations in Zebrafish Larvae Reveals a cxcl11 Chemokine Gene as a Marker of Macrophage Polarization During Mycobacterial Infection ', *Frontiers in Immunology* , p. 832. Available at: https://www.frontiersin.org/article/10.3389/fimmu.2019.00832.

Ruiz-Saenz, A. *et al.* (2018) 'HER2 Amplification in Tumors Activates PI3K/Akt Signaling Independent of HER3', *Cancer Research*, 78(13), pp. 3645–3658. doi: 10.1158/0008-5472.can-18-0430.

Rush, J. S. *et al.* (2012) 'Endosomal Accumulation of the Activated Epidermal Growth Factor Receptor (EGFR) Induces Apoptosis', *Journal of Biological Chemistry*, 287(1), pp. 712–722. doi: 10.1074/jbc.M111.294470.

Russell, R. E. K. *et al.* (2002) 'Alveolar macrophage-mediated elastolysis: roles of matrix metalloproteinases, cysteine, and serine proteases', *American Journal of Physiology-Lung Cellular and Molecular Physiology*, 283(4), pp. L867–L873. doi: 10.1152/ajplung.00020.2002.

Ryan, E. M., Whyte, M. K. B. and Walmsley, S. R. (2019) 'Hypoxia and reprogramming of host pathogen interactions', *Current Opinion in Physiology*, 7, pp. 15–20. doi: https://doi.org/10.1016/j.cophys.2018.11.004.

Rydell-Törmänen, K., Uller, L. and Erjefält, J. S. (2006) 'Direct evidence of secondary necrosis of neutrophils during intense lung inflammation', *European Respiratory Journal*, 28(2), pp. 268 LP – 274. doi: 10.1183/09031936.06.00126905.

Rytilä, P. *et al.* (2006) 'Airway neutrophilia in COPD is not associated with increased neutrophil survival'. European Respiratory Journal, pp. 1163–1169.

Ryzhov, S. *et al.* (2017) 'ERBB signaling attenuates proinflammatory activation of nonclassical monocytes', *American Journal of Physiology-Heart and Circulatory Physiology*, 312(5), pp. H907–H918. doi: 10.1152/ajpheart.00486.2016.

Saetta, M. *et al.* (1985) 'Loss of Alveolar Attachments in Smokers', *American Review of Respiratory Disease*, 132(4), pp. 894–900. doi: 10.1164/arrd.1985.132.4.894.

Saiwai, H. *et al.* (2010) 'The LTB4-BLT1 axis mediates neutrophil infiltration and secondary injury in experimental spinal cord injury', *The American journal of pathology*. 2010/03/19, 176(5), pp. 2352–2366. doi: 10.2353/ajpath.2010.090839.

Samarut, E., Lissouba, A. and Drapeau, P. (2016) 'A simplified method for identifying early CRISPR-induced indels in zebrafish embryos using High Resolution Melting analysis', *Bmc Genomics*, 17, p. 6. doi: 10.1186/s12864-016-2881-1.

Samson, A. L. *et al.* (2020) 'MLKL trafficking and accumulation at the plasma membrane control the kinetics and threshold for necroptosis', *Nature Communications*, 11(1), p. 3151. doi: 10.1038/s41467-020-16887-1.

dos Santos, G. T. *et al.* (2017) 'Impact of Her-2 Overexpression on Survival of Patients with Metastatic Breast Cancer', *Asian Pacific journal of cancer prevention : APJCP*, 18(10), pp. 2673–2678. Available at: %3CGo.

Sapey, E. *et al.* (2014) 'Phosphoinositide 3-kinase inhibition restores neutrophil accuracy in the elderly: toward targeted treatments for immunosenescence', *Blood*, 123(2), pp. 239–248. doi: 10.1182/blood-2013-08-519520.

Sasaki, T. *et al.* (2008) 'Phosphorylation regulates SIRT1 function', *PloS one*. 2008/12/24, 3(12), pp. e4020–e4020. doi: 10.1371/journal.pone.0004020.

Šašinková, M. *et al.* (2021) 'NSC348884 cytotoxicity is not mediated by inhibition of nucleophosmin oligomerization', *Scientific Reports*, 11(1), p. 1084. doi: 10.1038/s41598-020-80224-1.

Sassone-Corsi, P. (2012) 'The cyclic AMP pathway', *Cold Spring Harbor perspectives in biology*, 4(12), p. a011148. doi: 10.1101/cshperspect.a011148.

Saul, S. *et al.* (2021) 'Discovery of pan-ErbB inhibitors protecting from SARS-CoV-2 replication, inflammation, and lung injury by a drug repurposing screen.', *bioRxiv : the preprint server for biology*. doi: 10.1101/2021.05.15.444128.

Savale, L. *et al.* (2009) 'Shortened telomeres in circulating leukocytes of patients with chronic obstructive pulmonary disease.', *American journal of respiratory and critical care medicine*, 179(7), pp. 566–571. doi: 10.1164/rccm.200809-1398OC.

Sawant, K. V *et al.* (2016) 'Chemokine CXCL1 mediated neutrophil recruitment: Role of glycosaminoglycan interactions', *Scientific Reports*, 6(1), p. 33123. doi: 10.1038/srep33123.

Schett, G. and Neurath, M. F. (2018) 'Resolution of chronic inflammatory disease: universal and tissue-

specific concepts', *Nature Communications*, 9(1), p. 3261. doi: 10.1038/s41467-018-05800-6.

Schif-Zuck, S. *et al.* (2011) 'Saturated-efferocytosis generates pro-resolving CD11blow macrophages: Modulation by resolvins and glucocorticoids', *European Journal of Immunology*, 41(2), pp. 366–379. doi: https://doi.org/10.1002/eji.201040801.

Schmidt-Ioanas, M. *et al.* (2006) 'Apoptosis of peripheral blood neutrophils in COPD exacerbation does not correlate with serum cytokines', *Respiratory Medicine*, 100(4), pp. 639–647. doi: 10.1016/j.rmed.2005.08.011.

Schmiedel, B. J. *et al.* (2018) 'Impact of Genetic Polymorphisms on Human Immune Cell Gene Expression.', *Cell*, 175(6), pp. 1701-1715.e16. doi: 10.1016/j.cell.2018.10.022.

Schulz, R. *et al.* (2000) 'Enhanced Release of Superoxide from Polymorphonuclear Neutrophils in Obstructive Sleep Apnea', *American Journal of Respiratory and Critical Care Medicine*, 162(2), pp. 566–570. doi: 10.1164/ajrccm.162.2.9908091.

Schuster, S., Hurrell, B. and Tacchini-Cottier, F. (2013) 'Crosstalk between neutrophils and dendritic cells: a context-dependent process', *Journal of Leukocyte Biology*, 94(4), pp. 671–675. doi: 10.1189/jlb.1012540.

Schwartz, J. *et al.* (2009) 'Neutrophil Bleaching of GFP-Expressing Staphylococci: Probing the Intraphagosomal Fate of Individual Bacteria', *Journal of Immunology*, 183(4), pp. 2632–2641. doi: 10.4049/jimmunol.0804110.

Segovia-Mendoza, M. *et al.* (2015) 'Efficacy and mechanism of action of the tyrosine kinase inhibitors gefitinib, lapatinib and neratinib in the treatment of HER2-positive breast cancer: preclinical and clinical evidence', *American Journal of Cancer Research*, 5(9), pp. 2531–2561. Available at: %3CGo.

Sehnert, A. J. *et al.* (2002) 'Cardiac troponin T is essential in sarcomere assembly and cardiac contractility', *Nature Genetics*, 31(1), pp. 106–110. doi: 10.1038/ng875.

Selvarajah, S. *et al.* (2016) 'Multiple Circulating Cytokines Are Coelevated in Chronic Obstructive Pulmonary Disease.', *Mediators of inflammation*, 2016, p. 3604842. doi: 10.1155/2016/3604842.

Shannon, C. *et al.* (2005) 'Acute Inflammatory Response to Endotoxin in Mice and Humans', *Clinical and Vaccine Immunology*, 12(1), pp. 60–67. doi: 10.1128/CDLI.12.1.60-67.2005.

Sheshachalam, A. *et al.* (2014) 'Granule Protein Processing and Regulated Secretion in Neutrophils', *Frontiers in Immunology*, 5. doi: 10.3389/fimmu.2014.00448.

Shieh, J.-M. *et al.* (2014) 'CXCL1 Regulation in Human Pulmonary Epithelial Cells by Tumor Necrosis

Factor', *Cellular Physiology and Biochemistry*, 34(4), pp. 1373–1384. doi: 10.1159/000366344.

Sievers, F. *et al.* (2011) 'Fast, scalable generation of high-quality protein multiple sequence alignments using Clustal Omega', *Molecular systems biology*. School of Medicine and Medical Science, UCD Conway Institute of Biomolecular and Biomedical Research, University College Dublin, Dublin, Ireland., p. 539. doi: 10.1038/msb.2011.75.

Silva, M. T. (2011) 'Macrophage phagocytosis of neutrophils at inflammatory/infectious foci: a cooperative mechanism in the control of infection and infectious inflammation', *Journal of Leukocyte Biology*, 89(5), pp. 675–683. doi: https://doi.org/10.1189/jlb.0910536.

Sinden, N. J. and Stockley, R. A. (2010) 'Systemic inflammation and comorbidity in COPD: a result of overspill of inflammatory mediators from the lungs? Review of the evidence', *Thorax*, 65(10), pp. 930–936. doi: 10.1136/thx.2009.130260.

Singh, D. *et al.* (2011) 'Induced sputum genes associated with spirometric and radiological disease severity in COPD ex-smokers', *Thorax*, 66(6), pp. 489–495. doi: 10.1136/thx.2010.153767.

Skendros, P., Mitroulis, I. and Ritis, K. (2018) 'Autophagy in Neutrophils: From Granulopoiesis to Neutrophil Extracellular Traps', *Frontiers in cell and developmental biology*, 6, p. 109. doi: 10.3389/fcell.2018.00109.

Smith, J. (2002) 'Human Sir2 and the "silencing" of p53 activity.', *Trends in cell biology*, 12(9), pp. 404–406. doi: 10.1016/s0962-8924(02)02342-5.

Sogawa, Y. *et al.* (2011) 'Inhibition of neutrophil migration in mice by mouse formyl peptide receptors 1 and 2 dual agonist: indication of cross-desensitization in vivo.', *Immunology*, 132(3), pp. 441–450. doi: 10.1111/j.1365-2567.2010.03367.x.

Solomon, J. M. *et al.* (2006) 'Inhibition of SIRT1 catalytic activity increases p53 acetylation but does not alter cell survival following DNA damage.', *Molecular and cellular biology*, 26(1), pp. 28–38. doi: 10.1128/MCB.26.1.28-38.2006.

Soria, J. C. *et al.* (2015) 'Gefitinib plus chemotherapy versus placebo plus chemotherapy in EGFR-mutation- positive non-small-cell lung cancer after progression on first-line gefitinib (IMPRESS): a phase 3 randomised trial', *Lancet Oncology*, 16(8), pp. 990–998. doi: 10.1016/s1470-2045(15)00121-7.

Sousa, L. P. *et al.* (2010) 'PDE4 inhibition drives resolution of neutrophilic inflammation by inducing apoptosis in a PKA-PI3K/Akt-dependent and NF-kappa B-independent manner', *Journal of Leukocyte Biology*, 87(5), pp. 895–904. doi: 10.1189/jlb.0809540.

Staali, L. *et al.* (2006) 'Streptococcus pyogenes bacteria modulate membrane traffic in human neutrophils and selectively inhibit azurophilic granule fusion with phagosomes', *Cellular Microbiology*, 8(4), pp. 690–703. doi: https://doi.org/10.1111/j.1462-5822.2005.00662.x.

Stapels, D. A. C., Geisbrecht, B. V and Rooijakkers, S. H. M. (2015) 'Neutrophil serine proteases in antibacterial defense', *Current Opinion in Microbiology*, 23, pp. 42–48. doi: 10.1016/j.mib.2014.11.002.

Stark, R., Grzelak, M. and Hadfield, J. (2019) 'RNA sequencing: the teenage years', *Nature Reviews Genetics*, 20(11), pp. 631–656. doi: 10.1038/s41576-019-0150-2.

Strassburg, A. *et al.* (2004) 'Enhanced PMN response in chronic bronchitis and community-acquired pneumonia', *European Respiratory Journal*, 24(5), pp. 772–778. doi: 10.1183/09031936.04.00139803.

Sun, L. *et al.* (2015) 'Ex Vivo and In Vitro Effect of Serum Amyloid A in the Induction of Macrophage M2 Markers and Efferocytosis of Apoptotic Neutrophils', *Journal of Immunology*, 194(10), pp. 4891–4900. doi: 10.4049/jimmunol.1402164.

Suter, T. M. *et al.* (2007) 'Trastuzumab-associated cardiac adverse effects in the herceptin adjuvant trial.', *Journal of clinical oncology : official journal of the American Society of Clinical Oncology*, 25(25), pp. 3859–3865. doi: 10.1200/JCO.2006.09.1611.

Szklarczyk, D. *et al.* (2021) 'The STRING database in 2021: customizable protein-protein networks, and functional characterization of user-uploaded gene/measurement sets.', *Nucleic acids research*, 49(D1), pp. D605–D612. doi: 10.1093/nar/gkaa1074.

Tang, D. *et al.* (2012) 'PAMPs and DAMPs: signal 0s that spur autophagy and immunity', *Immunological reviews*, 249(1), pp. 158–175. doi: 10.1111/j.1600-065X.2012.01146.x.

Tang, L. *et al.* (2018) 'Radioiodinated Small-Molecule Tyrosine Kinase Inhibitor for HER2-Selective SPECT Imaging.', *Journal of nuclear medicine : official publication, Society of Nuclear Medicine*, 59(9), pp. 1386–1391. doi: 10.2967/jnumed.117.205088.

Tardy, O. R. *et al.* (2021) 'The Epidermal Growth Factor Ligand Spitz Modulates Macrophage Efferocytosis, Wound Responses and Migration Dynamics During Drosophila Embryogenesis', *Frontiers in Cell and Developmental Biology*, 9, p. 851. doi: 10.3389/fcell.2021.636024.

Taylor, A. *et al.* (2014) 'SRF is required for neutrophil migration in response to inflammation.', *Blood*, 123(19), pp. 3027–3036. doi: 10.1182/blood-2013-06-507582.

Terzikhan, N. *et al.* (2016) 'Prevalence and incidence of COPD in smokers and non-smokers: the

Rotterdam Study', *European journal of epidemiology*. 2016/03/05, 31(8), pp. 785–792. doi: 10.1007/s10654-016-0132-z.

The UniProt Consortium (2021) 'UniProt: the universal protein knowledgebase in 2021', *Nucleic Acids Research*, 49(D1), pp. D480–D489. doi: 10.1093/nar/gkaa1100.

Thompson, A. B. *et al.* (1989) 'INTRALUMINAL AIRWAY INFLAMMATION IN CHRONIC-BRONCHITIS - CHARACTERIZATION AND CORRELATION WITH CLINICAL-PARAMETERS', *American Review of Respiratory Disease*, 140(6), pp. 1527–1537. doi: 10.1164/ajrccm/140.6.1527.

Todt, J. C. *et al.* (2013) 'Smoking decreases the response of human lung macrophages to double-stranded RNA by reducing TLR3 expression', *Respiratory Research*, 14(1), p. 33. doi: 10.1186/1465-9921-14-33.

Trubiroha, A. *et al.* (2018) 'A Rapid CRISPR/Cas-based Mutagenesis Assay in Zebrafish for Identification of Genes Involved in Thyroid Morphogenesis and Function', *Scientific Reports*, 8, p. 19. doi: 10.1038/s41598-018-24036-4.

Tsai, W. C. *et al.* (2000) 'CXC chemokine receptor CXCR2 is essential for protective innate host response in murine Pseudomonas aeruginosa pneumonia.', *Infection and immunity*, 68(7), pp. 4289–4296. doi: 10.1128/IAI.68.7.4289-4296.2000.

Tsuda, Y. *et al.* (2004) 'Three Different Neutrophil Subsets Exhibited in Mice with Different Susceptibilities to Infection by Methicillin-Resistant Staphylococcus aureus', *Immunity*, 21(2), pp. 215–226. doi: https://doi.org/10.1016/j.immuni.2004.07.006.

Tucker, K. A. *et al.* (1987) 'Characterization of a new human diploid myeloid leukemia cell line (PLB-985) with granulocytic and monocytic differentiating capacity.', *Blood*, 70(2), pp. 372–378.

Tuder, R. M. and Petrache, I. (2012) 'Pathogenesis of chronic obstructive pulmonary disease.', *The Journal of clinical investigation*, 122(8), pp. 2749–2755. doi: 10.1172/JCI60324.

Turato, G. *et al.* (2002) 'Airway inflammation in severe chronic obstructive pulmonary disease: relationship with lung function and radiologic emphysema.', *American journal of respiratory and critical care medicine*, 166(1), pp. 105–110. doi: 10.1164/rccm.2111084.

Uemoto, T., Abe, G. and Tamura, K. (2020) 'Regrowth of zebrafish caudal fin regeneration is determined by the amputated length', *Scientific Reports*, 10(1), p. 649. doi: 10.1038/s41598-020-57533-6.

Uhlen, M. *et al.* (2019) 'A genome-wide transcriptomic analysis of protein-coding genes in human

blood cells.', *Science (New York, N.Y.)*, 366(6472). doi: 10.1126/science.aax9198.

Uhlén, M. *et al.* (2015) 'Proteomics. Tissue-based map of the human proteome.', *Science (New York, N.Y.)*, 347(6220), p. 1260419. doi: 10.1126/science.1260419.

Vaguliene, N. *et al.* (2013) 'Local and systemic neutrophilic inflammation in patients with lung cancer and chronic obstructive pulmonary disease', *BMC Immunology*, 14(1), p. 36. doi: 10.1186/1471-2172-14-36.

Valabrega, G., Montemurro, F. and Aglietta, M. (2007) 'Trastuzumab: mechanism of action, resistance and future perspectives in HER2-overexpressing breast cancer', *Annals of Oncology*, 18(6), pp. 977–984. doi: 10.1093/annonc/mdl475.

Valenti, P. and Antonini, G. (2005) 'Lactoferrin: an important host defence against microbial and viral attack.', *Cellular and molecular life sciences : CMLS*, 62(22), pp. 2576–2587. doi: 10.1007/s00018-005-5372-0.

Vaquero, A. *et al.* (2004) 'Human SirT1 interacts with histone H1 and promotes formation of facultative heterochromatin.', *Molecular cell*, 16(1), pp. 93–105. doi: 10.1016/j.molcel.2004.08.031.

Vassilev, L. T. *et al.* (2006) 'Selective small-molecule inhibitor reveals critical mitotic functions of human CDK1', *Proceedings of the National Academy of Sciences*, 103(28), pp. 10660–10665. doi: 10.1073/pnas.0600447103.

Vaure, C. and Liu, Y. (2014) 'A comparative review of toll-like receptor 4 expression and functionality in different animal species', *Frontiers in immunology*, 5, p. 316. doi: 10.3389/fimmu.2014.00316.

Veglia, F., Sanseviero, E. and Gabrilovich, D. I. (2021) 'Myeloid-derived suppressor cells in the era of increasing myeloid cell diversity', *Nature Reviews Immunology*, 21(8), pp. 485–498. doi: 10.1038/s41577-020-00490-y.

Vivier, E. *et al.* (2008) 'Functions of natural killer cells', *Nature Immunology*, 9(5), pp. 503–510. doi: 10.1038/ni1582.

Vlahos, R. *et al.* (2006) 'Therapeutic potential of treating chronic obstructive pulmonary disease (COPD) by neutralising granulocyte macrophage-colony stimulating factor (GM-CSF)', *Pharmacology & Therapeutics*, 112(1), pp. 106–115. doi: 10.1016/j.pharmthera.2006.03.007.

Vlahos, R. *et al.* (2010) 'Neutralizing Granulocyte/Macrophage Colony-Stimulating Factor Inhibits Cigarette Smoke-induced Lung Inflammation', *American Journal of Respiratory and Critical Care Medicine*, 182(1), pp. 34–40. doi: 10.1164/rccm.200912-1794OC.

Vlahos, R. and Bozinovski, S. (2014) 'Role of alveolar macrophages in chronic obstructive pulmonary disease', *Frontiers in immunology*, 5, p. 435. doi: 10.3389/fimmu.2014.00435.

Vogel, C. L. *et al.* (2002) 'Efficacy and safety of trastuzumab as a single agent in first-line treatment of HER2-overexpressing metastatic breast cancer', *Journal of Clinical Oncology*, 20(3), pp. 719–726. doi: 10.1200/jco.20.3.719.

Vogelmeier, C. F. *et al.* (2017) 'Global Strategy for the Diagnosis, Management, and Prevention of Chronic Obstructive Lung Disease 2017 Report: GOLD Executive Summary (vol 53, pg 128, 2017)', *Archivos De Bronconeumologia*, 53(7), pp. 411–412. doi: 10.1016/j.arbres.2017.06.001.

Walmsley, S. R. *et al.* (2005) 'Hypoxia-induced neutrophil survival is mediated by HIF-1alpha-dependent NF-kappaB activity.', *The Journal of experimental medicine*, 201(1), pp. 105–115. doi: 10.1084/jem.20040624.

Wang, J. *et al.* (2017) 'Visualizing the function and fate of neutrophils in sterile injury and repair', *Science*, 358(6359), pp. 111 LP – 116. doi: 10.1126/science.aam9690.

Wang, K. H. *et al.* (2012) 'Promotion of epithelial-mesenchymal transition and tumor growth by 17 beta-estradiol in an ER+/HER2(+) cell line derived from human breast epithelial stem cells', *Biotechnology and Applied Biochemistry*, 59(3), pp. 262–267. doi: 10.1002/bab.1022.

Wang, K. Q. *et al.* (2003) 'Inhibition of neutrophil apoptosis by type 1 IFN depends on cross-talk between phosphoinositol 3-kinase, protein kinase C-delta, and NF-kappa B signaling pathways', *Journal of Immunology*, 171(2), pp. 1035–1041. doi: 10.4049/jimmunol.171.2.1035.

Wang, K. Q. *et al.* (2012) 'Cyclin-Dependent Kinase 9 Activity Regulates Neutrophil Spontaneous Apoptosis', *Plos One*, 7(1), p. 6. doi: 10.1371/journal.pone.0030128.

Wang, Y. *et al.* (2017) 'Incidence and risk of infections associated with EGFR-TKIs in advanced non-small-cell lung cancer: a systematic review and meta-analysis of randomized controlled trials', *Oncotarget*, 8(17), pp. 29406–29415. doi: 10.18632/oncotarget.14707.

Wang, Y. J. *et al.* (2018) 'Role of inflammatory cells in airway remodeling in COPD', *International Journal of Chronic Obstructive Pulmonary Disease*, 13, pp. 3341–3348. doi: 10.2147/copd.s176122.

Wang, Z., Gerstein, M. and Snyder, M. (2009) 'RNA-Seq: a revolutionary tool for transcriptomics', *Nature reviews. Genetics*, 10(1), pp. 57–63. doi: 10.1038/nrg2484.

Ward, C. *et al.* (1999) 'NFkB Activation Is a Critical Regulator of Human Granulocyte Apoptosis in Vitro*', *Journal of Biological Chemistry*, 274(7), pp. 4309–4318. doi: 10.1074/jbc.274.7.4309.

Wee, P. and Wang, Z. X. (2017) 'Epidermal Growth Factor Receptor Cell Proliferation Signaling Pathways', *Cancers*, 9(5), p. 45. doi: 10.3390/cancers9050052.

Wei, X.-W. *et al.* (2020) 'Mutational landscape and characteristics of ERBB2 in non-small cell lung cancer.', *Thoracic cancer*, 11(6), pp. 1512–1521. doi: 10.1111/1759-7714.13419.

Weiss, S. T. *et al.* (1995) 'Relation of FEV1 and peripheral blood leukocyte count to total mortality. The Normative Aging Study.', *American journal of epidemiology*, 142(5), pp. 493–503. doi: 10.1093/oxfordjournals.aje.a117665.

Weyand, C. M. and Goronzy, J. J. (2000) 'Association of MHC and rheumatoid arthritis: HLA polymorphisms in phenotypic variants of rheumatoid arthritis', *Arthritis Research & Therapy*, 2(3), p. 212. doi: 10.1186/ar90.

Whelan, R. S. *et al.* (2012) 'Bax regulates primary necrosis through mitochondrial dynamics', *Proceedings of the National Academy of Sciences of the United States of America*, 109(17), pp. 6566–6571. doi: 10.1073/pnas.1201608109.

Whyte, M. K. B. *et al.* (1993) 'IMPAIRMENT OF FUNCTION IN AGING NEUTROPHILS IS ASSOCIATED WITH APOPTOSIS', *Journal of Immunology*, 150(11), pp. 5124–5134. Available at: %3CGo.

Wieduwilt, M. J. and Moasser, M. M. (2008) 'The epidermal growth factor receptor family: Biology driving targeted therapeutics', *Cellular and Molecular Life Sciences*, 65(10), pp. 1566–1584. doi: 10.1007/s00018-008-7440-8.

Wiesmann, N. *et al.* (2019) 'Phosphoproteome Profiling Reveals Multifunctional Protein NPM1 as part of the Irradiation Response of Tumor Cells', *Translational Oncology*, 12(2), pp. 308–319. doi: https://doi.org/10.1016/j.tranon.2018.10.015.

Williams, C. S. *et al.* (2015) 'ERBB4 is over-expressed in human colon cancer and enhances cellular transformation', *Carcinogenesis*, 36(7), pp. 710–718. doi: 10.1093/carcin/bgv049.

Williams, M., Todd, I. and Fairclough, L. C. (2021) 'The role of CD8 + T lymphocytes in chronic obstructive pulmonary disease: a systematic review.', *Inflammation research*, 70(1), pp. 11–18. doi: 10.1007/s00011-020-01408-z.

Witko-Sarsat, V. *et al.* (2000) 'Neutrophils: Molecules, Functions and Pathophysiological Aspects', *Laboratory Investigation*, 80(5), pp. 617–653. doi: 10.1038/labinvest.3780067.

Wo, H. M. *et al.* (2018) 'The Efficacy and Toxicity of Gefitinib in Treating Non-small Cell Lung Cancer: A Meta-analysis of 19 Randomized Clinical Trials', *Journal of Cancer*, 9(8), pp. 1455–1465. doi:

10.7150/jca.23356.

Wong, S. H. and Lord, J. M. (2004) 'Factors underlying chronic inflammation in rheumatoid arthritis.', *Archivum immunologiae et therapiae experimentalis*, 52(6), pp. 379–388.

Woodruff, P. G. *et al.* (2010) 'Safety and Efficacy of an Inhaled Epidermal Growth Factor Receptor Inhibitor (BIBW 2948 BS) in Chronic Obstructive Pulmonary Disease', *American Journal of Respiratory and Critical Care Medicine*, 181(5), pp. 438–445. doi: 10.1164/rccm.200909-1415OC.

World Health Organisation (2019) 'Global Health Observatory (GHO) data: Mortality and global health estimates.' http://origin.who.int/gho/mortality_burden_disease/causes_death/top_10/en/: World Health Organisation.

Wright, H. L. *et al.* (2013) 'RNA-seq reveals activation of both common and cytokine-specific pathways following neutrophil priming.', *PloS one*, 8(3), p. e58598. doi: 10.1371/journal.pone.0058598.

Wu, C.-L. *et al.* (2021) 'A Review of CXCL1 in Cardiac Fibrosis', *Frontiers in cardiovascular medicine*, 8, p. 674498. doi: 10.3389/fcvm.2021.674498.

Wynn, T. A. and Vannella, K. M. (2016) 'Macrophages in Tissue Repair, Regeneration, and Fibrosis', *Immunity*, 44(3), pp. 450–462. doi: 10.1016/j.immuni.2016.02.015.

Xu, Y. F. *et al.* (2013) 'Cigarette smoke (CS) and nicotine delay neutrophil spontaneous death via suppressing production of diphosphoinositol pentakisphosphate', *Proceedings of the National Academy of Sciences of the United States of America*, 110(19), pp. 7726–7731. doi: 10.1073/pnas.1302906110.

Xu, Y., Loison, F. and Luo, H. R. (2010) 'Neutrophil spontaneous death is mediated by down-regulation of autocrine signaling through GPCR, PI3Kgamma, ROS, and actin.', *Proceedings of the National Academy of Sciences of the United States of America*, 107(7), pp. 2950–2955. doi: 10.1073/pnas.0912717107.

Yadavilli, S. *et al.* (2009) 'Ribosomal protein S3: A multi-functional protein that interacts with both p53 and MDM2 through its KH domain.', *DNA repair*, 8(10), pp. 1215–1224. doi: 10.1016/j.dnarep.2009.07.003.

Yakes, F. M. *et al.* (2002) 'Herceptin-induced inhibition of phosphatidylinositol-3 kinase and Akt is required for antibody-mediated effects on p27, cyclin D1, and antitumor action', *Cancer Research*, 62(14), pp. 4132–4141. Available at: %3CGo.

Yamaoka, K. (2016) 'Janus kinase inhibitors for rheumatoid arthritis.', *Current opinion in chemical*

biology, 32, pp. 29–33. doi: 10.1016/j.cbpa.2016.03.006.

Yamaura, K. *et al.* (2014) 'Live cell off-target identification of lapatinib using ligand-directed tosyl chemistry', *Chemical Communications*, 50(91), pp. 14097–14100. doi: 10.1039/c4cc05885b.

Yan, D. *et al.* (2015) 'Gefitinib upregulates death receptor 5 expression to mediate rmhTRAIL-induced apoptosis in Gefitinib-sensitive NSCLC cell line', *Oncotargets and Therapy*, 8, pp. 1603–1610. doi: 10.2147/ott.s73731.

Yao, H. W. *et al.* (2013) 'SIRT1 redresses the imbalance of tissue inhibitor of matrix metalloproteinase-1 and matrix metalloproteinase-9 in the development of mouse emphysema and human COPD', *American Journal of Physiology-Lung Cellular and Molecular Physiology*, 305(9), pp. L615–L624. doi: 10.1152/ajplung.00249.2012.

Yarden, Y. and Sliwkowski, M. X. (2001) 'Untangling the ErbB signalling network', *Nature Reviews Molecular Cell Biology*, 2(2), pp. 127–137. doi: 10.1038/35052073.

Yipp, B. G. *et al.* (2012) 'Infection-induced NETosis is a dynamic process involving neutrophil multitasking in vivo', *Nature Medicine*, 18(9), pp. 1386–1393. doi: 10.1038/nm.2847.

Yipp, B. G. and Kubes, P. (2013) 'NETosis: how vital is it?', *Blood*, 122(16), pp. 2784–2794. doi: 10.1182/blood-2013-04-457671.

Yoon, I.-S. *et al.* (2011) 'Ribosomal protein S3 is phosphorylated by Cdk1/cdc2 during G2/M phase.', *BMB reports*, 44(8), pp. 529–534. doi: 10.5483/bmbrep.2011.44.8.529.

Yu, P. *et al.* (2021) 'Pyroptosis: mechanisms and diseases', *Signal Transduction and Targeted Therapy*, 6(1), p. 128. doi: 10.1038/s41392-021-00507-5.

Yu, Y. and Sun, B. (2020) 'Autophagy-mediated regulation of neutrophils and clinical applications', *Burns & Trauma*, 8, p. tkz001. doi: 10.1093/burnst/tkz001.

Yuyun, X. *et al.* (2021) 'Metabolomic analysis of spontaneous neutrophil apoptosis reveals the potential involvement of glutathione depletion', *Innate immunity*. 2020/09/10, 27(1), pp. 31–40. doi: 10.1177/1753425920951985.

Yvan-Charvet, L. and Ng, L. G. (2019) 'Granulopoiesis and Neutrophil Homeostasis: A Metabolic, Daily Balancing Act', *Trends in Immunology*, 40(7), pp. 598–612. doi: 10.1016/j.it.2019.05.004.

Zarrin, A. A. *et al.* (2021) 'Kinase inhibition in autoimmunity and inflammation', *Nature Reviews Drug Discovery*, 20(1), pp. 39–63. doi: 10.1038/s41573-020-0082-8.

Zhang, J. S. *et al.* (2012) 'Delayed apoptosis by neutrophils from COPD patients is associated with altered bak, bcl-xl, and mcl-1 mRNA expression', *Diagnostic Pathology*, 7, p. 8. doi: 10.1186/1746-1596-7-65.

Zhang, Y., Parmigiani, G. and Johnson, W. E. (2020) 'ComBat-seq: batch effect adjustment for RNA-seq count data', *NAR Genomics and Bioinformatics*, 2(3). doi: 10.1093/nargab/lqaa078.

Zhao, D. *et al.* (2018) 'Small airway disease: A different phenotype of early stage COPD associated with biomass smoke exposure', *Respirology*, 23(2), pp. 198–205. doi: https://doi.org/10.1111/resp.13176.

Zhao, S., Ye, Z. and Stanton, R. (2020) 'Misuse of RPKM or TPM normalization when comparing across samples and sequencing protocols.', *RNA (New York, N.Y.)*, 26(8), pp. 903–909. doi: 10.1261/rna.074922.120.

Zhao, X. *et al.* (2012) 'Neratinib reverses ATP-binding cassette B1-mediated chemotherapeutic drug resistance in vitro, in vivo, and ex vivo', *Molecular pharmacology*. 2012/04/04, 82(1), pp. 47–58. doi: 10.1124/mol.111.076299.

Zhou, L. *et al.* (2014) 'CDK1 switches mitotic arrest to apoptosis by phosphorylating Bcl-2/Bax family proteins during treatment with microtubule interfering agents.', *Cell biology international*, 38(6), pp. 737–746. doi: 10.1002/cbin.10259.

Zhu, A. *et al.* (2014) 'Sputum myeloperoxidase in chronic obstructive pulmonary disease', *European journal of medical research*, 19(1), p. 12. doi: 10.1186/2047-783X-19-12.

Zlotnik, A. and Yoshie, O. (2000) 'Chemokines: A New Classification System and Their Role in Immunity', *Immunity*, 12(2), pp. 121–127. doi: https://doi.org/10.1016/S1074-7613(00)80165-X.

8 Appendices

Appendix 1. Summary of pharmacological reagents used in experiments

Reagent	Manufacturer	Figure	Experimental model	Concentration
Gefitinib	Toku-E, G039-100mg	Figure 3.1	Human neutrophils	1, 5, 25, 50 µM
Lapatinib	Adooq Bioscience, A11752	Figure 3.1	Human neutrophils	1, 5, 25, 50 µM
Sapitinib AZD8931	Cayman Chemical, 24196	Figure 3.1	Human neutrophils	1, 5, 25, 50 µM
Neratinib HKI-272	Selleck, S2150	Figure 3.1	Human neutrophils	1, 5, 25, 50 µM
		Figure 3.3 Figure 3.5 Figure 3.15	Zebrafish larvae	10 µM
		Figure 4.1	Human neutrophils	5, 25, 50 µM
		Figures 4.2 – 4.22	Mouse	20 mg/kg
		Figures 5.8 – 5.15	Human neutrophils	25 µM
Tyrphostin AG825	Santa Cruz Biotechnology, sc-202045	Figure 3.3 Figure 3.8 Figure 3.9 Figure 3.12	Zebrafish larvae	10 µM
CP-724,714	AdooQ Bioscience, A10242	Figure 3.3 Figure 3.8 Figure 3.9 Figure 3.12	Zebrafish larvae	10 µM
EX527	Santa Cruz Biotechnology, sc-203044	Figure 5.15	Human neutrophils	5, 25 µM
NSC348884	Selleck, S8149	Figure 5.15	Human neutrophils	5, 25 µM
NU6102	Abcam, ab144317	Figure 5.15	Human neutrophils	5, 25 µM
Dibutyryladenosine 3',5'-cyclic monophosphate sodium salt (db-cAMP)	Sigma Aldrich, D0627	Figures 5.8 – 5.15	Human neutrophils	500 µM